Institut für Wasserbau · Universität Stuttgart

Mitteilungen

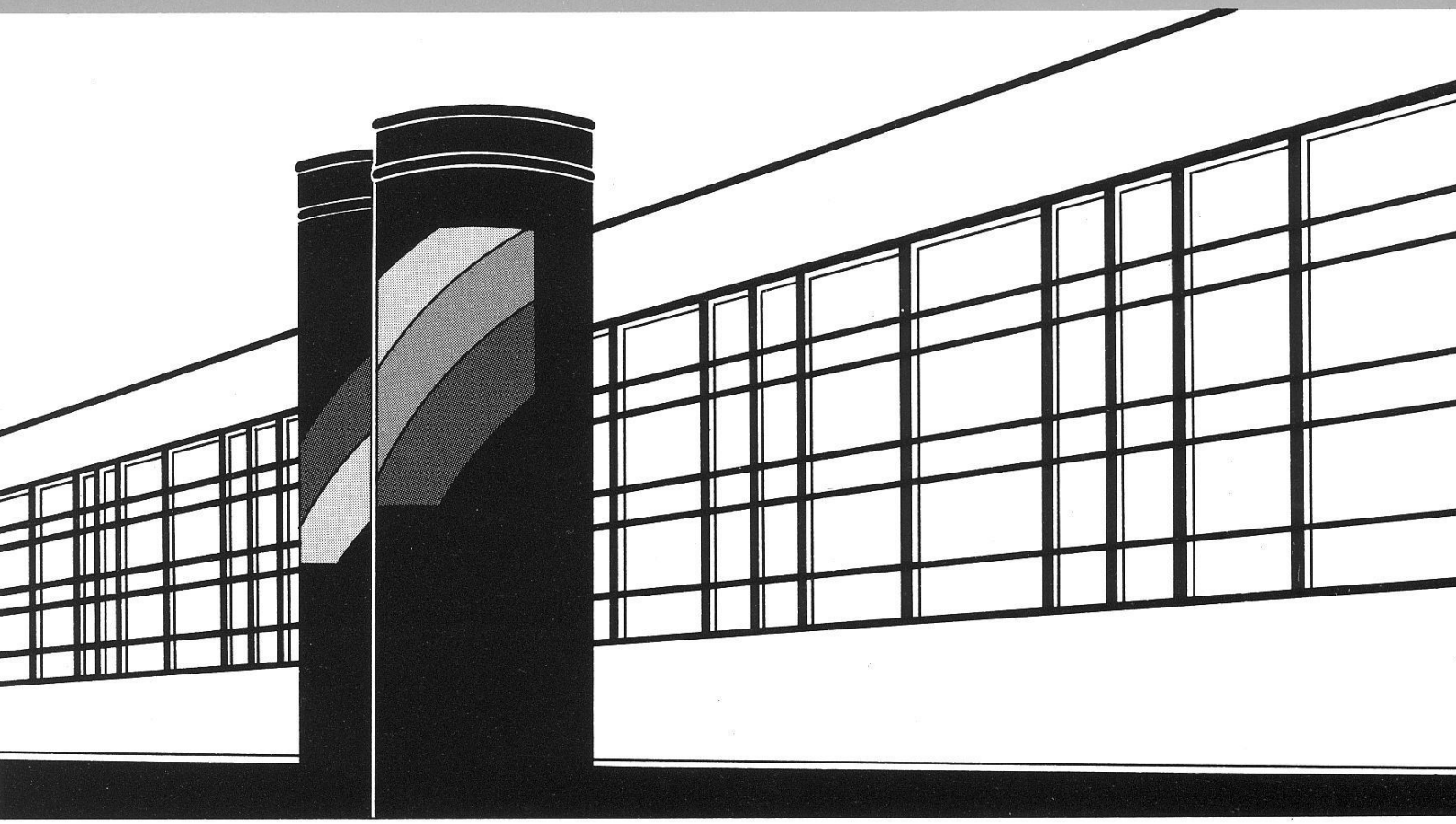

Heft 180 Saqib Ehsan

Evaluation of Life Safety Risks Related to Severe Flooding

Evaluation of Life Safety Risks Related to Severe Flooding

Von der Fakultät Bau- und Umweltingenieurwissenschaften der
Universität Stuttgart zur Erlangung der Würde eines
Doktor-Ingenieurs (Dr.-Ing.) genehmigte Abhandlung

Vorgelegt von
Saqib Ehsan
aus Gujranwala, Pakistan

Hauptberichter:	Prof. Dr.-Ing. Silke Wieprecht
Mitberichter:	Prof. Dr.-Ing. Jürgen Köngeter
	PD Dr.-Ing. Walter Marx
Tag der mündlichen Prüfung:	9. März 2009

Institut für Wasserbau der Universität Stuttgart
2009

Heft 180

Evaluation of Life Safety Risks Related to Severe Flooding

von
Dr.-Ing.
Saqib Ehsan

Eigenverlag des Instituts für Wasserbau der Universität Stuttgart

D93 Evaluation of Life Safety Risks Related to Severe Flooding

Titelaufnahme der Deutschen Bibliothek

Ehsan, Saqib:
Evaluation of Life Safety Risks Related to Severe Flooding/ von Saqib Ehsan. Institut für Wasserbau, Universität Stuttgart. - Stuttgart: Inst. für Wasserbau, 2009

(Mitteilungen / Institut für Wasserbau, Universität Stuttgart: H. 180)
Zugl.: Stuttgart, Univ., Diss., 2009
ISBN 978-3-933761-84-2
NE: Institut für Wasserbau <Stuttgart>: Mitteilungen

Herausgegeben 2009 vom Eigenverlag des Instituts für Wasserbau
Druck: Document Center S. Kästl, Ostfildern

ACKNOWLEDGEMENT

First of all, I am very thankful to God who gave me courage to complete this doctoral research. Then I am thankful to Prof. Dr.-Ing. Silke Wieprecht and ENWAT (International Doctoral Program Environment Water) for giving me the opportunity to start my Ph.D. research at the Institute of Hydraulic Engineering, Universität Stuttgart. I would like to thank Prof. Dr.-Ing. Silke Wieprecht for her kind supervision and guidance. I am also thankful to PD Dr.-Ing. Walter Marx for giving me valuable suggestions and for his encouragement throughout my research work. I would also like to thank Prof. Dr.-Ing. Jürgen Köngeter for his advices.

I would like to acknowledge the support of respective authorities in Pakistan, mainly Water and Power Development Authority (WAPDA) and National Engineering Services Pakistan (Pvt.) Ltd. (NESPAK) for providing me the necessary data of Mangla dam and Jhelum river valley. I am thankful to my all friends and colleagues for their encouragement and motivation.

Finally, I would like to thank my parents, wife, brothers and sisters for their continuous support and encouragement.

Saqib Ehsan

CONTENTS

LIST OF FIGURES

LIST OF TABLES

ABBREVIATIONS AND ACRONYMS

AEP	Annual Exceedance Probability
ALARP	As Low As Reasonably Practicable
ANCOLD	Australian National Committee on Large Dams
ETA	Event Tree Analysis
GA	Geometric Aggregate
HF	High Force
ICOLD	International Committee of Large Dams
IR	Individual Risk
LF	Low Force
LOL	Loss of Life/ No. of dead people
MCA	Multi-Criteria Analysis
MCE	Maximum Credible Earthquake
MCL	Maximum Conservation Level
MDF	Maximum Design Flood
OBE	Operating Basis Earthquake
PAR	Population at Risk/ No. of People at Risk
PMF	Probable Maximum Flood
SE	Side Erosion Index
SL	Stream Length
SOP	Safe Operating Procedure
VL	Valley Length
WAPDA	Water and Power Development Authority (Pakistan)
WT	Warning Time

ABSTRACT

The flooding risk has always been considered to be very important for the risk safety management of dams. The extreme flooding downstream of a dam could be either due to dam failure or sometimes it can occur without failure. In both cases, it poses serious risks to people and property downstream of the dam. In this study, the risk assessment for the Jhelum river valley downstream of Mangla dam has been carried out. Mangla dam is one of the large earth and rock-fill dams in the world. The height of the main dam is about 125 m above riverbed after the raising of about 9.15 m (30 ft) which was planned to be completed in 2008. For this research, Mangla dam has been considered with raised conditions.

The main aim of this research is to develop an improved method for loss of life estimation due to extreme flooding (with and without dam failure) downstream of a dam and to analyze the pattern of impacts depending on the downstream valley shape on possible life loss. The project reach is about 329 km long downstream of Mangla dam including different hydraulic structures. It has been modeled for unsteady flow conditions by using MIKE 11 (1D). Different catastrophic flooding scenarios with and without dam failure have been taken into consideration. Based on flood routing results, the flood severity indication has been done downstream of the dam for different flooding scenarios. In order to have more meaningful and realistic results, a new criterion for flood severity has been developed.

For more precise and realistic estimates of possible life loss due to extreme flooding downstream of the dam, an improved and elaborate loss of life (*LOL*) estimation method has also been developed and loss of life (*LOL*) has been estimated for different flooding scenarios. In order to generalize the *LOL* results of Jhelum river valley for other river valleys in the world, new valley shapes have been produced according to the suggested changes and hydraulic modeling under unsteady flow conditions for different flooding scenarios has been carried out. This study provides new useful guidelines for the better risk assessment of existing and planned dams in Pakistan and in other parts of the world.

ZUSAMMENFASSUNG

EINLEITUNG

Das Auftreten von Hochwasserereignissen stellt schon seit jeher eine Gefahr für den Menschen und sein Eigentum dar. Insbesondere die extremen Überflutungen unterstrom von Staudämmen und Talsperren bergen ein erhöhtes Risiko für die dort lebende Bevölkerung. Ursachen für Überflutungen unterstrom von Dämmen können durch deren Versagen oder durch andere Gründe hervorgerufen werden. Heutzutage wird aufgrund des hohen Schadenspotentials das Versagen von Dämmen sorgfältiger untersucht und dokumentiert als in der Vergangenheit. Aufgrund von Statistiken zum Verlust an Menschenleben und Vermögensschäden ist es völlig gerechtfertigt, dass Dammbetreiber die Versagensrisiken und die Schadenspotenziale, welche von Dämmen ausgehen, besser verstehen. Die Sicherheit von Staudämmen ist ein sehr wichtiger Bestandteil des Stauraummanagements, welcher in den vergangenen Jahren nicht immer ausreichend Rechnung getragen wurde. Außerdem war die genaue Einbeziehung der Dammversagensrisiken bisher nicht Bestandteil des Dammbaus. (*Dam Safety Inspection Manual (2003)* [20]), (*Bowles (1996)* [9])

Dieses Projekt beinhaltet eine Risikobetrachtung für verschiedene extreme Hochwasserereignisse und für den Fall des Dammversagens. Zusätzlich werden die Schadenspotentiale unterstrom des Damms, die durch die Hochwasserwelle aus Dammversagen beziehungsweise durch extreme Hochwasserereignisse, denen der Damm widerstanden hat, entstehen, analysiert. Das Risiko ist definiert als die Kombination von Versagenswahrscheinlichkeit und Schadenspotential (Kosten). Das auftretende Risiko kann durch verschiedene Maßnahmen in der Bauausführung, Überwachung und Wartung verringert werden.

Eine Beurteilung dieses Risikos kann wertvolle Informationen bezüglich strukturellen Verbesserungsmaßnahmen und nicht strukturellen Maßnahmen zur Minderung des Risikos liefern. Für zahlreiche ältere Dämme wurde in der damaligen Planungsphase keine angemessene Risikobeurteilung für die Flutwellenausbreitung bei Dammversagen oder bei anderen Schadenszenarien durchgeführt. (*Dam Safety Inspection Manual (2003)* [20]), (*Bowles (1996)* [9])

Der Zahl der Todesopfer wird als bedeutendster Aspekt der Schadensanalyse betrachtet. Abschätzungen zur Anzahl von Todesfällen dienen vornehmlich für folgende Zwecke: (*Aboelata et al. (2003)* [1])

- Reduzierung der menschlichen Sicherheitsrisiken im Zusammenhang mit Dämmen
- Bewertung der existierenden und verbleibenden Risiken von Dämmen
- Entscheidungsunterstützung für strukturelle- und nicht strukturelle Maßnahmen im Gefährdungsgebiet zur Risikominderung
- Abschätzung der Kosteneffizienz von risikomindernden Maßnahmen
- Verbesserung der Vorwarneffizienz und Evakuierungsplanung

In dieser Studie wurde die Risikobeurteilung für das Jhelum-Tal unterhalb des Mangla-Dammes durchgeführt. Der Mangla-Damm am Jhelum-Fluss ist ein Erd- und Steinschüttdamm und wurde 1967 fertig gestellt. Die ursprüngliche Höhe des Hauptdamms beträgt 115.85 m (*Pakistan Water Gateway* [50]), (*WAPDA (2001)* [77]). Im Jahr 2004 wurde eine Erhöhung des Dammes um circa 9.15 m beschlossen und im 2008 fertig gestellt (*WAPDA (2007)* [88]). Im Rahmen dieser Studie ist die Erhöhung des Damms bereits berücksichtigt.

HAUPTZIEL UND METHODE DER FORSCHUNG

Das Hauptziel dieses Forschungsprojekts ist die Entwicklung einer verbesserten Methode zur Abschätzung von Todesfällen aufgrund extremer Hochwasserereignisse mit und ohne Dammversagen sowie die Analyse des Einflusses der Talform im überflutungsgebiet auf die zu erwartenden Schäden. Als Untersuchungsgebiet wurde das Jhelum-Tal unterstrom des Mangla-Damms in Pakistan für die Durchführung dieser systematischen Studien ausgewählt. Die untersuchte Fließstrecke umfasst 329 km und wurde für instationäre Fließbedingungen basierend auf einer GIS-Datengrundlage mit MIKE 11 (1D) numerisch simuliert. Die verfügbare Datengrundlage bestand vornehmlich aus Fließquerschnitten, Daten zu hydraulischen Bauwerken, Standorten von bewohnten Häusern und Informationen über die Zusammensetzung der Bevölkerung. MIKE 11 wurde von DHI, Dänemark entwickelt und ist ein weltweit anerkanntes und vielseitiges Werkzeug zur Simulation von 1D-Strömungsverhältnisssen in Fließgewässern, Seen/Stauseen, Bewässerungskanälen und weiteren Binnengewässersystemen. Zusätzlich bietet MIKE 11 die Implementierung von

verschiedenen hydraulischen Bauwerken (*MIKE 11 Short Introduction (2005)* [65]). Vor der hydrodynamisch-numerischen 1D-Modellierung wurde eine Wahrscheinlichkeitsanalyse durchgeführt, um die Versagenswahrscheinlichkeit des Damms zu berechnen.

Die Entscheidung für eine 1D-Modellierung erfolgte aufgrund folgender Gründe.

- Sehr langer Flussabschnitt (329 km)
- Große Abstände zwischen den Verfügbaren Querschnitten (durchschnittlich circa 4 km)
- Keine verfügbaren Daten zwischen den Querschnitten
- Zu hoher Rechenaufwand für 2D-und 3D-Modellierung

Daher war die 1D-Modellierung die einzige Möglichkeit, die gesamte Fließstrecke zu simulieren, da 2D- und 3D-Modelle detaillierte Daten benötigen. Insgesamt wurden verschiedene Überflutungsszenarien für die instationäre Strömungssimulation mit und ohne Dammversagen betrachtet.

PHASEN DER FORSCHUNG

Die Forschungsarbeit gliedert sich in die folgenden Phasen:

Phase 1: Berechnung der Summe der Versagenswahrscheinlichkeit für den Mangla-Damm

Phase 2: Aufbau des eindimensionalen Modells unterstrom des Mangla-Damms inklusive Kalibrierung und Validierung für instationäre Strömungssimulationen

Phase 3: Simulationen für verschiedene extreme Hochwasserszenarien

Phase 4: Bestimmung der Hochwasserintensität unterstrom des Mangla-Damms unter Berücksichtigung der vorliegenden Kriterien und Entwicklung eines neuen verbesserten Kriteriums zur Ermittlung von Hochwasserintensitäten

Phase 5: Entwicklung einer verbesserten Methode zur Abschätzung der Anzahl von Todesfällen

Phase 6: a) Abschätzung der Todesfälle für verschiedene Hochwasserszenarien

b) Bestimmung des maximalen Ausmaßes an Todesfällen in Bezug zur Entfernung zum Damm

Phase 7: Analyse des Einflusses der Talform auf die Todesfälle

DURCHFÜHRUNG DER FORSCHUNGSARBEIT

Für die Wahrscheinlichkeitsanalyse wurden verschiedenen Versagens-Szenarien mit ihrer jeweiligen Auftretenswahrscheinlichkeit für den Mangla-Damm berücksichtigt. Naturgefahren wie Überschwemmungen und Erdbeben waren schon immer sehr kritisch für den Mangla-Damm. Alle berücksichtigten Versagens-Szenarien wurden qualitativ mit Ereignisbäumen analysiert, um die Summe der jährlichen Versagenswahrscheinlichkeit zu berechnen. Die anhand der vorliegenden Normen durchgeführten Analysen zeigen, dass die berechnete Summe der Versagenswahrscheinlichkeit des Mangla-Damms relativ hoch ist und rechtfertigt damit eindeutig die Notwendigkeit der weiteren Risikobewertung des Mangla-Damms.

Mithilfe der verfügbaren Daten wurde eine numerische hydrodynamische Modellierung für das Jhelum-Tal, unterstrom des Mangla-Damms, durchgeführt. Das Flood Routing wurde für einen 329 km länger Abschnitt des Jhelum-Tals unterstrom des Mangla-Damm, mit MIKE 11 für instationäre Strömungsbedingungen und bei verschiedenen Hochwasser-Szenarien durchgeführt. Das Versagen des Mangla-Damms aufgrund überströmen und infolge dessen Breschebildung durch Erosion wurde auch mit MIKE 11 für verschiedene Damm-Bruch-Szenarien, die auf der Grundlage von Fallstudien beruhen, modelliert. Weiterhin wurden die Abfluss Ganglinien für verschiedene Bruch-Szenarien ermittelt. Anschließend wurden die Ergebnisse des Flood-Routings für verschiedene Hochwasser-Szenarien mit und ohne Dammbruch miteinander verglichen

Die Ergebnisse des Flood-Routings der verschiedenen Hochwasser-Szenarien wurde für die Ermittlung der Hochwasserintensität an verschiedenen Stellen unterhalb des Mangla-Damms genutzt. Diese Information spielt eine sehr wichtige Rolle für die Bewertung des Hochwasserrisikos und der Schadensabschätzung. Dabei wurden verschiedene Kriterien für die Hochwasserintensität mit unterschiedlichen Definitionen aus der Literatur berücksichtigt und die Ergebnisse verglichen. Um realistische und sinnvolle Informationen über die

Hochwasserintensität abzuleiten, wurde ein neues verbessertes Kriterium für die Ermittlung und Bewertung der Hochwasserintensität entwickelt.

Verschiedene verfügbare Methoden für die Schätzung der zu erwartenden Todesfälle wurden untersucht. Für präzisere und realistischere Schätzungen wurde eine neue umfangreiche Methode zur Schätzung der Todesfälle entwickelt. In dieser Methode wurden verschiedene wichtige Faktoren, die sich aus den verfügbaren Daten ergeben, mit Hilfe einer Plausibilitäts-Analyse ausgewertet.

Um die Ergebnisse der vorliegenden Untersuchungen des Jhelum-Tals auch für andere Flusstäler in der Welt zu anwendbar zu machen, wurde die Auswirkung der unterstromigen Talform auf mögliche Verluste an Menschenleben aufgrund extremer Hochwasser analysiert. Verschiedene Änderungen am Tal zum Beispiel das Tal-Gefälle und die Breite wurden in den Simulationen der Hochwasser-Szenarien mit und ohne Dammbruch berücksichtigt. Die Todesfälle wurden auch entsprechend der neuen Methode für verschiedene Hochwasser-Szenarien mit den verschiedenen Talformen geschätzt. Schließlich wurden auch die Restrisiken für verschiedene Hochwasser-Szenarien bei verschiedenen Talformen geschätzt.

Diese innovative Forschung ist Teil der Idee des Technologietransfers zwischen Europa und Pakistan und zielt darauf ab bestehenden und geplanten Dämmen in Pakistan als auch in Europa und in anderen Teilen der Welt neue Leitlinien für eine bessere Risikobewertung bereit zu stellen.

1 INTRODUCTION

1.1 INTRODUCTION AND IMPORTANCE OF RESEARCH

Floods have always been a danger to people and property. Especially the extreme flooding downstream of a dam poses extra risk to the people living there. This high flooding downstream of a dam can happen with and without dam failure. Dam failures are severe threats to life and property and are now being recorded and documented more thoroughly than in the past. Life and property loss statistics justify the need for dam owners to better understand the risks of failure and the hazards to the public posed by dams. Dam safety is a very essential part of reservoir management. In the past, reservoir managers have not always given adequate attention to dam safety. Moreover, the precise consideration of dam failure risks has not been practiced by the dam engineering profession. (*Dam Safety Inspection Manual (2003)* [20]), (*Bowles (1996)* [9])

This research will include risk assessment for different catastrophic flood events as well as for dam collapse situations and damage analysis downstream of the dam due to flood wave propagation after a possible dam break as well as extreme flood events that the dam has resisted. Risk is defined as the probability of failure combined with the arising cost due to failure (damage potential): It can be lowered by good practice of construction, controlling and maintenance.

Risk assessment can provide valuable information on the risk reduction characteristics and potential benefits of structural and non-structural risk reduction options. For many aging dams, proper risk assessment for dam collapse and damage analysis downstream of the dam due to flood wave propagation (with and without dam break) was not carried out at the time of dam planning. (*Dam Safety Inspection Manual (2003)* [20]), (*Bowles (1996)* [9])

Life loss is the most severe damage. Life loss estimation is mainly needed for the following purposes, (*Aboelata et al. (2003)* [1])

- For reducing the life safety risks related to dams
- For evaluating the existing and residual risks of dams
- For deciding structural and non-structural risk reduction measures in affected areas

- For the estimation of cost effectiveness of risk reduction measures in affected areas
- For improving the warning efficiency and evacuation planning

This innovative study is committed to the idea of technology transfer between Europe and Pakistan and it is intended to give new guidelines for better risk assessment of existing and planned dams in Pakistan as well as in Europe and in other parts of the world.

1.2 MAIN AIM AND METHOD OF RESEARCH

The main aim of this research is to develop an improved method for life loss estimation due to extreme flooding (with and without dam failure) downstream of a dam and to analyze the impact of the downstream valley shape flooding scenarios and subsequently on life loss. In this study, the Jhelum river valley downstream of Mangla dam in Pakistan has been taken into consideration as a basis for systematic studies. The project reach is about 329 km long and it has been modeled for unsteady flow conditions based on GIS and other official data by using MIKE 11 (1D). MIKE 11 developed by the DHI Denmark is a well known and multipurpose engineering tool for modeling 1D-open channel flow conditions in rivers, lakes/reservoirs, irrigation canals and other inland water systems with the provision of different hydraulic structures (*MIKE 11 Short Introduction (2005)* [65]). Different flooding scenarios with and without dam failure have been considered for the unsteady flow simulations.

1.3 INTRODUCTION OF PROJECT AREA

1.3.1 Mangla Dam

Mangla dam was completed in 1967 and is one of the large earth and rock-fill dams in the world. It is located on Jhelum river, south-east of the Pakistani capital Islamabad in Mirpur district of Azad Kashmir, Pakistan [95] (figure 1.1). The original height of the main dam is about 115.85 m above riverbed (*Pakistan Water Gateway* [50]), (*WAPDA (2001)* [77]). The raising of the dam by about 9.15 m started in 2004 and it was planned to be completed in 2008 (*WAPDA (2007)* [88]). In this study, Mangla dam has been considered with raised conditions. The planned raising would increase the dam elevation from 376.22 m asl (1234 ft) to 385.37 m asl (1264 ft) and maximum conservation level (MCL) from 366.46 m asl (1202 ft)

to 378.66 m asl (1242 ft) (*WAPDA (2003)* [85], [86]) (figure 1.2). The crest length of the main dam is about 2,561 m (*WAPDA (2004)* [82]). The original catchment area of the reservoir is about 33,360 km^2 and the water surface area (at conservation level) is about 253 km^2 (*WAPDA (2001)* [77]). The salient features of Mangla dam have been shown in table 1.1.

Figure 1.1: Location of Mangla dam [92]

Table 1.1: Salient features of Mangla dam

Feature	**Detail**
Main dam height (original)	115.85 m (above riverbed)
Main dam height (after raising)	125 m (above riverbed)
Gross storage (original)	7.25 E+9 m^3
Net storage (original)	6.59 E+9 m^3
Catchment area of reservoir (original)	33,360 km^2
Water surface area of reservoir (original) (at maximum conservation level)	253 km^2
Power generation (existing capacity)	1,000 MW
Elevation of dam crest (original)	376.22 m asl (1234 ft)
Elevation of dam crest (after raising)	385.37 m asl (1264 ft)
Maximum conservation level (original)	366.46 m asl (1202 ft)
Maximum conservation level (after raising)	378.66 m asl (1242 ft)
Crest length of main dam	2,561 m
Design capacity of main spillway	28,583 m^3/s
Design capacity of emergency spillway	6,452 m^3/s
Maximum design flood (MDF) (recently reevaluated)	61,977 m^3/s
Maximum design flood level	384.15 m asl (1260 ft)
72-hrs volume of MDF hydrograph	7.11 E+9 m^3
Estimated peak outflow at MDF level (through all outlets)	36,309 m^3/s
Peak horizontal ground acceleration of maximum credible earthquake (MCE)	0.40g

Figure 1.2 shows a typical section of the main dam which illustrates the existing and raised conditions of Mangla dam.

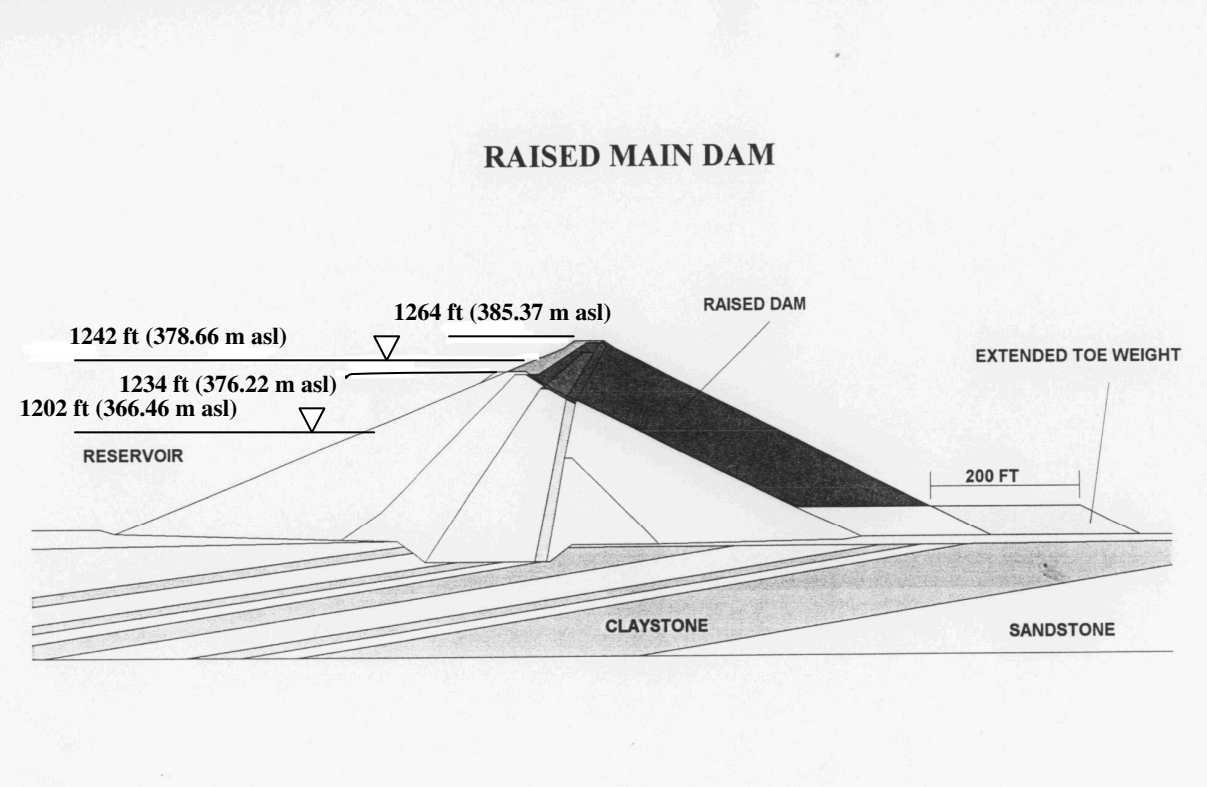

Figure 1.2: Typical section of raised main dam

1.3.2 Outlets of Mangla Reservoir

The Mangla reservoir has four outlets, main spillway, emergency spillway, power house/irrigation valves and jari outlet. The two spillways are mainly designed for flood control. Other outlets do not play any role in passing floods because of their low capacities (for their specific purposes). Figure 1.3 depicts the layout of Mangla dam. (*WAPDA (2001)* [77])

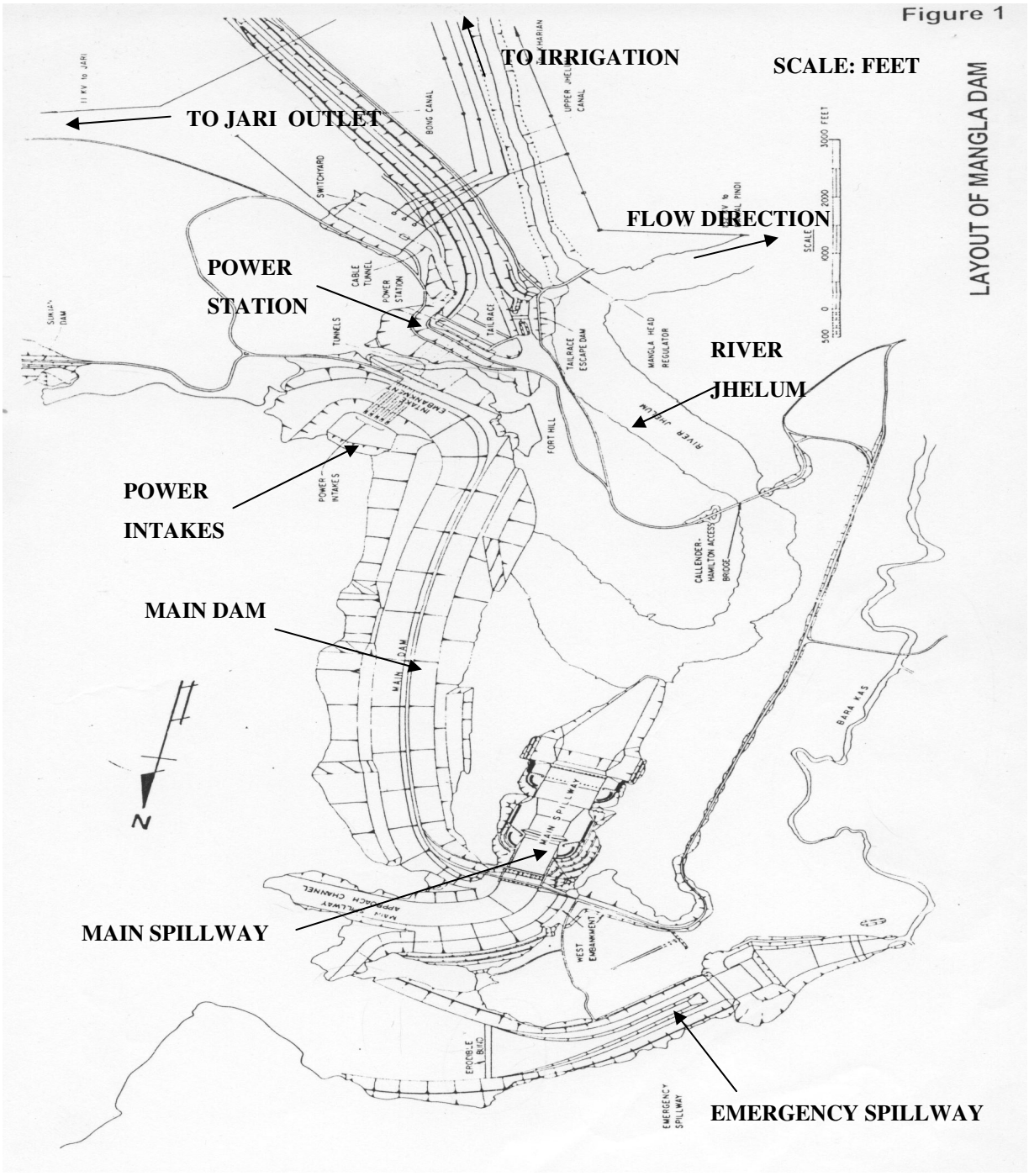

Figure 1.3: Layout of Mangla dam [77]

The reservoir is mainly operated to meet irrigation requirements with power generation being the secondary objective. The original design capacity of the main spillway is about 28,583 m^3/s. The main spillway is designed for following purposes (*WAPDA (2001)* [77]),

- to pass floods through the reservoir with the minimum rise in water level
- to release water before the occurrence of floods

- to supplement irrigation indents above the release capacity of power plants/irrigation valves and discharge that extra portion of flow during the time when reservoir is at maximum conservation level

When the reservoir is at maximum conservation level or rising close to it then spillway gates are operated to ensure that the conservation level is not exceeded. The main spillway is an orifice type structure. Each of nine orifices is controlled by a radial gate where each is 10.975 m (36 ft) wide and 12.195 m (40 ft) high. Under the raised conditions of the dam, the discharge capacity of the main spillway would be kept the same as its original capacity by raising the orifice floor by 5 ft to restrict the opening area of each gate (*WAPDA (2004)* [78]). Moreover, the headwall and abutment monoliths would also be raised by 9.15 m (30 ft). The structure of the main spillway with its different parts is shown in figure 1.4. (*WAPDA (2004)* [78]), (*WAPDA (2001)* [80])

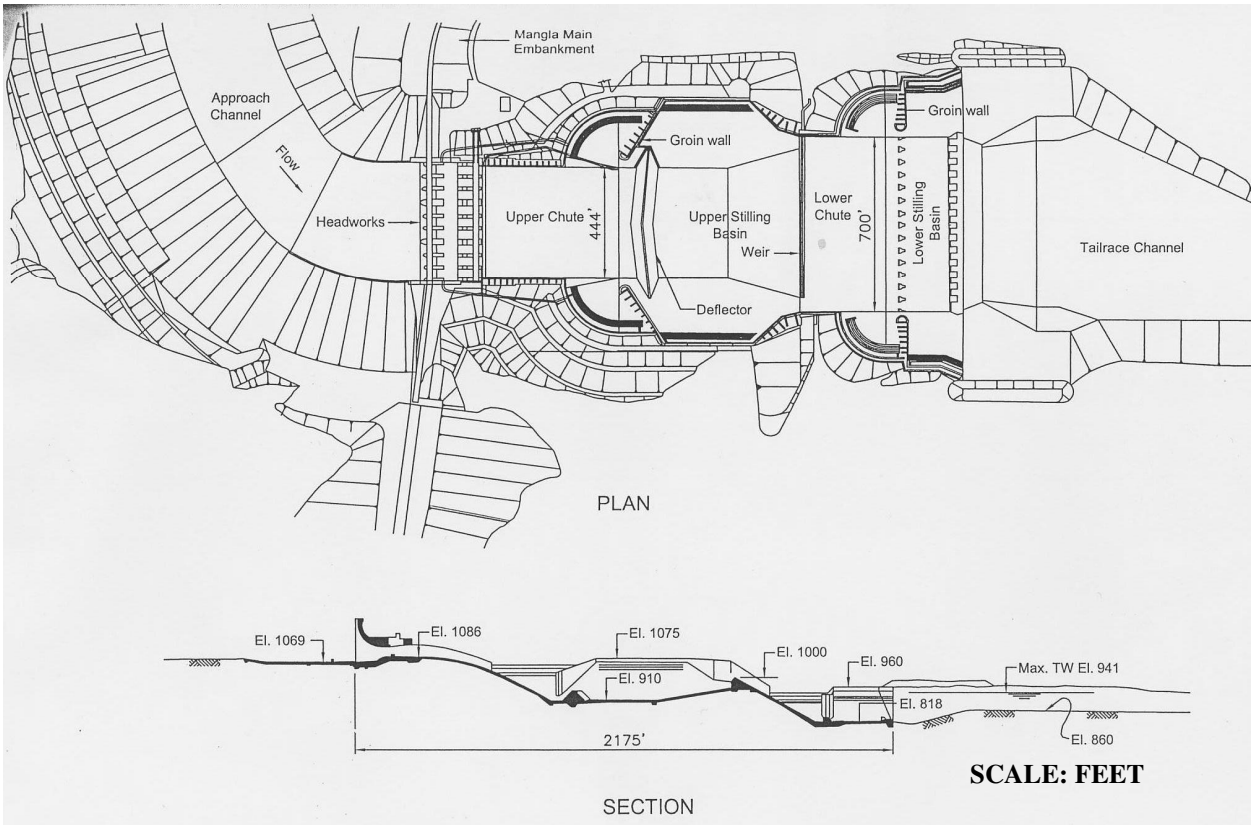

Figure 1.4: Structure of Main spillway [78]

The design capacity of the emergency spillway (figure 1.3) is about 6,452 m^3/s. The emergency spillway is an overflow type structure. The existing spillway structure has a

control weir, chute and bucket. The emergency spillway is designed to operate when the capacity of the main spillway is exceeded. This spillway has not been operated yet, because in the past no high flood occurred exceeding the main spillway capacity. Under the raised condition of the dam, this spillway would have a crest level of 378.66 m asl (1242 ft), maximum conservation level and its discharge capacity would remain the same as its original capacity. A control weir in the approach channel of the emergency spillway has been proposed for raised conditions. The proposed control weir would make the rim of the raised reservoir and dissipate the extra energy of the spilling water. This weir will be built at the entrance of the approach channel. (*WAPDA (2001)* [77]), (*WAPDA (2004)* [79]), (*WAPDA (2001)* [80]), (*WAPDA (2001)* [84])

1.3.3 Jhelum River Valley

The Jhelum river valley downstream of Mangla dam is about 329 km long up to the upstream of Trimmu barrage with various hydraulic structures. The main hydraulic structures are Jhelum bridges, Rasul barrage, Malikwal bridge and Khushab bridge (figure 1.5). There are five tributaries between Mangla dam and Rasul barrage, Suketar nallah, Bandar kas, Jabba kas, Kahan river and Bunha river (figure 1.5). Moreover, figure 1.5 illustrates also the confluence point of the Jhelum river and Chenab river. Available data of the downstream valley include mainly the river cross-sections, data of hydraulic structures, location of houses along the flood plains and population data (98-census). Different other features of the Jhelum river valley are also shown in figure 1.5.

According to 98-census data [94], there are more than one million people at risk of flooding downstream of Mangla dam along the project reach. Most of the population along the project reach is rural and people are engaged in agriculture. The Mangla dam supplies electric power to downstream areas and also irrigates the downstream fields of agriculture. The project area also covers some urban populated areas along the Jhelum river valley like Jhelum city, Pind Dadan Khan, Malikwal, Bhera, Khushab, Jouharabad, Sahiwal etc. Figure 1.6 shows the view of Jhelum river valley downstream of Mangla dam.

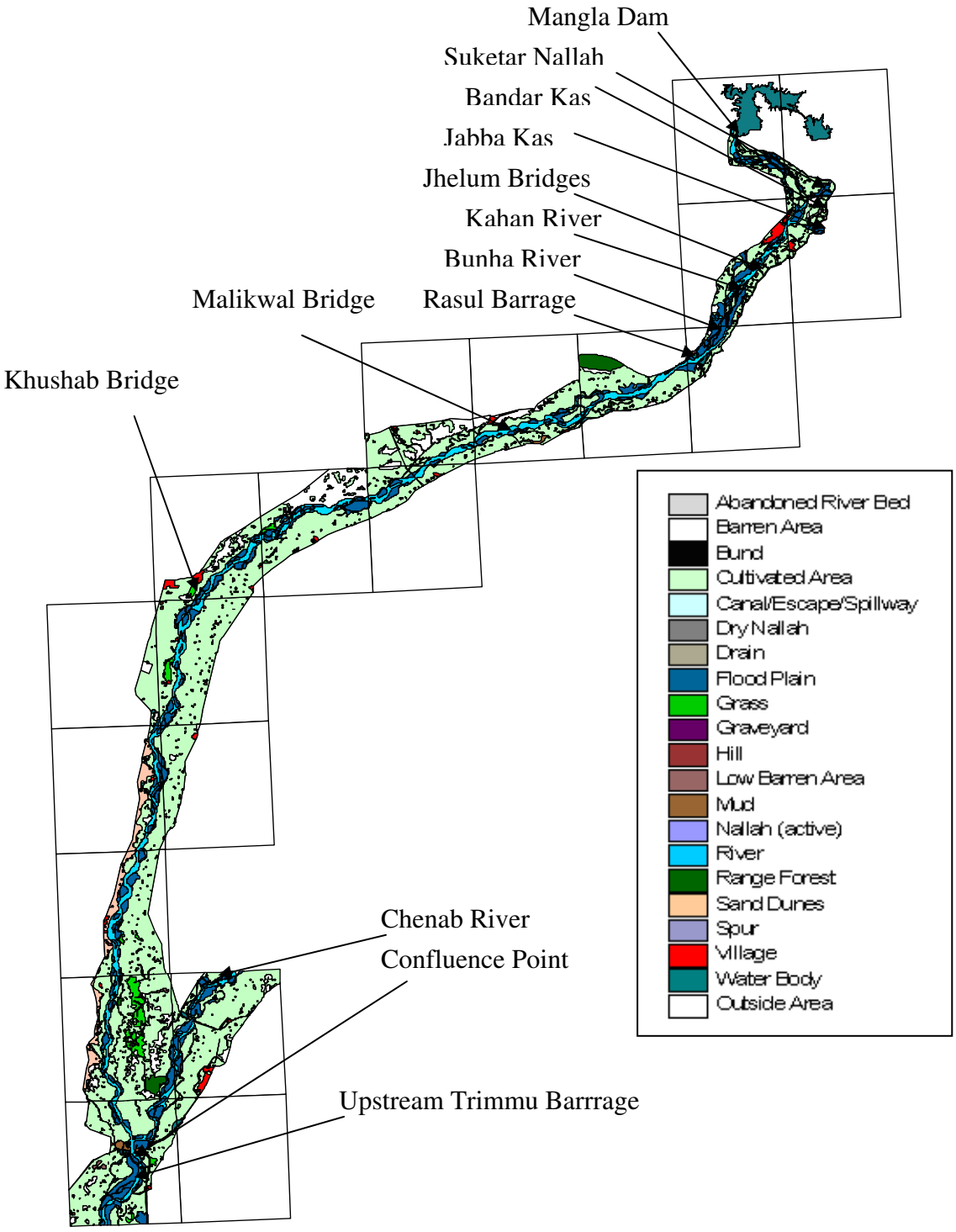

Figure 1.5: Jhelum river valley downstream of Mangla dam

Figure 1.6: View of Jhelum river valley downstream of Mangla dam, Pakistan [93]

1.4 RESEARCH PHASES CARRIED OUT

The research work has been divided into the following phases.

Phase 1: Computation of the overall failure probability of Mangla dam

Phase 2: One dimensional model setup downstream of Mangla dam: calibration and validation for unsteady flow conditions

Phase 3: Model runs for different extreme flooding scenarios

Phase 4: Flood severity indication downstream of Mangla dam according to available criteria and development of an improved criterion for flood severity indication

Phase 5: Development of an improved method for life loss estimation

Phase 6: a) Life loss estimation for different flooding scenarios

b) Determination of the maximum extent of life loss related to downstream distance from the dam

Phase 7: Analysis of the impact of the downstream valley shape on life loss

2 COMPUTATION OF OVERALL FAILURE PROBABILITY FOR MANGLA DAM

2.1 INTRODUCTION

This chapter focuses on the computation of overall failure probability of Mangla dam in Pakistan. In this study, Mangla dam has been considered with raised conditions (detail in section 1.3.1). For the computation of overall failure probability, different failure scenarios have been considered with respect to possible natural hazards. The probability analysis has been carried out by using the event tree method. Using the available data, the failure probabilities for different considered scenarios have been analyzed qualitatively and then expressed in a quantitative manner.

2.2 FAILURE SCENARIOS

Different failure scenarios have been taken into consideration depending on their possible occurrence for Mangla dam. Natural hazards like floods and earthquakes have always been very crucial for Mangla dam. The catchment of Mangla reservoir lies in the region of heavy rainfall (*WAPDA (2001)* [77]) and moreover, the Mangla dam project is located close to seismically active zones (*WAPDA (2004)* [87]). In case of extreme events, Mangla dam has a possible risk of failure. As Mangla dam is an earth and rock-fill dam, extreme flooding upstream of the dam could pose risks of overtopping, loss in geotechnical strength of the dam and loss in structural strength of main components. In the same way, catastrophic earthquake can also cause sudden loss in geotechnical strength of Mangla dam and structural strength of main components. Keeping in view the possible impacts of extreme hazards on Mangla dam, following failure scenarios have been considered and analyzed.

1- Overtopping failure of main dam (by flood)
2- Geotechnical strength failure of main dam (by flood)
3- Main dam failure by liquefaction in fill (by earthquake)
4- Structural failure of main spillway (by flood)
5- Structural failure of main spillway (by earthquake)

For all cases, the maximum conservation level (normal operating conditions) after raising of the Mangla dam has been taken into consideration.

2.3 INITIATING EVENTS FOR DAM FAILURE

Following are the considered initiating events (loading states) for different failure scenarios of Mangla dam.

- Maximum design flood (MDF)
- Maximum credible earthquake (MCE)

2.3.1 Maximum Design Flood (MDF)

For Mangla dam, MDF is considered to be the probable maximum flood (PMF) (*Binnie and Partners (1971)* [7]). By definition, 'the probable maximum flood (PMF) is the greatest flood which could ever be experienced' (*Binnie Deacon (1959)* [6]). The PMF at Mangla was first estimated in 1959 as 73,580 m^3/s (2.60 million cusecs) and reevaluated in 1992 as 66,505 m^3/s before the occurrence of the high flood of September 1992 (*WAPDA (2001)* [81]). But the volume under inflow hydrograph remained almost the same, about 8.39 E+9 m^3 (*WAPDA (2001)* [81]). The exceptionally high flood of 1992 (peak inflow: 30,847 m^3/s) made it necessary to further reevaluate the so-called PMF (MDF for Mangla dam). Recently it has been evaluated as 61,977 m^3/s (2.19 million cusecs) with 72-hrs inflow volume of about 7.11 E+9 m^3 (*WAPDA (2003)* [86]). In Mangla dam literature, the term 'PMF' is not in accordance with the current PMF standards. Currently for design purposes, PMF is expressed in terms of its probability of occurrence which is usually very low. According to the specifications given by (*DIN 19700-11 (2004)* [24]), Mangla dam comes into the category of 'class1'. The annual exceedance probability (AEP) for an extreme flood, BHQ_2 (more than MDF) is suggested to be 1.0 E-4 (*DIN 19700-11 (2004)* [24]). Moreover, the PMF is believed to be much higher than BHQ_2 (*DIN 19700-11 (2004)* [24]) and obviously its AEP would be quite lower than 1.0 E-4. According to ANCOLD standards (*McDonald (1999)* [44]), the AEP of PMF must also be lower than 1.0 E-4. The so-called PMF (MDF for Mangla dam) is not the actual PMF according to the current standards. In this probability analysis, this recently estimated MDF (61,977 m^3/s) has been taken into account.

2.3.2 Annual Exceedance Probability for MDF

By definition, annual exceedance probability (AEP) is the probability that an event of a given magnitude, or any greater magnitude will occur in one year (*Fell et al. (2000)* [28]). The available record of past floods (figure 2.1) is not too long to have a very good estimation of AEP for MDF at Mangla dam. The AEP for MDF (61,977 m^3/s) has been estimated by the extrapolation of available annual flood peak frequency curve as shown in figure 2.1. Considering the available flood frequency data, it is also believed that even with more record of floods the return period for MDF occurrence would not be much higher than 200 years. However, the estimated AEP for MDF is considered to be reliable for this study.

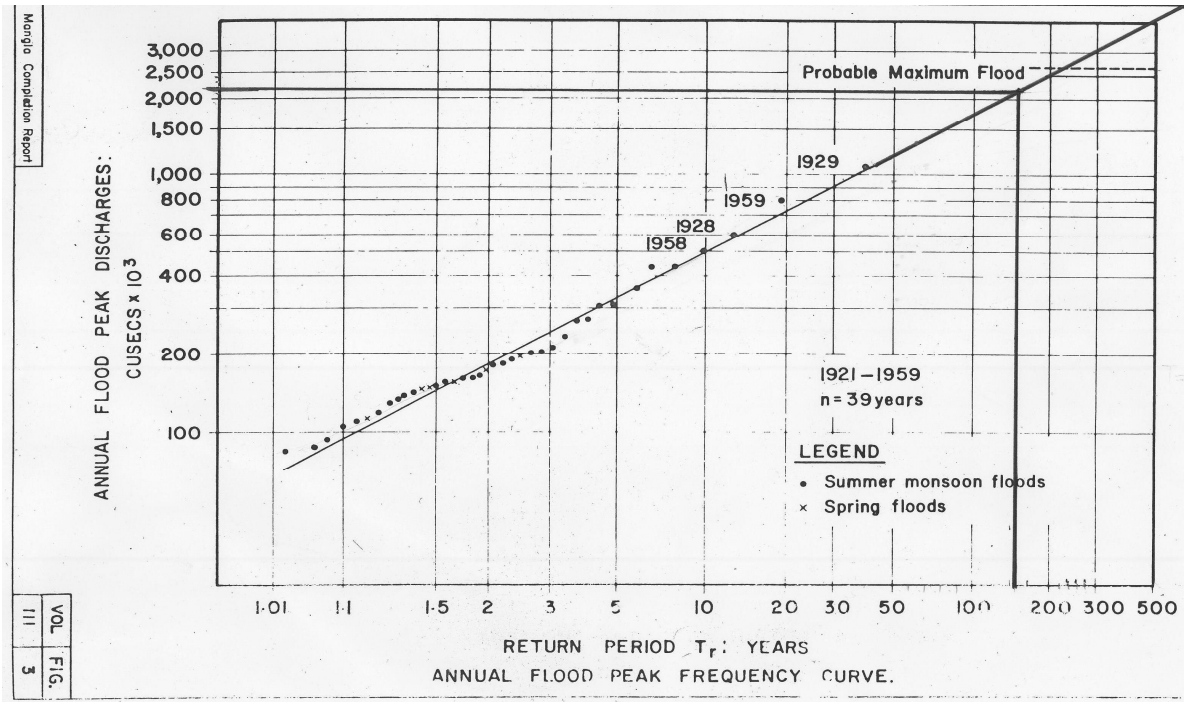

Figure 2.1: Annual flood peak frequency curve for Mangla dam [7]

Following is the derived AEP (P_e) for MDF given by equation (2.1),

Return period (T) = 156 years (by extrapolation of existing curve)

$$P_e = \frac{1}{T} = \frac{1}{156} = 6.41 \text{ E-3 (adopted for analysis)} \qquad (2.1)$$

The estimated AEP for MDF occurrence, 6.41 E-3 seems to be relatively high. According to (*DIN 19700-11 (2004)* [24]) for class1 dams, the AEP for MDF (BHQ_1) should be 1.0 E-3 and for an extreme flood (BHQ_2) it must be 1.0 E-4. Further the maximum limit of AEP (high

hazard category) for MDF is 1.0 E-4 (*McDonald (1999)* [44]). The estimated AEP for MDF does not meet the requirements of (*DIN 19700-11 (2004)* [24]) and also ANCOLD standards (*McDonald (1999)* [44]).

2.3.3 Maximum Credible Earthquake (MCE)

According to ICOLD guidelines, 'the MCE is the largest reasonable conceivable earthquake that appears along a recognized fault or within a geographically defined tectonic province under the presently known or presumed tectonic framework'. The Mangla dam project is located close to the axis of the Hazara-Kashmir syntaxial bend and seismically active tectonic features are present on both sides of this axis. The figure 2.2 shows seismic conditions in the Mangla region. (*WAPDA (2004)* [87])

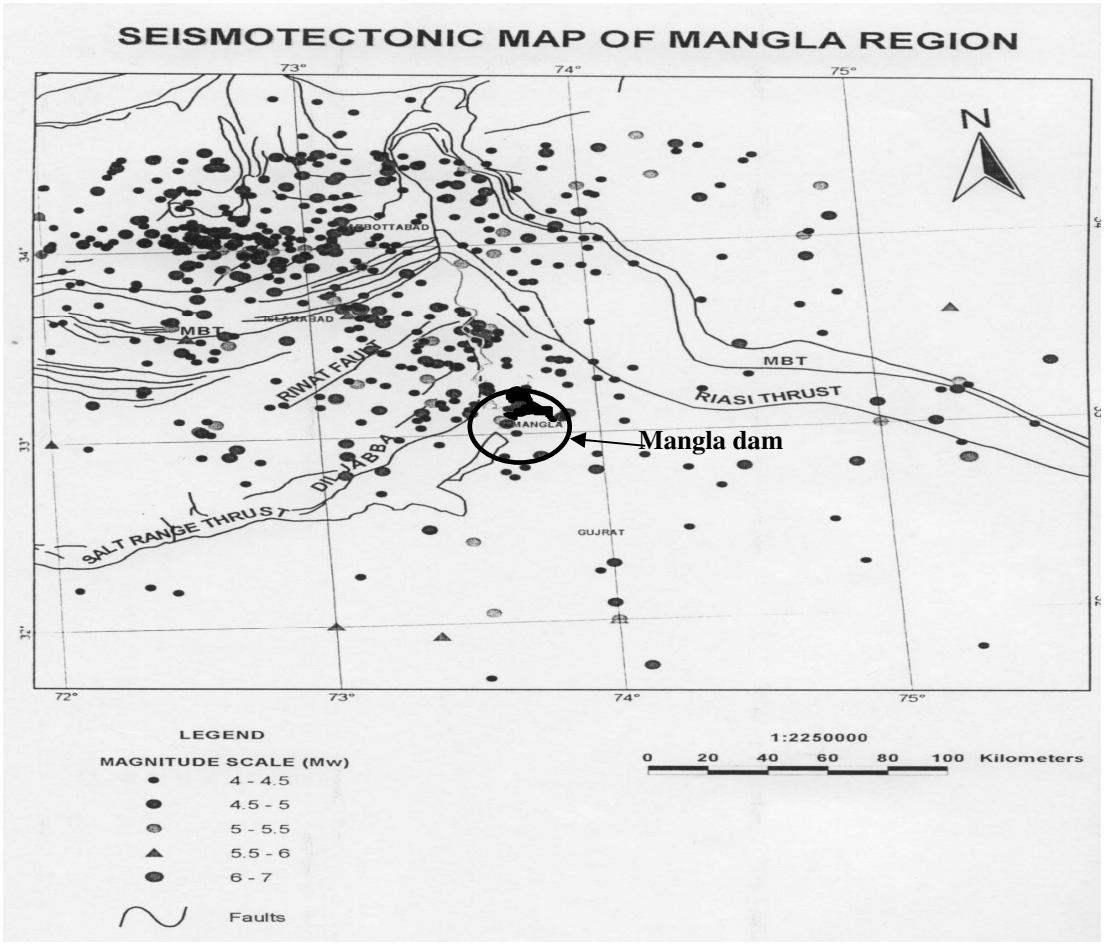

Figure 2.2: Seismotectonic map of Mangla region [87]

For the design of Mangla dam, the peak horizontal ground acceleration of 0.11g was used. The peak horizontal ground acceleration of 0.14g associated with the operating basis

earthquake (OBE) has been recommended for Mangla dam for project life of 100 years. OBE represents the level of ground motion at the dam site at which only minor damage is acceptable. After recent feasibility studies for Mangla raising, the peak horizontal ground acceleration of 0.40g has been recommended for MCE condition (*WAPDA (2004)* [87]). In this probability analysis, this recently recommended value of peak horizontal ground acceleration (0.40g) for MCE has been considered.

2.3.4 Annual Exceedance Probability for MCE

In figure 2.3, the total hazard curve shows the annual frequency of exceedance (AEP) for MCE acceleration as about 0.00008 (return period of about 12,500 years). (*WAPDA (2004)* [87])

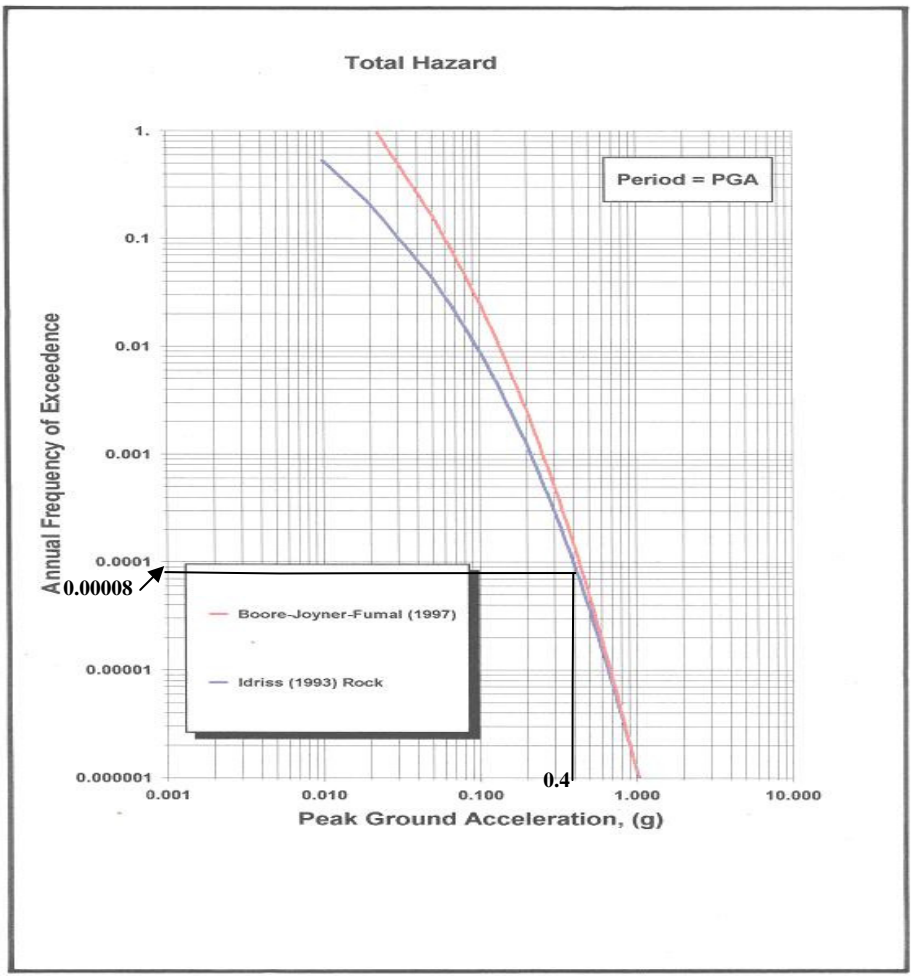

Figure 2.3: Total hazard curve for peak ground acceleration [87]

Following shows the computation of AEP (P_e) for MCE,

$$P_e = 1 - \left(1 - \frac{1}{T}\right)^n \qquad (2.2)$$

Here,

T =12500 years

n =1 year (as annual probability required)

So, $$P_e = 1 - \left(1 - \frac{1}{12500}\right) = 8.0 \text{ E-5}$$

This annual exceedance probability (AEP) for MCE has been used in this probability analysis.

2.4 EVENT TREE ANALYSIS (ETA)

All selected failure scenarios have been analyzed with event trees. Event tree analysis (ETA) is one of the techniques available to the engineer for conducting a reliability or safety analysis of a dam. An event tree is constructed to provide specific qualitative and quantitative information about a system, in particular its vulnerability and reliability. This method is used to identify the possible outcomes and their probabilities of occurrence due to an initiating event. Event trees provide a logical structure within which a variety of considerations of concern about a particular dam can be taken. Problems are decomposed into small parts and then joined together. The basic question addressed in ETA analysis is, 'what happens if…', e.g. what happens if there is an extremely high flood. (*Hartford and Baecher (2004)* [34])

2.4.1 Elements of Event Trees

The construction of an event tree is from left to right and begins with an initiating event. The elements of an event tree can be considered to be the components of the lines of reasoning from the initiating event to different consequences. In figure 2.4, the arrangement of different elements of an event tree has been given. (*Hartford and Baecher (2004)* [34])

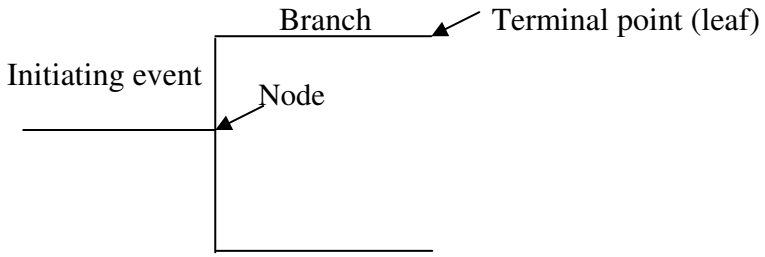

Figure 2.4: Elements of an event tree [34]

Initiating Event

An event tree begins with a defined initiating event. This event can be a natural hazard, such as extreme flood or a strong earthquake, or an internal failure of the system. As mentioned in previous sections, two initiating events for this study have been considered, maximum design flood (MDF) and maximum credible earthquake (MCE).

Branches

The branches of an event tree are simple graphic links through the sequence of system states to the terminal point as shown in figure 2.4. Each branch is unique and all branches have at least one common element, the initiating event.

Nodes

The nodes of an event tree depict the transitions from one system state to one or more new states. Typically, event tree structures are binary, success/failure, yes/no. Nodes could also show multiple outcomes such as 100%, 80%, 50%, 30%, and 0% of functional capability of the system. In this study, event trees have been developed as binary structures.

Terminal Points (leaves)

The terminal point is simply the end of a branch which shows a particular consequence or outcome, depending on all the preceding events/system states.

2.4.2 System States

Once the initiating event is defined, the response of the considered system is determined and success and failure states are carefully defined. The system states are logically ordered for a particular system depending on the expected response of system due to an initiating event.

2.4.3 Probability Computation in Event Trees

For computing the probability of outcomes in event trees, following steps should be taken into account.

1) Determination of Probability for Initiating Events

Probability for the initiating events is determined from the available data and information of the system under consideration (Mangla dam in this study). As discussed in section 2.3, annual exceedance probabilities for Mangla dam have been determined for two selected initiating events, maximum design flood (MDF) and maximum credible earthquake (MCE).

2) Assigning the Conditional Probabilities for Different System States

The conditional probabilities for different system states are predicted on the basis of available data. Generally, the conditional probabilities are judgmental probabilities as there is no statistical basis on which to base them. Judgmental probabilities are a measure of the degree of confidence in the prediction of a particular outcome as determined by evidence (*Hartford (1998)* [35]), (*Foster and Fell (1999)* [29]). Guidelines and methods for the estimation of judgmental probabilities are given by (*Vick (1992)* [72]) and (*Hartford (1998)* [35]). Different mapping schemes which relate verbal descriptors of likelihood to quantitative probabilities have been suggested for assigning conditional probabilities in event trees by (*Canadian Standard Association (1993)* [16]), (*Johansen et al. (1997)* [39]), (*Vick (1992)* [72]) and (*Whitman (1984)* [89]). In table 2.1, a mapping scheme suggested by (*Vick (1992)* [72]) and (*Foster and Fell (1999)* [29]) is shown. There is a degree of subjectivity in these assessments but the estimates should be best estimates, not biased towards the conservative (*Foster and Fell (1999)* [29]).

Table 2.1: Mapping scheme based on [29] and [72]

Verbal descriptor		**Probability**
Event is virtually certain	0.9-0.99	0.99
Event is very likely	0.5-0.9	0.9
Event is likely	0.1-0.5	0.5
Event is very unlikely	0.01-0.1	0.1
Event is virtually impossible or extremely unlikely	< 0.01	0.01

For some conditional probabilities, it may be justifiable to assign even lower probabilities than those indicated by table 2.1 (*Foster and Fell (1999)* [29]). Higher probabilities should be assigned where there are several important 'higher likelihood' factors (*Foster and Fell (1999)* [29]). In this study, the assigned conditional probabilities in event trees base not only on the above mentioned guidelines but also on self- judgment. Depending on the available factors for the estimation of conditional probabilities in different failure scenarios, the probability thresholds have also been interpolated accordingly as shown in table 2.1. For example, the probability limit for 'event is not likely' is not directly mentioned in table 2.1 so it will be considered between 0.1-0.5.

3) Calculation on Event Trees

The calculation process in event trees is straightforward. It is simple multiplication of branch probabilities along any path that yields the probability related to that terminal point. The addition of different path probabilities leading to failure would give the total failure probability of the system due to a particular initiating event. In the same manner, the sum of the total failure probabilities for different initiating events would give the overall failure probability of the system under consideration. (*Fell et al. (2000)* [28]), (*Hartford and Baecher (2004)* [34])

4) Computational Check for Event Trees

Following two checks are mainly applied to event trees.

- The sum of the conditional probabilities of sibling branches should be equal to 1.0.

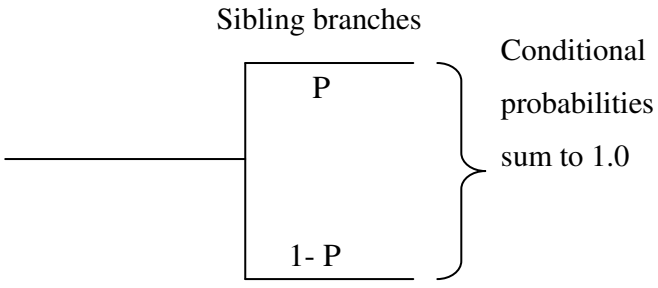

Figure 2.5: 1st Computational check for event trees [34]

- The sum of the path probabilities for a particular initiating event should be equal to the probability of the initiating event. (figure 2.6)

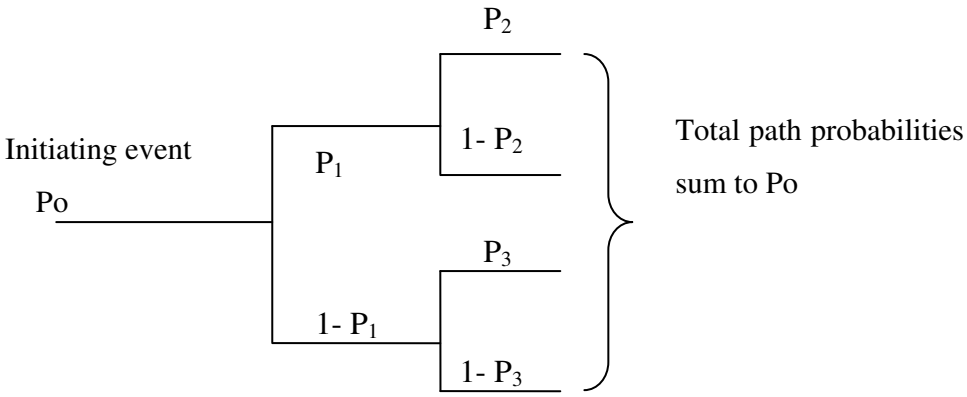

Figure 2.6: 2nd Computational check for event trees [34]

$$P_0.P_1.P_2 + P_0.P_1.(1- P_2) + P_0.(1-P_1).P_3 + P_0.(1-P_1).(1- P_3) = P_0$$

$$P_0 = P_0$$

2.5 PROBABILITY ANALYSIS FOR MANGLA DAM

This section emphasizes the probability analysis for Mangla dam with respect to different selected failure scenarios. As already mentioned, all selected failure scenarios have been analyzed with event trees. In the following, for the selected failure scenarios different factors affecting the construction of event trees (specific for each failure scenario) have been discussed separately.

2.5.1 Overtopping Failure of Main Dam (by MDF)

Basics

In this scenario overtopping failure of main dam (Mangla) has been analyzed due to the occurrence of maximum design flood (MDF) at maximum conservation level (378.66 m asl). In this probability analysis, the recently estimated MDF value of 61,977 m^3/s with 72-hrs inflow volume of about 7.11 E+9 m^3 (table 1.1) has been considered (*WAPDA (2003)* [86]). Figure 2.7 shows the overtopping failure of an embankment dam.

.

Figure 2.7: Overtopping failure of an embankment dam [36]

Reservoir Level and Outflow at MDF

After the raising of Mangla dam, the main dam height and crest elevation will be about 125 m (above riverbed) and 385.37 m asl respectively (table 1.1). According to the available research studies, the estimated reservoir level at maximum design flood (61,977 m^3/s) will be about 384.15 m asl (1260 ft) (table 1.1). The estimated peak discharge of outflow hydrograph at MDF will be about 36,309 m^3/s through all outlets (*WAPDA (2003)* [86]).

Available Outlets

The available outlets of Mangla dam have been discussed in section 1.3.2 and shown in figure 1.3. The original design capacity of the main spillway (figure 1.4) is about 28,583 m^3/s (table 1.1). For the safe functioning of the main spillway, the maximum discharge capacity in raised condition would remain the same as its original design capacity. This would be done by raising the orifice floor by 5 ft to restrict the opening area of each gate. (*WAPDA (2004)* [78])

The design capacity of the emergency spillway (figure 1.3) is about 6,452 m^3/s (table 1.1). The existing spillway structure has a control weir, chute and bucket. The maximum discharge capacity of the emergency spillway will almost remain the same after the raising of the dam. Currently only the main spillway is in operation. There are many establishments existing in the escape channel (BARA KAS) which is about 4 km long and spillway operation could pose severe risks. Figure 2.8 shows existing establishments in the escape channel area (BARA KAS). (*WAPDA (2001)* [80])

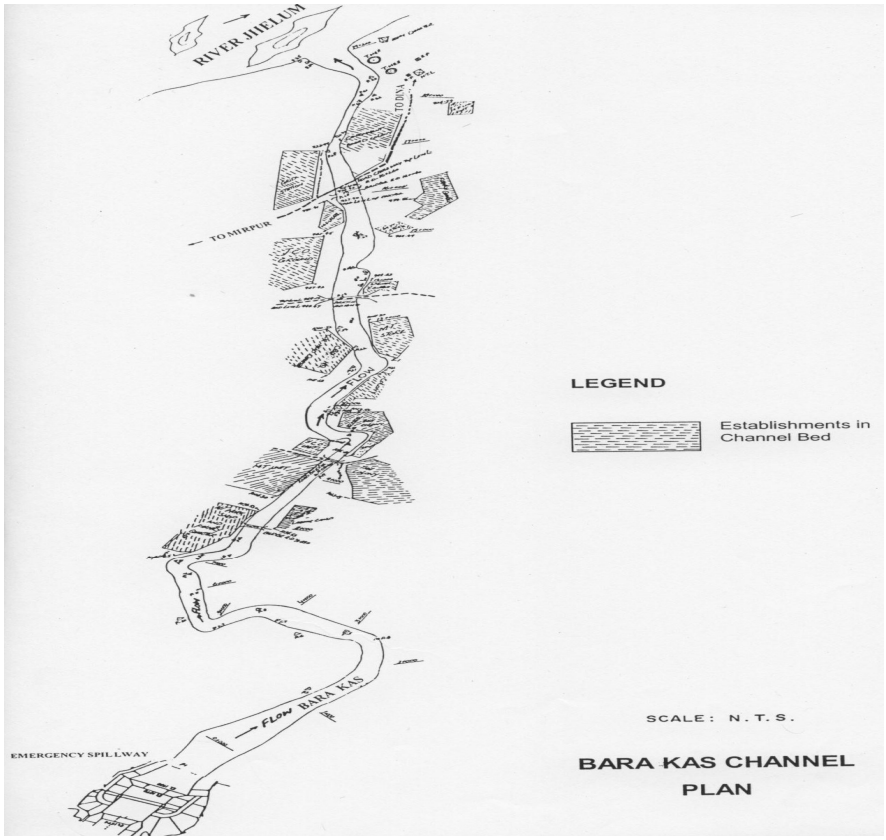

Figure 2.8: BARA KAS Channel with establishments [80]

The total worth and replacement cost of these establishments are quite high. An alternate emergency spillway at Bhangla ridge along the south western periphery of Mangla reservoir was also planned but not recommended due to a very high cost factor (higher than the worth and replacement cost of establishments) and serious environmental impacts. Finally, it was suggested to ensure the availability of the existing emergency spillway at the time of need. This can only be done by removing establishments from the tail channel (*WAPDA (2001)* [80]). For this probability analysis, emergency spillway has also been considered in operation. However, it is strongly urged to make the emergency spillway available in the near future by removing the establishments in order to avoid any uncertain situation.

Comparison of Spillway Capacities with Maximum Design Flood (MDF)

Both spillways have been considered in operation with the raised dam. According to the available studies (*WAPDA (2003)* [86]) the estimated peak discharge of outflow hydrograph at MDF will be about 36,309 m^3/s (table 1.1) through all outlets with the maximum flood level of 384.15 m asl (adopted design flood level). The maximum part of the peak outflow at MDF will be through the spillways (peak Q: 35,035 m^3/s) (table 1.1) and the rest will be through tunnels for other purposes (*WAPDA (2003)* [86]).

Estimation of Conditional Probabilities for Overtopping Failure of Main Dam

The conditional probabilities have been estimated for considered system states of an event tree for an overtopping failure of main dam by MDF. Different relevant factors have been taken into account.

Rise in reservoir level up to dam crest: According to available studies (*WAPDA (2003)* [86]) at MDF level (384.15 m asl) both spillways can cope with the estimated peak outflow by passing through its maximum amount (35,035 m^3/s). A freeboard of about 1.22 m is available at MDF level (384.15 m asl) with respect to the dam crest level (385.37 m asl). In order to compare it with the required freeboard, the estimated maximum probable wave run-up and wind setup (~ 1.51 m) at MDF level (384.15 m asl) by (*WAPDA (2004)* [82]) have been considered. With the addition of proper safety margin the required freeboard will be obviously quite higher than the available freeboard. However, the available freeboard of about 1.22 m is very close to the minimum limits (at least 1 m or not less than 3 ft) specified by (*CBCWSEP* [15]), (*DVWK (1997)* [25]) and (*NAC* [49]). Further at MDF level the surcharge storage above maximum conservation level has been estimated as about 1.85 E+9 m^3 by (*WAPDA (2003)* [86]). This estimated surcharge storage at MDF level is within the provision made in the design of dam, 2.23 E+9 m^3 (*WAPDA (2001)* [81]). The dam authorities in Pakistan also claim that this MDF level (384.15 m asl) or slightly lower level can be retained by pre-releases of the reservoir according to standing operating procedures (SOPs) which are based on qualitative and quantitative forecast (*Ehsan (2005)* [26]), (*WAPDA (2003)* [86]). Depending on different factors discussed above, it is concluded that the rise in reservoir level up to crest level for overtopping of the main dam is not likely to occur. As in table 2.1 there is no direct threshold available for 'event is not likely'. So in this case an interpolated probability value of *0.25* has been predicted for this system state by considering all factors and the available thresholds in table 2.1.

Main dam failure by overtopping: If reservoir level rises up to dam crest then there could be different possibilities of overtopping. For this system state following three cases of overtopping have been considered for the estimation of conditional probability.

- overtopping by only few centimeters and dam remains intact
- overtopping by a small water wave and dam still remains intact
- overtopping by a huge water wave and dam fails

The mangla reservoir would contain very big volume of water at dam crest level. At that stage a rapid increase in water level above dam crest due to high winds or heavy rainfall is also possible to happen. Because the catchment of Jhelum river above Mangla falls within the region of active monsoon and the probable period of MDF occurrence is also considered to be in monsoon season (*WAPDA (2001)* [81]). Then the possibility of the occurrence of a huge water wave is more as compared to other two cases of overtopping. The first overtopping case is considered to be extremely unlikely and a conditional probability of 0.01 (table 2.1) is assigned. The second case of overtopping is believed to be very unlikely and a conditional probability of 0.1 is given. Further the overtopping failure by a huge water wave is assumed to be likely as compared to the other cases. The conditional probability of 0.4 has been selected for this overtopping case by interpolating the available thresholds in table 2.1. Finally the conditional probability for this system state will be the sum of the assigned probabilities for three cases, (0.01+0.1+0.4) *0.51*.

No rise in reservoir level up to dam crest and dam failure: When there is no rise in reservoir level up to dam crest then dam failure by overtopping is almost impossible to occur. At the same time there would also be a very low probability of other failures which can not be neglected. Due to MDF level (384.15 m asl) and low available freeboard (~ 1.22 m) there could be crest settlement or development of sinkholes. According to (*Foster and Fell (1999)* [29]), the crest settlement or sinkhole mechanism can occur due to low freeboard and relatively narrow crest. In this case, the dam crest is quite broad (about 12 m) but freeboard is not so high (very close to minimum limits). Depending on above discussion a very low conditional probability of *0.05* (interpolated value from table 2.1) is chosen for this system state in order to consider the very less possibility of such failure.

Event Tree for Overtopping Failure of Main Dam (by* MDF*)

Figure 2.9 describes this failure scenario in terms of an event tree which is based on the estimated conditional probabilities.

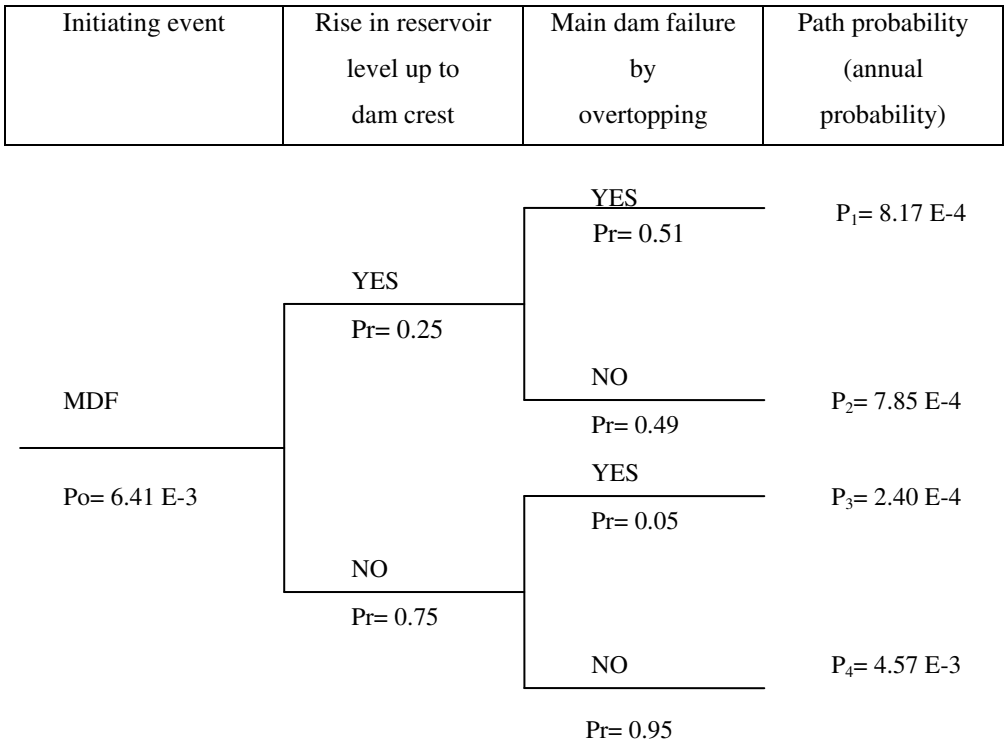

Figure 2.9: Event tree for overtopping failure of main dam by MDF

Check: Total path probability 'P' = $P_1+P_2+P_3+P_4$ = 6.41 E-3 = Po (OK)

Total annual failure probability = P_1+P_3 = 1.06 E-3

Total annual no failure probability = P_2+P_4 = 5.35 E-3

2.5.2 Geotechnical Strength Failure of Main Dam (by MDF)

Basics

In this failure scenario, the stability of the main dam has been analyzed against the geotechnical strength failure due to the occurrence of maximum design flood (MDF). The pore pressure in the dam core plays a very important role in this regard. High pore pressure in the dam core causes loss of geotechnical strength (*Hartford and Baecher (2004)* [34]). There are different modes of geotechnical strength failure, failure due to embankment cracking, slope failure, dam crest settlement etc. But in this scenario general meaning of geotechnical strength failure has been considered (depending on the available data) instead of specifying any typical failure mode. Here increase of the pore pressure ratio within the core has been judged as representative for various mechanisms of geotechnical dam failure. The failure probability analysis of the main dam core has been done for the raised dam, crest elevation of 385.37 m asl.

Pore Pressure in the Main Dam Core and Geotechnical Stability of Main Dam

The pore pressure ratio, 'r_u' is the ratio of the pore water pressure (u) to the vertical overburden pressure (σ_v) at a given point in a body of soil (dam core in this case) [91].

$$r_u = \frac{u}{\sigma_v} \tag{2.3}$$

The main dam core is of rolled clay surrounded by rolled sand stone and gravel fill at upstream of dam. A pore pressure ratio (r_u) of 0.5 was adopted for the existing dam on the basis of all pore pressure readings in 1967. For main dam, it has been observed that comparatively high pore pressure developed in clay because of its low coefficient of consolidation and that the load of the reservoir as well as that of the fill contributed to the pressure. In 1998, records showed decrease in the pore pressure ratio (r_u), 0.4 or less in the bottom half and 0.3 or less in the top half of core at maximum reservoir operating level. However, this reduction in the pore pressure of the existing core is due to the considerable dissipation of extra pressure and consolidation that occurred during the past years of operation. According to available studies, the pore pressure ratio (r_u) in the newly raised part of the main dam core is assumed to be not more than 0.3. (*WAPDA (2001)* [83]), (*WAPDA (2004)* [82])

Moreover, the results of slope stability analysis by (*WAPDA (2004)* [82]) and (*WAPDA (2001)* [83]) show the stability of the existing upstream and downstream slope of the main dam. The static stability analysis of the main dam locations by (*WAPDA (2004)* [82]) also gives acceptable factors of safety. Further the expected crest settlement at deepest sections of the raised main dam has been estimated to be quite low (~ 0.46 m) (*WAPDA (2004)* [82]). The above discussion confirms the geotechnical stability of the main dam.

Estimation of Conditional Probabilities for Geotechnical Failure of Main Dam

The conditional probabilities for considered system states of an event tree for the geotechnical strength failure of main dam by MDF have been judged by taking into account the available geotechnical information.

<u>*Considerable rise in pore pressure of the main dam core*</u>: Dam raising would certainly increase the pore pressure in the dam core due to following factors,

- additional fill load (9.15 m raising)
- water load (as the reservoir level rises)

The additional fill load will not make any significant contribution to pore pressure in existing core as raising is only 7.3% (9.15 m) of the total main dam height, 125 m (above riverbed after raising). Moreover, the water load for maintaining maximum conservation level, 378.66 m asl is also not expected to cause unexpected increase in pore pressures. As in past years of dam operation, pore pressure in the dam core has decreased due to consolidation and pressure dissipation. As a result of consolidation the response to additional load will be lower than previous load increments (*WAPDA (2001)* [83]). So at maximum conservation level (378.66 m asl) with raised conditions, pore pressure in the main dam core is expected to be small. Due to MDF occurrence, the reservoir level would increase to 384.15 m asl (*WAPDA (2003)* [86]). The pore pressure would certainly be higher than the pore pressure at maximum conservation level due to additional water loading of MDF. The change in reservoir level at MDF is about 5.49 m with respect to the maximum conservation level (378.66 m asl) which is not so high to cause unexpected rise in pore pressure of the main dam core. However, the increase in pore pressure at MDF would cause some reduction in the strength of fill. Keeping in view all conditions discussed above, an unexpected increase in pore pressure of the main dam core at MDF level (384.15 m asl) is not likely to occur. Depending on the qualitative description of the likelihood a conditional probability of *0.25* is proposed for this system state by interpolating the available thresholds in table 2.1.

Geotechnical strength failure of the main dam: If there is considerable increase in pore pressure of the main dam. Then there could be different possibilities of a geotechnical strength failure. As discussed above, the pore pressure plays an important role in maintaining the strength of dam fill. Due to unexpected rise in pore pressure the dam fill can lose its strength and cracking, sliding or slope failure of the dam may occur. So in case of considerable rise in pore pressure of dam fill the geotechnical strength failure is likely to occur. For this system state a conditional probability of *0.5* has been selected by the available thresholds in table 2.1.

No considerable rise in pore pressure of the main dam and dam failure: When there is no considerable rise in pore pressure of the main dam then the geotechnical strength failure (cracking, sliding or slope failure) is also not possible to occur. But there could always be a very low probability of dam failure due to other reasons. The dam failure may occur due to

excessive seepage, internal erosion or piping etc. A very low probability of *0.05* is assigned to this system state by interpolating the available thresholds in table 2.1.

Event Tree for the Geotechnical Strength Failure of Main Dam (by* MDF*)

Figure 2.10 shows an event tree which represents quantitatively the likelihood of geotechnical strength failure of the main dam due to MDF occurrence.

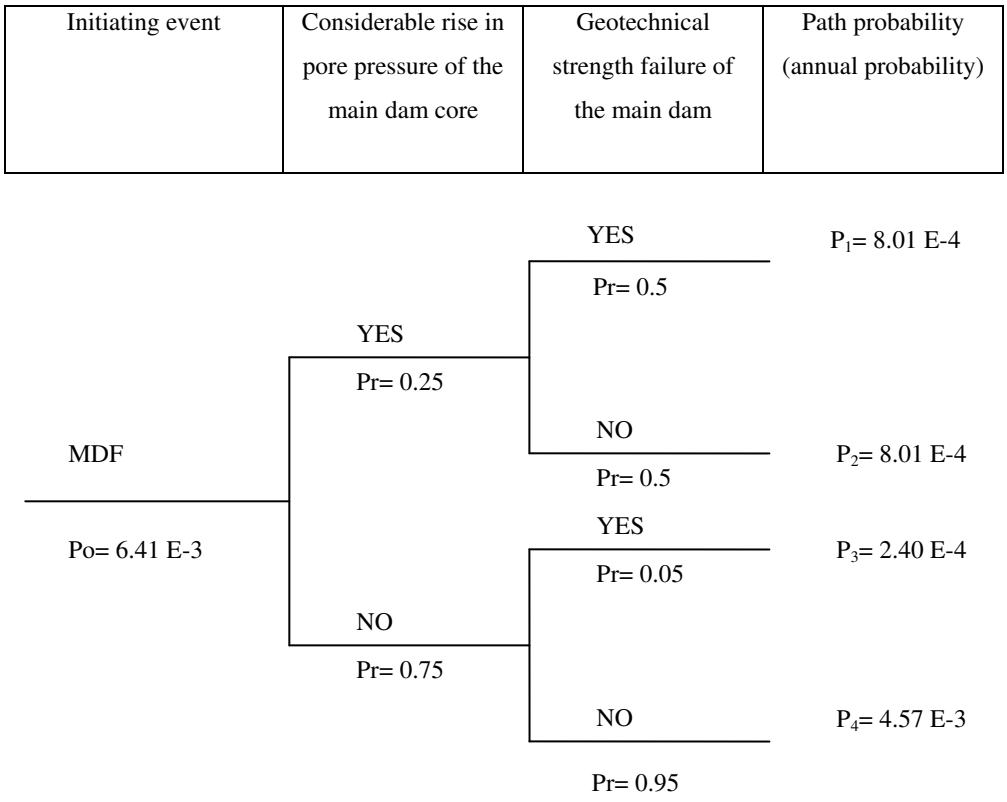

Figure 2.10: Event tree for the geotechnical strength failure of main dam by MDF

Check: Total path probability 'P' = $P_1+P_2+P_3+P_4$ = 6.41 E-3 = Po (OK)

Total annual failure probability = P_1+P_3 = 1.04 E-3

Total annual no failure probability = P_2+P_4 = 5.37 E-3

2.5.3 Main Dam Failure by Liquefaction in Fill (by MCE)

Basics

In this scenario, main dam failure by liquefaction in fill due to the maximum credible earthquake (MCE) has been analyzed. Seismic liquefaction refers to a sudden loss in stiffness

and strength of soil as a result of cyclic loading of an earthquake (*Seid-Karbasi and Byrne (2004)* [64]).

Liquefaction in Fill

Liquefaction of fill in the dam can occur due to large drop in stiffness and strength of soil due to seismic movements (*Byrne and Seid-Karbasi (2003)* [14]), (*Dahms (2004)* [19]). This loss in strength results from a tendency of soils to contract under cyclic loading and if such contraction is prevented or restricted by the presence of water in the pores that can not escape, then it causes increase in pore water pressure and reduction in effective stress. If the effective stress drops to zero, 100 % pore pressure rise, the strength and stiffness also drop to zero and soil behaves like a heavy liquid (*Seid-Karbasi and Byrne (2004)* [64]). As a result of liquefaction in fill part of a dam may slump and slide off the structure that could cause total failure of the dam as shown in figure 2.11.

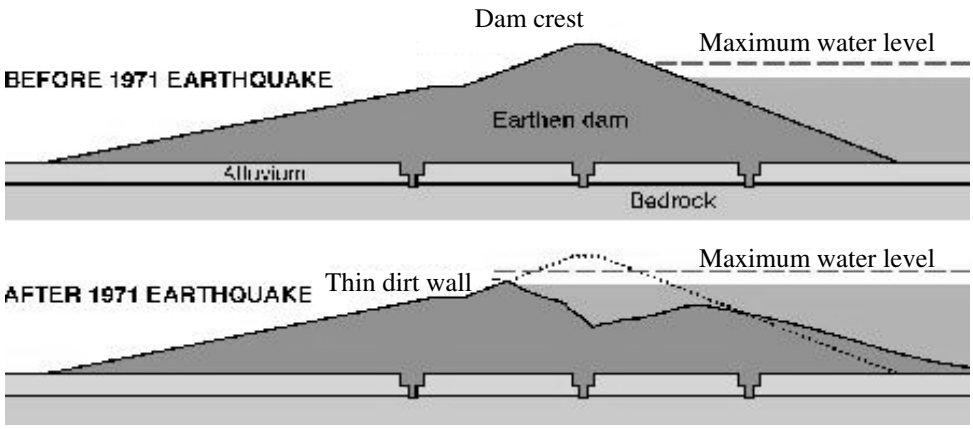

Figure 2.11: Liquefaction failure of an earth dam [19]

The severeness of liquefaction in fill depends on the magnitude of the earthquake which causes rapid increase in pore pressure with extreme loss in strength of fill. For Mangla dam, it is quite clear that the maximum credible earthquake (MCE) is the largest conceivable event that could occur in the tectonic environment in which the project is located (*WAPDA (2004)* [87]). MCE is also expected to be an extreme event with respect to the recommended value of peak horizontal ground acceleration of 0.40g, which is more than three times the original design value, 0.11g.

Estimation of Conditional Probabilities for Liquefaction Failure in Fill of Main Dam

The conditional probabilities for considered system states of an event tree for the liquefaction failure of main dam by MCE have been assessed by considering the available information and other factors.

Rapid increase in pore pressure: Pore pressure plays a vital role in the occurrence of liquefaction in fill. For Mangla dam, the main dam core being the central part with fill load on both sides plays a prominent role in the development of pore pressure in the main dam fill. During the past years of Mangla dam operation, pore pressure in the existing core has reduced (less than design value) due to consolidation and dissipation of pore pressure (*WAPDA (2001)* [83]). At maximum conservation level (378.66 m asl) with raised conditions, pore pressure in the main dam core is expected to be normal (as mentioned in section 2.5.2). In the available studies, dynamic deformation analysis of the main dam for MCE has been carried out for normal drawdown and steady seepage conditions by Newmark's method (*WAPDA (2004)* [82]). It has been concluded that the deformations under MCE are within safe limits. But the weak point is the assumption made for this deformation analysis which is not realistic at all. It was assumed that the pore pressure will not change and there will not be any loss of strength during an earthquake (*WAPDA (2004)* [82]). So the impact of MCE can not be underestimated. Because MCE loading is expected to be extremely high, the possibility of sudden increase in pore pressure of the main dam core is relatively high. Keeping in view all factors, a conditional probability of *0.7* has been selected for this system state by interpolating the available thresholds in table 2.1.

Main dam failure by liquefaction in fill: Due to a rapid increase in pore pressure a huge loss in strength and stiffness of the fill material can occur (*Byrne and Seid-Karbasi (2003)* [14]), (*Dahms (2004)* [19]). This loss in strength of fill can finally result into a liquefaction failure by slumping and sliding. Depending on the high magnitude of peak horizontal ground acceleration, 0.40g (more than three times the original design value, 0.11g) and very high likelihood of rapid increase in pore pressure of fill at MCE, the liquefaction in fill is more than likely to occur. So a very high conditional probability of *0.85* for this system state has been judged by considering the relevant factors and interpolating the related thresholds in table 2.1.

No rapid increase in pore pressure and dam failure: If pore pressure in the main dam does not increase rapidly at MCE then the dam failure by liquefaction in fill is not possible to occur. The impact of MCE loading is considered to be higher than MDF loading. So there is a possibility of dam failure due to other reasons like failure of main spillway or other dam components. But in this system state the likelihood of such failure at MCE is very unlikely. Considering all possible factors and thresholds in table 2.1, a conditional probability of *0.1* has been chosen for this system state.

Event Tree for Main Dam Failure due to Liquefaction in Fill (by* MCE*)

Based on the estimated conditional probabilities for liquefaction failure of the main dam, figure 2.12 shows the related event tree.

Initiating event	Rapid increase in pore pressure	Main dam failure by liquefaction in fill	Path probability (annual probability)

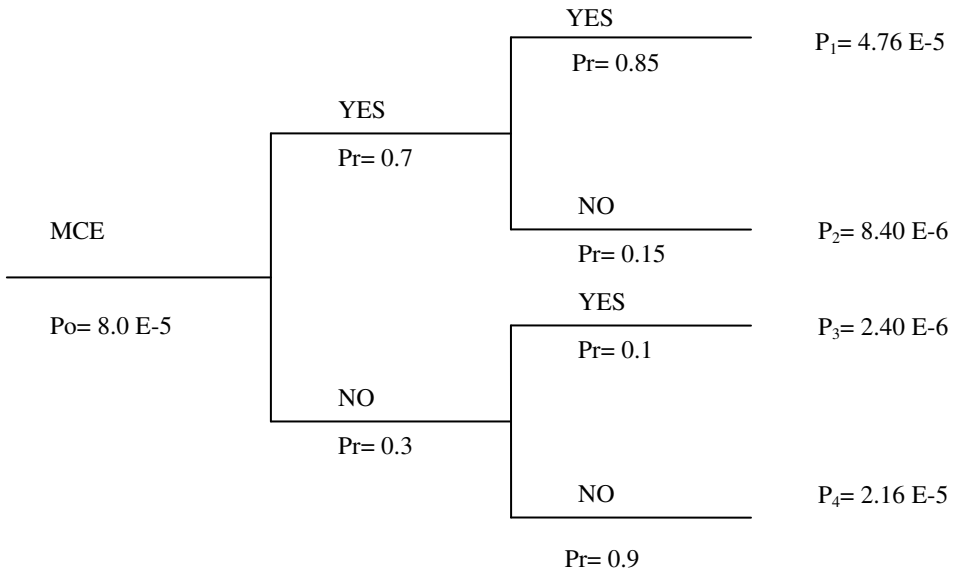

Figure 2.12: Event tree for main dam failure due to liquefaction in fill by MCE

Check: Total path probability 'P' = $P_1+P_2+P_3+P_4$ = 8.0 E-5 = Po (OK)

Total annual failure probability = P_1+P_3 = 5.0 E-5

Total annual no failure probability = P_2+P_4 = 3.0 E-5

2.5.4 Structural Failure of Main Spillway (by MDF)

Basics

The dam failure may occur due to the structural failure of dam components. The structural failure can result in a significant release of the reservoir and may eventually cause a dam breach with total release of the reservoir (*Dam Safety Inspection Manual (2003)* [20]). In this failure scenario, Mangla dam failure due to the structural failure of the main spillway (figure 1.4) has been focused. For the probability analysis, the overall structural stability of the main spillway due to the occurrence of maximum probable flood (MDF) has been analyzed. Figure 2.13 shows the gated structure and abutments of the main spillway. (*WAPDA (2004)* [78]), (*WAPDA (2001)* [84])

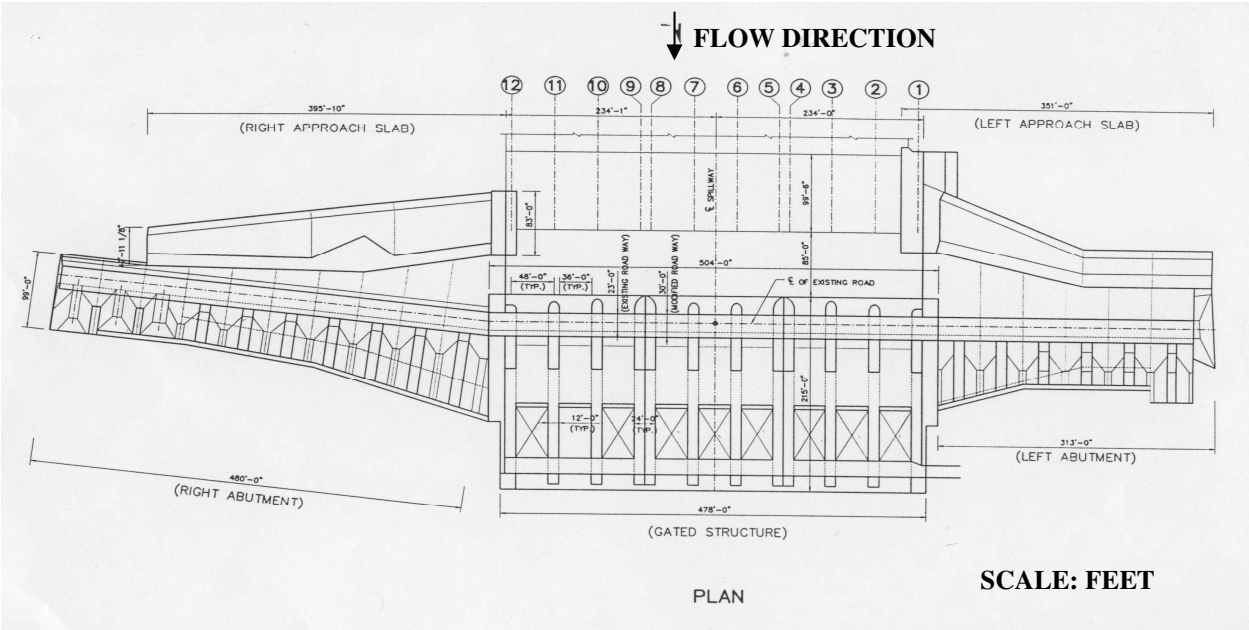

Figure 2.13: Plan of main spillway structure [84]

The main spillway was originally designed with the provision of the future dam raising by 12.195 m (40 ft). In this case, the main spillway has been considered with 9.15 m (30 ft) dam raising (detail in section 1.3). The main spillway would have its maximum discharge capacity at MDF level (reservoir level of 384.15 m asl) (*WAPDA (2004)* [78]), (*WAPDA (2003)* [86]). Following sections emphasize the stability of different parts of the main spillway against structural failure based on the available stability criteria. The right and left abutments of the main spillway have been shown separately in figure 2.14 and figure 2.15.

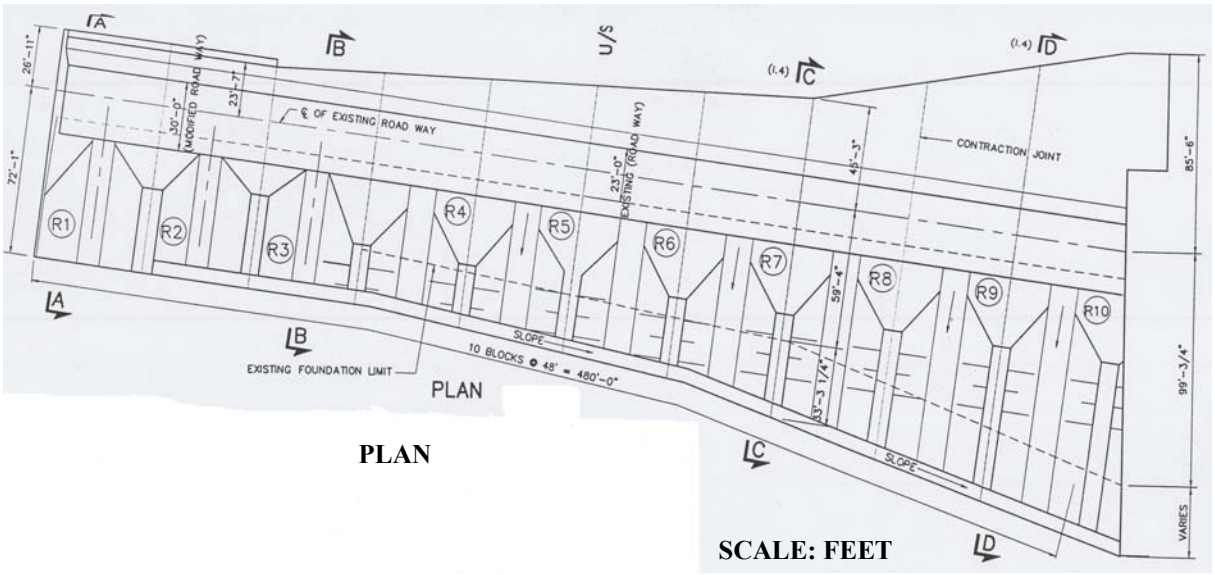

Figure 2.14: Right abutments of main spillway [84]

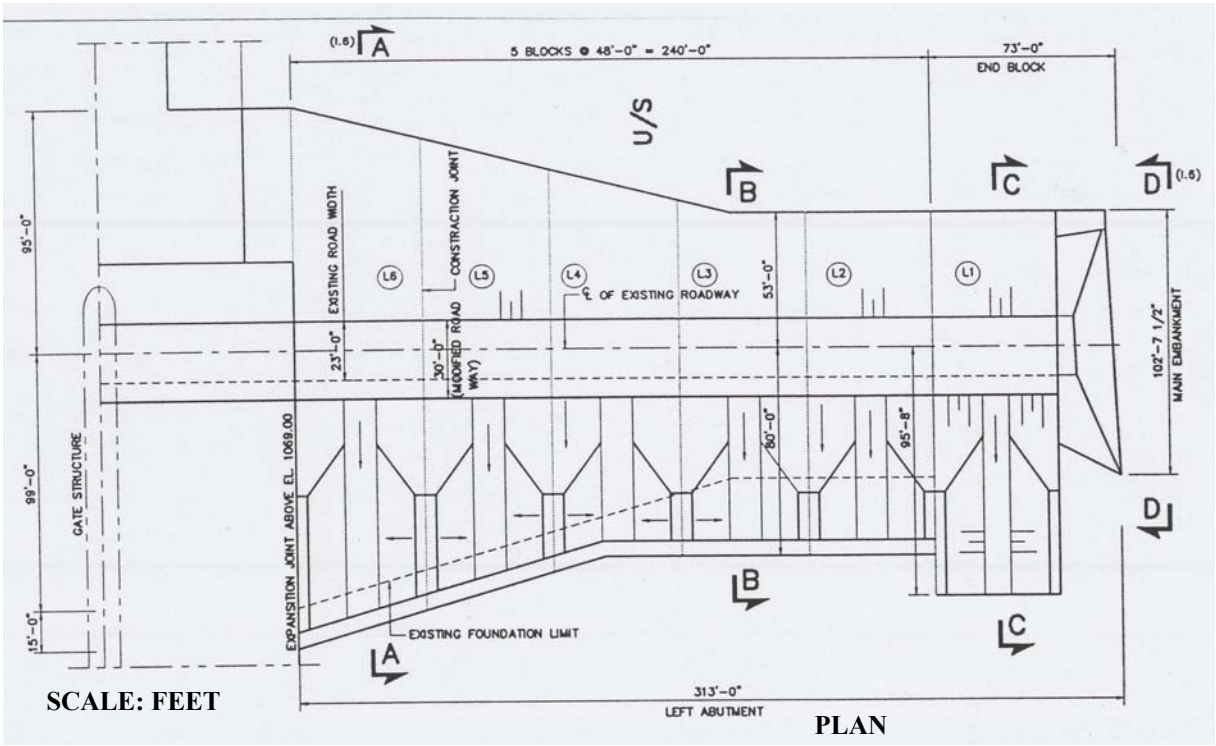

Figure 2.15: Left abutments of main spillway [84]

Estimation of Conditional Probabilities for Structural Failure of Main Spillway

The conditional probabilities for considered system states of an event tree for the structural failure of the main spillway by MDF have been judged by taking into account relevant factors.

Structural failure of the main spillway: The results of structural stability analysis with respect to the raised conditions and updated design criteria for different parts of the main spillway under different loadings including MDF are already available in the literature of Mangla dam. The structural stability of the main spillway has been analyzed against two modes of structural failure, sliding and overturning. The overall structural stability of the main spillway can only be ensured by safety against different modes of structural failure. In order to estimate the likelihood of structural failure, available results of stability analysis for the main parts of the main spillway with raised conditions have been taken into consideration.

In table 2.2, the available stability results for MDF loading have been shown. According to updated design criteria, for MDF loading the factor of safety against sliding should be greater than 1.0 and the allowable foundation pressure is 1273.62 N/m^2 (26.6 lb/ft^2). The foundation bearing pressure mainly contributes to an overturning failure. (*WAPDA (2004)* [78])

Table 2.2: Available results of stability analysis for MDF loading of main spillway [78]

Analyzed sections (figs. 2.13, 2.14 and 2.15)	Estimated factor of safety against sliding	Max. foundation bearing pressure (N/m^2)
Central gated monolith	2	699.53
L3	1.87	504.66
L4	1.95	592.76
L5	1.97	662.18
L6	2.02	757.94
R4	1.78	424.70
R5	1.73	424.22
R6	1.77	439.10
R7	1.84	418
R8	1.88	472.10
R9	2.07	824
R10	2.23	845.60

The results are well within the allowable limits for all analyzed sections. The factor of safety against sliding for all analyzed sections is considerably greater than 1.0. The maximum foundation bearing pressures are also well below the allowable foundation pressure. The results show the overall structural stability of the main spillway against MDF loading. Based

on available stability results, it is clear that at MDF loading the structural failure of the main spillway is very much unlikely to occur. Keeping in view all factors and interpolating the related thresholds in table 2.1, a very low probability of *0.05* has been assigned to this system state.

Ultimate dam failure: The structural failure of the main spillway at MDF loading will definitely affect the whole dam. As the main spillway is one of the most important components of the dam. Its structural failure can release a large amount of water from the reservoir and finally it can breach the dam structure by total release of the reservoir (*Dam Safety Inspection Manual (2003)* [20]). The ultimate dam failure due to the structural failure of the main spillway is likely to occur at MDF loading. For this system state a conditional probability of *0.5* has been estimated by using the guidelines in table 2.1.

No structural failure of the main spillway and ultimate dam failure: If there is no structural failure of the main spillway at MDF loading then the ultimate dam failure is not possible to occur. But at the same time there is always a possibility of other types of dam failure. At MDF loading the dam failure can occur due to crest settlement/sinkholes, piping, internal erosion and other geotechnical reasons. But the probability of such failure is considered to be very low. So a conditional probability of *0.05* has been chosen for this system state by interpolating the related thresholds in table 2.1.

Event Tree for the Structural Failure of Main Spillway (by* MDF*)

Figure 2.16 shows an event tree which gives the failure probability for this scenario according to the estimated conditional probabilities for considered system states.

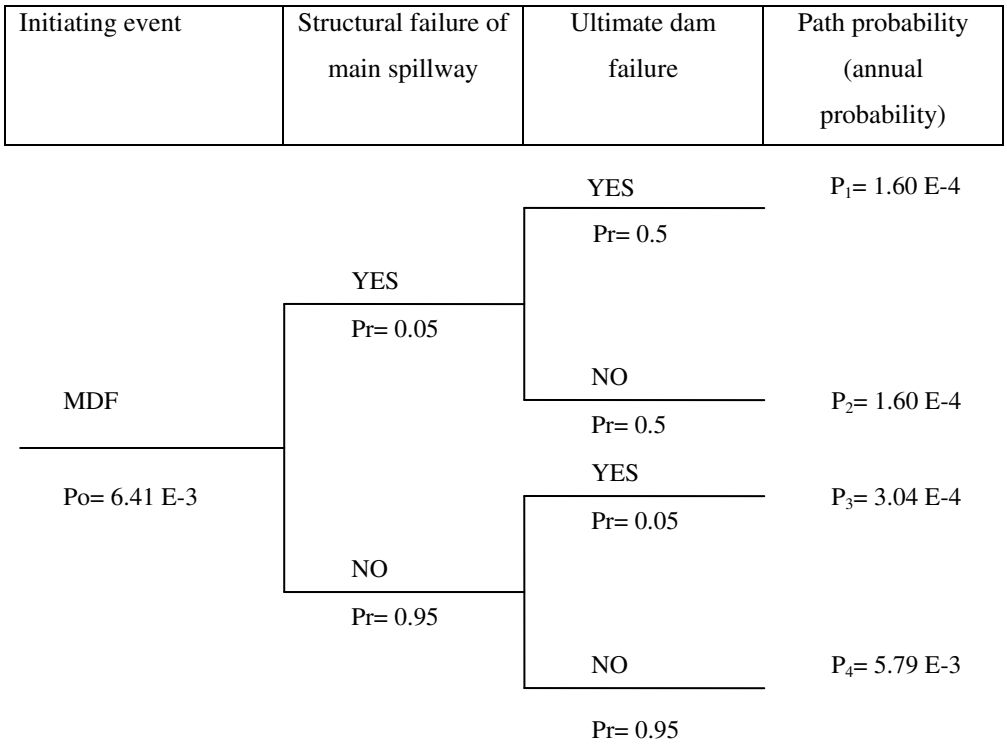

Figure 2.16: Event tree for the structural failure of main spillway by MDF

Check: Total path probability 'P' = $P_1+P_2+P_3+P_4$ = 6.41 E-3 = Po (OK)

Total annual failure probability = P_1+P_3 = 4.65 E-4

Total annual no failure probability = P_2+P_4 = 5.95 E-3

2.5.5 Structural Failure of Main Spillway (by MCE)

Basics

In this dam failure scenario the main spillway stability against structural failure due to the occurrence of maximum credible earthquake (MCE) at maximum conservation level has been analyzed. The main spillway structure with raised conditions and concepts of structural stability analysis have already been discussed in section 2.5.4. In the following, safety of the main spillway against structural failure due to MCE has been discussed.

Estimation of Conditional Probabilities for Structural Failure of Main Spillway

The conditional probabilities for considered system states of an event tree for the structural failure of the main spillway by MCE have been assessed by taking into consideration relevant factors.

Structural failure of the main spillway: In this case the available results of stability analysis for the gated and abutment monoliths have been considered. The results of stability analysis are available for MCE loading (0.40g) at maximum conservation level. According to the updated design criteria for MCE loading at maximum conservation level, factor of safety against sliding should be greater than 1.0. The occurring foundation pressure should be below the threshold value of 1273.62 N/m^2 (26.6 lb/ft^2) (the same as MDF loading) (*WAPDA (2004)* [78]). Depending on the available results, the values of foundation pressures (mainly contributing to an overturning failure) and factor of safety against sliding for MCE have been compared with the stability standards. Table 2.3 shows the available stability results for MCE loading (0.40g) at maximum conservation level.

Table 2.3: Available stability results for MCE loading (0.40g) of main spillway [78]

Analyzed sections (figs. 2.13, 2.14 and 2.15)	Estimated factor of safety against sliding	Max. foundation bearing pressure (N/m^2)
Central gated monolith	1.03	993.52
L3	1	774.70
L4	1.01	873.82
L5	1.04	948.99
L6	1.04	1077.78
R4	1	705.75
R5	1	722
R6	1	739.27
R7	1.01	721.10
R8	1.02	772.79
R9	1.05	1224.30
R10	1.07	1249.67

The estimated safety factors against sliding are almost equal to the minimum allowable value for all sections. However, this shows the stability against sliding. Further, the maximum foundation pressures are below the allowable pressure. Although for some sections they are close to the allowable value. The results show the overall structural stability of the main spillway at MCE but the impact of MCE loading for possible sliding failure should not be underestimated. As the MCE event is considered to be more severe than MDF. Depending on all factors, it is concluded that the structural failure of the main spillway due to MCE is very

unlikely to occur. Following the available thresholds in table 2.1, a conditional probability of *0.1* has been suggested for this system state.

Ultimate dam failure: Due to the structural failure of the main spillway at MCE the ultimate failure of the dam can also occur. A huge amount of water can release from the reservoir and eventually dam break could happen (*Dam Safety Inspection Manual (2003)* [20]). The overall impact of MCE loading is expected to be higher than MDF loading. So the ultimate failure of the dam due to structural failure of the main spillway is more than likely to occur. Considering all factors, a conditional probability of *0.6* has been estimated for this system state by interpolating the related thresholds in table 2.1.

No structural failure of the main spillway and ultimate dam failure: If the structural failure of the main spillway does not occur at MCE loading then the there is no likelihood of ultimate dam failure. But the likelihood of dam failure due to other reasons can not be ignored. At MCE loading the ultimate dam failure can occur due to geotechnical problems or failure of other dam components. However, the probability of such failure is expected to be very low. But the impact of MCE is considered to be more than MDF. So a conditional probability of *0.1* has been assigned to this system state by analyzing all factors and considering the guidelines in table 2.1.

Event tree for the Structural Failure of Main Spillway (by* MCE*)

Figure 2.17 describes this failure scenario in terms of an event tree and gives the failure probability in a quantitative manner by using the estimated conditional probabilities.

Initiating event	Structural failure of main spillway	Ultimate dam failure	Path probability (annual probability)

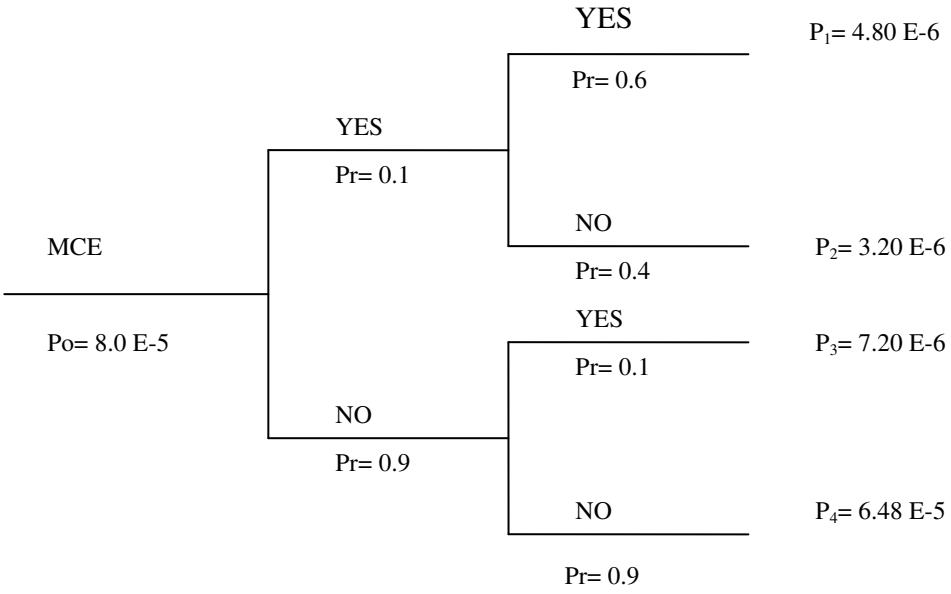

Figure 2.17: Event tree for the structural failure of main spillway by MCE

Check: Total path probability 'P' = $P_1+P_2+P_3+P_4$ = 8.0 E-5 = Po (OK)

Total annual failure probability = P_1+P_3 = 1.20 E-5

Total annual no failure probability = P_2+P_4 = 6.80 E-5

2.6 OVERALL ANNUAL FAILURE PROBABILITY FOR MANGLA DAM

The overall failure probability will be the sum of the total failure probabilities due to different initiating events for the selected failure scenarios. Following are the total annual failure probabilities from the event tree analyses of the selected failure scenarios: (table 2.4)

Table 2.4: Total annual failure probabilities

Considered failure scenarios	**Total annual failure probability (Pr)**
Overtopping failure of main dam (by MDF)	1.06 E-3
Geotechnical strength failure of main dam (by MDF)	1.04 E-3
Main dam failure by liquefaction in fill (by MCE)	5.00 E-5
Structural failure of main spillway (by MDF)	4.65 E-4
Structural failure of main spillway (by MCE)	1.20 E-5

Overall annual failure probability of Mangla dam

$$P_{overall} = P_{MDF} + P_{MCE} = 2.56\text{ E-}3 + 6.20\text{ E-}5$$

$$\mathbf{P_{overall} = 2.63\text{ E-}3}$$

The computed overall failure probability value is comparatively very high. There are no fixed universal standards available for an overall failure probability of a dam. However, different researchers have given different probability estimates. Table 2.5 shows a relation between verbal probability and an exact value (*Rettemeier et al. (2000)* [57]), (*Idel (1986)* [37]). Table 2.5 is different from table 2.1 because it gives the qualitative descriptions and quantitative values for the comparison of annual failure probabilities. On the other hand, table 2.1 provides verbal descriptors and thresholds for the estimation of conditional probabilities which are required in event trees.

Table 2.5: Probability of failure verbally and quantitative [37]

Verbal Probability	Quantitative Probability
Totally unlikely	$< 10^{-6}$
With a degree of probability verging on certainly unlikely	10^{-5}
Unlikely	10^{-4}
Not impossible	10^{-3}
Possible	10^{-2}
Likely	$1\text{-}10^{-1}$

According to probability limits shown in table 2.5, the overall failure probability of Mangla dam comes between 'Not impossible' and 'Possible'. The above probability values (table 2.5) are reasonable for having a good understanding of the computed failure probability.

2.7 SUMMARY

Based on the available data and information of Mangla dam, different possible dam failure scenarios have been taken into consideration. All considered failure scenarios have been analyzed qualitatively with event trees in order to compute the overall annual failure probability. According to the available standards, the computed overall failure probability of Mangla dam is quite high and it clearly justifies the need of further risk assessment study on Mangla dam.

3 NUMERICAL HYDRODYNAMIC MODELING

3.1 INTRODUCTION

In the previous chapter, the overall failure probability of Mangla dam has been computed by taking into account different possible failure scenarios. Because of comparatively high failure probability, further risk assessment study on Mangla dam has been carried out. This chapter describes the steps of numerical hydrodynamic modeling carried out for the Jhelum river valley downstream of Mangla dam. Figure 3.1 shows the top view of Mangla dam and its reservoir.

Figure 3.1: Top view of Mangla dam (by Google earth)

The project reach downstream of Mangla dam is about 329 km long with different hydraulic structures (figure 1.5). There are five tributaries between Mangla dam and Rasul barrage. No gauges exist at the tributaries. Only 25, 50 and 100 years peak discharge values are available. Figure 3.2 shows different available features for a part of Jhelum river valley in a closer view.

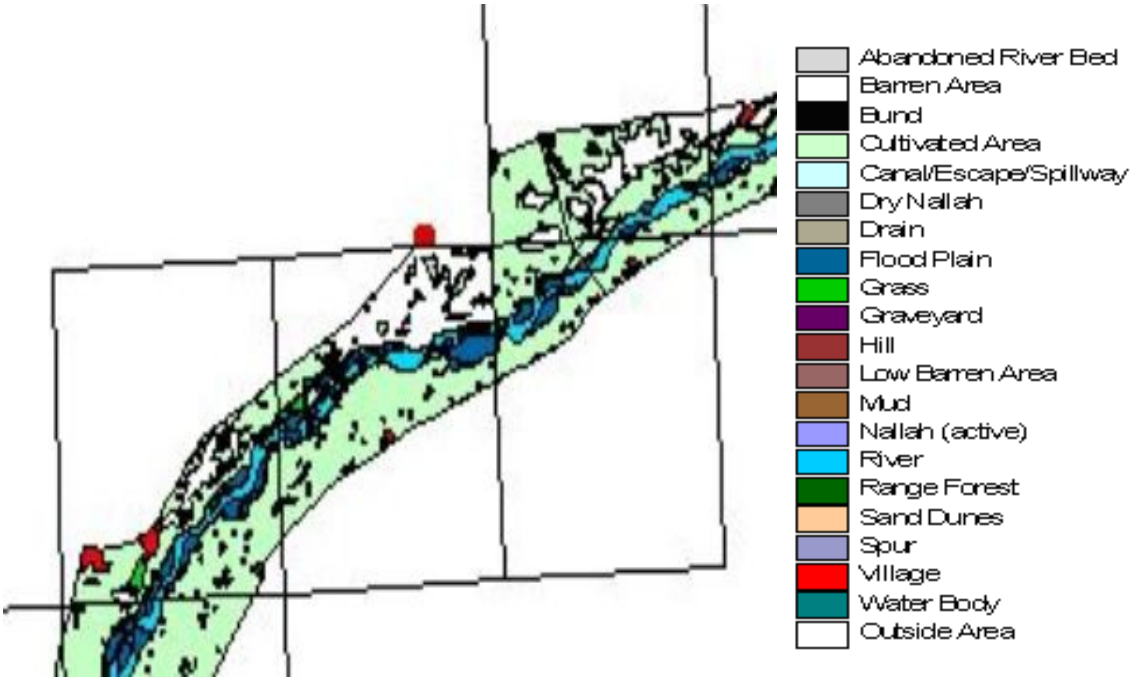

Figure 3.2: Available features of Jhelum river valley

3.2 1D-MODELING

According the available GIS and other official data one dimensional modeling for unsteady flow conditions has been carried out by using the model tool MIKE 11. The 1D-modeling approach has been chosen because of the following reasons.

- Very long river reach of 329 km
- Long distance between the available consecutive downstream cross-sections (average 4 km)
- No data available in between the cross-sections
- 2D and 3D modeling requires high computational efficiency and it is quite time consuming

In this situation 1D-modeling was the only option as for 2D and 3D modeling very close cross-sections with more detailed data are needed. There are about 82 available cross-sections for the investigated part of Jhelum river valley. The river valley is very broad and shallow with a gentle longitudinal average slope of about 0.0004. Because of unavailability of reliable roughness data, an average value of 0.05 (Manning's 'n') has been adjusted for calibration and further used for all considered scenarios. For all modeling scenarios, the upstream and downstream boundary conditions are an outflow hydrograph at Mangla dam and respectively

the water levels upstream of Trimmu barrage as shown in figure 1.5. According to data availability different hydraulic structures have been defined at the respective downstream locations. Moreover, the contributions of five tributaries between Mangla dam and Rasul barrage have also been added as inflow boundaries.

3.2.1 Theory of Flood Routing in MIKE 11

For unsteady flow simulations the computations depend on hydrodynamic flow conditions. One dimensional flood routing in MIKE 11 is based on an implicit finite difference scheme developed by (*Abbott and Ionescu (1967)* [2]). MIKE 11 is capable of using kinematic, diffusive or dynamic and vertically integrated equations of conservation of continuity and momentum (the 'de Saint Venant' equations), as required by the user. The basic equations are derived considering the conservation of mass and conservation of momentum. The resulting equations are mentioned below (*MIKE 11 Reference Manual (2004)* [54]).

$$\frac{\partial Q}{\partial x} + \frac{\partial A}{\partial t} = q \tag{3.1}$$

$$\frac{\partial Q}{\partial t} + \frac{\partial\left[\alpha \frac{Q^2}{A}\right]}{\partial x} + gA\frac{\partial h}{\partial x} + \frac{gQ|Q|}{C^2 AR} = 0 \tag{3.2}$$

Where

Q = discharge (m^3/s)

A = flow area (m^2)

q = lateral inflow (m^3/s)

h = stage above datum (m)

C = chezy resistance coefficient ($m^{1/2}/s$)

R = hydraulic or resistance radius (m)

α = momentum distribution coefficient

The transformation of the de Saint Venant equations to a set of implicit finite difference equations is performed in a computational grid consisting of alternating 'Q- points and h-

points', points where the discharge (Q) and water level (h) are computed at each time step as shown in figure 3.3.

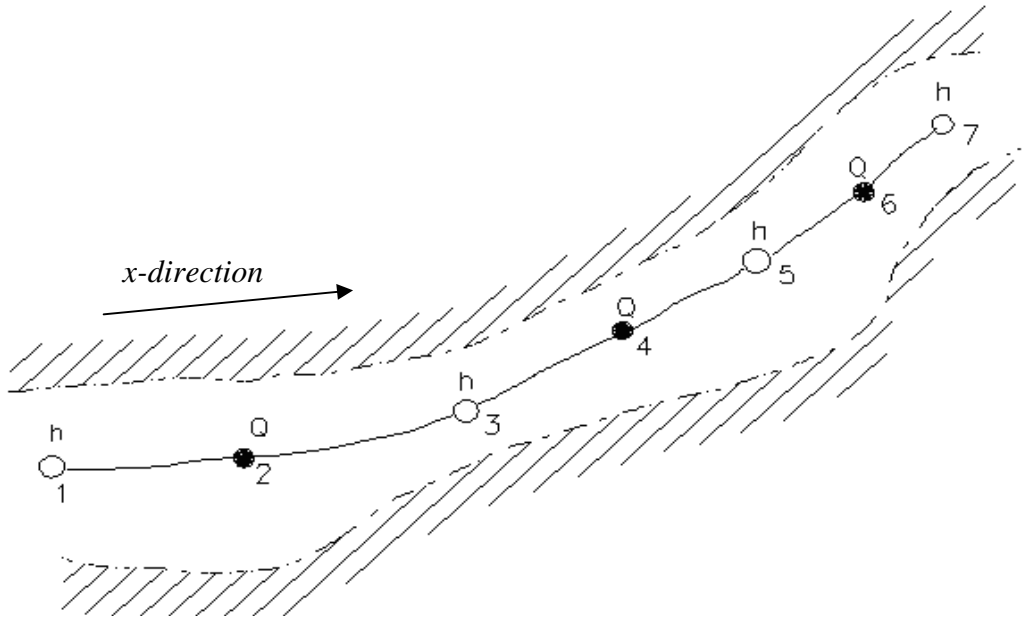

Figure 3.3: Channel section with computational grid [54]

The computational grid is generated automatically by the model on the basis of the user requirements. The Q-points are always placed midway between neighboring h-points, while the distance between h-points may differ. As a rule, the discharge will be defined as positive in the positive x-direction (increasing chainage). The adopted numerical scheme is a 6-point Abbott-scheme which is an implicit finite difference scheme.

3.2.2 Calibration

For calibration of the model, the 1997 flood (peak Q downstream of Mangla dam: 12,798 m^3/s) in the Jhelum river has been taken into consideration. The available outflow hydrograph (97-flood) downstream of Mangla dam has been taken as upstream boundary condition in the model. The available time varying water level upstream of Trimmu barrage after the confluence point (figure 1.5) has been defined as downstream boundary condition. For tributaries, the 25-years peak discharge values have been used to define the boundary conditions. Different hydraulic structures have also been defined according to the available data. Figure 3.4 and 3.5 show the available upstream and downstream boundary conditions for 97-flood.

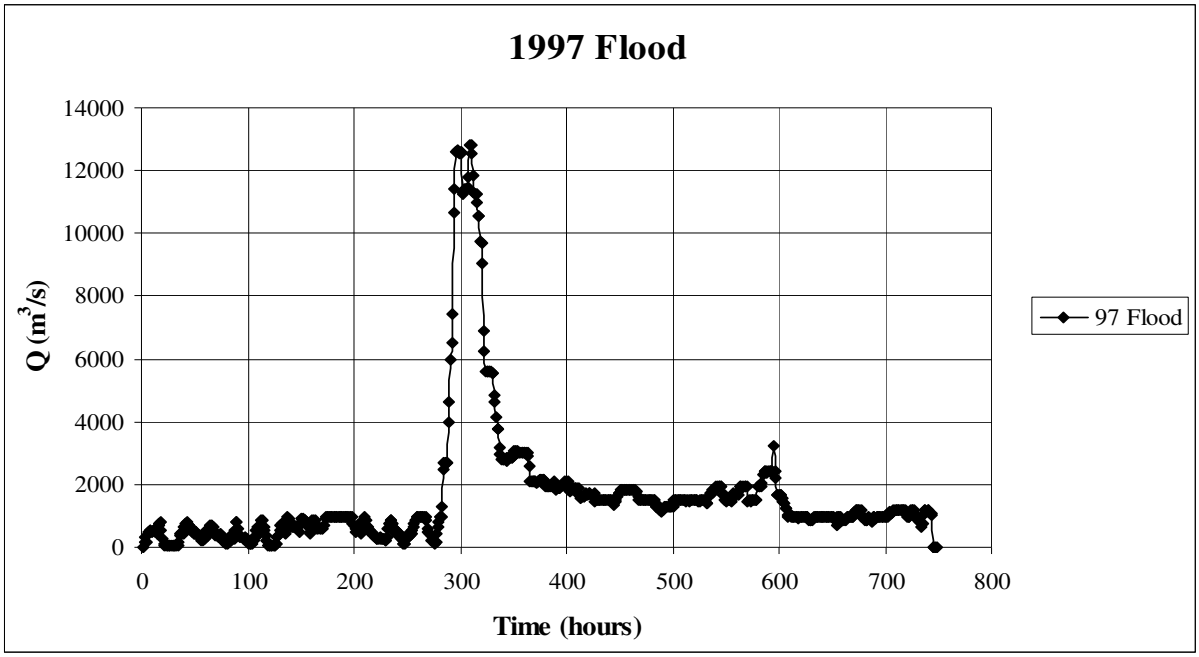

Figure 3.4: Outflow hydrograph at Mangla dam for 1997 flood

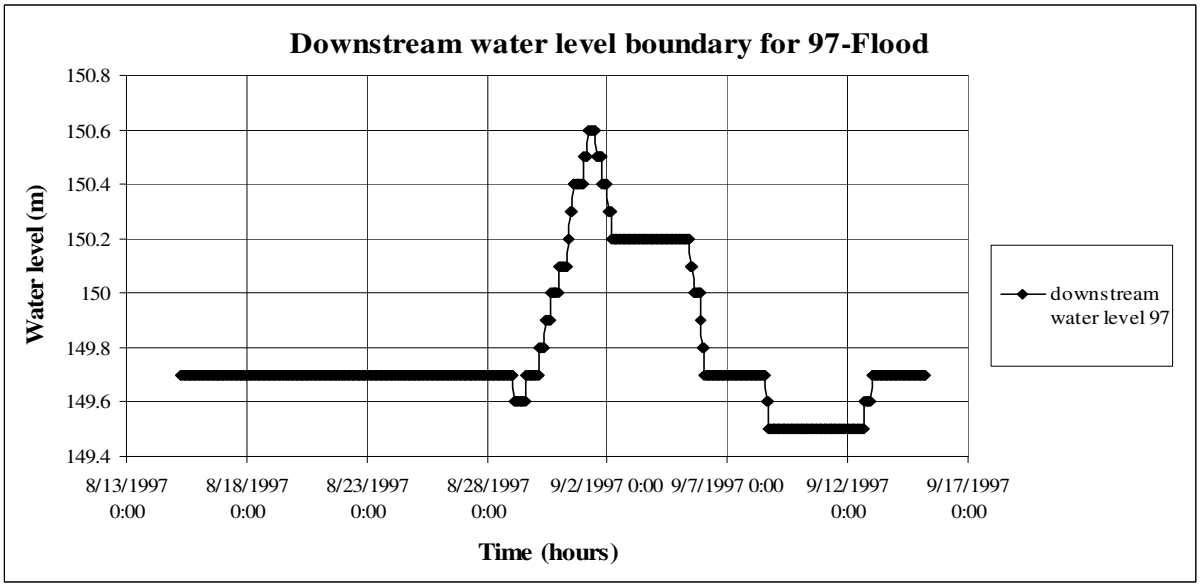

Figure 3.5: Downstream water level at Trimmu barrage as boundary condition for 97- flood

During the simulation, the water level exceeded the specified maximum elevation at many cross-sections. MIKE 11 suggests to prevent crashing of simulation by restricting the cross-sections by implementing vertical walls at both sides as boundaries (figure 3.6). For having meaningful and reliable results, it is important to ensure that the maximum elevation of the cross-sections should be specified in such a way that the maximum expected water levels do not exceed these thresholds. (*MIKE 11 Reference Manual (2004)* [54])

The default calculation in MIKE 11 suggests an extrapolation of the cross-sections with vertical walls as shown in figure 3.6.

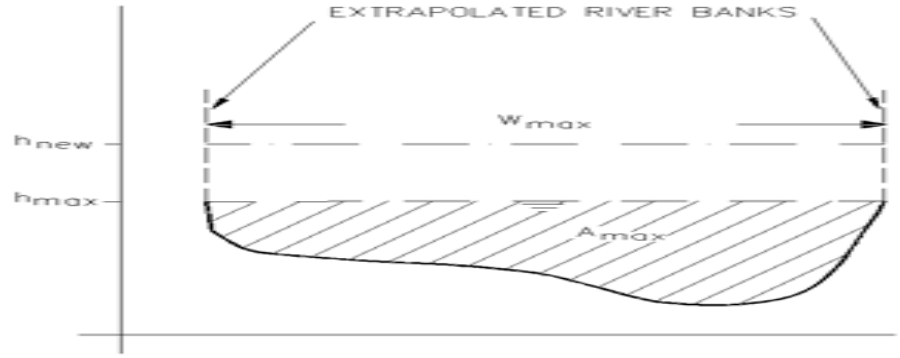

Figure 3.6: Default calculation of areas above the maximum specified height by MIKE 11[54]

But the extrapolation ought to be done in a more realistic way than suggested by MIKE 11. To ensure a more realistic geometry of cross-sections, available cross-section and GIS data were considered as guidelines for extrapolation. Knowing the expected maximum water levels, the step by step extrapolation of the cross-sections was done for considered scenarios. Following points were taken into consideration for the extrapolation of a cross-section (figure 3.7).

- Using information from the neighboring cross-sections
- Comparing features available in GIS Map
- Assuming average elevation change with respect to distance

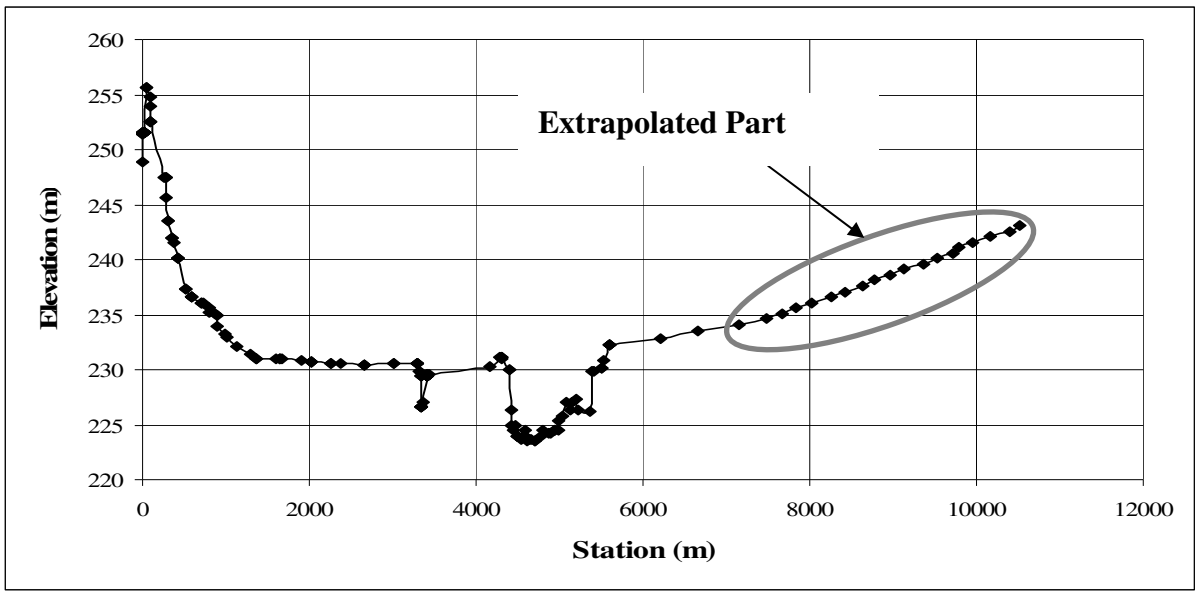

Figure 3.7: Extrapolation of the cross-sections

After necessary extrapolation of cross-sections unsteady flow simulation was run for the 1997 flood. Depending on the available data, the calibration could be proven only with the existing measured data of Rasul barrage as shown in figure 3.8. The discharge increases in the beginning due to the contribution of tributaries and then decreases along the reach. The discharge decreases due to the retention of upstream hydrograph along the reach and local impoundment on flood plains.

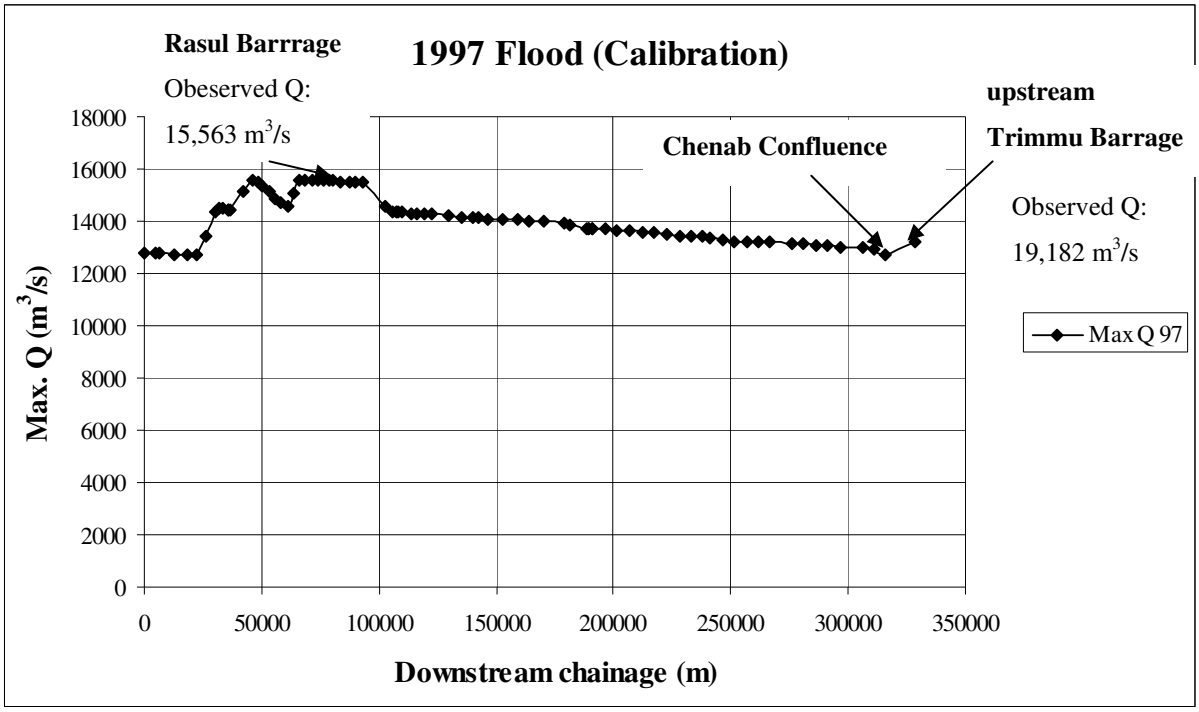

Figure 3.8: Calibration of the model for 1997 flood

Due to unavailability of the reliable data at the confluence point, Chenab's contribution has not been considered. The observed discharge at Trimmu upstream is higher than the computed value because of Chenab's contribution at the time of the 97-flood. For the 1997 flood, time varying water level upstream of Trimmu barrage with respect to Chenab's contribution is available. But for validation and other considered flooding scenarios, always a new water level boundary is required depending on the Chenab's contribution. Unfortunately, not enough data are available at the confluence point to estimate the water level with respect to Chenab's contribution for other scenarios. In order to simplify the situation, the effect of the downstream boundary condition on the results was analyzed for the 1997 flood as shown in figure 3.9. It was found that there is no significant impact of the change of downstream boundary condition on discharges and water levels computed in an unsteady analysis with MIKE 11 for first 286 km. There were only very small differences in the last 43 km. So the

results of the last downstream section have been ignored for all scenarios and a constant water level (optimized for a stable simulation) has been used as the downstream boundary condition for validation and other scenarios.

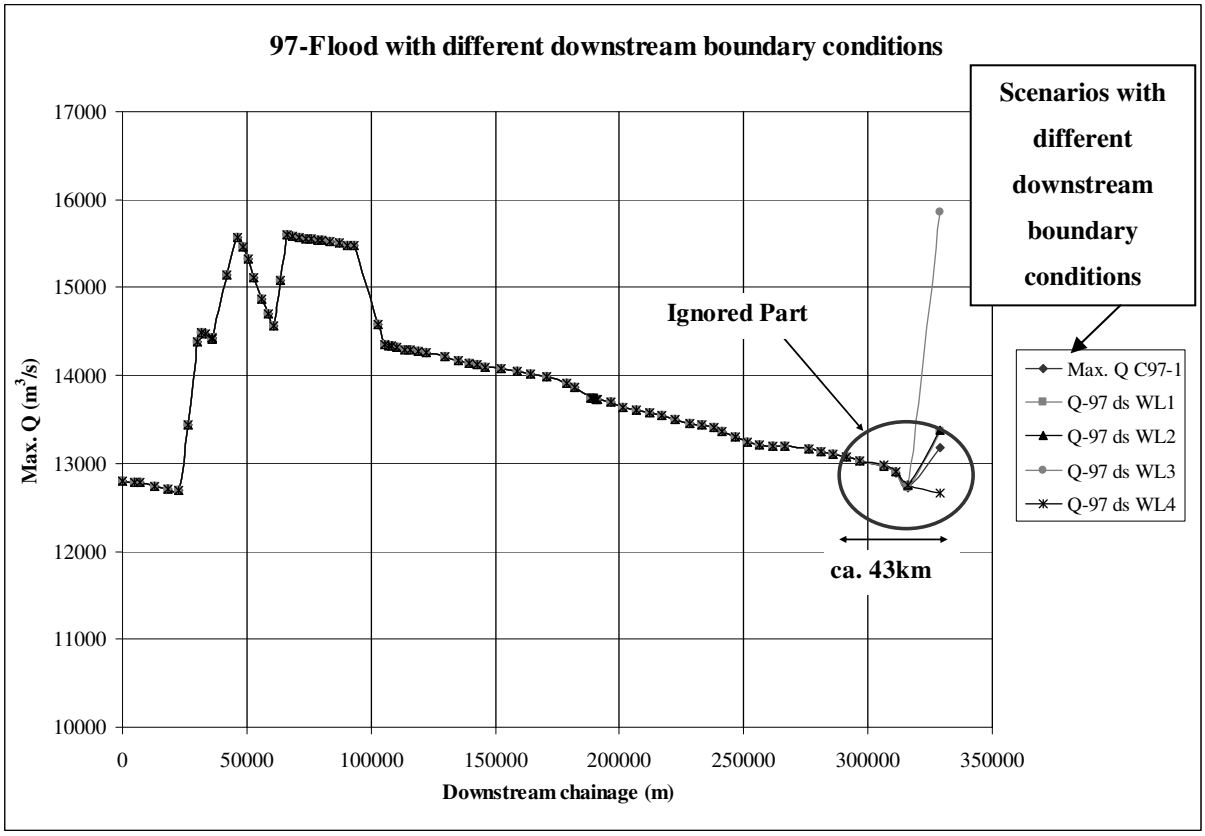

Figure 3.9: Impact of different water levels on results (97-flood)

3.2.3 Validation

For validation of the model, the past highest flood of 1992 (peak *Q* downstream of Mangla dam: 26,293 m^3/s) has been considered. Figure 3.10 shows the outflow hydrograph at Mangla dam for 1992 Flood. For the purpose of validation the contribution of tributaries was kept the same as in case of calibration (97-flood) for the unsteady flow simulation. The exact discharge data of tributaries is not available for different flood events due to nonexistence of gauges. Only 25, 50 and 100 years peak discharge values are available. So the actual contribution of tributaries at the time of 92-flood and other considered scenarios could be quite different. The contribution of tributaries makes some uncertainty. But its overall impact on results would be very small. Figure 3.11 shows the flood routing results for 1992 flood.

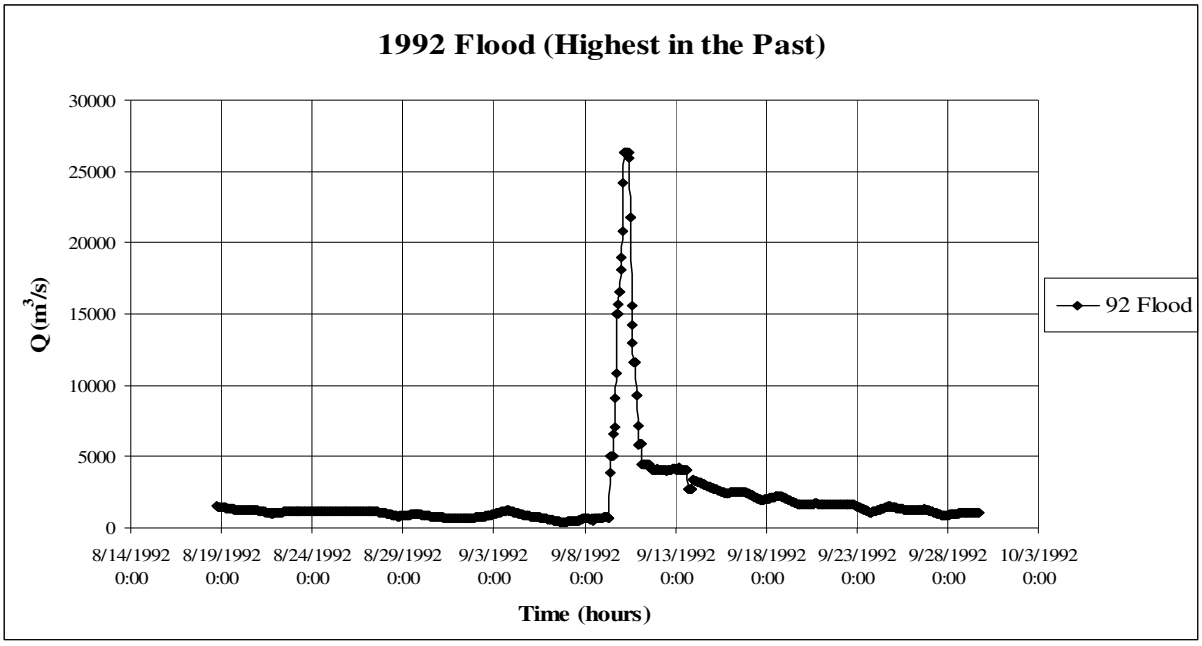

Figure 3.10: Outflow hydrograph at Mangla dam for 1992 flood

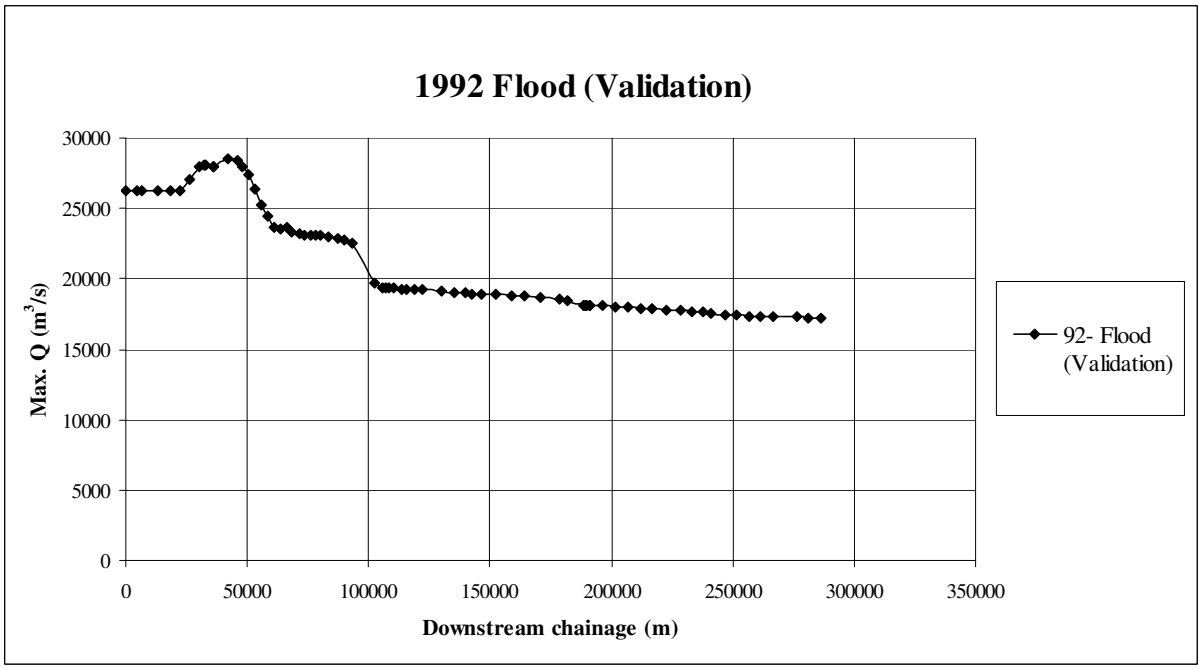

Figure 3.11: Validation of the model for 1992 flood

3.3 HIGHER FLOODING SCENARIOS

The project reach has been modeled for different high flooding scenarios. The hydrographs for two high flooding scenarios 40,000 and 50,000 m^3/s (figure 3.12) have been extrapolated from the available outflow hydrograph of 1992, the highest flood event in the past at Mangla. The peak outflow of 40,000 m^3/s can be taken as an outflow downstream of Mangla dam

without dam failure, because it is close to the maximum discharge capacity of the spillways (~35,035 m^3/s) (*WAPDA (2003)* [86]). But the peak outflow of 50,000 m^3/s could be an outflow after dam failure. The available inflow hydrograph of maximum design flood (MDF: 61,977 m^3/s) has been taken into consideration for flood routing downstream of the dam. It has also been assumed to be an outflow after dam failure. The analysis of dam failure (overtopping) for Mangla dam has also been done in order to determine the possible outflow hydrographs for different failure cases (section 3.4). Figure 3.12 and 3.13 show the extrapolated hydrographs and the available MDF hydrograph marked by grey line.

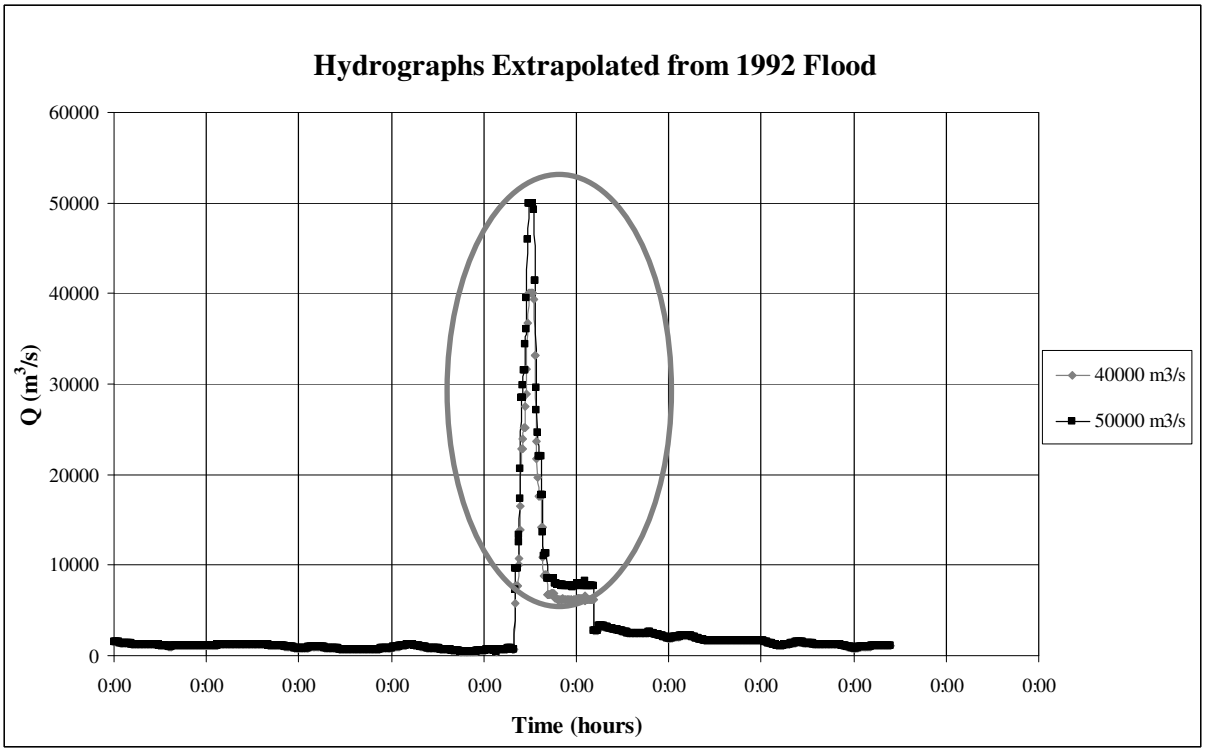

Figure 3.12: Hydrographs extrapolated from 92-flood

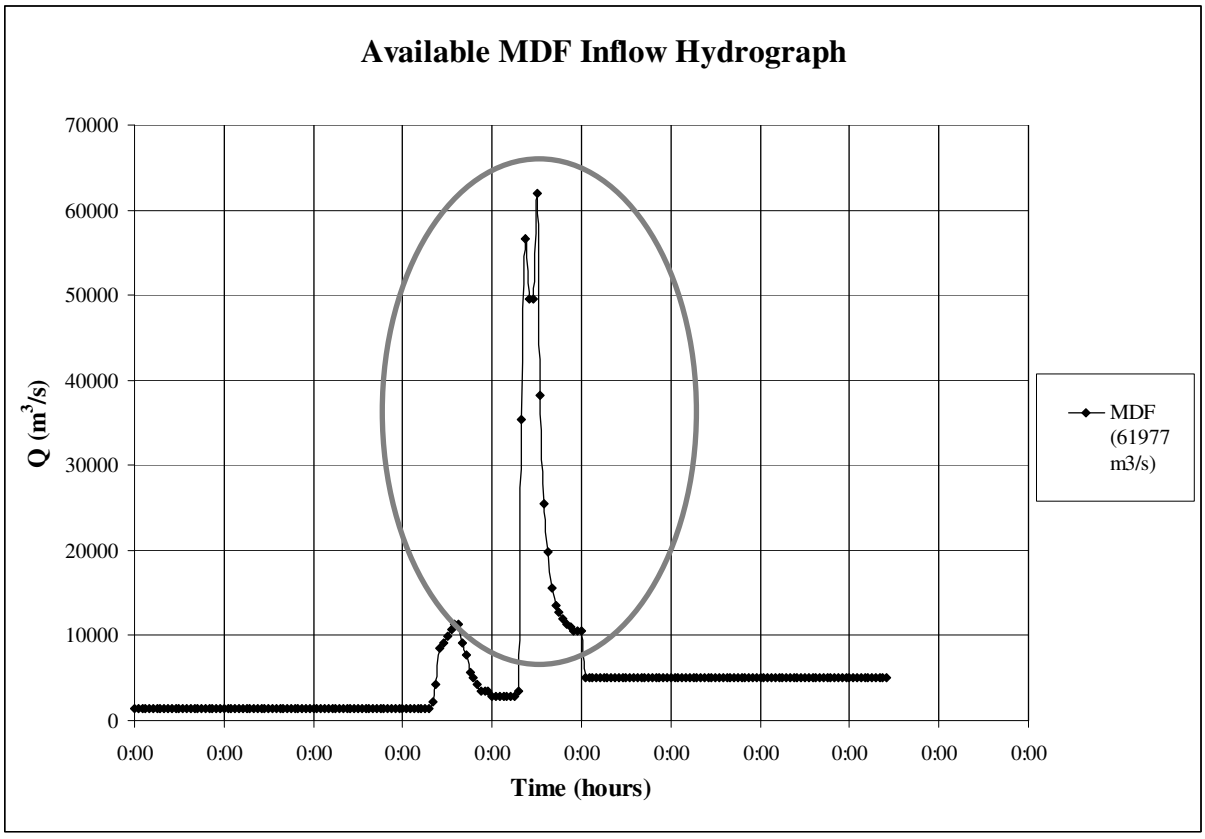

Figure 3.13: Available MDF inflow Hydrograph

3.4 DAM BREAK MODELING

Now the overtopping failure of Mangla dam with raised conditions will be analyzed. Depending on the available data, the parametric approach has been used to estimate the breach geometry and simulate the breach growth as a linear process in order to determine the breach outflows.

3.4.1 Estimation of Breach Parameters

The breach parameters have been estimated by using different available relations based on case studies. Three cases of dam breach have been considered for the computation of the breach geometry. (table 3.1)

Table 3.1: The estimated breach parameters

Case 1	**Case 2**	**Case 3**
Z = 1.4 (Overtopping)	Z = 1.4 (Overtopping)	Z = 1.4 (Overtopping)
d_{ovtop} = 0.61 m	d_{ovtop} = 0.61 m	d_{ovtop} = 0.61 m
h_w = 83.9 m	h_w = 62.92 m	h_w = 41.95 m
h_b = 83.29 m	h_b = 62.31 m	h_b = 41.34 m
HB = 302.08 m asl	HB = 323.05 m asl	HB = 344 m asl
B_{bot} = 231.13 m asl	B_{bot} = 185.34 m asl	B_{bot} = 139.54 m asl

Following is the description of parameters, (*Wahl (1998)* [75]), (*Wahl (2004)* [76])

h_d = Height of dam (m) (in this case, 125 m after raising)

CL = Crest level of dam (m) (in this case, 385.37 m asl after raising)

Z = Breach side slope factor (Z horizontal: 1 vertical); 1.4 for overtopping (*Froehlich (1995a)* [31]),(*Froehlich (1995b)* [32]), (*Froehlich (1987)* [30])

d_{ovtop} = Maximum overtopping depth (m) (0.15 to 0.61 m); 0.61 m considered in this case (*Singh and Snorrason (1982)* [66]), (*Singh and Snorrason (1984)* [67])

h_w = Hydraulic depth of water at dam at failure, above breach bottom (m), (*Reclamation (1988)* [71]), (*Johnson and Illes (1976)* [38])

h_b = Height of breach (m), (h_w - d_{ovtop})

HB = Breach bottom level (m), (CL – h_b)

B_{bot} = Breach bottom width (m), by $B_{avg} = 2.5h_w + C_b$ (*Von Thun and Gillette (1990)* [74]), (*Dewey and Gillette (1993)* [23]) where B_{avg} is the average breach width and C_b is a function of reservoir storage, and B_{top}/B_{bot} =1.29 (*Singh and Scarlatos (1988)* [68]) where B_{top} is the breach top width and B_{bot} is the breach bottom width

Figure 3.14 shows the main parameters of the breach in an idealized way.

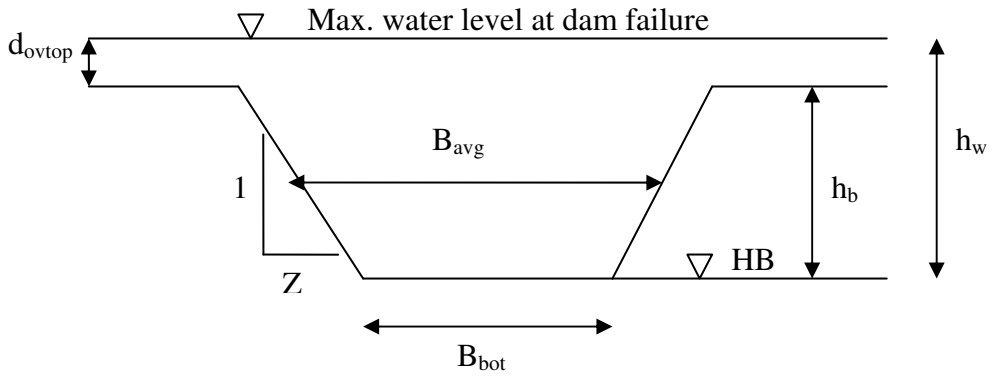

Figure 3.14: Parameters of an idealized dam breach

In large reservoirs, the peak discharge occurs when the breach reaches its maximum depth and width (*Wurbs (1987)* [90]), (*Wahl (1998)* [75]), (*Wahl (2004)* [76]).

3.4.2 Dam Break Setup in MIKE 11

In order to have more realistic results, an erosion based overtopping failure has been analyzed by using MIKE 11 dam break module. The time to failure is related to the full development of the breach with respect to erosion after the initiation of dam failure. In the following, the theoretical background and model setup of dam break analysis in MIKE 11 have been discussed.

Theoretical Background in MIKE 11

In MIKE 11, an erosion based breach development is modeled only by using the energy equation. The initial and the final breach shape must be specified. During the development of the breach the trapezoid increases in size and changes the shape to a linear spline as shown in figure 3.15. (*MIKE 11 Reference Manual (2004)* [54])

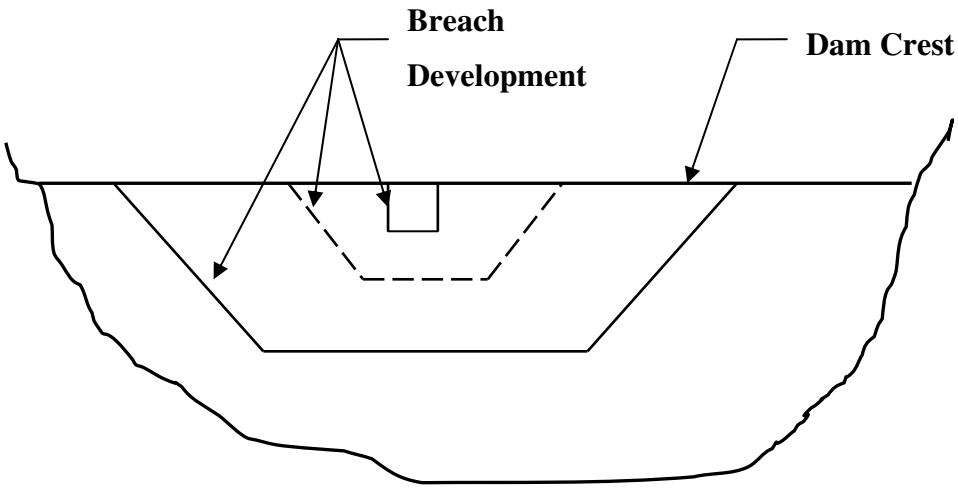

Figure 3.15: Linear development of the breach

The increase of the breach during a time step is calculated from the actual prevailing conditions in the breach itself. The (*Engelund-Hansen (1967)* [27]) sediment transport formula is used to compute the sediment transport in the breach. The flow resistance is calculated as the total dimensionless shear stress, based on the Engelund formulation for flow resistance, *q-q´* relationship. (*MIKE 11 Reference Manual (2004)* [54])

The sediment transport rate (q_t) is calculated from the Engelund-Hansen formula in terms of m^2/s per meter-width of pure sediment. By application of the sediment continuity equation in the breach, the change in breach level (dH_b) in a time interval (d_t) is given in equation (3.3),

$$\frac{dH_b}{d_t} = \frac{q_t}{L_b(1-\varepsilon)} \tag{3.3}$$

Where

H_b = breach level (m)

q_t = sediment transport rate (m^2/s)

ε = porosity of the sediment (%)

L_b = breach length in the direction of flow (m)

t = time

Modeling the variation of the breach width perpendicular to the flow direction is more difficult to relate to the classical theories of sediment transport. This is why for the

development of a wall boundary layer along the often very steep side walls of the breach the theories for bed load and suspended load do not apply. As an approximation, the sediment transport at the sloping walls is assumed to be proportional to that in the central part of the breach. The coefficient of proportionality *SE* (side erosion index) relates the increase in breach width (W_b) to breach depth (h_b) as shown in equation (3.4), (*MIKE 11 Reference Manual (2004)* [54])

$$\frac{dW_b}{dh_b} = 2.SE \qquad (3.4)$$

Where

W_b = breach width (m)

h_b = breach depth (m)

SE = side erosion index, generally the side erosion index (*SE*) is in the range of 0.5-1.0

Dam Break Setup in MIKE 11

The reservoir is modeled as a water level point in the model. This point also corresponds to the upstream boundary of the model where the inflow hydrograph is specified. So the surface storage area of the dam is expressed as a function of the water level. The dam break structure is located at the discharge point with the reservoir. Depending on the available data, the dam geometry and different material properties were defined (*WAPDA (2001)* [83]), (*Tingsanchali and Khan (1998)* [69]). According to the available options in the model, an overtopping failure setup was made according to the following conditions. (*MIKE 11 User Guide (2004)* [70])

- When the water level in the reservoir exceeds the dam crest level (385.37 m), failure will initiate
- The volume of water in Mangla reservoir at overtopping should be about 1.15 E+10 m^3 (max. storage capacity at crest level by the extrapolation of available data)

No sufficient information was available for the exact estimation of the side erosion index (*SE*) required in the model. The erosion increases with the increase in *SE* and vice versa. So two cases of erosion with respect to the side erosion index were considered for different dam failure cases, *SE*: 0.75 (mean value) and 0.6. The estimated breach parameters (table 3.1) were inputted accordingly in the model for different failure cases with respect to the two erosion

cases as shown in table 3.2. Finally, the model was run with unsteady flow conditions for an erosion based overtopping failure.

Table 3.2: Breach Parameters for different cases of dam break simulations

Erosion Case1	Breach Parameters for Dam break simulations with ***SE = 0.75***		
Breach case1	Z = 1.4	HB = 302.08 m	B_{bot} = 231.13 m
Breach case2	Z = 1.4	HB = 323.05 m	B_{bot} = 185.34 m
Breach case3	Z = 1.4	HB = 344 m	B_{bot} = 139.54 m
Erosion Case2	Breach Parameters for Dam break simulations with ***SE = 0.6***		
Breach case1	Z = 1.4	HB = 302.08 m	B_{bot} = 231.13 m
Breach case2	Z = 1.4	HB = 323.05 m	B_{bot} = 185.34 m
Breach case3	Z = 1.4	HB = 344 m	B_{bot} = 139.54 m

3.4.3 Outflow Hydrographs for Different Failure Cases

According to the breach parameters for different cases (table 3.2) and dam break setup, simulations were run for three failure cases in order to determine the outflow hydrographs after failure. Figure 3.16 and 3.17 show the computed outflow hydrographs for two erosion cases. The maximum outflow for the worst case of failure is more than 300,000 m^3/s which could be the highest possible discharge after the failure of Mangla dam.

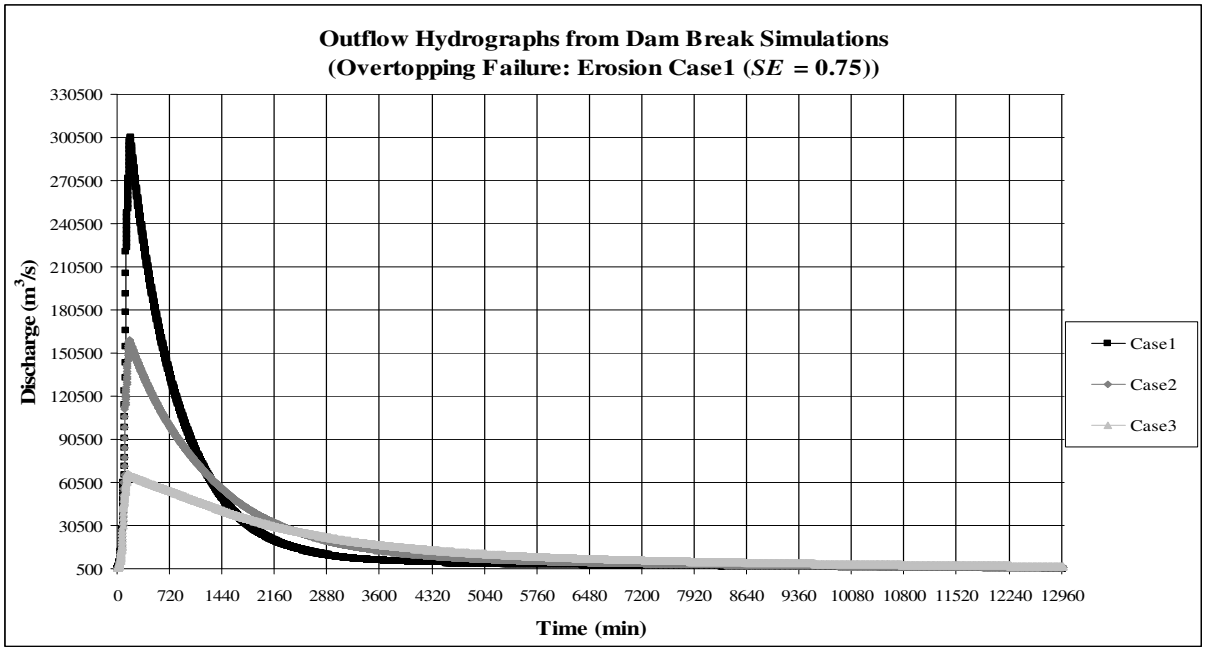

Figure 3.16: Outflow hydrographs from dam break simulations (Erosion case1: *SE* = 0.75)

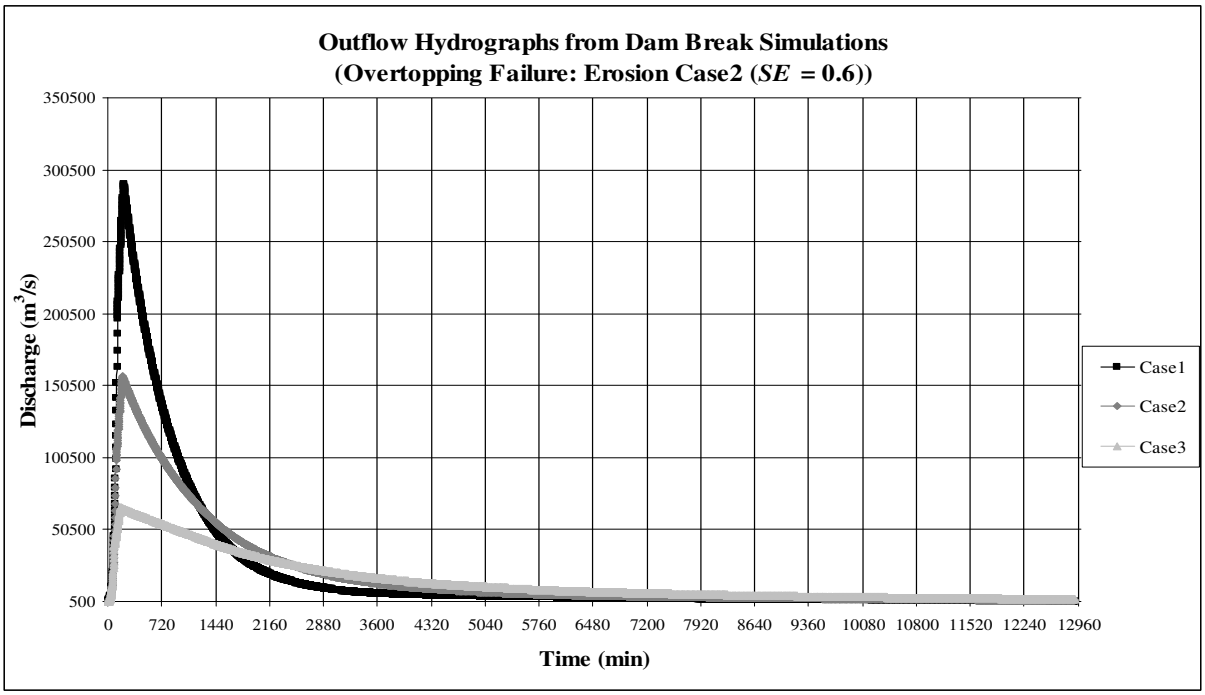

Figure 3.17: Outflow hydrographs from dam break simulations (Erosion case2: *SE* = 0.6)

The peak discharges for different failure cases are comparatively higher for the erosion case1. But there is no significant difference in peak discharges for the two cases of erosion. The main difference due to erosion is the difference in the time to failure (t_f) as shown below in figure 3.19. The time to failure is the breach formation time and it is related to the occurrence of the peak discharge at the full development of the breach (*Wahl (2004)* [76]). Due to more erosion, the breach erosion rate increases as shown in figure 3.18.

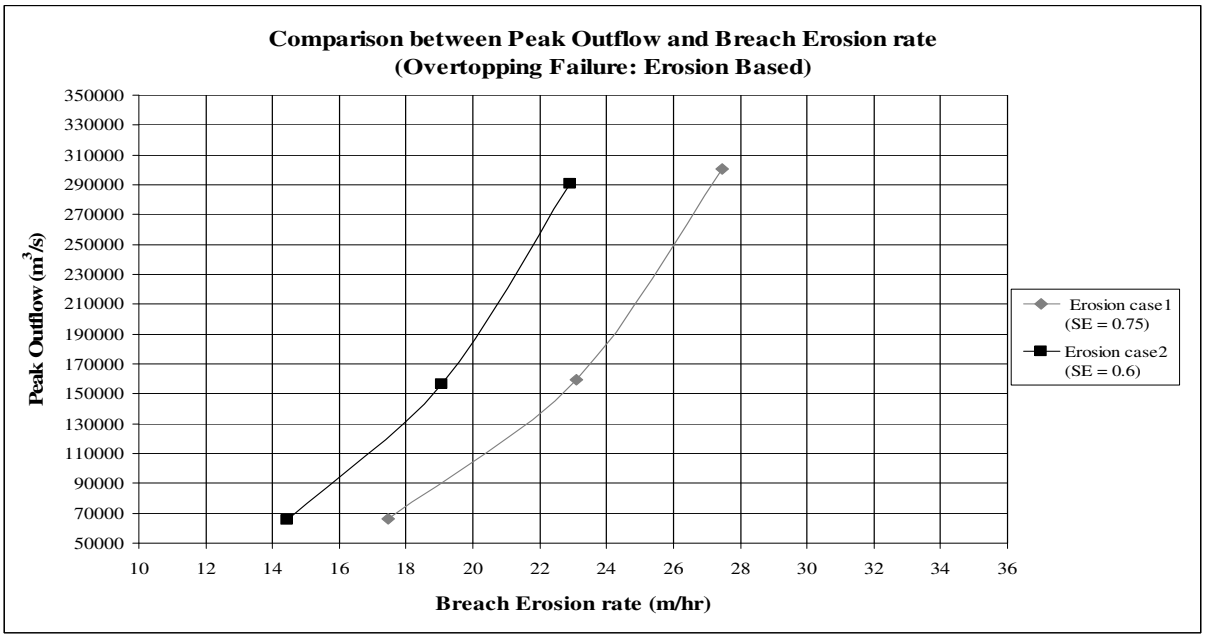

Figure 3.18: Comparison between peak outflow and breach erosion rate

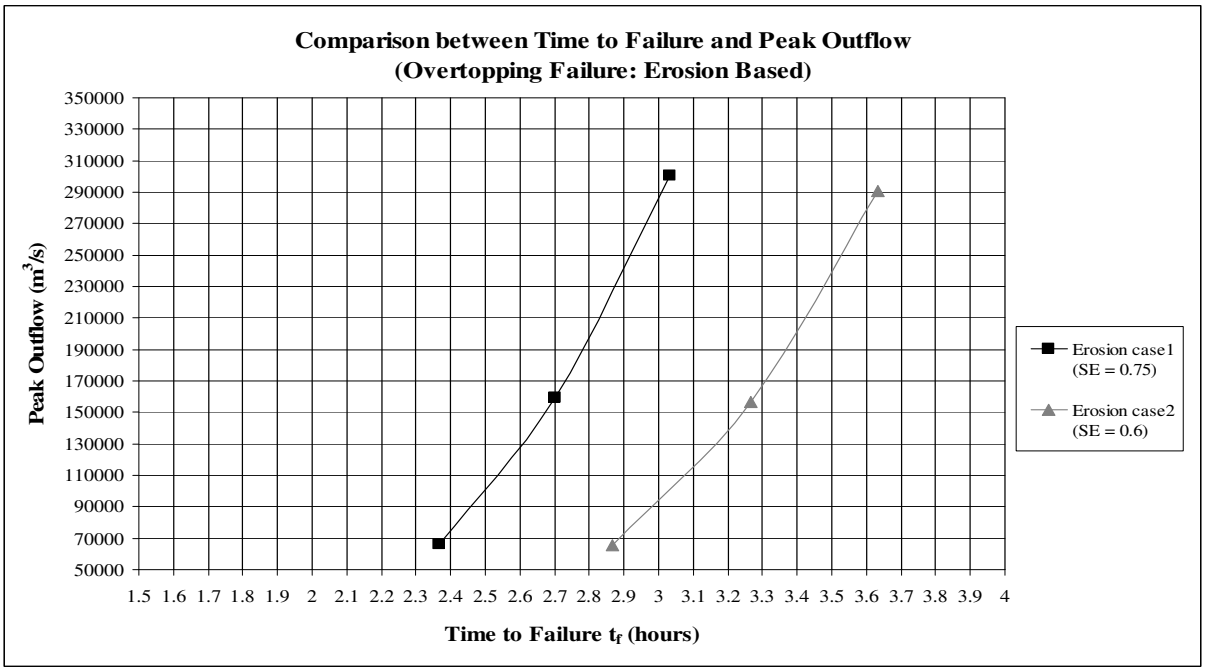

Figure 3.19: Comparison between peak outflow and time to failure

In the following, the results of all dam break simulations have been shown collectively in table 3.3.

Table 3.3: Results of the dam break simulations

Failure Cases	**Peak Outflow (m^3/s)**	**Time to Failure (hours)**	**Breach Erosion Rate (m/hr)**
Breach Case1 (*SE* = 0.75)	300,763	3.033	27
Breach Case2 (*SE* = 0.75)	159,627	2.7	23
Breach Case3 (*SE* = 0.75)	66,396	2.367	17
Breach Case1 (*SE* = 0.6)	290,835	3.633	22
Breach Case2 (*SE* = 0.6)	156,877	3.267	19
Breach Case3 (*SE* = 0.6)	65,777	2.867	14

3.4.4 Check of Impact of Dam Break Parameters

The analyses for checking the impact of different breach parameters were also carried out (see *Appendix B*). The effect of the change in different breach parameters on peak discharge and time to failure was analyzed. It has been found that the peak discharge increases with the increase in the side erosion index whereas time to failure decreases significantly with the

increase in the side erosion index. The additional input parameters for dam break simulations such as initial breach height and initial breach width which are not based on case studies have also been analyzed. The increase in initial breach width increases the peak discharge and reduces the time to failure. But the decrease in initial breach height causes increase in the peak discharge and time to failure. Moreover, the decrease in the side slope of the breach decreases the peak discharge and time to failure and vice versa.

3.5 RESULTS OF FLOOD ROUTING FOR DIFFERENT SCENARIOS

Regarding the hydraulic situation in the valley downstream of Mangla dam, two cases of bridges have been considered for the unsteady flow simulation of all flooding scenarios. In the first case, the model has been run for flow conditions with the existing bridges at different locations downstream of the dam, whereas in the second case model runs were made without bridges assuming that the bridges might have been washed off due to extreme flooding. For higher flooding scenarios the respective hydrographs (figure 3.12 and 3.13) have been used for flood routing. For dam failure cases, the outflow hydrographs by the erosion case1 (figure 3.16) have been considered for the unsteady flow simulations. The 1st erosion case gives comparatively higher peak outflows than the 2nd erosion case which is a worst case consideration. Depending on the available data, the maximum contribution of tributaries was considered for all scenarios. The necessary extrapolation of the cross-sections with respect to increase of the water levels was also done for different flooding scenarios. Figure 3.20 and 3.21 show maximum discharge for higher flooding scenarios (with and without bridges). The results of maximum discharge after dam break flood routing are shown in figure 3.22. In all scenarios the maximum discharge decreases along the reach due to retention of upstream hydrograph with respect to the shape of cross-sections. The random increase in the discharge in the upstream part of the reach is due to the contribution of the tributaries at different locations. In all flooding scenarios there is an overall increase in maximum discharge downstream of Mangla dam for the case where bridges have not been included for flood routing. In the first case (with bridges), there is local impoundment upstream of bridges which reduces the maximum discharge for entire downstream reach. But in the other case (without bridges) water flows down faster and spreads more over the flood plains in order to increase the overall flooding.

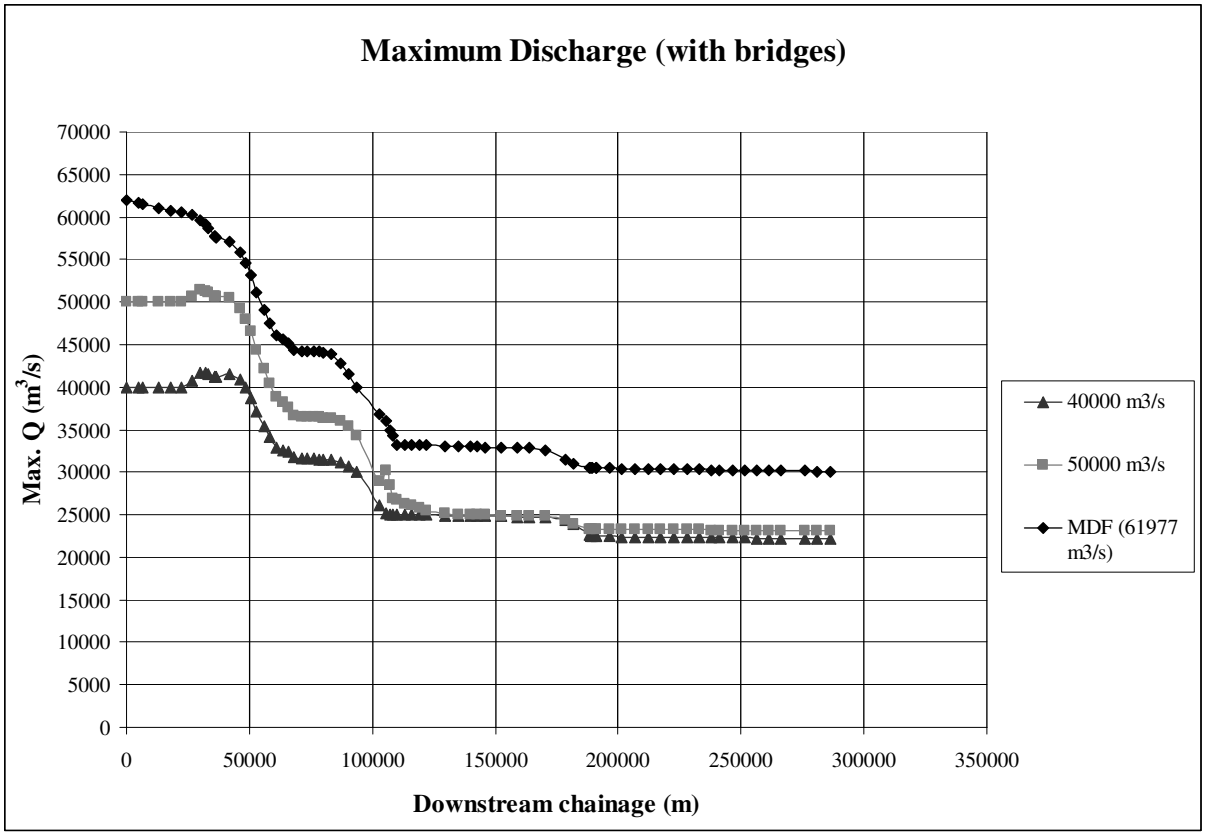

Figure 3.20: Maximum discharge for high flooding scenarios with bridges

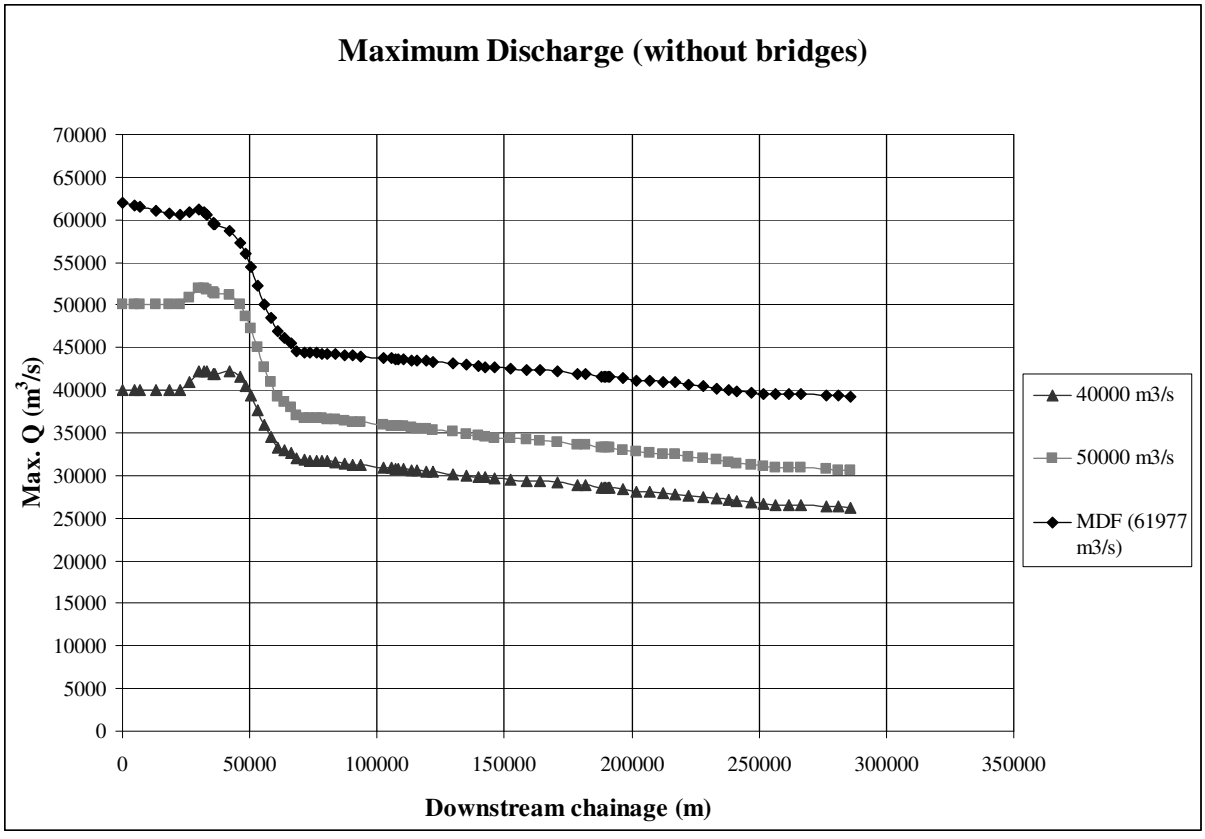

Figure 3.21: Maximum discharge for high flooding scenarios without bridges

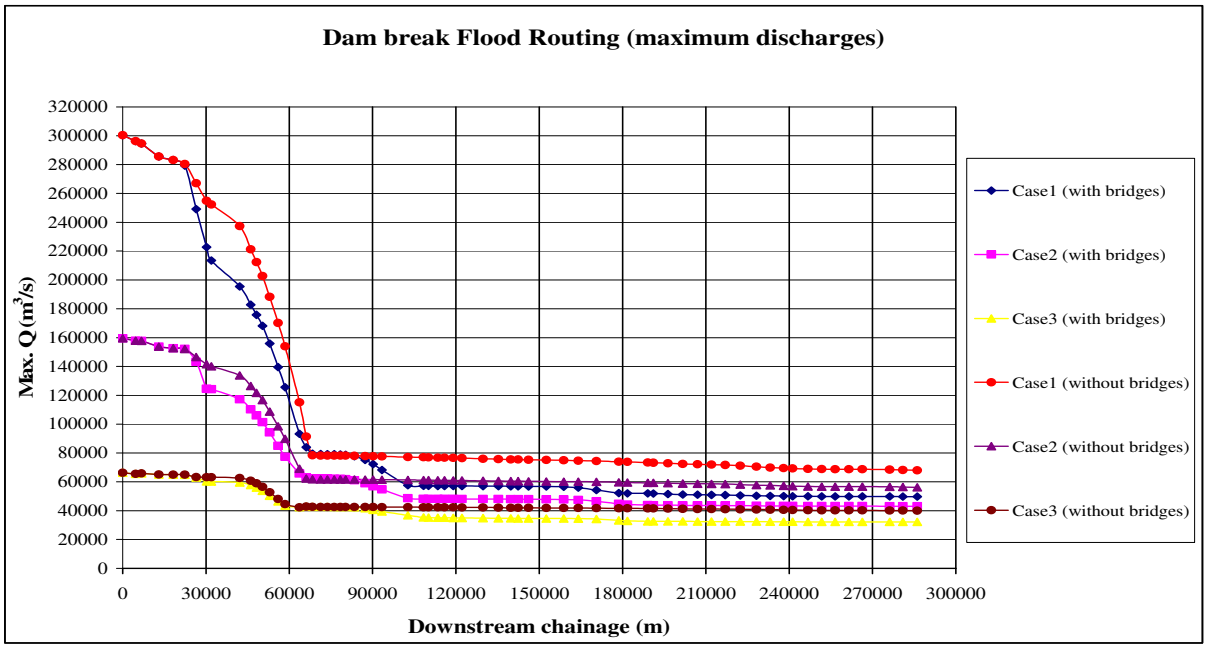

Figure 3.22: Maximum discharge after dam break flood routing

The results of maximum water level for high flooding scenarios and dam break flood routing downstream of Mangla dam are shown in figure 3.23 and figure 3.24. In all cases, the water levels upstream of Rasul barrage are higher than the water levels downstream of Rasul barrage due to possible impoundment upstream of Rasul barrage. For the case of bridges, the maximum water levels are higher than the water levels computed in the other case (without bridges) only for the locations upstream of bridges due to local impoundment.

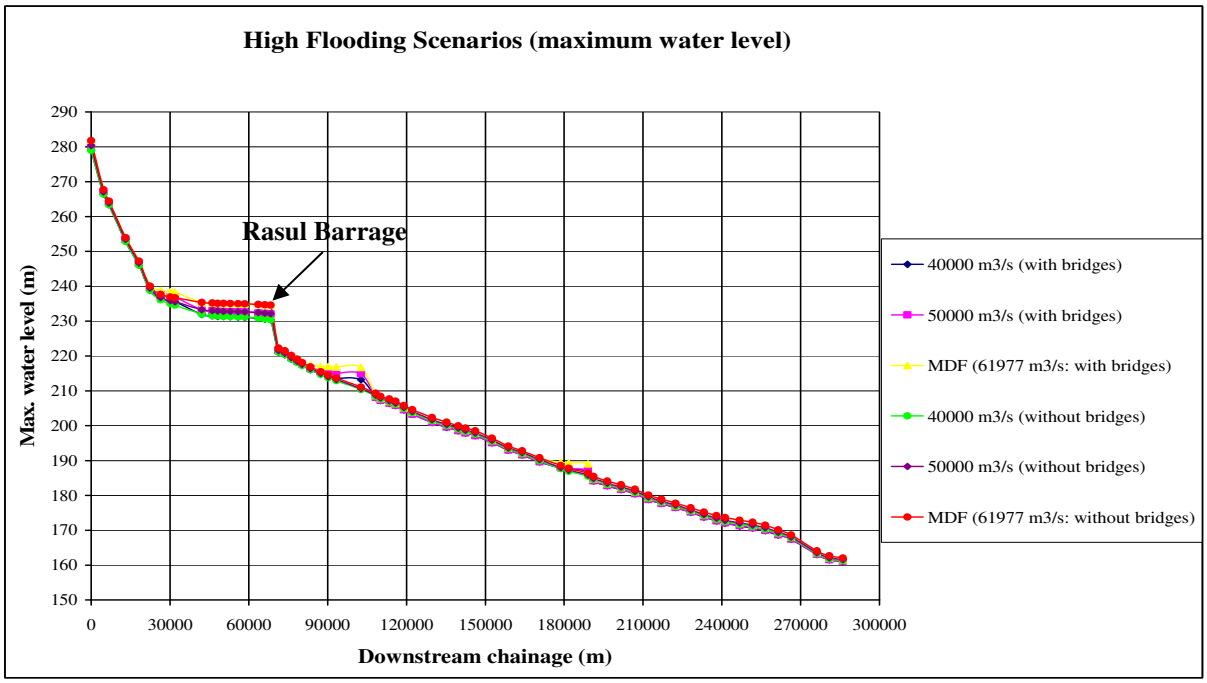

Figure 3.23: Maximum water level for high flooding scenarios

For all other river locations the maximum water levels are higher in the case of no bridges due to more inundation.

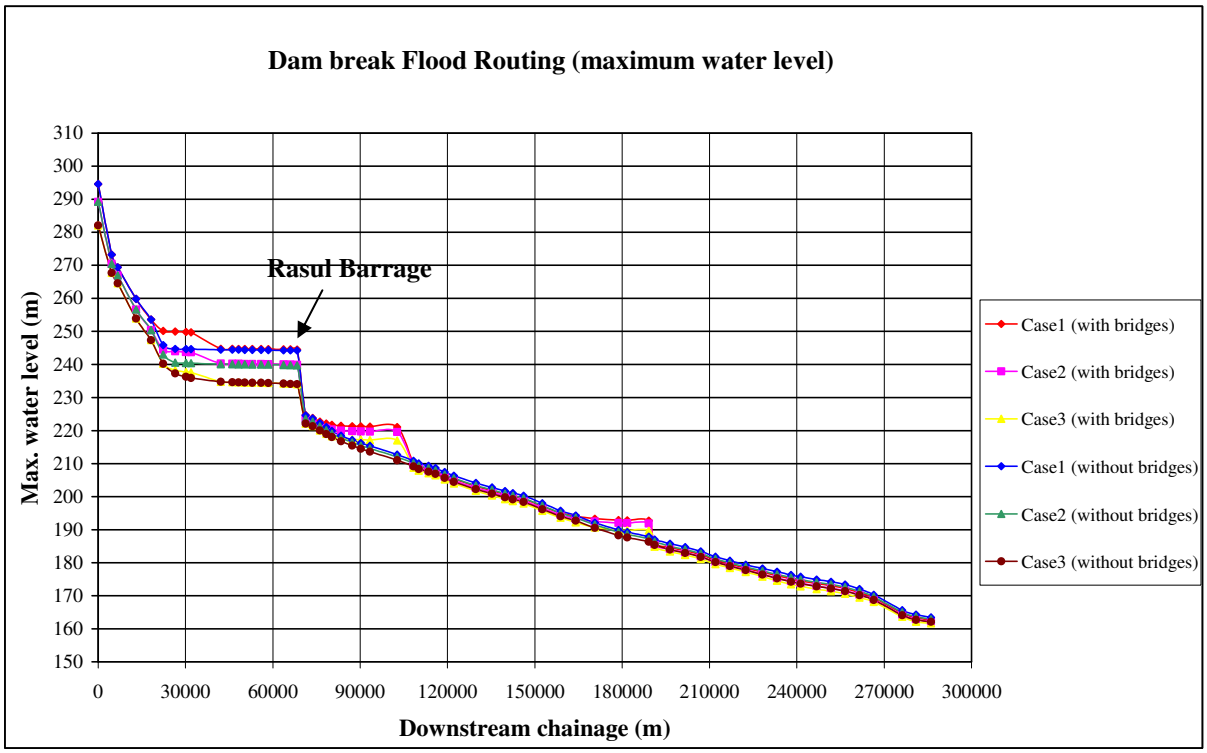

Figure 3.24: Maximum water level after dam break flood routing

3.6 SUMMARY

Depending on the available data, the 1D-hydrodynamic model has been calibrated and validated. Different flooding scenarios have been considered for unsteady flow simulations. Erosion based overtopping failure of Mangla dam has also been modeled by MIKE 11 with respect to different dam breach cases which are based on case studies. The outflow hydrographs for different failure cases have been determined. The maximum failure outflow for the worst case is more than 300,000 m^3/s. The results of flood routing for different flooding scenarios (with and without dam failure) have also been compared. The overall flooding downstream of the dam is more in the case of no bridges. Because in the case of no bridges, water flows down more rapidly and extends more over the flood plains. On the other hand in the case (with bridges) due to local impoundment upstream of bridges, the peak discharge decreases for the whole reach and the maximum water level increases only for the locations upstream of bridges.

4 FLOOD SEVERITY INDICATION

4.1 INTRODUCTION

The results of flood routing for different flooding scenarios computed in the previous chapter have been used in this chapter for flood severity indication downstream of the dam. The risk of flooding has always been a crucial issue in flood control projects. Especially in a river valley downstream of a dam, the flooding risk is seen more and more critical for safe flood plain management. Extreme flooding can occur due to dam failure but sometimes high outflows that exceed the downstream safe channel capacity can also cause significant flooding. The information about flood severity at different downstream river locations plays a very important role in dealing with flood risk assessment and damage estimation. Flood severity depends on many parameters such as flood discharge, flood velocity, flood depth, flood width and safe discharge capacity of channel. Different available flood severity criteria were studied. It was found that the available criteria do not include all important parameters for the computation of flood severity. The contribution of all essential parameters in flood severity calculation is very important for having reliable results. In order to have the combined effect of all necessary parameters and for more realistic and meaningful results, a new criterion of flood severity has been developed.

4.2 FLOOD SEVERITY DEFINITIONS

There are different criteria available for flood severity indication depending mainly on maximum discharge, safe channel capacity, flood width, flood depth and flood velocity. They are based on specific flood severity definitions depending on the expected damage to buildings and life loss. There are mainly two flood severity definitions available in the literature following the specific criteria. In the following, these two flood severity definitions have been discussed. (table 4.1) (*Clausen and Clark (1990)* [18]), (*Graham (1999)* [33]), (*RESCDAM (2000)* [58])

Table 4.1: Flood severity definitions [18], [33], [58]

Definition 1	**Definition 2**
High severity: total or major damage to buildings	High severity: clean sweep of area and little or no evidence of prior human and habitation remaining (rare type of flooding like e.g. Vajont dam, Italy)
Medium severity: partial or moderate structural damage, little damage to the major elements of buildings	Medium severity: destruction of houses but still trees and mangled homes remain for refuge
Low severity: inundation and no damage to structures	Low severity: no buildings are washed off their foundations

4.2.1 Flood Severity Criteria

Now the available criteria depending on different flood severity definitions are discussed.

For *definition 1,* the flood severity indication criteria are the following (*Clausen and Clark (1990)* [18]), (*Kelman (2002)* [42]), (*Reiter (2001)* [55]), (*Reiter (2000)* [56]), (*RESCDAM (2000)* [58]).

If $vh \geq 7$ (m^2/s) then high flood severity, (4.1)

where,
v = Average flow velocity of the flood water (m/s)
h = flood depth (structures are exposed to) (m)

if $7 > vh \geq 3$ (m^2/s) then medium flood severity, (4.2)
otherwise low severity.

The above mentioned *vh*- thresholds are applicable to materials that are mostly used in buildings such as concrete, brick and masonry.

For *definition 2,* the available criteria are incomplete. They are defined in the literature only for medium and low flood severity. There is no threshold available for high flood severity. As

no specific building type is mentioned in the literature (*Graham (1999)* [33]), the following criteria are assumed to be applicable to all common types of buildings.

if $DV > 4.6$ (m^2/s) then medium flood severity, (4.3)

otherwise low severity.

where,

$$DV = \frac{\left(Q_{df} - Q_{safe}\right)}{W_{df}} \ (m^2/s) \quad (4.4)$$

where

Q_{df} = discharge at a particular site caused by dam failure (m^3/s)

Q_{safe} = mean annual discharge or safe channel capacity at the same site (m^3/s)

W_{df} = maximum width of flooding caused by dam failure at the same site (m)

There is also another criterion for this flood severity definition depending on flood depth (h). This criterion is also incomplete as it gives thresholds only for medium and low flood severity. (*Graham (1999)* [33])

if $h \geq 10$ ft then medium flood severity, (4.5)

otherwise low severity.

It is quite obvious that flood severity does not depend only on one parameter. It is the combination of different parameters such as flood discharge, flood velocity, flood depth, and flood width. In this study, *DV* and *vh* criteria have been considered for a closer investigation as they include the key parameters for flood severity indication.

4.2.2 Flood Severity Indication downstream of Mangla Dam

The flood severity downstream of Mangla dam has been computed for different flooding cases by using the flood routing results of unsteady flow simulations (discussed in chapter 3). Additionally for flood severity calculation, the safe discharge capacity and safe water level for Jhelum river downstream of Mangla dam have also been computed as shown in figure 4.1 and 4.2. It has been done by running several steady flow simulations and analyzing the change in water levels at downstream cross-sections with respect to the location of flood plains and

establishments shown in the available GIS maps. The parameters can also be referred to as bank full discharge and bank full water level (related to bank full depth).

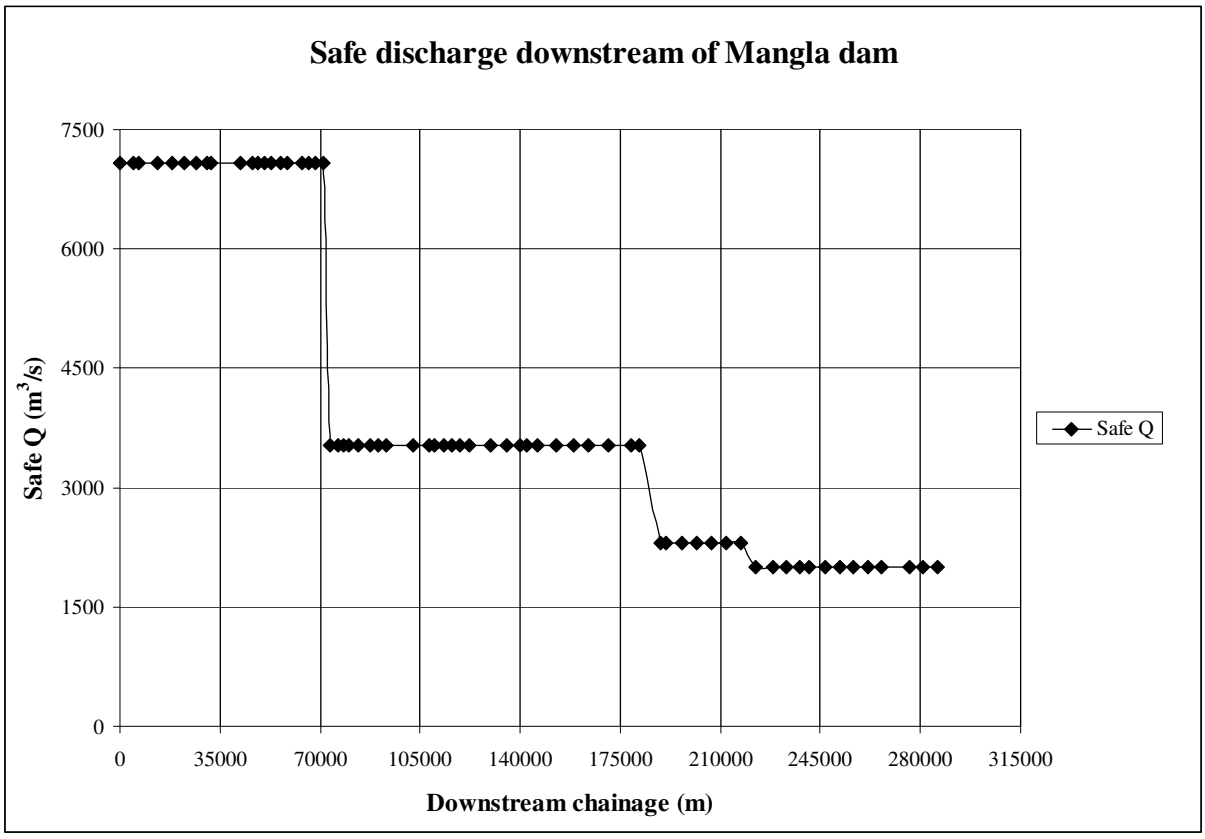

Figure 4.1: Safe discharge downstream of Mangla dam

Safe discharge capacity of a river cross-section is related to its size and shape and it shows the ability of a cross-section to carry a specific amount of discharge without overbank flooding. For this study, the safe discharge capacity has been estimated at each downstream cross-section. As shown in figure 4.1, there are significant changes in the safe capacity at some downstream locations. According to the available cross-section data, this is due to the change in the bank full area of respective cross-sections with respect to the change in their overall shape and hydraulic conditions. For all flooding scenarios the computed water levels have been compared with the safe water levels (figure 4.2) for the calculation of flood depth (h). In all scenarios, the computed water levels are higher than the safe water level as shown in figure 4.2.

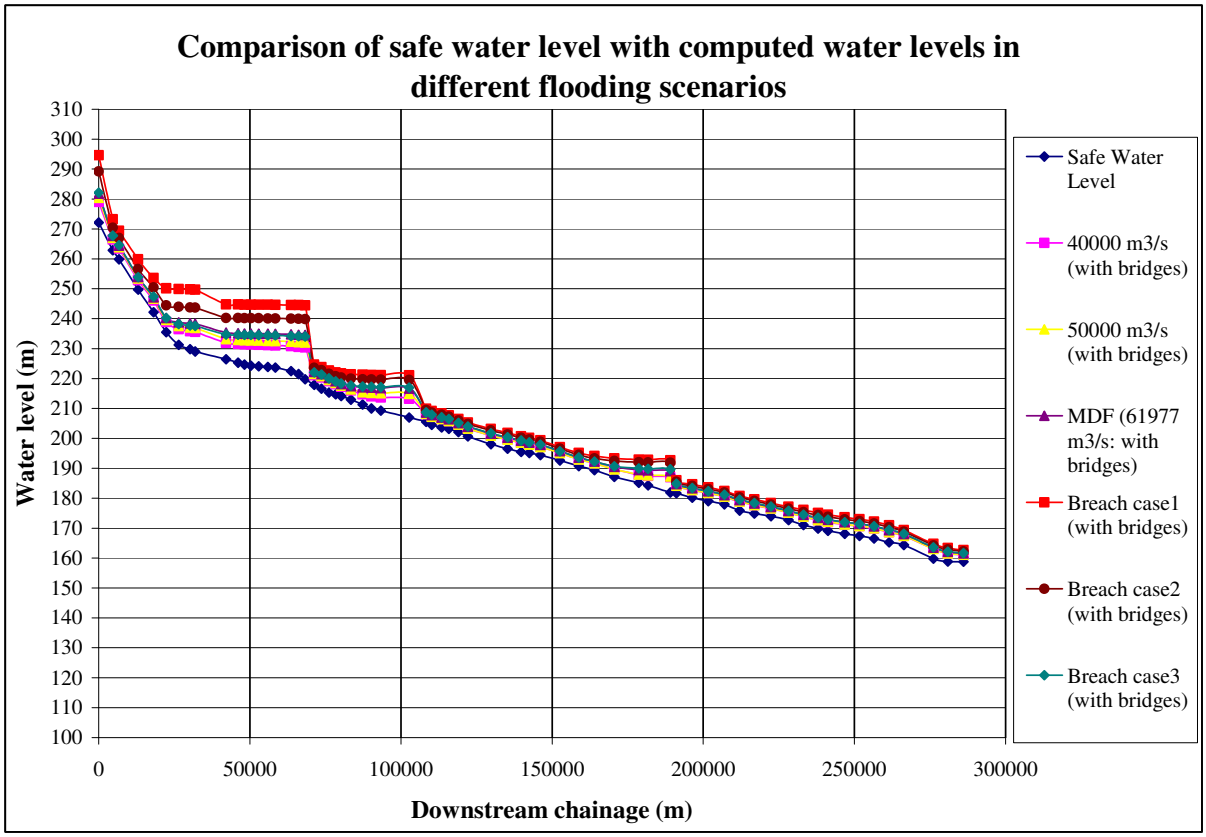

Figure 4.2: Comparison of safe water level with computed water levels

In figure 4.3 and 4.4, the points with different colors indicate the flood severity at downstream locations for different flooding cases (with and without dam failure) according to the available flood severity criteria. The flood severity at a downstream river location depends on hydraulic conditions (Q, v, h etc.) as well as the cross-sectional shape. The vh-criterion (definition 1) describes all flood severity categories (high, medium and low) (figure 4.3). It is obvious that overall flood severity increases with the increase in flooding. Figure 4.4 shows the flood severity according to the DV-criterion (definition 2) at different downstream locations. The flood severity criteria (definition 2) are incomplete because they give flood severity only for medium and low categories. The results of flood severity by both criteria (DV and vh) are quite different from each other. In the following section, both criteria have been compared.

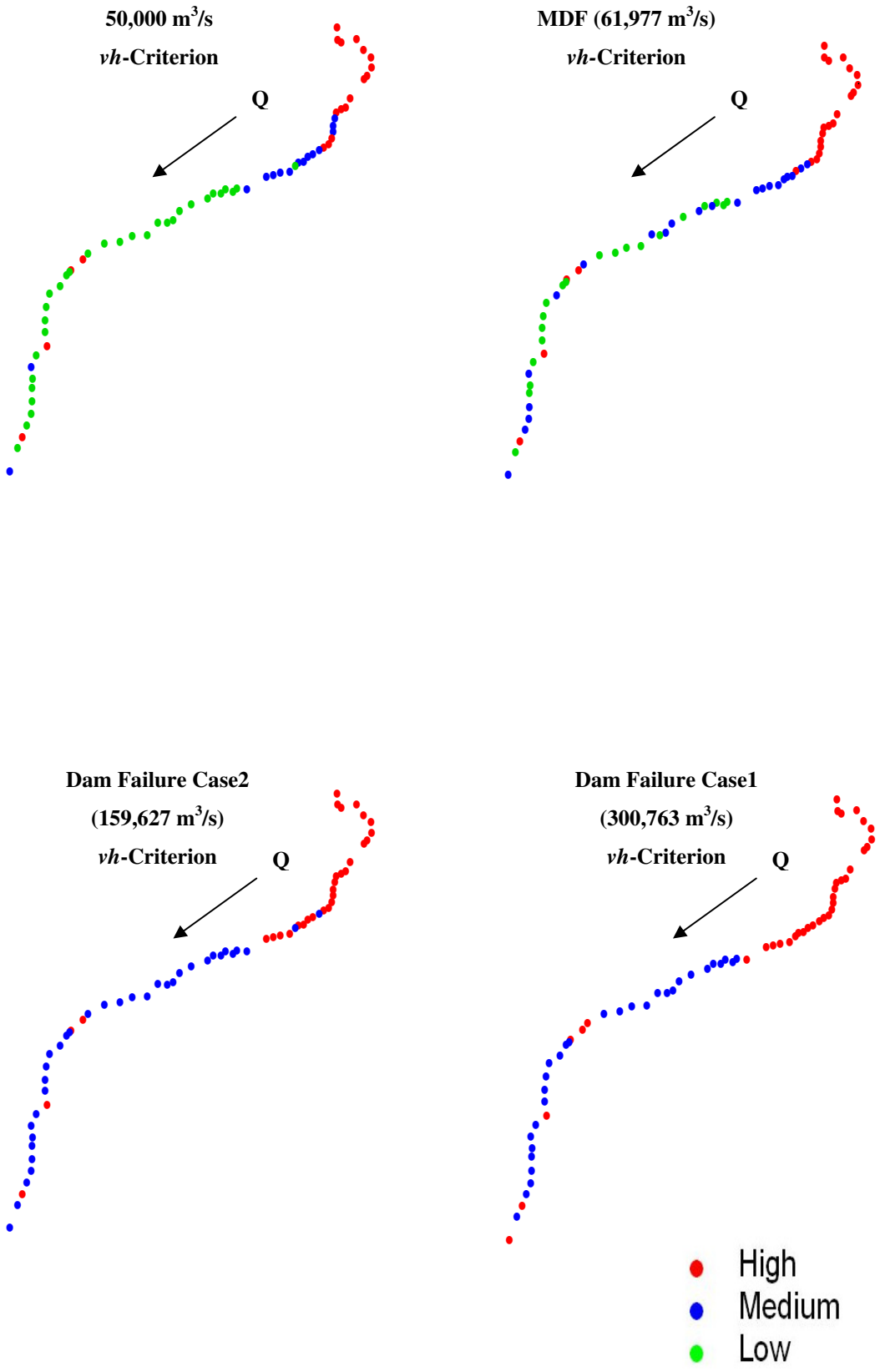

Figure 4.3: Flood severity indication downstream of Mangla dam (defn. 1: with bridges)

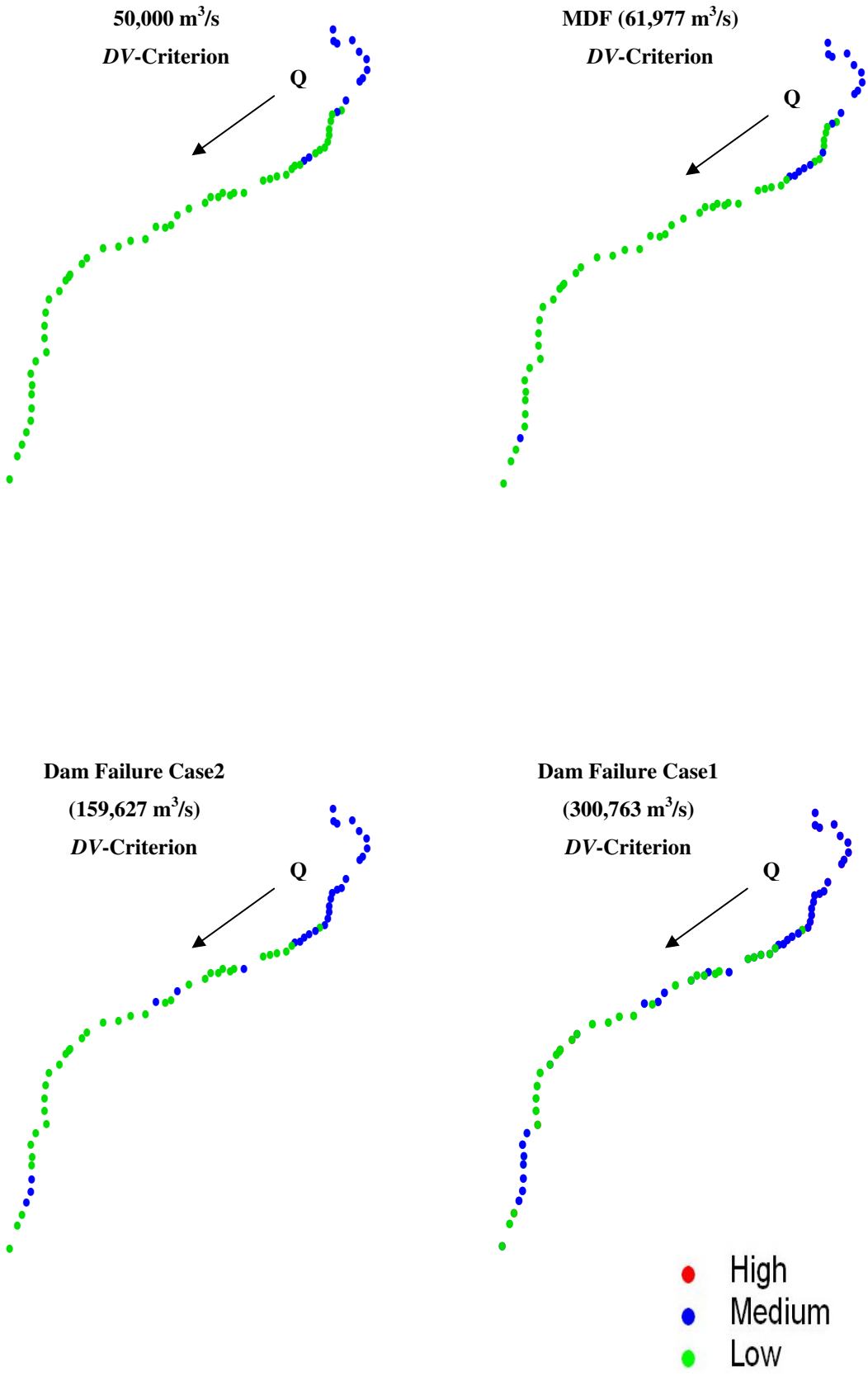

Figure 4.4: Flood severity indication downstream of Mangla dam (defn. 2: with bridges)

4.2.3 Comparison of Flood Severity Criteria

The criterion according to the definition 1 (table 4.1) fully describes the flood severity categories. On the other hand the two criteria following the definition 2 (table 4.1) are incomplete as they do not provide any threshold for high flood severity. Both definitions are quite different from each other with respect to different flood severity categories. In this study both definitions have been qualitatively compared. The definition 1 (table 4.1) is very common in literature and mostly used for flood severity indication. The definition 2 (table 4.1) seems to be more extreme in terms of flood severity categorization in comparison to definition 1 (table 4.1). For example, the high severity category by the definition 2 (table 4.1) shows a very extreme and rare event which could cause total clean sweep and it can not be compared with the high severity category by the definition 1 (table 4.1).

The high and medium severity categories by the definition 1 (table 4.1) are quite comparable to medium and low severity categories by the definition 2 (table 4.1). Moreover, low severity by the definition 2 (table 4.1) states that no buildings are washed off their foundations. This does not mean that there will be no damage. It can be qualitatively interpreted that there might be some partial damages but no complete destruction due to removal of foundations. It has also been proved by comparing the results of flood severity indication by both definitions for different flooding scenarios that the criteria by the definition 2 (table 4.1) show quite different results as compared to the criteria by the definition 1 (table 4.1). In this study, the definition 1 (table 4.1) has been considered for flood severity indication because it gives thresholds for all flood severity categories.

The two criteria *vh* and *DV* have the same units (m^2/s). Both have the same concept and are implicitly related to each other. They represent the same thing but in a different way. With respect to the *DV*-criterion (equation 4.4), the term '*vh*' can also be interpreted as specific flow, flow per unit width of the cross-section. Figure 4.5 represents the important parameters for both criteria in a typical river cross-section.

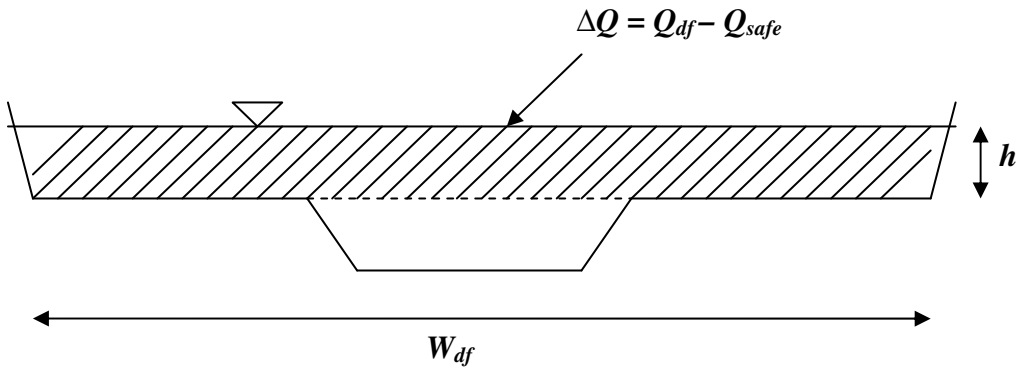

Figure 4.5: A typical river cross-section

DV-criterion is defined as

$$DV \sim \frac{Q}{W}$$

As $Q = v.A$ and $A = W.h$ (assuming a rectangular channel)

Then

$$DV \sim \frac{v.A}{\frac{A}{h}} = v.h$$

In principle,

$$DV \sim v.h$$

The *DV*-thresholds have been qualitatively derived for the definition 1 (table 4.1) by comparing the respective flood severity categories and *vh*-thresholds.

The *DV*-thresholds compared to *vh*-thresholds are as under,

Medium flood severity (definition 2) be equal to high flood severity (definition1)

Then, the DV''-threshold for high severity according to the definition 1 (table 4.1) will be 4.6 (m^2/s) and also

Low flood severity (definition 2) be equal to medium flood severity (definition1)

For this case, there is no *DV* limit available. Obviously it is less than 4.6 (m^2/s), but we need a DV''-threshold for medium severity as for *vh*-criterion is available, 3 (m^2/s). As *vh* and *DV* are qualitatively comparable, it is assumed that the ratio between their thresholds will be the same for medium severity (definition1) as for high severity (definition 1) (table 4.1).

So, a DV''-threshold has been derived by using the ratio between *vh* and *DV*,

$$\frac{vh}{DV} = \frac{7}{4.6} = 1.52$$

The DV''-threshold for medium severity according to the definition 1 (table 4.1) will be, DV'' = 3/1.52 = 1.97 (m^2/s), where '3' is the corresponding *vh*-threshold for medium severity. It can be said collectively for the DV''-criterion,

if $DV'' > 4.6$ (m^2/s) then high flood severity (4.6)

if $4.6 > DV'' > 1.97$ (m^2/s) then medium flood severity (4.7)

otherwise low severity.

So we have two indicators for flood severity. Now the results of flood severity by both criteria (*vh* and DV'') have been compared. Figure 4.6 shows the flood severity indication for different flooding scenarios according to the DV''-criterion. The results of flood severity indication in figure 4.3 have been compared with the results in figure 4.6. For the flooding cases of 50,000 m^3/s and MDF (61,977 m^3/s) the *vh*-criterion shows high severity for more upstream locations (figure 4.3) as compared to the corresponding results by DV''-criterion in figure 4.6. Moreover, the DV''-criterion (figure 4.6) illustrates medium severity for more locations and low severity for less number of locations in comparison to the results by the *vh*-criterion (figure 4.3) in the flooding cases of 50,000 m^3/s and MDF (61,977 m^3/s). For the worst case of dam failure (300,763 m^3/s) in figure 4.3 the *vh*-criterion shows high severity for more upstream locations and few downstream locations. While the DV''-criterion (figure 4.6) represents high severity for upstream locations and comparatively more downstream locations in the worst case of dam failure. The two indicators comprise key parameters for the determination of flood severity but they show differences in the expression of flood severity categories. The involvement of all necessary parameters (discharge, velocity, flood depth,

flood width and safe channel capacity) in flood severity computation is very important for having more realistic results. In order to have the collective impact of both indicators for flood severity indication in different categories they should be aggregated properly.

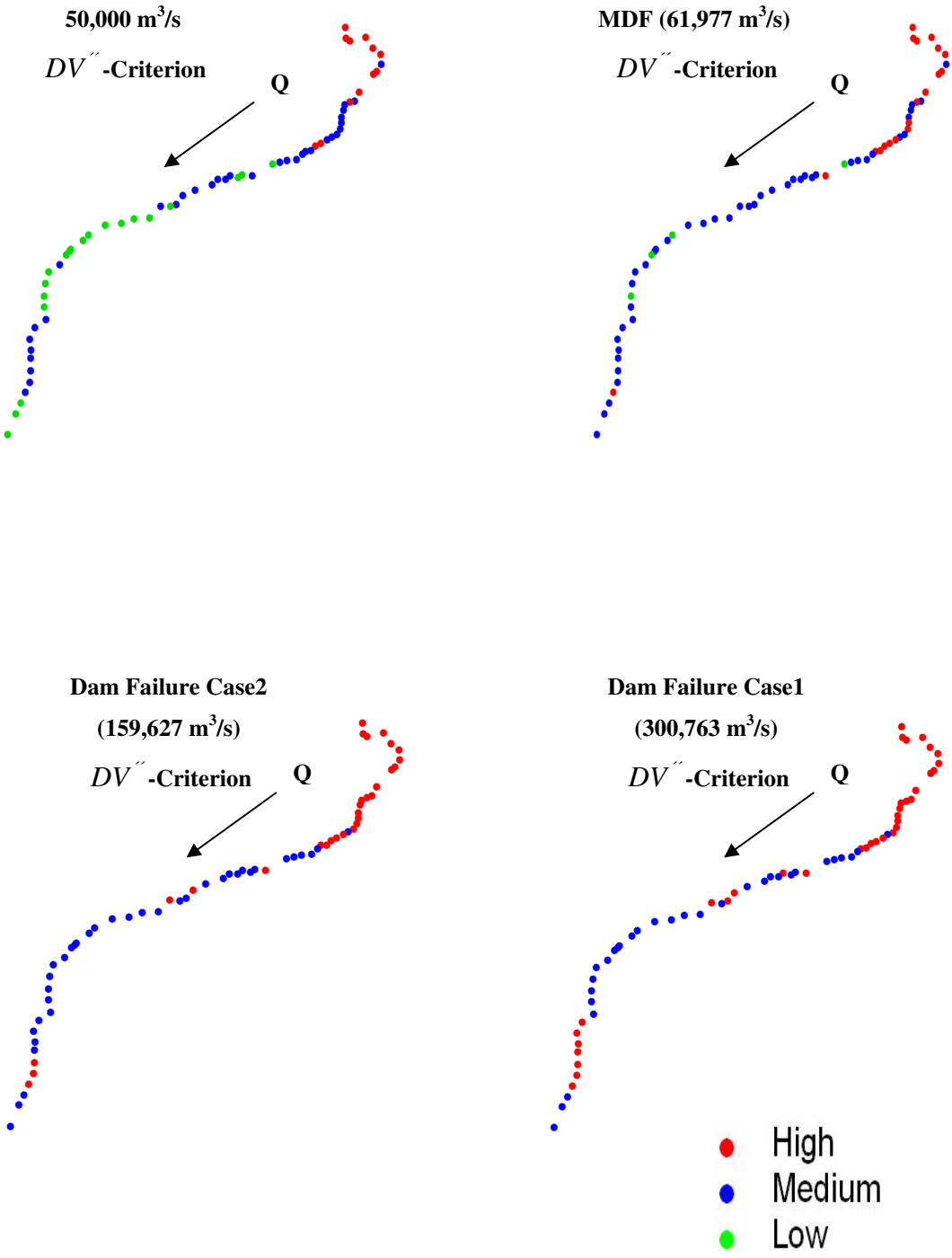

Figure 4.6: Flood severity indication by new $DV^{''}$-criterion (with bridges)

4.3 AGGREGATION OF FLOOD SEVERITY INDICATORS

Usually indicators are normalized before aggregation. Normalization means to bring different indicators to the same measurement units if indicators are expressed in different units in order to make them comparable. In this case, the two indicators have already the same units. Both indicators have the same conceptual basis and are related to each other. It is also mentioned in literature that sometimes there is no need to normalize the indicators, if the indicators are already expressed with the same standard. In such cases the normalization could obscure the issue and one may loose the inherent information contained in the indicators (*Nardo et al. (2004)* [48]), (*Nardo et al. (2005)* [47]). So in this case, no normalization is required before aggregation. Mainly following are the available aggregation methods, (*Cartwright et al. (2006)* [17]), (*Nardo et al. (2005)* [47]), (*Saisana (2005)* [62])

- Additive aggregation (Linear)
- Geometric aggregation
- Multi-criteria analysis (MCA)

4.3.1 Additive Aggregation (Linear)

There are different methods available for the additive aggregation of indicators. The mostly used method is linear aggregation, summation of weighted and normalized indicators. (*Cartwright et al. (2006)* [17]), (*Nardo et al. (2005)* [47]), (*Saisana (2005)* [62])

In general form by equation (4.8),

$$Y = \sum wI \quad \text{with} \ \sum w = 1 \tag{4.8}$$

$$Y = w_1 I_1 + w_2 I_2 + w_3 I_3 .....$$

Where Y is the additive aggregate, w is the relative weight of indicator and I is the normalized indicator value. In this aggregation technique, the poor performance of some indicators can be fully compensated by high values of other indicators. This full compensability is some times undesirable.

For linear additive aggregation, the indicators need to be mutually preferentially independent. This is a very important condition which should be fulfilled for getting a meaningful composite indicator. In other words, an additive aggregation exists only if the indicators are mutually preferentially independent (*Debreu (1960)* [21]), (*Keeney and Raiffa (1976)* [41]), (*Krantz et al. (1971)* [43]). In this study two indicators (*vh* and *DV*) have a very strong correlation which clearly shows the departure from independence. Table 4.2 shows the correlation between the two indicators for different considered scenarios.

Table 4.2: Correlation between *DV* and *vh*

***Q*-Cases**	**Correlation (*DV* and *vh*)**
40,000 m^3/s	0.865
50,000 m^3/s	0.892
MDF (61,977 m^3/s)	0.891
Failure Case1 (300,763 m^3/s)	0.913
Failure Case2 (159,627 m^3/s)	0.928
Failure Case3 (66,396 m^3/s)	0.867

So it is quite clear that in this case the additive aggregation is not applicable.

4.3.2 Geometric Aggregation

Here, the aggregate is the product of the indicators and the weights are exponents to each indicator as shown in the following equation (4.9) (*Cartwright et al. (2006)* [17]), (*Nardo et al. (2005)* [47]), (*Saisana (2005)* [62]).

$$Y = X_1^{w_1} X_2^{w_2} X_3^{w_3} \ldots \qquad (4.9)$$

Where Y is the aggregate, w is the relative weight of indicator and X is the indicator value.
When geometric aggregation is used, each indicator interacts with the values of all other indicators to change the value of the aggregate. This aggregation method is sensitive to low values of the indicators. For example, if only one indicator has a value of zero, then no matter how large the other indicators are, the value of the aggregate will be zero.

So it should be carefully decided to use this type of aggregation depending on individual indicator values. Moreover, in geometric aggregation weights describe the relative influence of indicators.

4.3.3 Multi-Criteria Analysis (MCA)

When different goals are equally legitimate and important, a non-compensatory logic might be essential. This is usually the case when highly different dimensions are aggregated into a composite. For instance, environmental indicators may have physical, social and economic factors. If the analyst analyzes that an increase in economic performance can not compensate a loss in social cohesion, or an aggravation in environmental sustainability then neither the linear nor the geometric aggregation is appropriate. A non-compensatory multi-criteria approach (MCA) can assure the non-compensability by finding a compromise between two or more legitimate goals (*Cartwright et al. (2006)* [17]), (*Munda (1995)* [46]), (*Nardo et al. (2005)* [47]), (*Saisana (2005)* [62]), (*Vincke (1992)* [73]).

In this method, weights are interpreted as 'importance coefficients', the greatest weight should be given to those components which are considered to be more important in the context of composite indicator (*Podinovskii (1994)* [52]), (*Roy (1996)* [61]), (*Vincke (1992)* [73]). In other aggregation methods, weights are the substitution rates (trade-offs) and do not show the importance of the indicators associated with respect to composite indicator. This method is usually appropriate for scenarios with small number of observations and indicators (*Cartwright et al. (2006)* [17]), (*Nardo et al. (2005)* [47]).

4.3.4 Considered Aggregation Method

In this study, additive aggregation can not be applied as the indicators are strongly dependent on each other (as discussed in section 4.3.1). It is perceived that for MCA, the considered sub-indicators are different in nature from each other and they are considered equally legitimate and important depending on their individual importance. For example, the progress index of a country might include different sub-indicators, universities, industry, medical facilities, imports, exports, infrastructure etc. All these sub-indicators are quite different in nature from each other but can be considered equally important for MCA. But in this case, both indicators are the same in nature and they do not show their specific individual significance with respect

to the composite indicator. So they do not fulfill the basic condition for MCA. Finally, for this case geometric aggregation has been chosen as it fits best to this situation. All indicators will interact with each other to change the value of the composite indicator. The composite indicator will show the combined effect of all indicators. The assigned weights will also express the relative influence of the indicators on the composite indicator. All indicator values are strictly positive as geometric aggregation is sensitive to low or zero values. The geometric aggregate will have the same unit as the indicators (*vh* and *DV*) and it will show the contribution of both indicators for flood severity indication.

4.3.5 Weighting of Indicators

Mostly weights are decided by experts or panels based on the assumed political or theoretical importance of each indicator. However, a major weakness of judicially assigned weights is the inevitable disagreement between the panelists. There are also different methods available for determining the weights. Each method is valid for a different purpose. No matter which method is used, weights are essentially the value judgments. While some analysts might select weights based only on statistical methods, others might reward or punish the indicators that are considered more or less influential depending on expert opinion to better express the policy priorities and some theoretical factors. Weights may also be selected to reflect the statistical quality of the data. Ideally, weights should show the contribution of each indicator to the overall composite (*Cartwright et al. (2006)* [17]), (*Nardo et al. (2005)* [47]).

In this study weights have been qualitatively estimated for both indicators (*vh* and *DV*). From literature there is no specific information available which could show the qualitative domination of one indicator on the other. In principle both indicators are very important for flood severity indication as they include typical relevant parameters. The *vh*-criterion is actually available in literature with its thresholds for all flood severity categories (definition 1) (table 4.1). While the original form of the *DV*-indicator for definition 2 (table 4.1) provides thresholds for only medium and low severity categories. Moreover, the DV''-thresholds have been qualitatively derived for all flood severity categories of definition 1 (table 4.1). This shows some domination of the *vh*-criterion on the DV''-criterion with respect to the original availability of all flood severity thresholds. However, the contribution of the DV''-criterion is quite critical for having a meaningful composite indicator. Before giving final weights to both indicators the impact of different weights has also been checked.

4.3.6 Check of Impact of Weights

The geometric aggregate of both indicators has been calculated with different combinations of weights. As the units of both indicators are the same and the sum of weights is equal to 1, the units of the aggregate will also be the same (m^2/s). The general form of the geometric aggregate in this case is given by equation (4.10),

$$GA\ (m^2/s) = vh^{w_1} DV^{w_2} \qquad \text{with } \sum w = 1 \qquad (4.10)$$

Thresholds for different flood severity categories will also change accordingly,

$$GA\ (\text{high/medium})\ (m^2/s) = 7^{w_1} \times 4.6^{w_2} \qquad (4.11)$$

$$GA\ (\text{medium/low})\ (m^2/s) = 3^{w_1} \times 1.97^{w_2} \qquad (4.12)$$

Following are the weight combinations considered for checking the impact of weights, (table 4.3)

Table 4.3: Weight combinations for checking of impact

Cases	w_1 **(*vh*)**	w_2 **(*DV*)**
1	0.5	0.5
2	0.6	0.4
3	0.7	0.3
4	0.8	0.2

The geometric aggregate (*GA*) has been computed with these combinations of weights for different flooding scenarios and then results of flood severity indication have been compared (see *Appendix A*). It has been found that there are no big differences in the results with different weight combinations for different flooding scenarios. The results of flood severity indication are the same at most of the locations but there are differences at very few locations. So it can be concluded that the geometric aggregate (*GA*) is not much sensitive to weights. Keeping in view the impact of different weights and discussion in the previous section (section 4.3.5), the suggested weights for indicators *vh* and $DV^{''}$ are *0.65* and *0.35* respectively. Collectively, the thresholds of geometric aggregate (*GA*) for different flood severity categories with respect to the definition 1 (table 4.1) can be shown as under,

GA (m^2/s) = $7^{0.65} \times 4.6^{0.35}$ for high/medium flood severity (4.13)

GA (m^2/s) = $3^{0.65} \times 1.97^{0.35}$ for medium/low flood severity (4.14)

It should be noted that these suggested weights are not fixed for the future. They might change for different cases depending on specific data/information available by that time. Anyhow, they give necessary guidance for estimating weights of flood severity indicators (vh and DV'') for geometric aggregation in future. The results of flood severity indication downstream of Mangla dam according to the GA-criterion for different flooding scenarios have been shown in figure 4.7. These results show the combined effect of both indicators (figure 4.3 and 4.6) for the definition 1 (table 4.1) of flood severity.

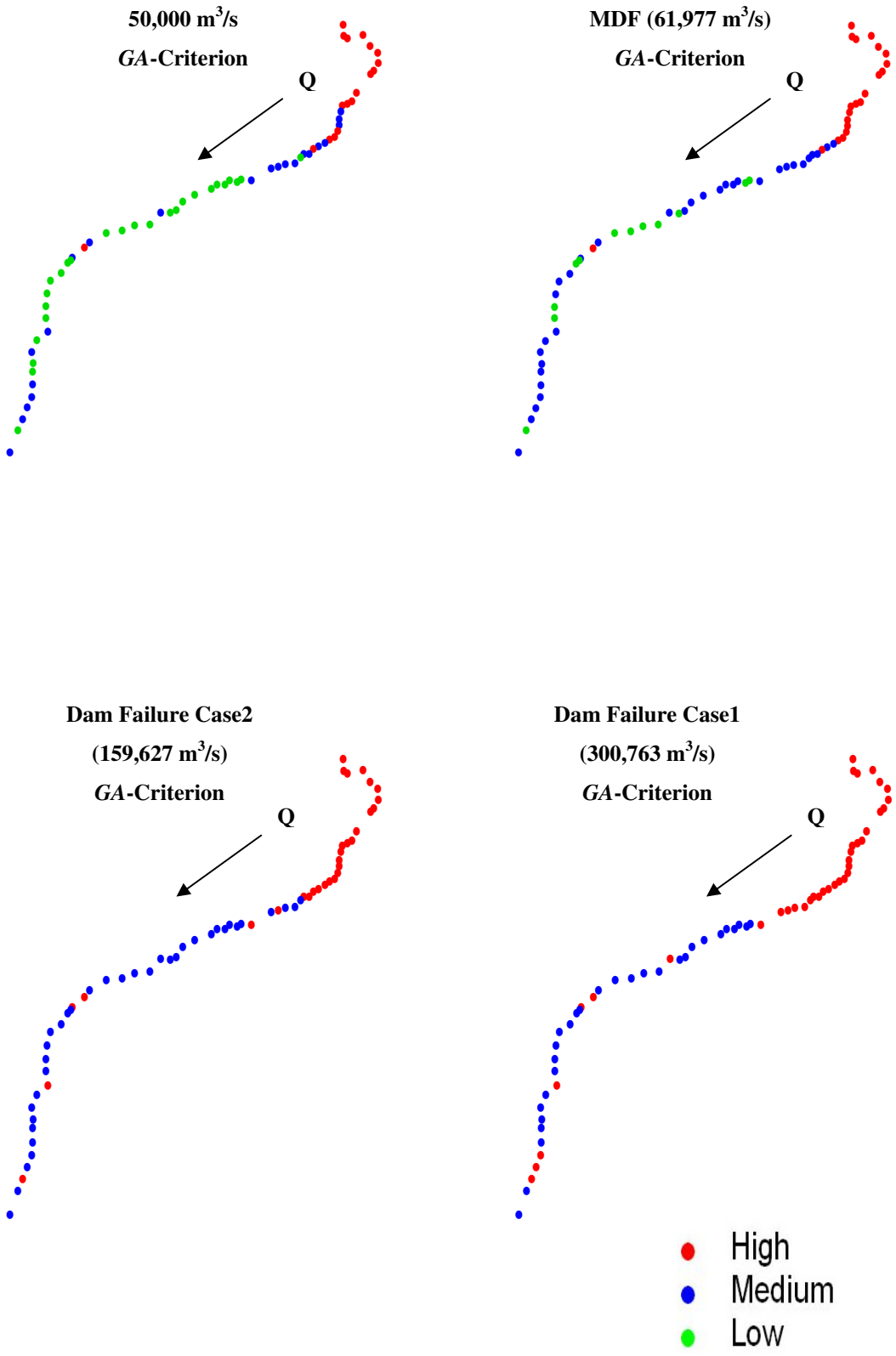

Figure 4.7: Flood severity indication according to *GA*-criterion (with bridges)

4.4 SUMMARY

Different available flood severity criteria following the specific flood severity definitions have been discussed. The results of flood severity indication downstream of Mangla dam by various available criteria have been compared for different flooding scenarios (with and without dam failure). Flood severity does not depend only on one parameter. Different important parameters such as flood discharge, flood velocity, flood depth, flood width and safe channel capacity directly influence the flood severity computation. For having more reliable and realistic results, an improved criterion (*GA*) for flood severity indication has been developed by thorough consideration of the available criteria and it includes necessary parameters responsible for flood severity downstream of a dam. The results of flood severity indication by the new criterion (*GA*) have also been compared for different flooding scenarios. The *GA*-criterion shows the combined impact of all important parameters involved in flood severity.

5 LOSS OF LIFE ESTIMATION

5.1 INTRODUCTION

The results of flood severity indication by the *GA*-criterion (chapter 4) have been used in loss of life estimation for different flooding scenarios downstream of Mangla dam. High flooding downstream of a dam could cause severe damages to people and property. The evaluation of the consequences due to catastrophic flooding downstream of a dam with and without dam failure is an important part of any dam safety study. The most severe damage is the loss of life which does not have any substitute. The extent of life loss is more in case of dam failure than that without failure. Life loss estimation is mainly needed for different important purposes. (mentioned in section 1.1)

Loss of life estimation depends on the number of people at risk, flood severity, warning efficiency and also other factors. Different available methods for loss of life (*LOL*) estimation have been studied and an improved and elaborate method for more realistic estimation of possible *LOL* has been developed.

5.2 METHODS FOR LOSS OF LIFE ESTIMATION

There are different methods available for life loss estimation in literature (*Brown and Graham (1988)* [13]), (*Dekay and McClelland (1993)* [22]), (*Graham (1999)* [33]), (*Reiter (2001)* [55]). It is not possible to estimate potential loss of life with complete accuracy and precision. Different methods are based on different factors and assumptions. So they can not always give the same estimates of life loss due to specific limitations. In the following, different available methods for loss of life estimation have been discussed.

5.2.1 *LOL* Estimation Method by Brown and Graham

In 1988, (*Brown and Graham (1988)* [13]) developed a procedure for life loss estimation based on 24 dam failures and major flash floods. Warning time used in the equations is defined as the elapsed time between the initiation of an official evacuation warning to the public and the arrival of dangerous flooding at population at risk (*PAR*). The equations are, (*Brown and Graham (1988)* [13]), (*Graham (1999)* [33])

When warning time is less than 15 minutes;

Loss of life = $0.5\ (PAR)$ (5.1)

When warning time is between 15 and 90 minutes;

Loss of life = $PAR^{0.6}$ (5.2)

When warning time is more than 90 minutes;

Loss of life = $0.0002\ (PAR)$ (5.3)

The examples of *LOL* estimation by this method for different warning categories have been shown in figure 5.1.

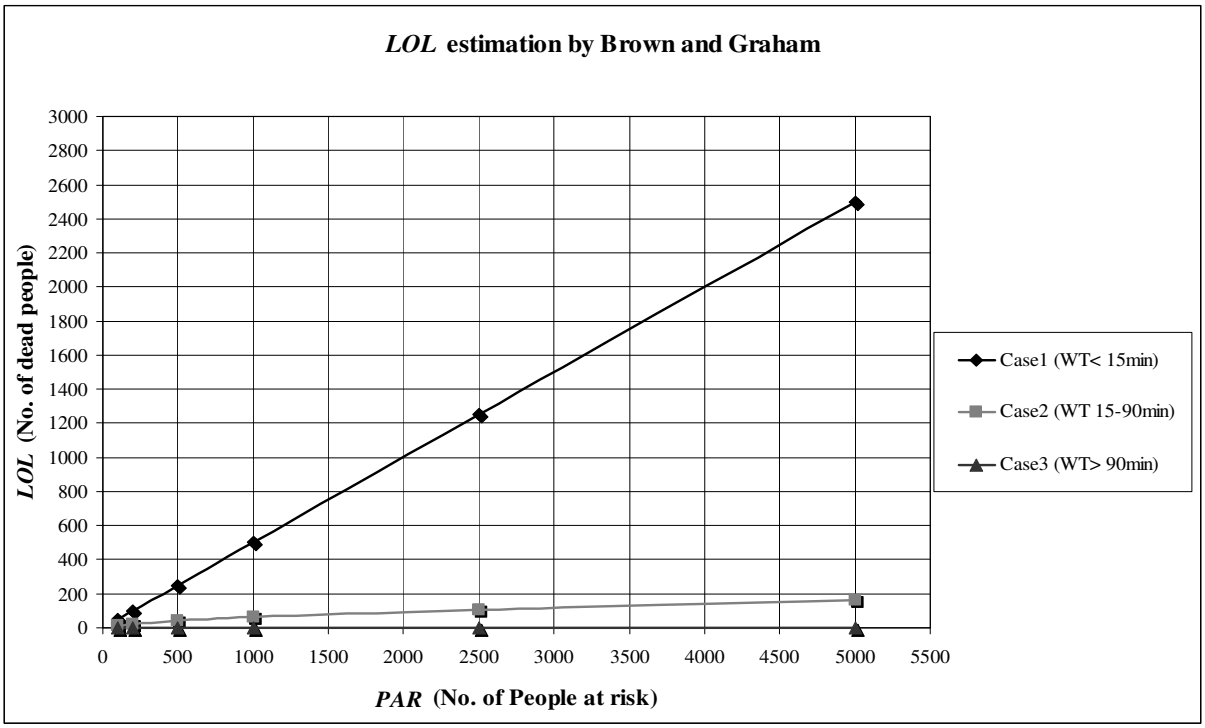

Figure 5.1: Examples of *LOL* estimation by Brown and Graham

It is quite obvious from above equations that the loss of life estimates will change widely depending on warning time. For example (figure 5.1), in an area with 5000 people at risk and warning time of less than 15 minutes, loss of life could be 2500 people whereas in another area with the same number of people at risk and the warning time of more than 90 minutes, estimated loss of life is only 1. This does not seem to be realistic. Warning time is an important parameter for life loss estimation. But the loss of life depends on many other factors which should also be considered in order to have more realistic estimates.

5.2.2 *LOL* Estimation Method by Dekay and McClelland

In 1993, (*Dekay and McClelland (1993)* [22]) presented a procedure for loss of life estimation with respect to the people at risk in a non-linear form. They have provided separate equations for high and low force (fatality) conditions. High force (*HF*) conditions mean that 20% or more of the flooded residences are either destroyed or heavily damaged (*Dekay and McClelland (1993)* [22]), (*Graham (1999)* [33]).

$$\text{Loss of life, } HF = \frac{PAR}{1 + 13.277(PAR^{0.440})\, e^{[2.982(WT) - 3.790]}} \qquad (5.4)$$

For low force (*LF*) conditions, where less than 20% of the flooded residences are either destroyed or heavily damaged loss of life is described as follows.

$$\text{Loss of life, } LF = \frac{PAR}{1 + 13.277(PAR^{0.440})\, e^{[0.759(WT)]}} \qquad (5.5)$$

Where *PAR* is the number of people at risk and *WT* is warning time in hours. Figure 5.2 illustrates the examples of *LOL* estimation by this method for both flood force conditions. Warning time used by Dekay and McClelland is the time in hours from the initiation of dam failure warning until the flood water reaches the community. The main difference between the two procedures is that the warning time is used as a continuous variable by Dekay and McClelland, whereas Brown and Graham placed warning time into three categories. Dekay and McClelland also recommended the use of their equations not for dams that fail without warning the areas with very large number of people at risk. In both methods, warning time has been considered as a major factor for loss of life estimation.

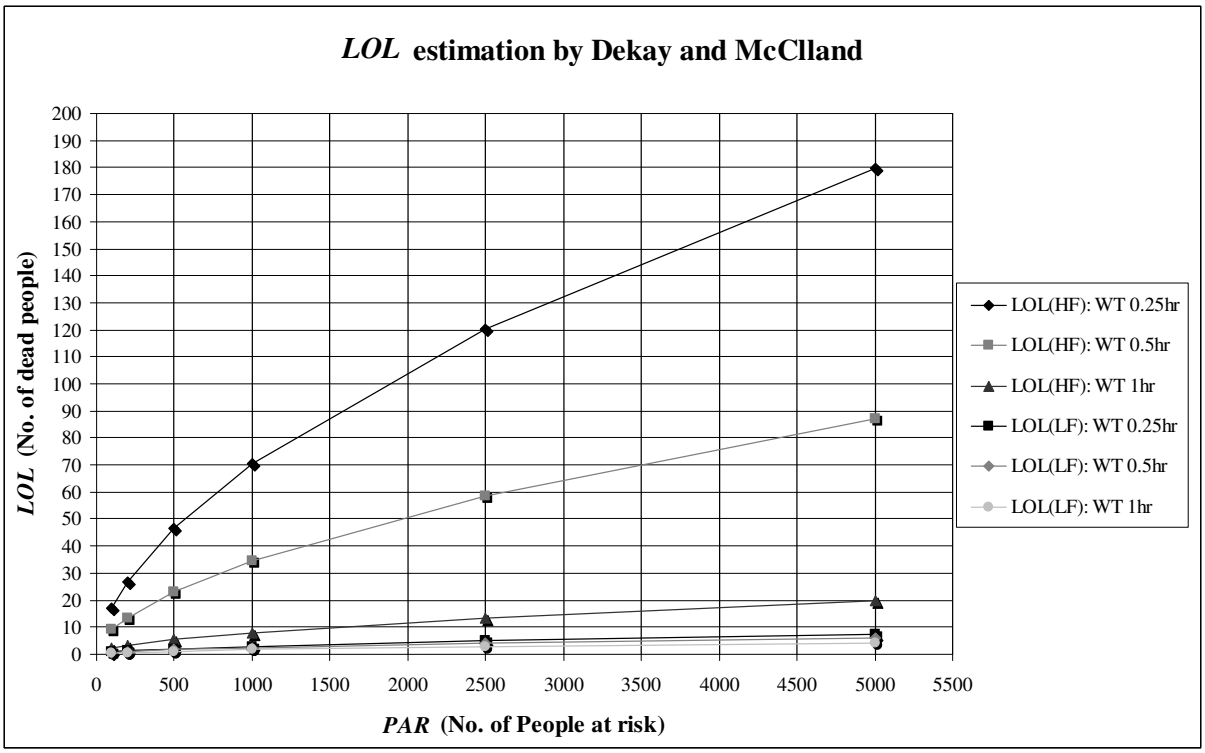

Figure 5.2: Examples of *LOL* estimation by Dekay and McClelland

5.2.3 *LOL* Estimation Method by Graham

After the identification of weaknesses in above mentioned methods, a new method for loss of life estimation was developed by Graham. This method depends on different factors such as flood severity, amount of warning and a measure of whether people understand the severity of the flooding. This method was developed by using a large data set of 40 floods (many due to dam failure). This method provides the suggested *fatality rates (Table 7)* (*Graham (1999)* [33]) based on flood severity, warning and awareness of the people about flood severity. The steps for life loss estimation by this method can be summarized as follows (*Graham (1999)* [33]).

- Determine dam failure scenarios to evaluate
- Determine time categories for which loss of life estimates are needed
- Determine when dam failure warnings would be initiated
- Determine area flooded for each dam failure scenario
- Estimate the number of people at risk for each dam failure scenario and time category
- Use the suggested *fatality rates* to estimate the loss of life
- Evaluate uncertainty

5.2.4 RESCDAM *LOL* Estimation Method

The method follows the principles introduced by (*Graham (1999)* [33]). The generalized equation for the calculation of loss of life due to dam failure flooding is given below, (*Reiter (2001)* [55])

$$LOL = PAR \times FAT_{BASE} \times IMPACT \times CORRFAT \quad (5.6)$$

Where

LOL = Loss of life caused by dam break flood

PAR = Population at risk

FAT_{BASE} = Base fatality rate of *PAR*, mean values from *(Table 7)* (*Graham (1999)* [33])

IMPACT= Additional impact factor to account for flood severity impact (SEV), living environment impact (LOC) and vulnerability impact (VUL) derived in the RESCDAM *LOL* method using public population register information on *PAR*. (Common max. value is 1.5)

CORRFAT= Correction factor to take the warning efficiency and possible emergency/rescue action into account in each sub-area (re-arranged values *(Table 7)* (*Graham (1999)* [33]))

This method includes more factors such as vulnerability factor, living environment factor and rescue factor important for having a good estimation of loss of life as compared to other available methods. But some of these factors should be considered in more detail. Moreover, there are still some other necessary factors that influence loss of life which have not been considered yet. As an extension of this method (equation 5.6), a new method has been developed in order to have more realistic, accurate and meaningful *LOL* estimation.

5.3 DEVELOPMENT OF AN IMPROVED METHOD FOR *LOL* ESTIMATION

Considering the weaknesses and useful ideas in the available methods (as discussed above), an improved and elaborate method for more realistic and precise estimation of life loss due to extreme flooding downstream of the dam has been developed. Depending on the available data of the Jhelum river valley downstream of Mangla dam in Pakistan, different factors have been taken into consideration. The generalized form of the method is as follows by equation (5.7),

$$LOL_i = PAR_i \times FAT_{BASE} \times F_{sv} \times F_{age} \times F_{mt} \times F_{st} \times F_h \times F_{war} \times F_{ev} \qquad (5.7)$$

Where

LOL_i = Loss of life at a particular location " i " downstream of the dam

PAR_i = Population at risk at a particular location " i " downstream of the dam

FAT_{BASE} = Base fatality rate of 0.15 from *(Table 7)* (*Graham (1999)* [33]) for the worst case of medium severity for definition 2 (table 4.1). An average value of 1.0 for all other factors with average conditions is assumed. The other factors could differ from 1.0 depending on the specific available information. These factors have been defined after a qualitative plausibility analysis according to the related information available in the literature.

F_{sv} : Flood severity factor based on flood severity indication (according to the new criterion, e.g. *GA*); it has been defined quantitatively in terms of the probability of life loss due to collapse of buildings.

High Severity	very likely	1.0
Medium Severity	unlikely	0.3
Low Severity	very unlikely	0.1

F_{age} : Age risk factor depending on different age groups in *PAR*; Based on the available data [94], three age groups have been defined, number of people in group *A* (<10yrs+ (>=65yrs)), *B* (10-15)yrs and *C* (15-64)yrs. This factor will change from 1.0 with respect to the likelihood of different age groups to be endangered. According to (*Ramsbottom et al. (2003)* [53]) the risk posed by the old people (relatively weak) depends on the relation between their specific percentage in the project area and their average percentage at national level. In the project area downstream of Mangla dam, the percentage of old people is around the national average percentage [94]. So 25% extra risk (*Ramsbottom et al. (2003)* [53]) has been considered for old people (>=65yrs) and also people with age (<10yrs) combined in group *A* (very weak people) as mentioned in equation (5.8).

No guideline is available about the risk posed by other age categories in group *B* and *C*. So for other age groups, the age risk has been reduced with respect to group *A* accordingly.

A	1+0.25 (0.25 is the extra risk)	1.25 (more than likely)
B	1+0.1	1.1 (likely)
C	1-0.2	0.8 (unlikely)

$F_{age} = 1.25 \times A\% + 1.1 \times B\% + 0.8 \times C\%$ (general form) (5.8)

Obviously this factor would be different for rural, urban and mixed areas. The percentages of different age groups will be used as weighting factors.

F_{mt} : Material risk factor: For flood severity indication, materials that are frequently used for house construction such as concrete, bricks, masonry etc (depending on available references) have been considered. But in the project area, there are also very low strength houses (earth bound with unbaked bricks). In literature such houses are named 'Kucha houses' [94]. The adopted flood severity criteria showed the damage potential for all common types of houses. But there will be certainly extra damage risk for Kucha houses. At the moment, there is no guidance available for the extra risk posed by Kucha type houses. So, it is assumed that extra risk (*Re*) for Kucha houses will be, *Re* = 1+ 0.5, 50% more than the risk for other house types.

$F_{mt} = 1 \times X\% + 1.5 \times Y\%$ (general form) (5.9)

Where, X = % of other types of houses, Y = % of Kucha houses (very low strength houses)
The percentage of Kucha houses is more in rural areas than in the urban areas. In above equation, the percentage of different house types will be used as weighting factor.

F_{st} : Storey risk factor: It is assumed that all types of houses (single and more storeys) will be damaged during high flood severity, because upper storeys can also collapse due to the failure of the ground storey. For medium and low severity cases, more storey houses could provide refuge to people in upper storeys and reduce the overall risk. So the suggested relation for the storey risk factor is,

$F_{st} = 1$ (for high severity and all types of houses)
$F_{st} = 1 - S\%$ (for medium and low severity) (5.10)

Where, S = % of more storey houses

The percentage of more storey houses will be used as weighting factor. In medium and low severity cases, this factor will be different for rural and urban areas.

F_h : Health risk factor: An average value of 1.0 was assumed with FAT_{BASE} for normal healthy *PAR*. According to the available data [94], there are about 3% disabled people in the project area (urban and rural). The overall risk would increase with respect to the percentage of disabled persons. In this case, the extra risk posed by disabled people will be very low but can not be ignored. According to (*Ramsbottom et al. (2003)* [53]) the risk posed by the disabled people depends on the relation between their specific percentage in the project area and their average percentage at national level As in this case, the percentage of disabled people is around the national average percentage [94]. So 25% extra risk for the disabled people has been considered (*Ramsbottom et al. (2003)* [53]).

$F_h = 1 \times H\% + 1.25 \times D\%$ (general form) (5.11)

Where, H = % of *PAR* with avg. health, D = % of disabled *PAR*
The percentage of *PAR* will be used as weighting factor in the equation.

F_{war} : Warning factor depending on the initiation of warning and flood travel time.
It has been defined quantitatively as the likelihood of no rescue for different warning time categories by interpreting Graham's warning definitions. Flood severity understanding for warning issuers defined by Graham has also been combined with the warning.

Warning time	Flood severity understanding	F_{war}
No	No	1
Some (15-60 min)	Vague/unclear	0.7
Adequate (> 60 min)	Precise/clear	0.3

Different warning time categories have been defined by Graham in the following way (*Graham (1999)* [33]).

1- No warning: This means that no warning is issued by the media or official sources in the particular area before the arrival of flood water. Only the possible sight or sound of the approaching flood will be considered as a warning.

2- Some warning: This means that the officials or media start warning in the particular area for 15 to 60 minutes before the arrival of flood water. Some people will be informed about flooding through friends, neighbors or relatives.
3- Adequate warning: This means that the officials or the media start warning in a particular area for more than 60 minutes before the arrival of flood water. Some people will be informed about flooding through friends, neighbors or relatives.

Flood severity understanding describes the ability of the warning issuers to comprehend the severity and the magnitude of the flooding. Depending on the available data and guidelines, the category of *'Many observers at dam'* has been considered for the warning initiation downstream of Mangla dam. (*Graham (1999)* [33])

F_{ev}: Ease of evacuation factor: It will depend on the warning efficiency and the available evacuation facilities, transportation. In principle, this factor would be different for urban and rural areas. Depending on the available data, urban and rural areas have not been considered separately. But more research is required to estimate the ease of evacuation in urban and rural areas. At the moment, no empirical value or guideline is available for ease of evacuation. So this factor has been defined quantitatively as the likelihood of no rescue for all combinations of population at risk (*PAR*) with respect to warning efficiency.

Warning time	Ease of evacuation	F_{ev}
No	No	1
Some (15-60 min)	Some	0.7
Adequate (> 60 min)	Good	0.3

5.4 *LOL* ESTIMATION FOR DIFFERENT FLOODING SCENARIOS

Using the new estimation method, possible *LOL* has been estimated for different flooding scenarios with and without dam failure. The flood routing and flood severity indication results of the flooding scenarios have been used in *LOL* estimation downstream of Mangla dam. Other necessary factors for *LOL* estimation have been discussed in the following sections.

5.4.1 *PAR* Downstream of Mangla Dam

For *LOL* estimation the number of people at risk (*PAR*) was required. According to the available census data (1998) and maps [94], *PAR* was estimated at the locations downstream of Mangla dam. Depending on the extent of flooding and available location of houses on the GIS map, the estimated *PAR* has been approximately related to the 92- flood (peak *Q*: 26,293 m^3/s). No extra information about the location of houses in the flood plains is available for more extreme scenarios. Obviously the population at risk (*PAR*) will be more for higher flooding scenarios.

For scenarios of higher flooding *PAR* has been increased quantitatively at each downstream location with respect to the ratio of flooded area in a higher flooding scenario to the flooded area in 92-flood. The *PAR* downstream of Mangla dam is both rural and urban, where rural *PAR* is more than urban *PAR*. Figure 5.3 shows the number of people at risk downstream of Mangla dam according to 98-census data [94] and the 92-flood event.

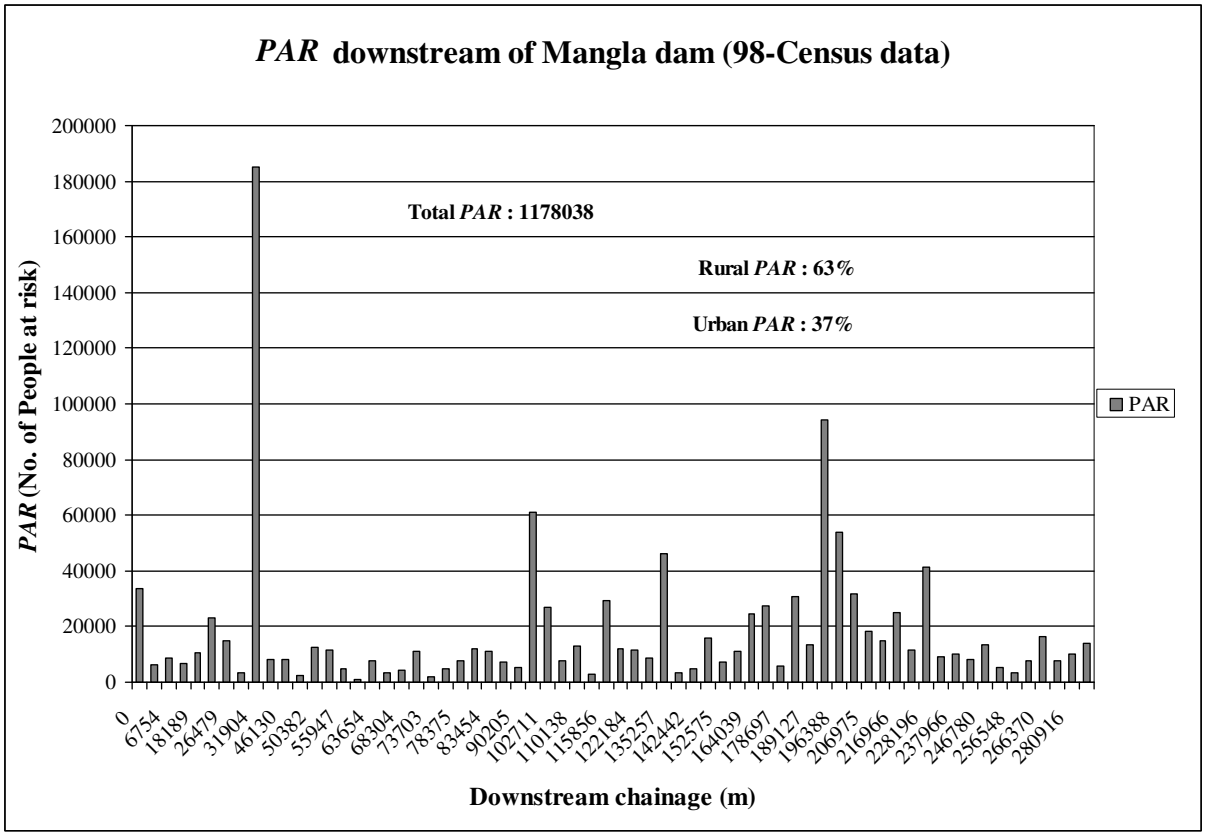

Figure 5.3: *PAR* downstream of Mangla dam (98-census data) and the 92-flood event

5.4.2 *LOL* Factors

Depending on the available data, all factors for loss of life computation have been estimated by following the procedure given by the new *LOL* estimation method. The flood severity factor will change accordingly with respect to the flood severity indication at different downstream locations. The age risk factor will be different for rural, urban and mixed *PAR* depending on the percentages of age groups considered. For the material risk factor the available percentages of Kucha houses in rural and urban areas have been considered. For the storey risk factor the houses with 5 and more rooms in rural areas and houses with 3-4 rooms and 5 and more rooms in urban areas have been considered as more storey houses. The percentage of disabled people in rural and urban areas is about the same. The downstream *PAR* is either rural or mixed. There is no downstream location where only urban *PAR* exists. So the risk factors dependent on *PAR* type have been calculated accordingly. Different categories of warning initiation have been considered for the computation of warning and evacuation factors with respect to the computed flood travel times (*Graham (1999)* [33]).

5.4.3 Results of *LOL* Estimation for Different Flooding Scenarios

In figure 5.4 the total *LOL* estimated for different flooding scenarios (50,000 m^3/s and MDF: 61,977 m^3/s) with and without bridges are shown. These two flooding scenarios have been assumed to be possible dam failure scenarios. Different categories of the warning initiation have been considered. The warning factors for the downstream locations are based on warning initiation and the computed flood travel times. The total loss of life increases with the delay in warning initiation and vice versa. The loss of life is more in case of no bridges due to increase in overall flooding.

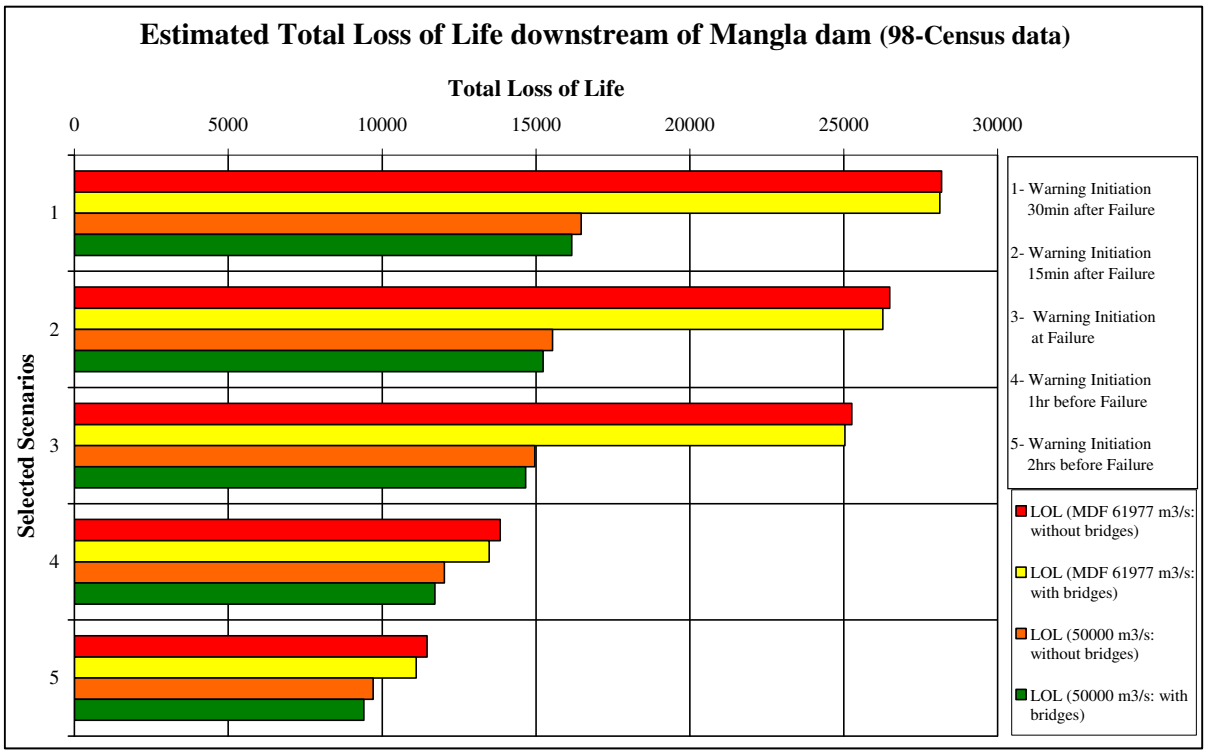

Figure 5.4: *LOL* estimates downstream of Mangla dam for different scenarios

The estimated *LOL* over the reach length downstream of Mangla dam has been shown in figure 5.5. In this case, the *LOL* has been estimated for the worst case of warning initiation of 30 minutes after failure. The major *LOL* occurs up to about 50 km downstream of the dam.

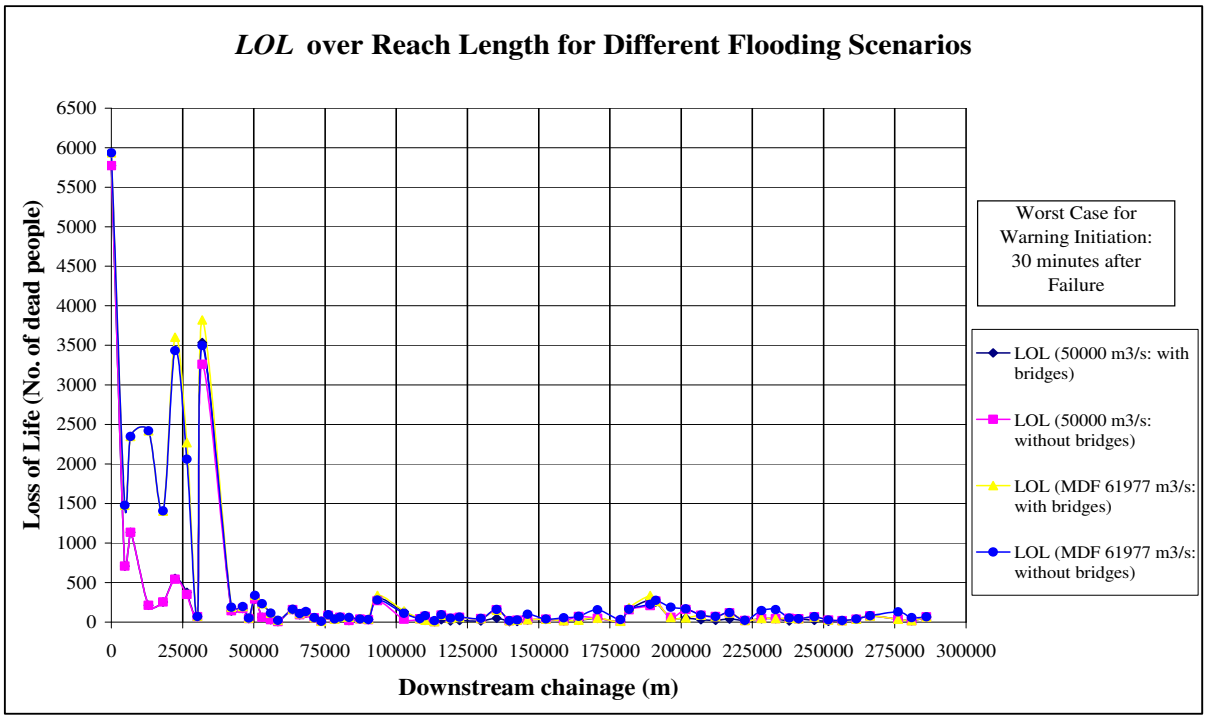

Figure 5.5: *LOL* over reach length for different flooding scenarios

5.4.3 Results of *LOL* Estimation for Dam Failure Cases

Loss of life estimation has been done by using the flood routing results of dam break simulations (sections 3.4 and 3.5). For *LOL* estimation the worst case of warning initiation of 30 minutes after the failure has been considered. Figure 5.6 shows the percentages of total loss of life for different dam failure cases (with and without bridges). The percentage of total loss of life is more in case of no bridges for different failure cases. The percentage of total loss of life has been calculated with respect to the corresponding *PAR* for different failure cases. The increase in *%LOL* is mainly due to increase in flooding which subsequently results in decrease of warning time for higher failure cases. The percentage of total *LOL* is the highest (close to 4%) for the case of maximum failure discharge without bridges. For other failure discharges, the percentages in both cases (with and without bridges) are very close to each other.

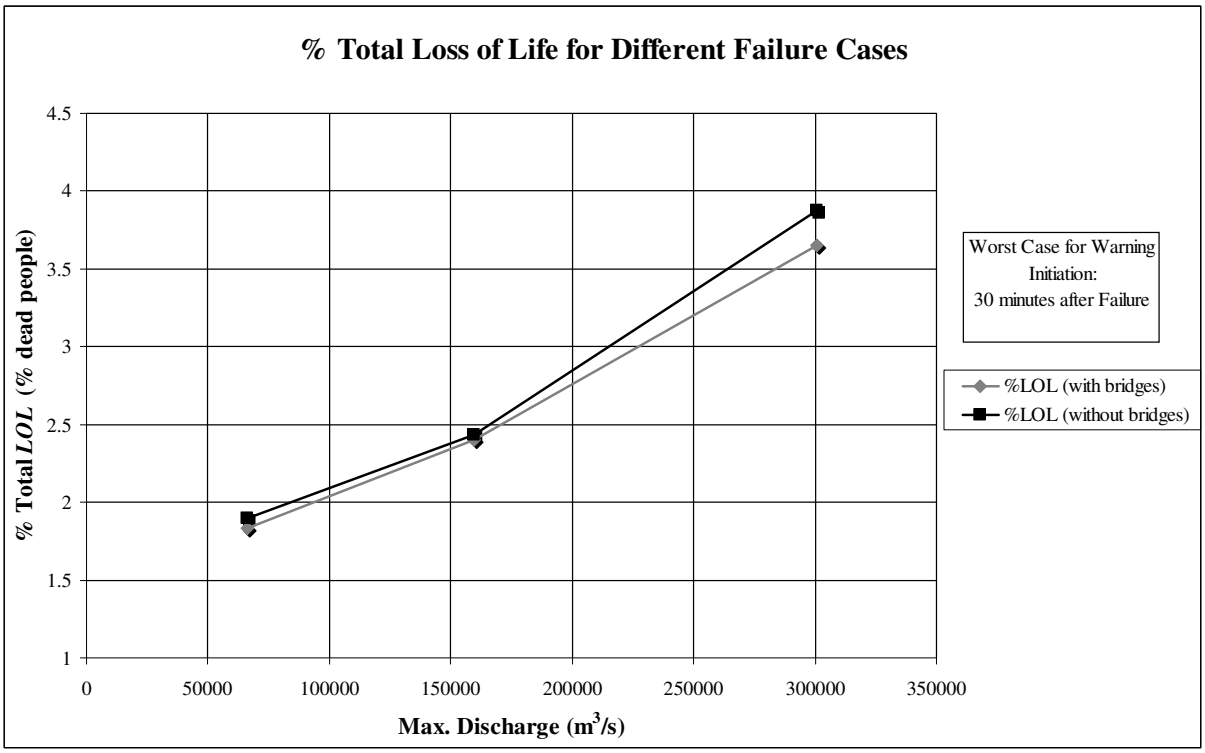

Figure 5.6: % Total loss of life for different failure cases

The estimated loss of life over the reach length for dam failure cases is shown in figure 5.7. In all failure cases the *LOL* at downstream locations (mainly up to first 50 km) is quite higher than the loss of life for other flooding scenarios (figure 5.5).

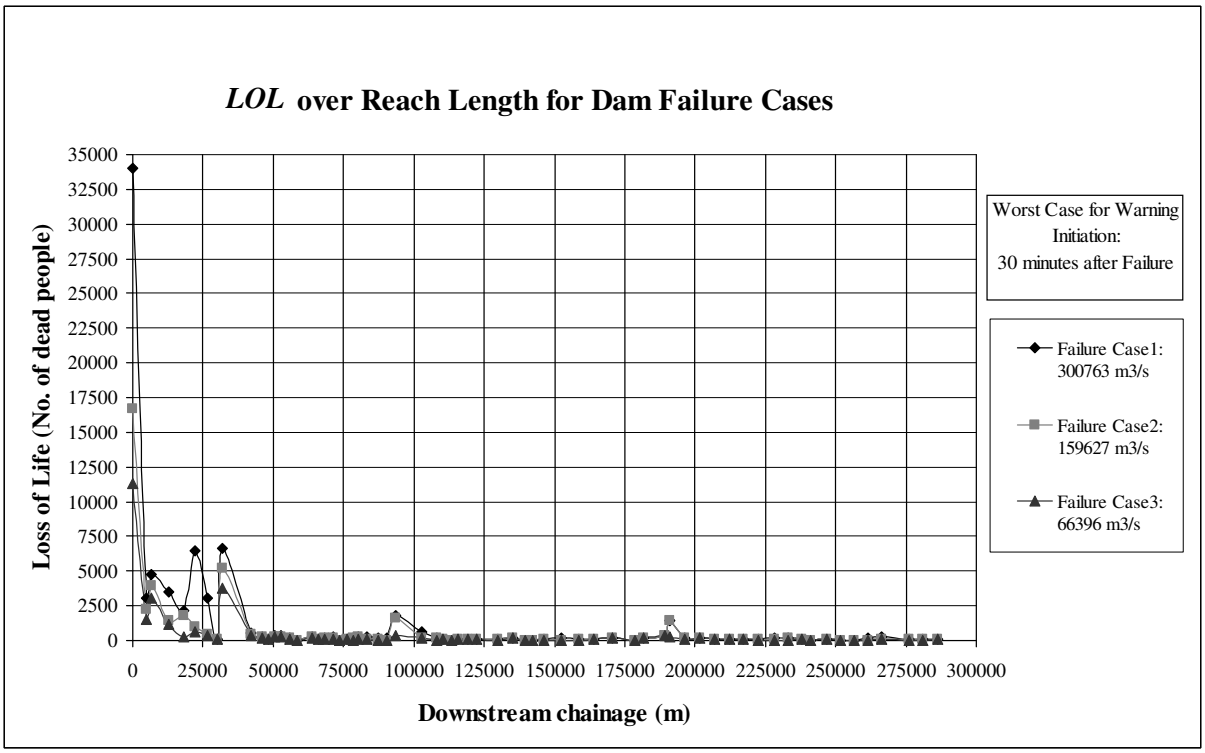

Figure 5.7: *LOL* over reach length for dam failure cases with bridges

5.5 COMPARISON OF *LOL* ESTIMATION METHOD WITH EXISTING DATA

In order to compare the *LOL* estimation method with the existing data, more than 40 past floods mentioned in (*Graham (1999)* [33]) have been taken into consideration. The flood data include population at risk (*PAR*), distance of *PAR* from dam, flood severity information (in terms of *DV*), warning information and fatalities. These data do not fulfill the requirements of this *LOL* estimation method. For the actual validation of this method, detailed authentic information is needed in order to estimate different *LOL* factors. Getting access to reliable data for a specific flood event is very difficult and time consuming. As an attempt, the loss of life due to past floods and computed *LOL* in considered flooding scenarios have been compared with respect to the specific flood severity and warning information. For this purpose, the available data of Brush creek flood (1977) in Kansas City have been considered (*Graham (1999)* [33]) which comprise 2380 people at risk, flood severity (*DV*= 2.3 m^2/s), some warning (categorized by Graham) and 20 deaths. Because only for the Brush creek flood different downstream locations from the considered flooding scenarios with approximately the same flood severities (in terms of *DV*) were found for comparison. The loss of life derived by *PAR* ratio with respect to Brush creek flood at different locations has been compared with the loss of life computed at those locations by the suggested method with the same warning

conditions (as in Brush creek flood). Loss of life in both cases (by *PAR* ratio and computation) is almost the same in different scenarios as shown in figure 5.8. This is not a true validation of this method. As due to unavailability of data, all suggested *LOL* factors have not been taken into account for the considered flood event (Brush creek flood). However, this is an effort to partially validate this method.

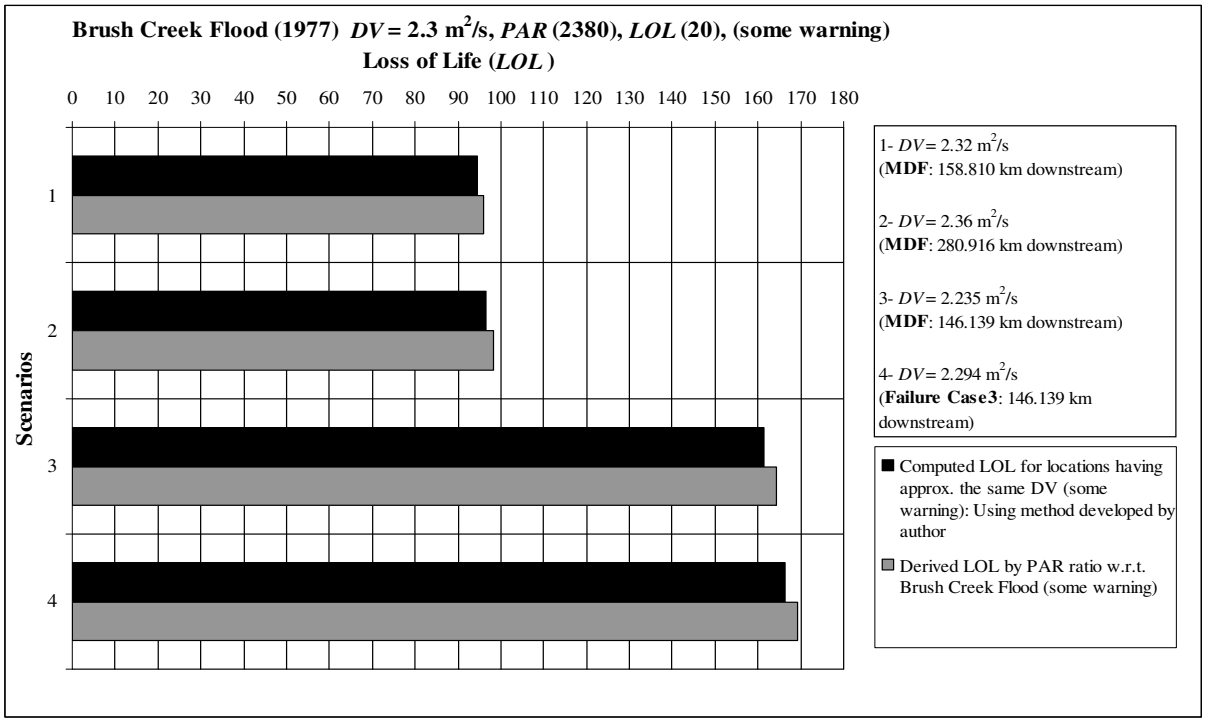

Figure 5.8: Comparison of *LOL* estimation method with existing data

5.6 EXTENT OF *LOL* IN TERMS OF THE DOWNSTREAM DISTANCE

In the literature, there is no exact guideline available about the extent of life loss downstream of the dam due to dam failure. There are some statements available about small and very large dams which are based on the empirical data of past events. The extent of loss of life has been discussed in terms of the downstream distance mainly for smaller dams. Based on the available data base of small dams, different predictions have been made for the possible extent of life loss downstream of very large dams. Some of these past predictions can not be considered to be correct due to the unavailability of data for very large dams. This study provides realistic and precise estimation of possible loss of life downstream of the very large Mangla dam in Pakistan for different dam failure cases. The results of this study verify some predictions and also adjust some ideas about the possible extent of life loss downstream of very big dams due to dam failure.

5.6.1 Verification of Some Predictions

Based on the dam failure data, it was stated by Graham that a high percentage of life loss due to dam failure occurs in the first 25 km downstream of the dam. Further it was said that for smaller dams this downstream distance is considerably less than 25 km. It was also predicted that there may be some very high dams or those storing very large quantities of water where severe flooding could extend to 161 km or more downstream of the dam. In these cases, the loss of life studies may be extended for more than 50 km downstream of the dam. (*Graham (1999)* [33]) The above statements have been verified by this study as explained in the following.

- Firstly, this study verifies the general statement of Graham about the occurrence of high percentage of life loss due to dam failure in the first 25 km downstream of the dam. In figure 5.9, it is clearly shown that about 68% of the total loss of life occurs up to 25 km downstream of Mangla dam for different failure cases.

- Secondly, the results of this research clearly verify that for very high dams with very large storage capacity severe flooding could extend to 161 km or more downstream of the dam. In this study Mangla dam in Pakistan has been considered as one of the large earth and rock-fill dams in the world. The extension of flood severity up to 286 km in the Jhelum river valley downstream of Mangla dam for different failure cases has been illustrated in figures 3.22 and 4.7.

- Thirdly, this study also verifies the prediction about the extension of loss of life studies for more than 50 km downstream of the dam. In this research life loss estimation has been done for 286 km of the Jhelum river valley downstream of Mangla dam as shown in figure 5.9.

5.6.2 Adjustments to Earlier Predictions

This study also adjusts some past predictions about the extent of life loss downstream of the dam due to dam failure. Graham stated that generally the life loss for more than 50 km

downstream of a dam should be very small as compared to the life loss estimated for the areas closer to the dam. Further it was stated that the life loss from 50 km to onwards downstream of the dam would not change the results of the dam safety recommendation (*Graham (1999)* [33]). The contradiction has been described in the following.

- The results of this study clearly contradict the Graham's statements about the extent of life loss for more than 50 km downstream of a dam. In this study the estimated loss of life for more than 50 km downstream of Mangla dam is not very small. The loss of life up to 50 km downstream of Mangla dam is about 80% of the total loss of life for different failure cases as illustrated in figure 5.9. The 20% life loss occurs after 50 km up to 286 km downstream of the dam. The life loss increases to 90% of the total loss of life up to 100 km downstream and then the remaining 10% occurs up to 286 km downstream. The loss of human beings is the most severe damage due to extreme flooding downstream of a dam with or without dam failure. In figure 5.9, the life loss of 20% after 50 km downstream shows considerable number of fatalities for different dam failure cases.

- Finally, this 20% loss of life after 50 km downstream to onwards 286 km can not be ignored for dam safety studies of very large dams like Mangla dam. It will certainly influence the results of a dam safety recommendation. This study emphasizes the consideration of possible loss of life due to dam failure for more than 50 km downstream of very large dams for any dam safety recommendation.

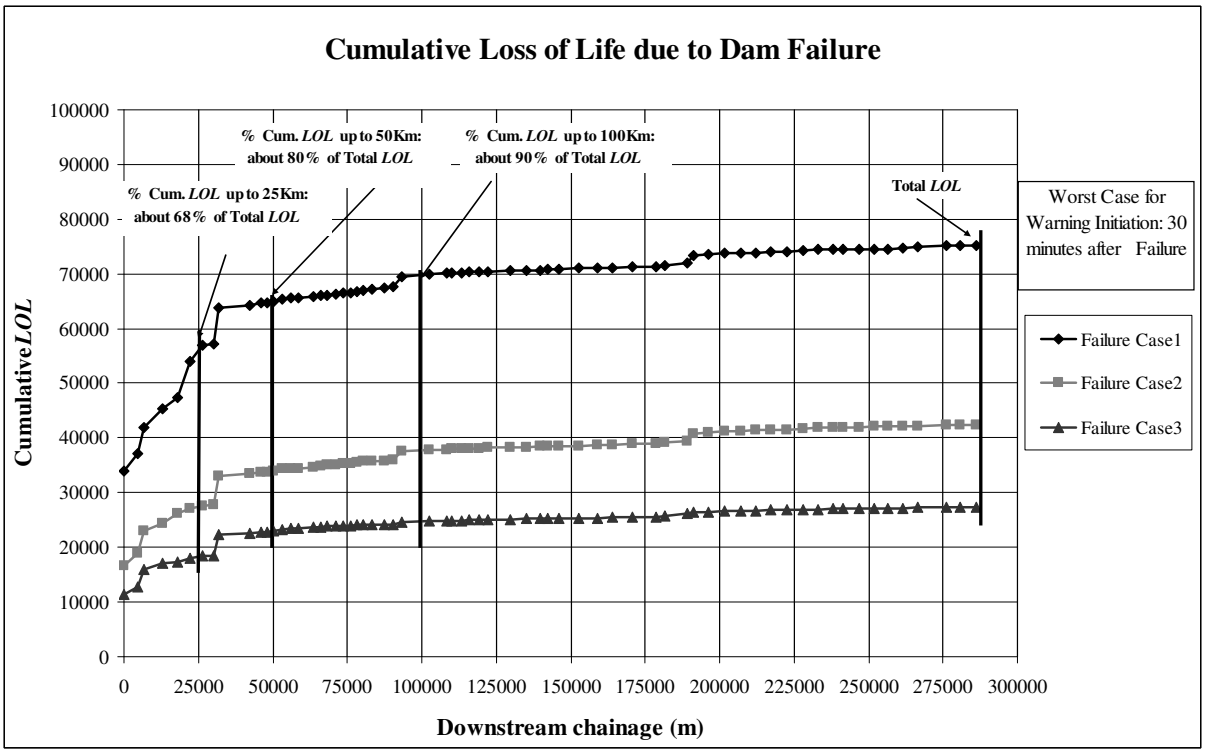

Figure 5.9: Cumulative loss of life due to dam failure (with bridges)

5.7 RISK DETERMINATION

The residual risks for Mangla dam have been determined for different dam failure cases. By definition, risk is the combination of the probability of occurrence and possible consequences (damages). It can be categorized in two ways (*ANCOLD (2003)* [3]), (*ANCOLD (1994a)* [4]), (*ANCOLD (1994b)* [5]), (*Bowles (2007)* [10]), (*McDonald (1999)* [44]), (*Ramsbottom et al. (2003)* [53]):

- Individual risk
- Societal risk

In the following, both types of risks have been discussed separately.

5.7.1 Individual Risk

Individual risk is the frequency at which an individual may be expected to sustain a given level of harm (loss of life in this case) from the occurrence of specific hazards. It is computed by averaging the probable risk of life loss over the population at risk (*PAR*) in a particular area

due to a specific event. The annual individual risk can be calculated by equation (5.12) (*ANCOLD (2003)* [3]), (*McDonald (1999)* [44]), (*Ramsbottom et al. (2003)* [53]).

Individual risk/year = (Total *LOL*/Total *PAR*)* Annual probability of occurrence (5.12)

In this case, the individual risk per year has been computed for different dam failure cases with respect to the overall annual failure probability of *2.63 E-3* (chapter 2) and estimated *LOL* for different failure cases. Figure 5.10 shows the computed individual risk per year for the considered failure cases of Mangla dam.

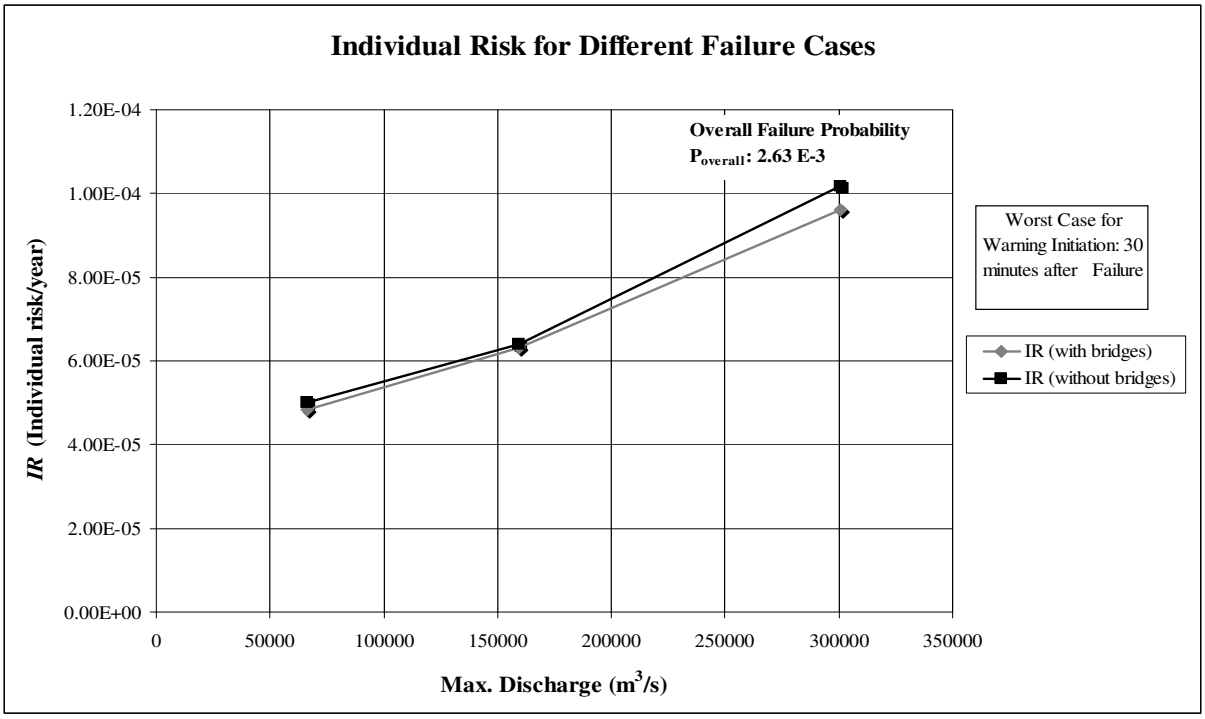

Figure 5.10: Individual risk for different failure cases of Mangla dam

According to the recent guidelines of Australian National Committee on Large Dams (ANCOLD) the limit of individual tolerable risk for existing dams is 1 in 10,000/year (*ANCOLD (2003)* [3]), (*Bowles (2007)* [10]). ANCOLD guidelines consider the ALARP principle (as low as reasonably practicable) which emphasizes the further reduction of residual risks (*Bowles (2004)* [11]), (*Bowles (2003)* [12]). As shown in figure 5.10, the individual risk per year for the worst case of dam failure is exceeding the maximum limit of ANCOLD and it can be considered to be intolerable or unacceptable for Mangla dam. For the other two cases of dam failure the annual individual risk is tolerable as it is within the limits (1.0 E-4).

5.7.2 Societal Risk

Societal risk is the relationship between the failure probability and the number of people suffering from a given level of harm (loss of life) in a given population due to specific hazards. It is determined by the F-N chart, where F is the cumulative frequency of events per year (failure probability of dam) and N is the number of fatalities due to dam failure (*ANCOLD (2003)* [3]), (*Bowles (2007)* [10]), (*McDonald (1999)* [44]).

In this case, the overall failure probability of Mangla dam (*2.63 E-3*) has been considered for the determination of the societal risk by the F-N chart. Figure 5.11 shows the F-N chart for societal risk according to recent guidelines of societal tolerable risk by (*ANCOLD (2003)* [3]) for existing dams. The dark black line shows the limit of tolerability. Risks are tolerable only if they satisfy the ALARP principle, 'reducing risks as low as reasonably practicable' (ALARP). ALARP is the main consideration in fulfilling the requirements for tolerability of risks under common law legal systems (*Bowles (2007)* [10]), (*Bowles (2004)* [11]), (*Bowles (2003)* [12]).

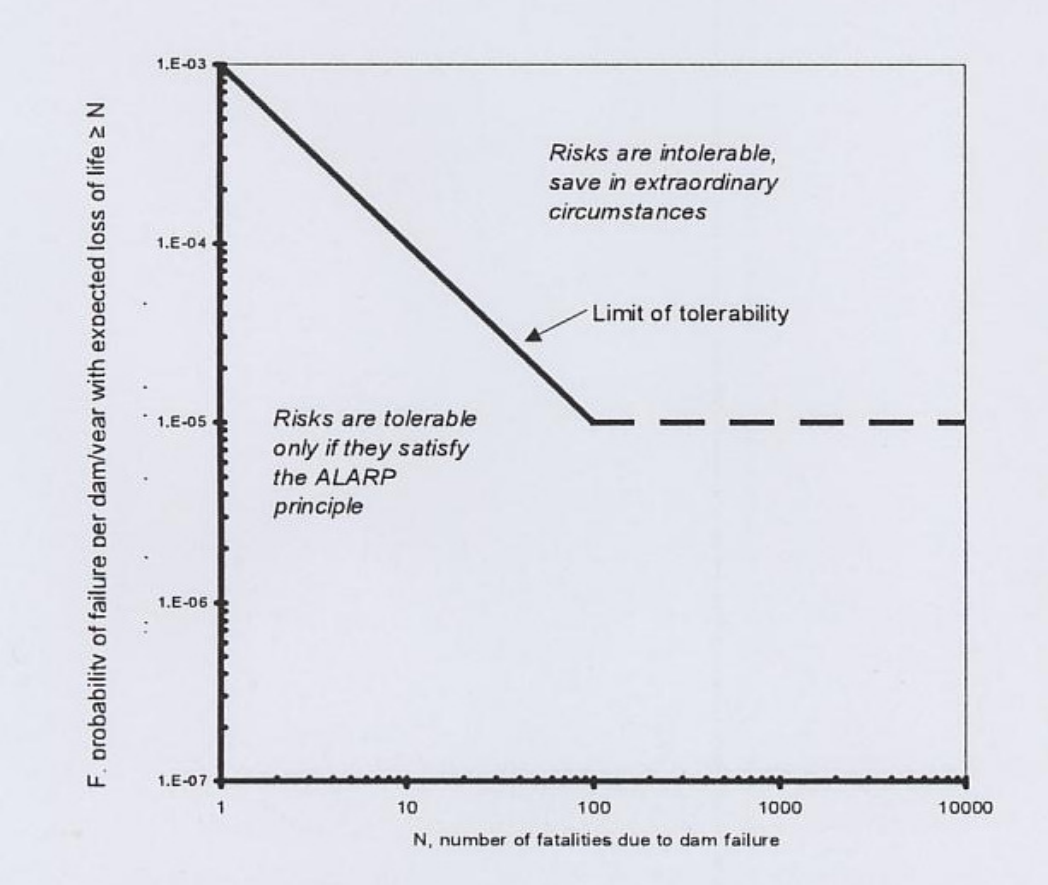

Figure 5.11: ANCOLD (2003) Societal risk guideline for existing dams [10]

The computed overall failure probability is beyond the probability limit given in F-N chart. Moreover, the total loss of life (number of fatalities) in all dam failure cases is also very high as shown in figure 5.9. Actually the dam was built with the safe design principles available in the past in order to fulfill the risk safety requirements in future. But now due to more advancement in research, the risk safety standards have become more severe for dams with respect to extreme events. According to the current standards, the societal risk for Mangla dam is not in the acceptable limits due to high probability of failure and loss of life in all failure cases. It is strongly recommended that the existing risk reduction measures (structural and non-structural) for Mangla dam should be improved and new measures should also be introduced to minimize the possible residual risks (individual and societal) due to dam failure.

5.7.3 Possible Reduction in Societal Risk

Both the failure probability and expected loss of life are very crucial for the determination of societal risk. In order to have a clear understanding, possible reduction in societal risk has been analyzed. This analysis will be helpful for planning new dams in Pakistan as well as in other parts of the world. In this case, the societal risk for Mangla dam is unacceptable due to high overall probability of failure and estimated loss of life. The overall failure probability of Mangla dam (*2.63 E-3*) is based on the annual failure probabilities of the following considered scenarios (detail in chapter 2).

- Overtopping failure of main dam (by MDF): Pr = 1.06 E-3
- Geotechnical strength failure of main dam (by MDF): Pr = 1.04 E-3
- Main dam failure by liquefaction in fill (by MCE): Pr = 5.0 E-5
- Structural failure of main spillway (by MDF): Pr = 4.65 E-4
- Structural failure of main spillway (by MCE): Pr = 1.20 E-5

$$P_{overall} = P_{MDF} + P_{MCE} = 2.56\text{ E-}3 + 6.20\text{ E-}5$$

$$\mathbf{P_{overall} = \ 2.63\ E\text{-}3}$$

The computed overall probability of failure is quite high mainly due to very high annual exceedance probability (AEP) of MDF (*6.41 E-3*) used in the probability computation by event trees in three failure scenarios (by MDF) mentioned above. Ideally the AEP of the maximum design flood (MDF) should be quite low as expressed in table 5.1 (*McDonald (1999)* [44]).

Table 5.1: Recommended design flood exceedance probabilities by ANCOLD [44]

Incremental Flood Hazard Category	Annual Exceedance Probability (AEP)
High	PMF to 1 in 10,000
Significant	1 in 10,000 to 1 in 1000
Low	1 in 1000 to 1 in 100

The MDF for Mangla dam is considered to be the probable maximum flood (PMF), 61,977 m^3/s. So it has been considered in the 'High' category as shown in table 5.1. Different overall failure probabilities have been computed by using event trees with different lower annual probabilities of MDF in the respective failure scenarios.

The conditional probabilities have been kept the same as discussed in chapter 2. Only the AEP of MDF has been changed for different scenarios. Table 5.2 shows different overall failure probabilities with respect to different annual probabilities of MDF as initiating event in respective scenarios. The computed failure probabilities of the scenarios by MCE (maximum credible earthquake) have not been changed.

Table 5.2: Overall failure probabilities with different lower annual probabilities of MDF

Considered Annual Exceedance Probability for MDF (Initiating event)	Total Annual Failure Probability of the Scenarios by MDF	Total Annual Failure Probability of the Scenarios by MCE	Overall Annual Failure Probability
1.0E-4	4.00E-5	6.20E-5	1.02E-4
1.0E-5	4.00E-6	6.20E-5	6.60E-5
1.0E-6	4.00E-7	6.20E-5	6.24E-5
1.0E-7	4.00E-8	6.20E-5	6.204E-5
1.0E-8	4.00E-9	6.20E-5	6.20E-5

The overall failure probability reduces with the decrease in the AEP of MDF and comes in the range of the F-N chart for societal risk (figure 5.11). For societal risk, the overall failure probabilities mentioned above cross the limit of tolerability due to very high loss of life (number of fatalities) estimated for different dam failure cases (figure 5.9).

Figure 5.12 illustrates the societal risk with different overall failure probabilities based on different AEPs of MDF. Obviously the societal risk for very big dams could be very high due to higher expected loss of life.

For very big dams, if the failure probability is less than 1.0 E-5 then the societal risk can be considered to be tolerable even with the expected number of fatalities of more than 10,000. For smaller dams, comparatively high probability of failure and expected loss of life under the limit of tolerability could result in tolerable societal risk. The expected loss of life could be quite higher due to the failure of very big dams as compared to smaller dams. Societal risk for new dams can be reduced by considering the failure probability in tolerable range for dam design (based on acceptable AEP of possible hazards) and planning necessary structural and non-structural risk reduction measures to reduce the possible loss of life in case of dam failure.

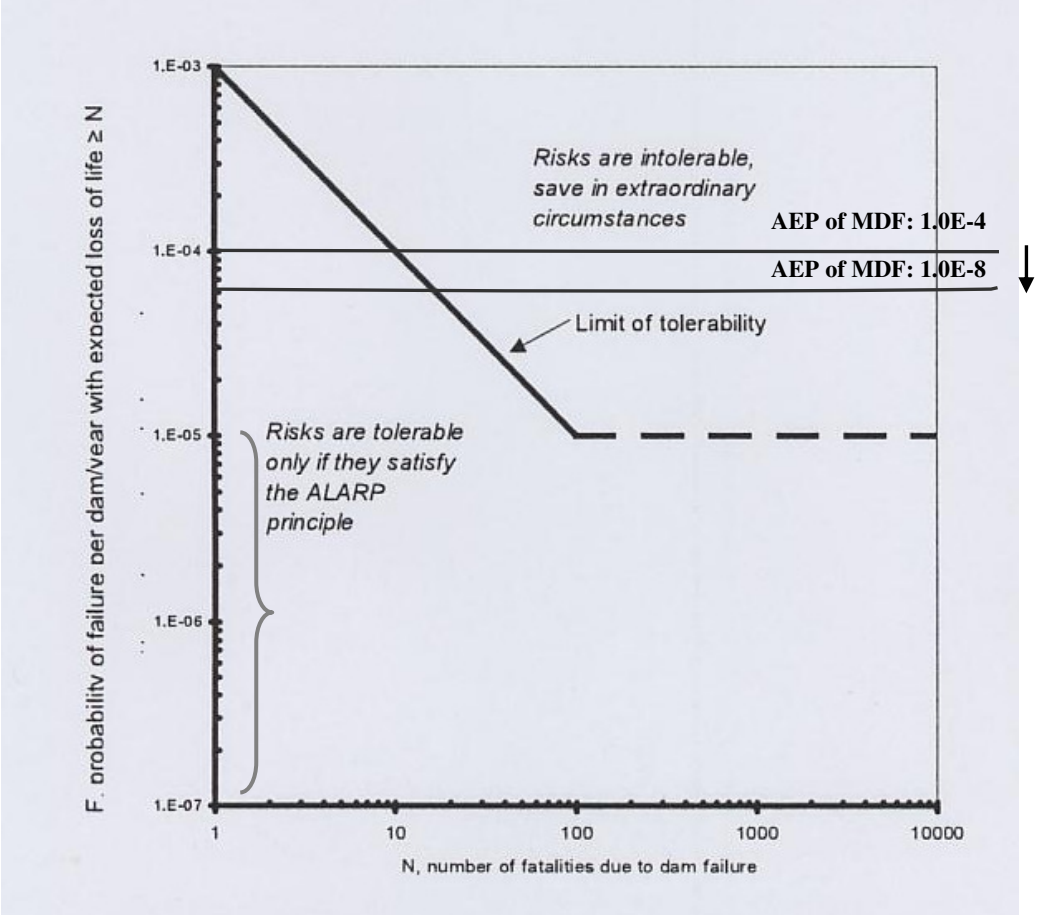

Figure 5.12: Societal risk with different annual probabilities of MDF

5.8 SUMMARY

Different available *LOL* estimation methods have been discussed. For more realistic and precise estimation a new method for *LOL* estimation has been developed. Different flooding scenarios have been considered for loss of life estimation downstream of the dam. The maximum percentage of possible *LOL* estimated for the worst case of dam failure is close to 4% of total *PAR* which seems to be very high. The *LOL* estimation method has also been compared with the existing data of past floods (detail in section 5.5). The extent of loss of life in terms of downstream distance has been determined. This study verifies and also adjusts some past predictions about the extent of possible *LOL* downstream of the dam due to dam failure (detail in section 5.6).

Moreover, the individual and societal risks for Mangla dam due to dam failure have been analyzed by considering the overall failure probability and estimated loss of life. Individual risk per year for the worst case of dam failure exceeds the limit of individual tolerable risk (1 in 10,000) given by (*ANCOLD (2003)* [3]). Also, the societal risk of Mangla dam is not allowable due to high overall probability of failure and estimated loss of life. The possible reduction in societal risk with respect to overall failure probability has also been discussed. This risk determination gives useful information about the magnitude of possible risks due to dam failure for other very big dams like Mangla dam (section 5.7). It also gives an insight to reduce the residual risks for new dams in Pakistan as well as in other parts of the world. For existing dams the residual risks (individual and societal) due to dam failure can be minimized by improving the existing risk reduction measure and also by adopting new enhanced structural and non-structural risk reduction measures. But for new dams these risks can be reduced by considering the dam failure probability in tolerable range for dam design (based on the acceptable AEP of possible hazards) and planning proper structural and non-structural risk reduction measures. For Mangla dam the specific high residual risks due to dam failure can be decreased by the following measures,

- Relocation of the people living near flood plains to safe places
- Increase in the flood severity understanding of *PAR* (mostly rural)
- Proper repair and improvement of the existing safety measures like dikes, bunds, levees etc.
- Enhancement in the warning efficiency and evacuation planning

6 IMPACT OF DIFFERENT CHANGES IN THE VALLEY SHAPE ON POSSIBLE *LOL*

6.1 INTRODUCTION

According to *LOL* estimation in the previous chapter, the residual risks for Mangla dam due to dam failure are not permissible. For other dams in the world the residual risks could be different with respect to the possible *LOL* in extreme cases. The downstream valley shape strongly affects the loss of life in case of extreme flooding. For different valley shapes downstream of the dams the loss of life will be different. In order to generalize the computed loss of life results of Jhelum river valley downstream of Mangla dam also for other river valleys in the world, the impact of downstream valley shapes on loss of life has been analyzed. For this purpose, different changes in the valley shape downstream of Mangla dam have been suggested. First the Jhelum river valley has been classified according to the available river classification systems and then artificial new valley shapes have been produced. Unsteady flow simulations have been run for different scenarios of the suggested changes in the valley shape. The *LOL* estimation has been done for different scenarios of valley shapes by using the new *LOL* estimation method (section 5.3).

6.2 RIVER CLASSIFICATION SYSTEMS

Different classification schemes have been developed based on different purposes. The categorization of river systems by channel morphology is justified in order to achieve to some extent the following objectives (*Rosgen (1994)* [59]).

- Predict the behavior of a river from its appearance
- Develop specific hydraulic and sediment relations for a given morphological channel type and state
- Provide a mechanism to extrapolate site-specific data collected on a given stream reach to those of similar character
- Provide a reliable frame of reference of communication for those working with river systems in a variety of professional disciplines

River classification systems are very important for knowing the features of a river valley. They provide useful guidelines for understanding the geometry of river cross-sections. Different important parameters of the river valley can also be calculated according to these classification systems. In this research, different river classification systems have been studied in order to classify the Jhelum river valley downstream of Mangla dam. Then different changes in the important shape parameters of the downstream valley have been suggested which could affect the possible loss of life due to extreme flooding downstream of the dam. In the following, river classification systems by (*Rosgen (1994)* [59]), (*Rosgen (1996)* [60]) and (*Montgomery and Buffington (1993)* [45]) have been discussed.

6.2.1 Rosgen Classification System

The Rosgen stream classification system is based on a hierarchical approach. The advantage of hierarchical assessment is that it provides the physical, hydrologic and geomorphic context for linking the driving forces and response variables at all scales of inquiry (*Rosgen (1996)* [60]). The hierarchical approach is a process-based procedure. It was developed by formulating morphological process relationships at the reach level and then determining how to extrapolate these relationships to a larger scale (*Rosgen (1996)* [60]). The hierarchical system has four levels of assessment, *Level I* to *Level IV* (figure 6.1). These levels start at a broad geomorphic scale and progress down to a detailed-specific description and assessment. The level of required data collection and analysis increases as the resolution improves through the levels. (*Patterson (2003)* [51]), (*Rosgen (1994)* [59]), (*Rosgen (1996)* [60])

- ***Level I*** is defined as the broad geomorphic characterization level. This level characterizes the stream on the broad scale by integrating the landform and valley morphology with the channel relief, channel pattern, shape, and dimension. The required data for this level can be taken from topographic and landform maps and aerial photography.
- ***Level II*** is defined as the morphological description level. This level is more detailed than *Level I*. In this level, measured field data of reference reaches are used for the morphological description of the stream types. These data include channel entrenchment, dimensions, patterns, profile and boundary materials. *Level II* provides consistent quantitative morphological assessment at a higher resolution than *Level I*.

- ***Level III*** describes the existing condition or state of the stream. This classification level is reach and feature specific. The existing condition is based on the stability, response potential and function of the stream. Additional field parameters, such as riparian vegetation, sediment supply, flow regime, etc. are measured in the field for this classification level.
- ***Level IV*** is defined as the validation level. Field measurements are made to verify process relationships inferred in the preceding levels of assessment. These relationships are specific to the respective stream type. These relationships can be used to interpret data from gauge stations and research sites for similar stream types.

In this study, *Level I* and *Level II* have been considered to suggest possible changes in the valley shape.

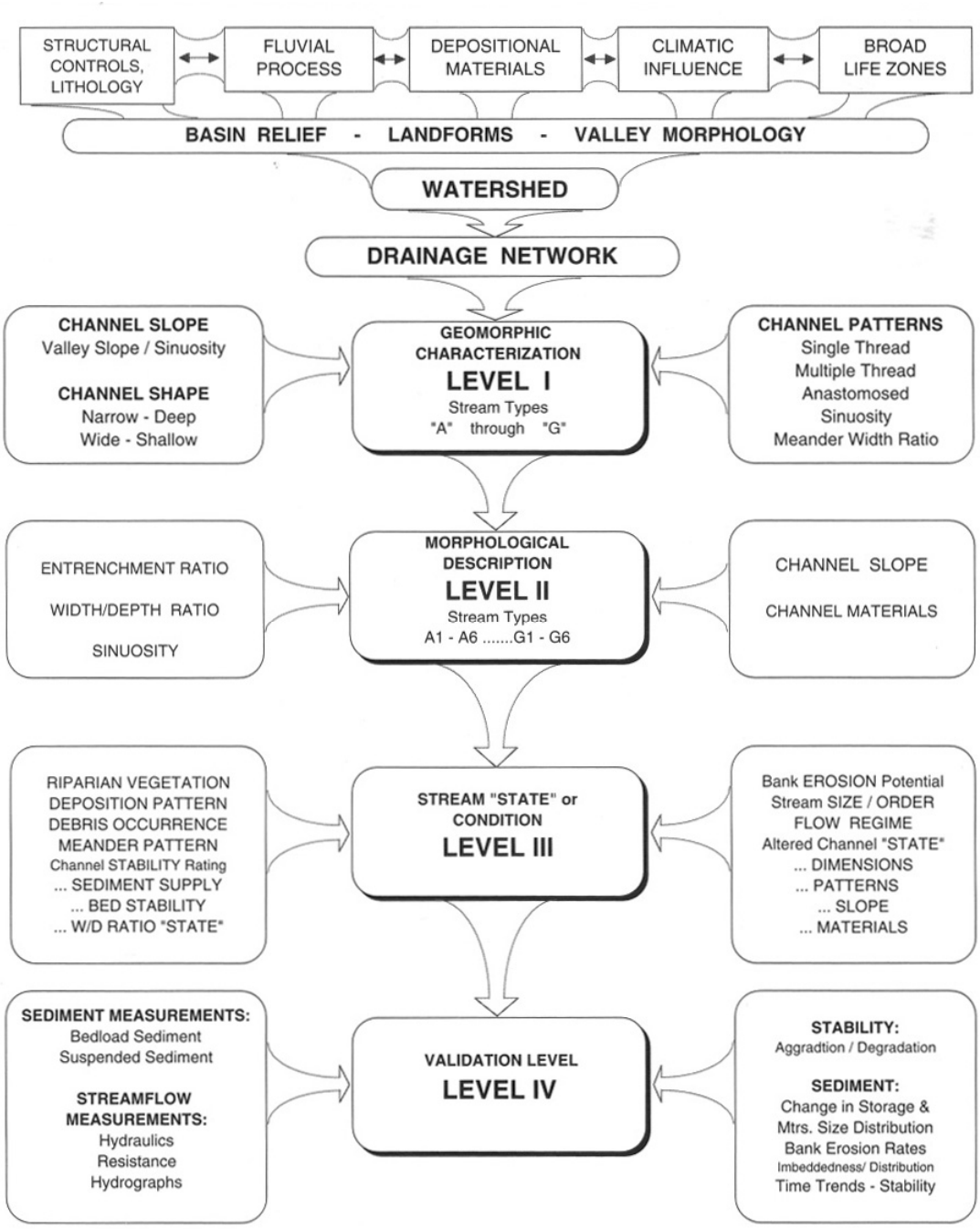

Figure 6.1: Rosgen Hierarchy [60]

Collectively, the classification of natural rivers by Rosgen with respect to different important parameters is illustrated in figure 6.2.

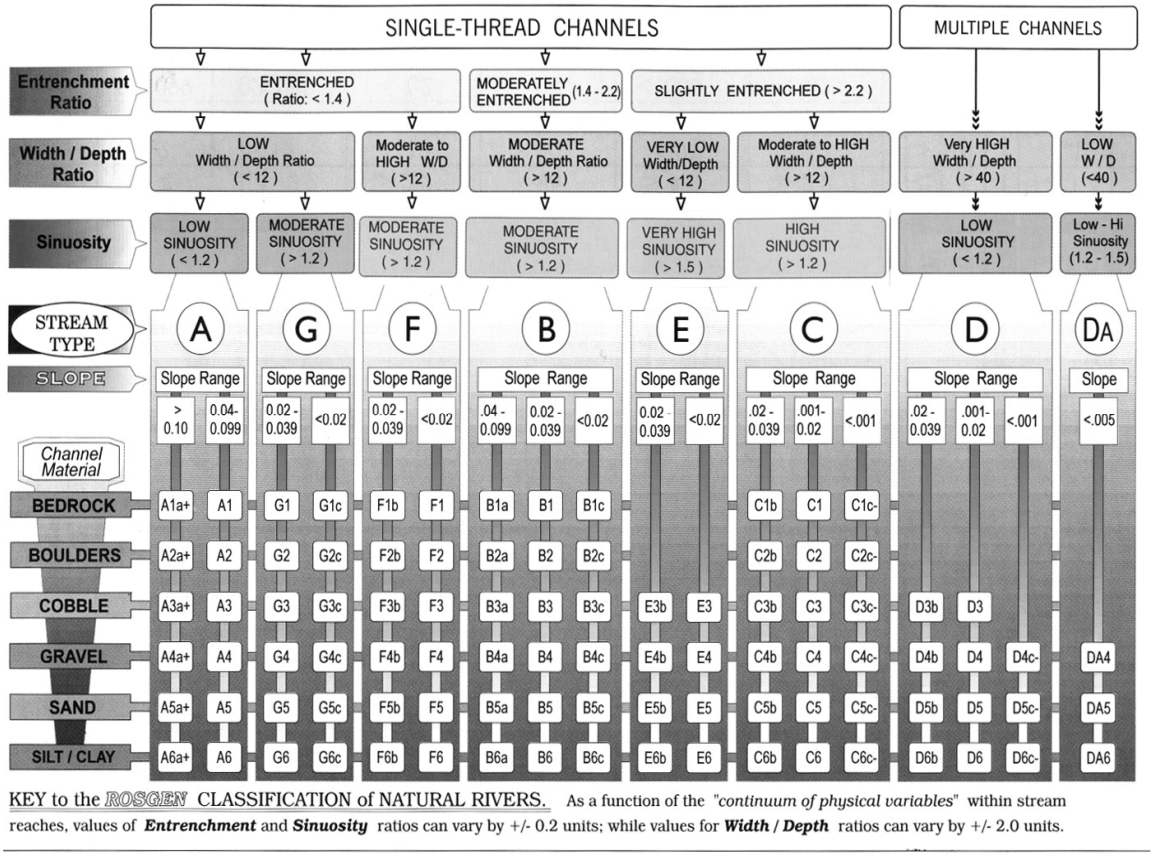

KEY to the ROSGEN CLASSIFICATION of NATURAL RIVERS. As a function of the "*continuum of physical variables*" within stream reaches, values of ***Entrenchment*** and ***Sinuosity*** ratios can vary by +/- 0.2 units; while values for ***Width / Depth*** ratios can vary by +/- 2.0 units.

Figure 6.2: The key to Rosgen classification of natural rivers [60]

6.2.2 Montgomery and Buffington Classification System

The Montgomery and Buffington classification system is a classification of landscape and channel form that gives a base for interpreting channel morphology, assessing channel condition and predicting response to natural and anthropologic disturbance. Channel types are defined based on channel morphology, sediment transport processes and sediment flux characteristics as controlled by hydraulic discharge and sediment supply. It uses maps and aerial photos to classify reach boundaries by estimating stream gradients, degree of valley confinement, channel meander patterns and significant changes in predominant rock types. (*Montgomery and Buffington (1993)* [45]), (*Patterson (2003)* [51])

Montgomery and Buffington channel classification includes a range of scales over which various factors affect channel characteristics. A natural division of scales that shows differences in processes and controls channel morphology is given by geomorphic province, watershed, valley segment, channel reach and channel unit scales. Channel morphology at

each of these scales is associated, but represents different levels of resolution. Each level of this spatial hierarchy gives a framework for comparing channels at finer scales.
(*Montgomery and Buffington (1993)* [45]), (*Patterson (2003)* [51])

***Geomorphic Province Level**:* Geomorphic provinces are areas of comparable landforms that have hydrologic, erosional and tectonic processes. Geomorphic provinces are likely to be surrounded by major physiographic, climatic and geological features. They are useful for stratifying areas where similar watersheds might be found. Most watersheds within a geomorphic province have comparatively the same controls on channel processes and morphology.

***Watershed Level**:* A watershed can be separated into hill slopes and valleys. The different hill slopes and valley morphologies will indicate fundamental differences in sediment production and transport processes. Hill slopes are the undivided portions of the landscape that are zones of sediment production and transport. Valleys are regions of the landscape that take runoff and sediment transport through down slope.

***Valley Segment Level**:* Valley segments define parts of the valley with similar morphologies and governing geomorphic processes. The system recognizes three kinds of valley reaches: colluvial, bedrock and alluvial. Colluvial, bedrock and alluvial valleys are classified based on dominant types of sediment input and transport processes (*Bisson and Montgomery (1996)* [8]).

***Channel Reach Level**:* Montgomery defines a reach as “a length of channel that exhibits a consistent association of bed forms or channel units and is many channel widths long.” The boundaries of the reaches are based on average gradient and apparent degree of valley confinement. A change in slope may specify a reach boundary. There are different categories used by Montgomery and Buffington to differentiate between channel types; predominant bed material, bed form pattern (sinuosity), dominant roughness elements, dominant sediment sources, typical slope, typical confinement and pool spacing.

Figure 6.3 illustrates an idealized stream showing the general distribution of channel types from the hilltop down through the channel network (*Montgomery and Buffington (1993)* [45]).

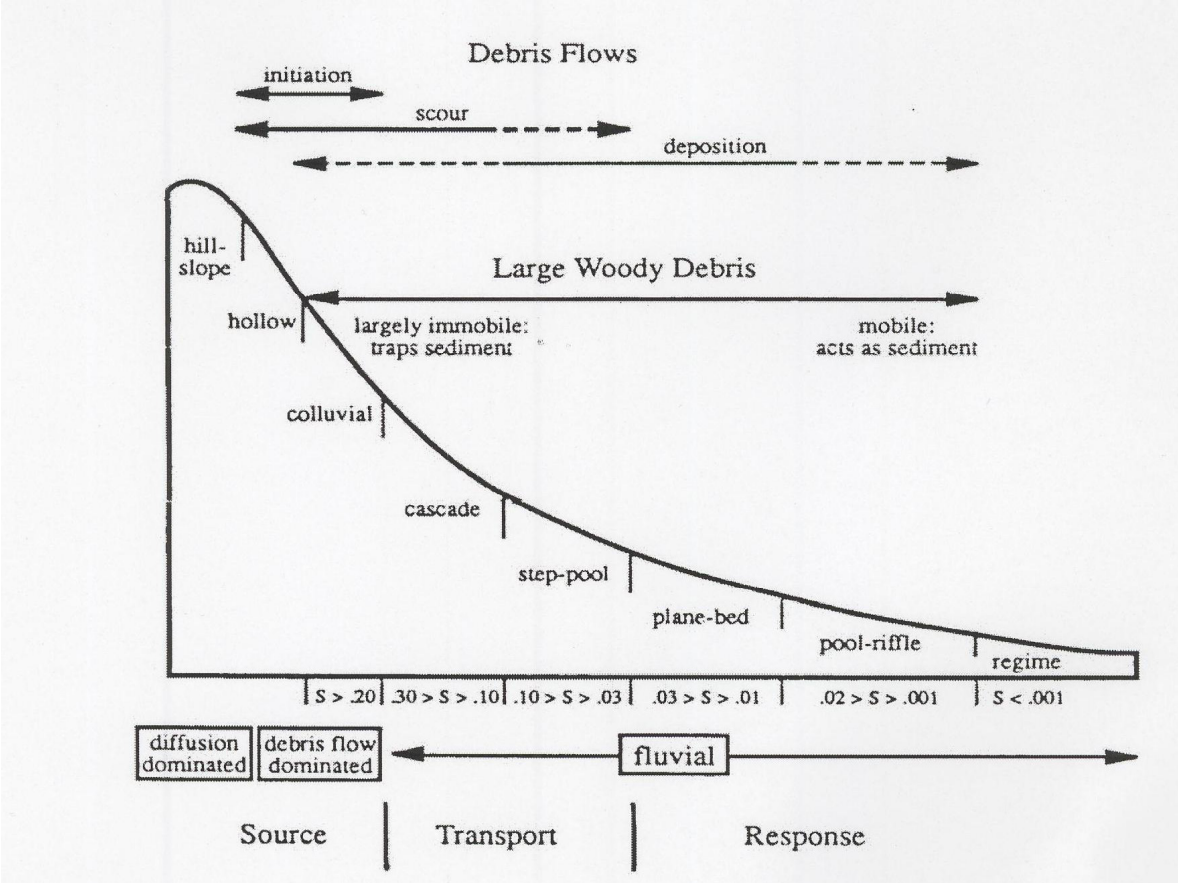

Figure 6.3: Idealized stream showing the general distribution of channel types [45]

From the above discussion, the description of slope categories for different channel types by Montgomery and Buffington has been taken into consideration. Different guidelines from both classification systems have been used in this study to classify the Jhelum river valley and suggest the changes in the valley shape (as discussed in section 6.2).

6.3 CLASSIFICATION OF JHELUM RIVER VALLEY

Depending on the available data, the classification of Jhelum river valley downstream of Mangla dam has been done with respect to following parameters (*Rosgen (1994)* [59]).

- Sinuosity
- Slope
- Width

6.3.1 Sinuosity

Sinuosity is the ratio of stream length to valley length. It shows the meandering behavior of a river. It can be calculated in the following way by figure 6.4.

River Sinuosity = Stream length (SL)/Valley length (VL) (6.1)

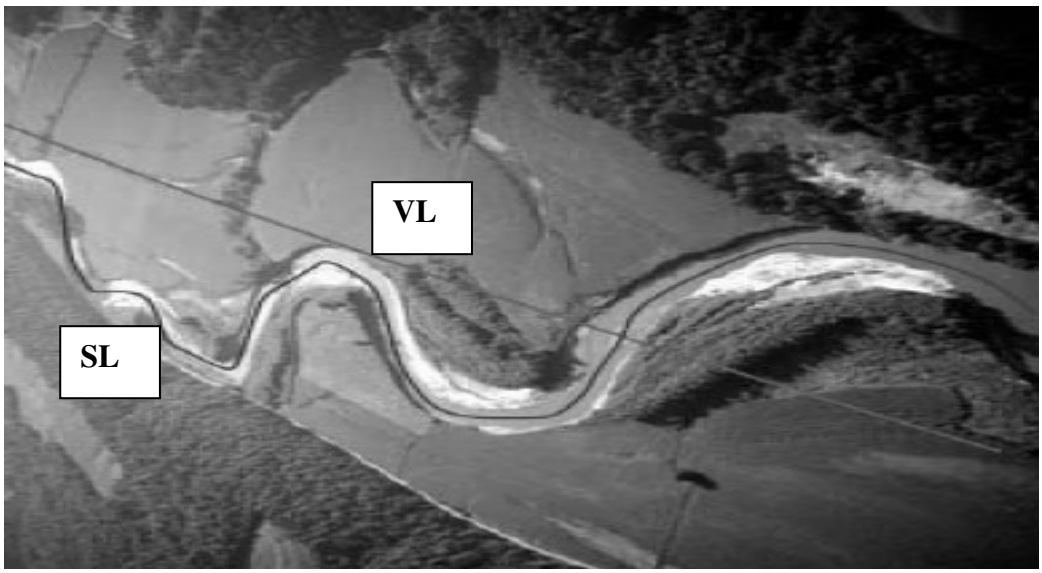

Figure 6.4: Sinuosity of a river [40]

According to the available data, the sinuosity of Jhelum river valley has been computed to be 1.27 which comes into the category of moderate sinuosity according to (*Rosgen (1994)* [59]).

6.3.2 Slope

Slope or gradient is the ratio of vertical distance to horizontal distance. Channel slope is a measure of how far the channel drops over a horizontal distance. Channel slope is one of the important factors that influence the flow velocity in the channel. For Jhelum river valley downstream of Mangla dam, slope has been computed at all locations (between the consecutive cross-sections). The mean slope of the Jhelum river valley is about 0.0004. So it comes into the category of gentle slope (<0.001) (*Montgomery and Buffington (1993)* [45]).

6.3.3 Width

Width is also a very important parameter in a river valley. It is considered in the following two ways,

- Width/Depth ratio (with respect to bank full discharge)
- Entrenchment ratio (detail in section 6.4.2)

According to the computed width/depth ratios at downstream cross-sections, the Jhelum river valley has been classified as *'very broad and shallow valley'*. Moreover, the Jhelum river valley comes into the categories of *'moderately entrenched'* and *'slightly entrenched'* according to the computed entrenchment ratios at the downstream cross-sections. The entrenchment ratio will be discussed in detail in section 6.4.2.

6.4 SUGGESTED CHANGES IN THE VALLEY SHAPE

Keeping in view the available data/information and above discussion, following changes in Jhelum river valley have been suggested for the sake of generalizing hydrodynamics and *LOL*-results for other valley shapes downstream of the dams (as discussed in section 6.1).

- Changes in valley slope
- Changes in valley width

Both parameters are very important in a river valley. They influence the flooding quite significantly. The suggested changes have been discussed separately in the following sections.

6.4.1 Suggested Changes in Valley Slope

As already mentioned, the Jhelum river valley is very broad and shallow with a mean slope of 0.0004. According to figure 6.3, this mean slope comes into the category of 'regime' with slope<0.001 (*Montgomery and Buffington (1993)* [45]). For such very broad and shallow rivers, valley is usually not so steep. Figure 6.5 illustrates different zones of a river valley from upstream source to downwards. The Jhelum river valley can be considered in Zone 3.

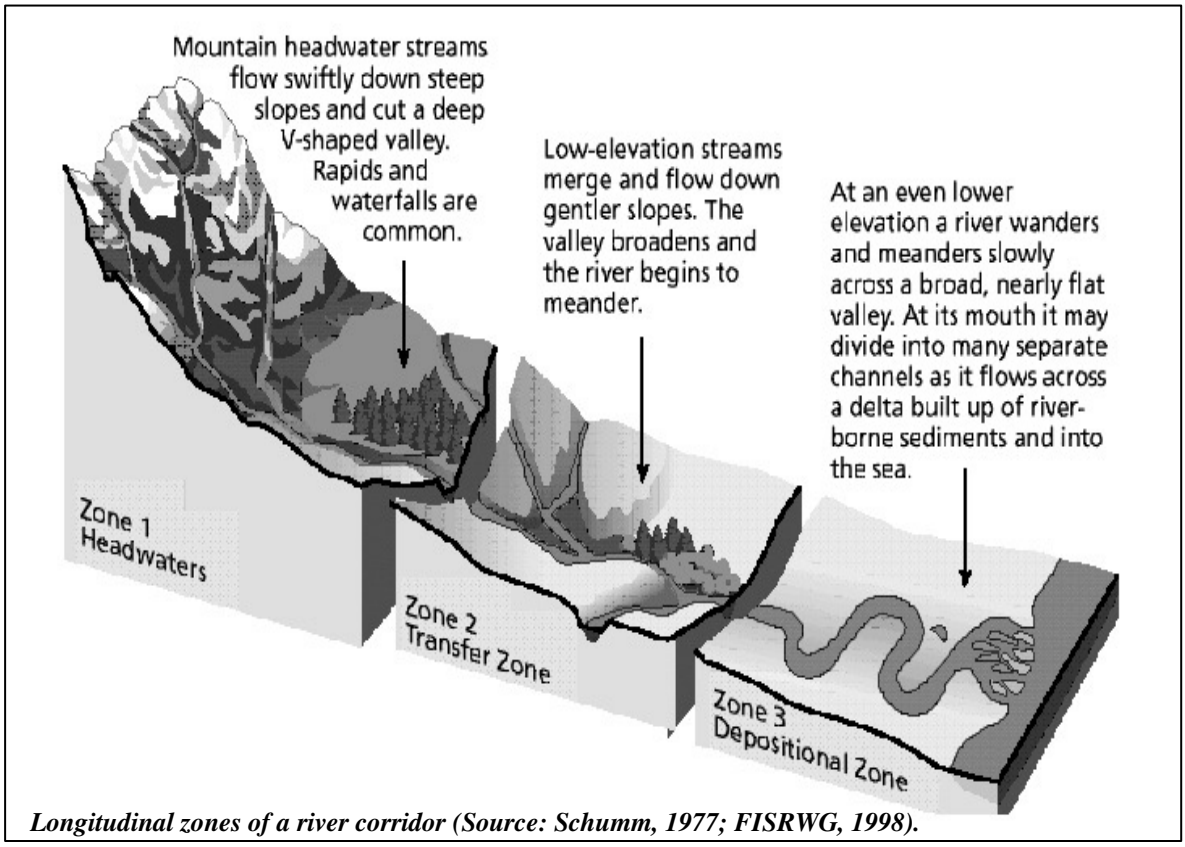

Figure 6.5: Different zones of a river valley [63]

In order to analyze the effect of valley slope on loss of life due to extreme flooding downstream of the dam, different valley shapes have been produced with the following suggested valley slopes. These valley slopes have been maintained the same through the whole reach (between the consecutive cross-sections) for different valley shapes.

Investigated Valley Slopes

- 0.0004, 0.0007, 0.0009, 0.001, 0.0015

Different slope values have been considered up to 0.001 starting from the mean value of 0.0004. Additionally, a higher slope of 0.0015 has also been considered in order to have an example of the pool-riffle category (0.02<S>0.001). All other parameters have been kept the same for these valley shapes. Figure 6.6 shows the bed levels of cross-sections for suggested valley slopes and the original valley slope downstream of Mangla dam.

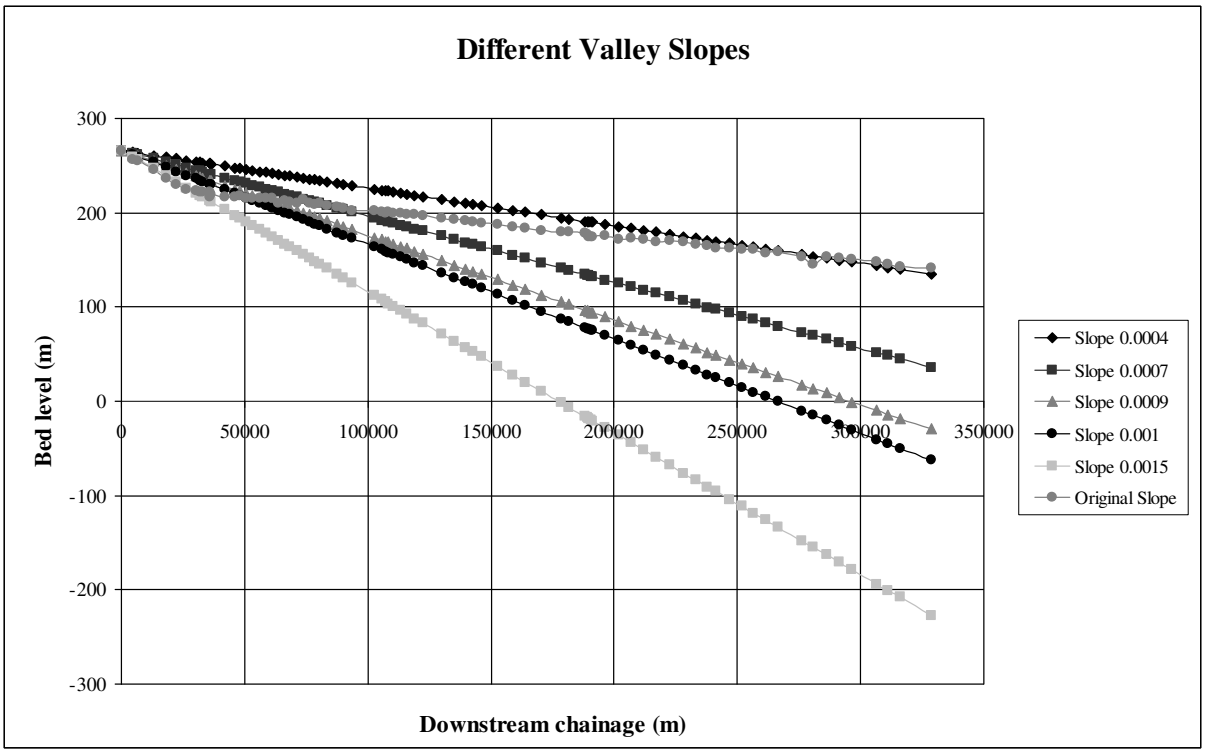

Figure 6.6: Bed levels of downstream cross-sections for different valley slopes

6.4.2 Suggested Changes in Valley Width

Depending on the data availability, different changes in the width of valley have been suggested. The changes in valley width have been considered in terms of entrenchment ratio. By definition, the entrenchment ratio is the ratio of the width of flood-prone area to bank full surface width of the channel. The flood prone width is defined as the width measured at an elevation that is twice the maximum bank full water depth. This flood prone elevation has also been related to a frequent flood (50 years or less return period) by field observations (*Rosgen (1994)* [59]), (*Rosgen (1996)* [60]). The computation of entrenchment ratio is illustrated in figure 6.7.

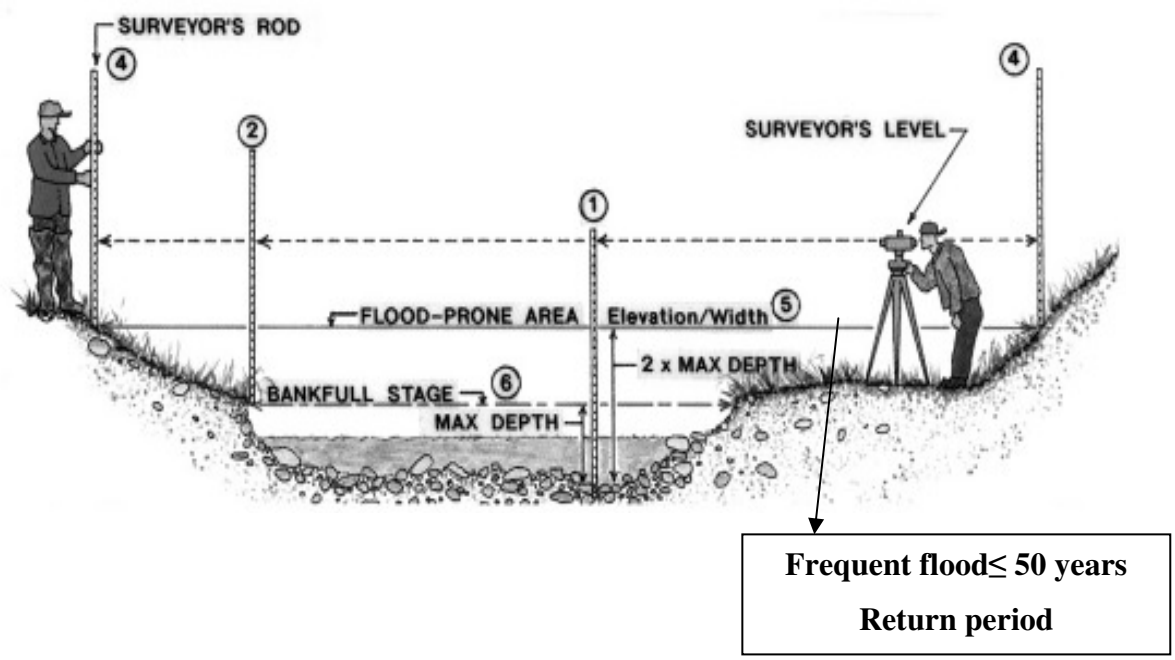

Figure 6.7: Computation of entrenchment ratio [60]

The entrenchment ratio can be categorized in the following way (*Rosgen (1994)* [59]), (*Rosgen (1996)* [60]).

1 – 1.4	entrenched
1.41 – 2.2	moderately entrenched
> 2.2	slightly entrenched (well-developed flood plain)

According to the available cross-section data, it was not possible to determine the flood prone width at an elevation that is twice the maximum bank full depth. As the elevation at twice the bank full depth was exceeding the maximum cross-section limits for most of the cross-sections due to broadness and shallowness of the Jhelum river valley as illustrated in figure 6.8.

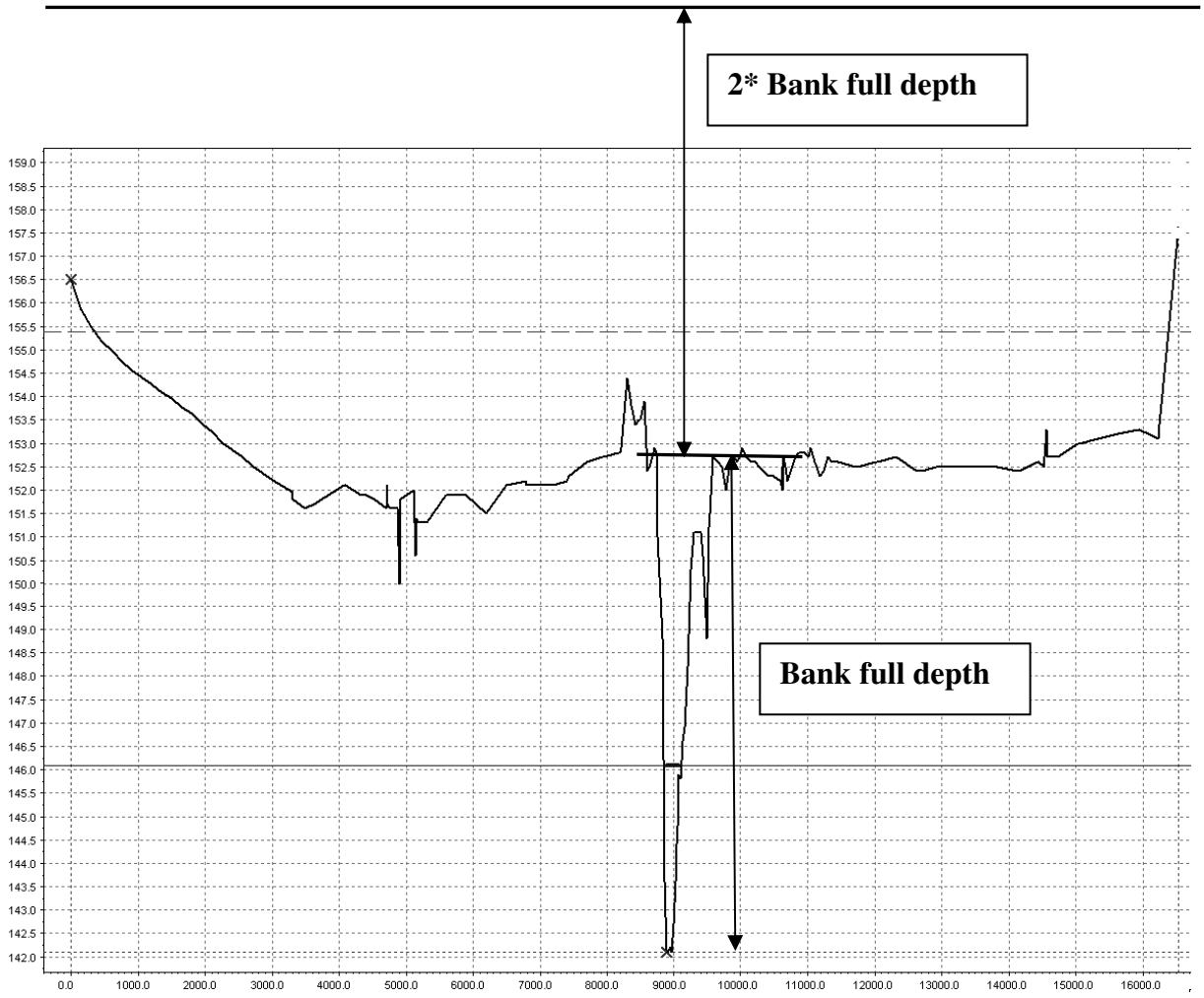

Figure 6.8: Flood prone elevation exceeding the maximum cross-section limits

In this case, the available definition of flood prone elevation with respect to a frequent flood (50 years or less return period) has been considered. The criteria of entrenchment by (*Rosgen (1994)* [59]) have been developed for streams and small rivers. For such streams and small rivers the flood of 50 years or less return period can be a frequent flood. But for large river valleys like Jhelum river valley it is considered that a flood of 5-15 years return period would have significant impact. Moreover, the highest flood in the past (92-flood) in Jhelum river downstream of Mangla dam had return period of 35 years (figure 2.1) and it was a rare event. So depending on available data, the results of 1997 flood (8 years return period) (figure 2.1) have been considered for the computation of entrenchment ratio. As already mentioned, the Jhelum river valley has been classified as *'moderately entrenched'* and *'slightly entrenched'*

with respect to the computed entrenchment ratios at downstream cross-sections. Figure 6.9 shows the channel types with different entrenchment ratios.

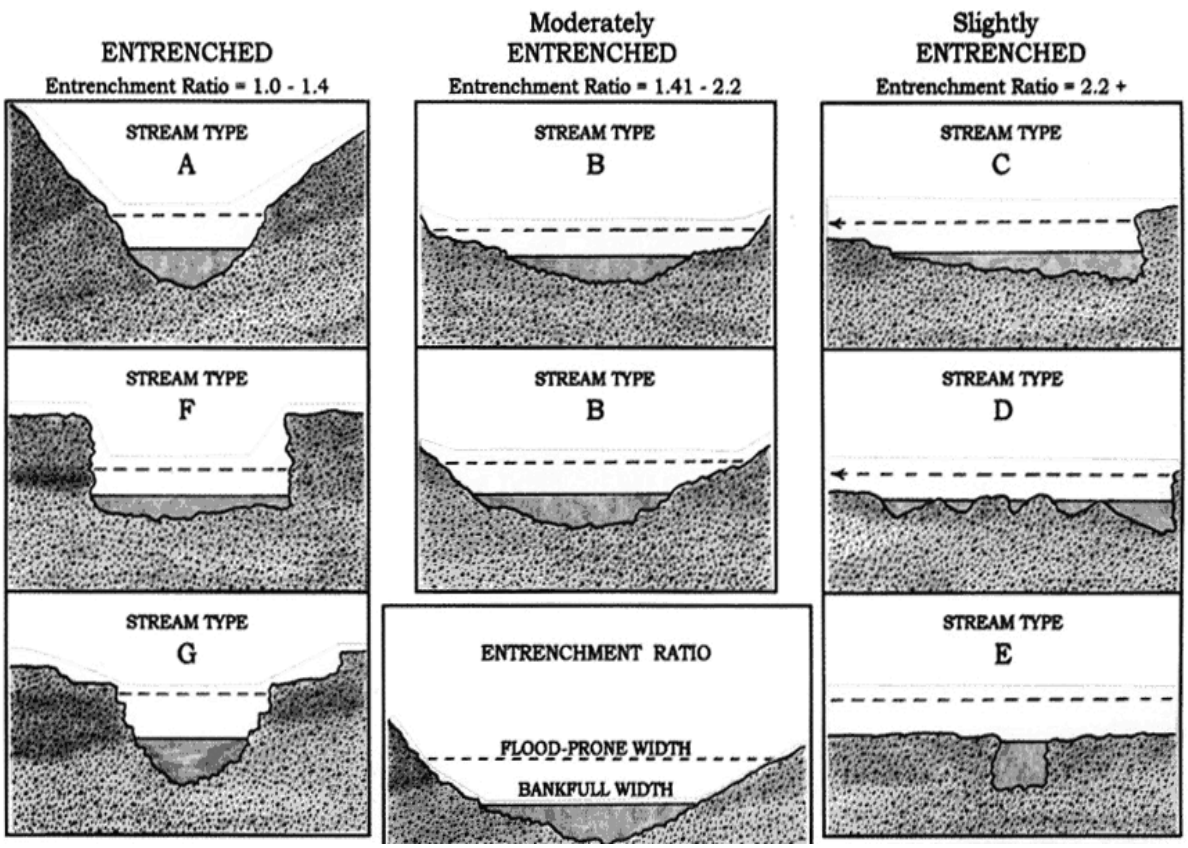

Figure 6.9: Examples of channel entrenchment [60]

For this study, different valley shapes have been produced with the following suggested entrenchment ratios (for 97-flood of 8 years return period) in order to analyze their impact on possible loss of life.

Investigated Valley Widths

- 1.4, 1.8, 2.2, 2.6

For different valley shapes the entrenchment ratios have been kept the same for all downstream cross-sections. The bank full width has not been changed. Only the flood prone width of cross-sections has been changed accordingly to have respective entrenchment ratios for different valley shapes. As an example figure 6.10 and 6.11 illustrate a typical cross-section of Jhelum river with different entrenchment ratios.

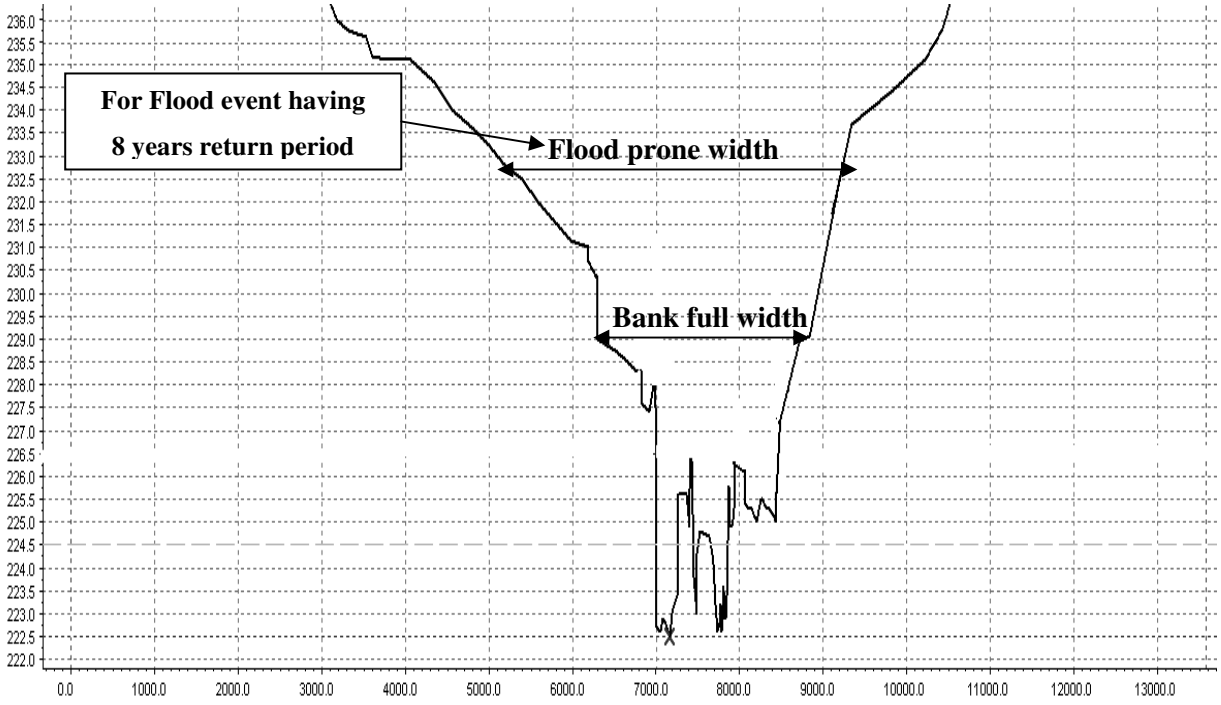

Figure 6.10: Typical cross-section with entrenchment ratio 1.4 for Jhelum river

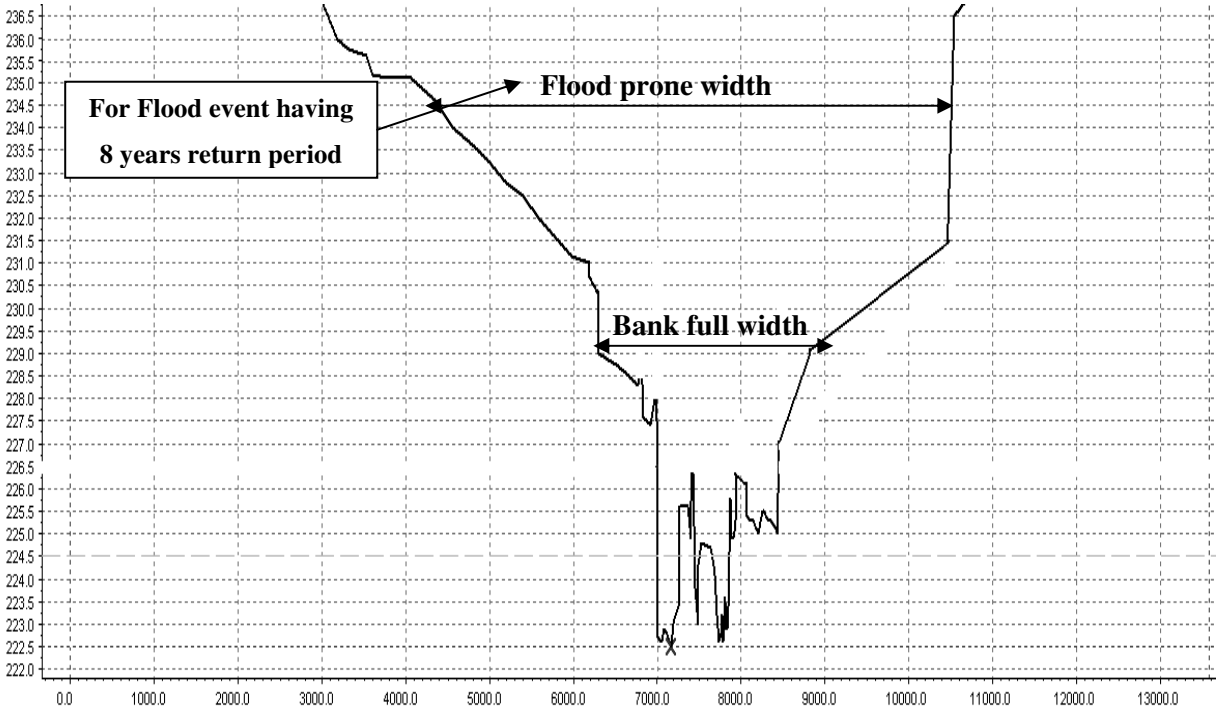

Figure 6.11: Typical cross-section with entrenchment ratio 2.2 for Jhelum river

6.5 UNSTEADY FLOW MODELING

For different valley shapes with the suggested changes, unsteady flow modeling with MIKE 11 has been carried out. In order to avoid the possible numerical instabilities due to the changing position of hydraulic structures with respect to the changes in valley shape, hydraulic structures (weirs and bridges) have not been considered in all modeling scenarios. Depending on the requirement, necessary extrapolation of cross-sections has also been done (as discussed in section 3.2.2). Different flooding scenarios with and without dam failure have been modeled. The computed outflow hydrographs from dam break modeling (for erosion case1: section 3.4.3) and additionally the outflow hydrographs with peak discharge of 40,000 m^3/s and 26,293 m^3/s (92-flood: highest in the past) have been considered for the upstream boundary in different flood routing scenarios of valley slopes and widths. The downstream water level boundary changes with respect to change in elevation in case of varying valley slope. While in varying valley width, the downstream boundary remains the same. In the following sections, the results of different flood routing scenarios have been discussed.

6.5.1 Results of Flood Routing for Different Valley Slopes

Different unsteady flow simulations were run for the scenarios of suggested slope changes. The results of discharge and water level from the flood routing of failure outflow (case1) have been shown in figure 6.12 and 6.13. It is quite obvious from the results that with the increase in slope, discharge increases and the water level decreases. In general, any thing falling down from higher elevation would have more impact as compared to that falling from lower elevation. With an increase in valley slope the flowing water accelerates due to increase in elevation (between river cross-sections). Because of this fast flow and increase in elevation, water does not accumulate itself to increase water levels. The water levels for different valley slopes have been relatively represented with respect to the corresponding bed levels of cross-sections (figure 6.6). The differences in the results at downstream locations are very significant for different slope cases. In other words, it can be said that the steeper the valley, the higher the discharges and vice versa. Also, the steeper the valley the lower the water levels and vice versa.

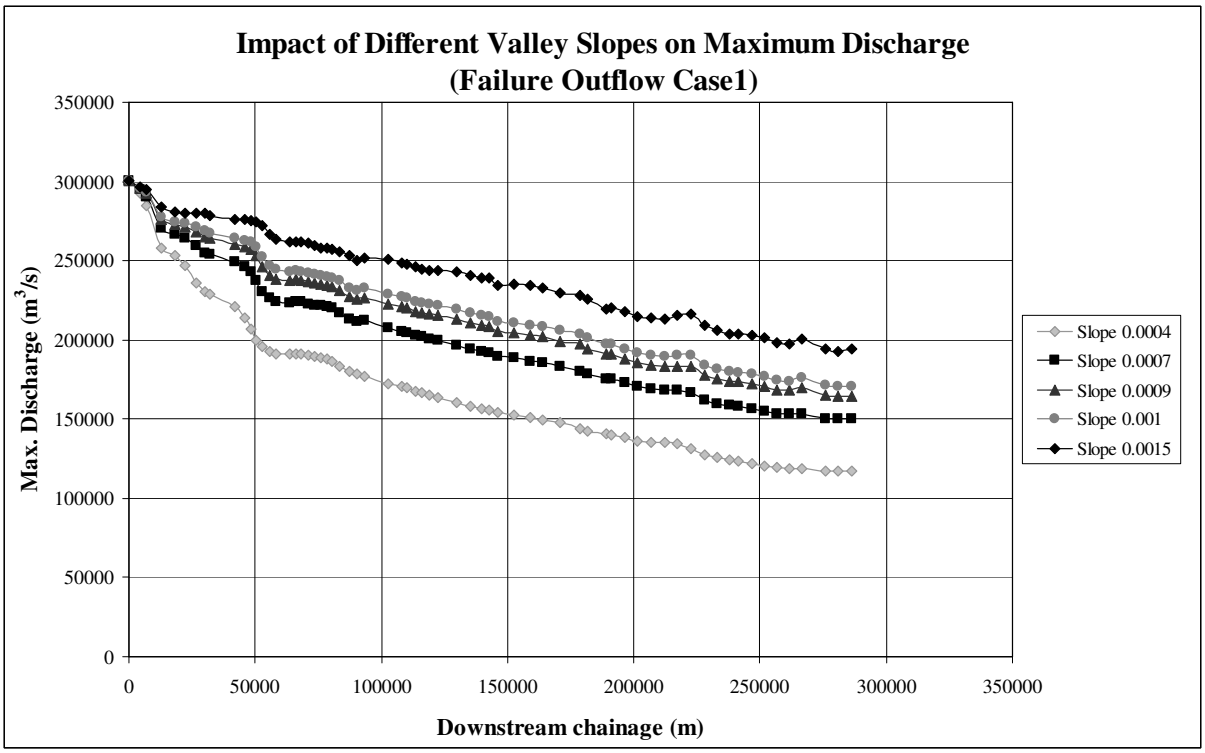

Figure 6.12: Impact of valley slopes on discharge (failure outflow case1)

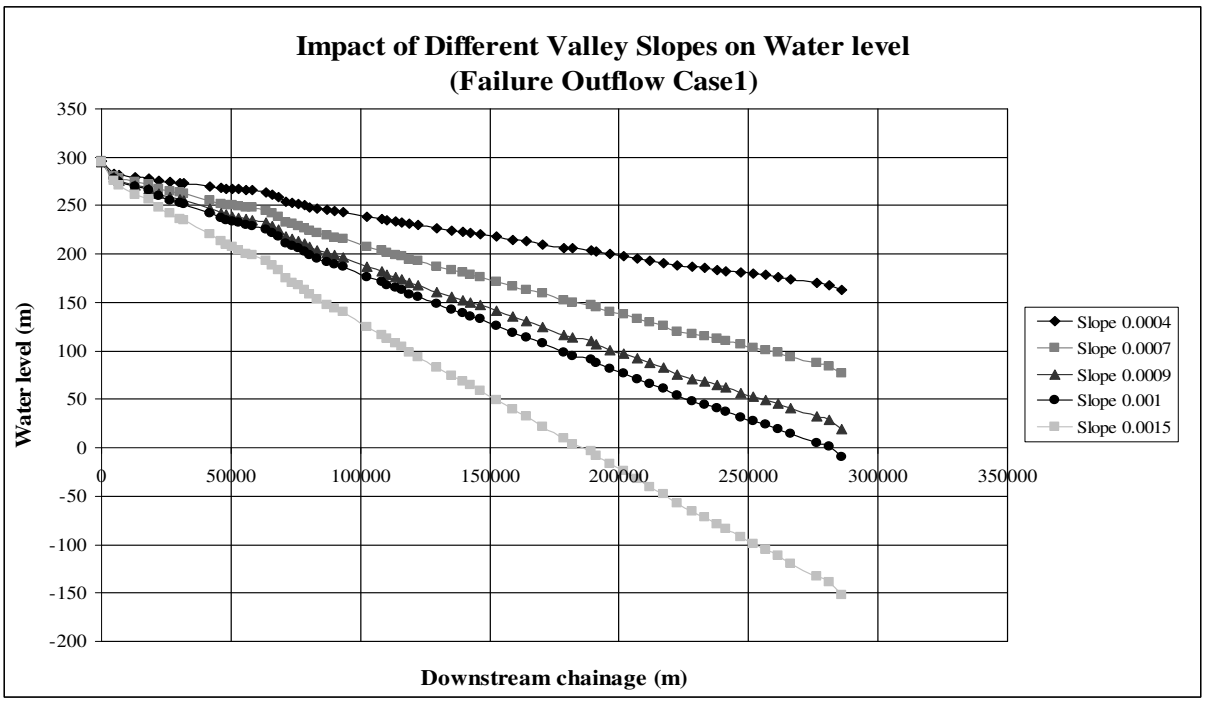

Figure 6.13: Impact of valley slopes on water level (failure outflow case1)

For other modeling scenarios (as mentioned in section 6.5), the flood routing results have also the same characteristics as in this case of failure outflow.

6.5.2 Results of Flood Routing for Different Valley Widths

The flood routing results of failure outflow (case1) for different valley widths (entrenchment ratio) have been shown in figure 6.14 and 6.15. The results of other flooding scenarios also represent the same character. The differences in the results for different valley width cases are not as big and significant as in the case of valley slopes. But they show the impact of change in valley width on discharges and water levels. In order to have a clear understanding, the closer views of results for a part of the project reach have been shown. It is very clear from the results that both the discharge and water level decrease with the increase in valley width (entrenchment ratio) and vice versa. In other words, the broader the valley the lower the discharge and water level and vice versa. Due to increase in the width of a river cross-section the flowing water extends more along the flood plains to accommodate itself. This process decelerates the flowing water and also reduces the water level.

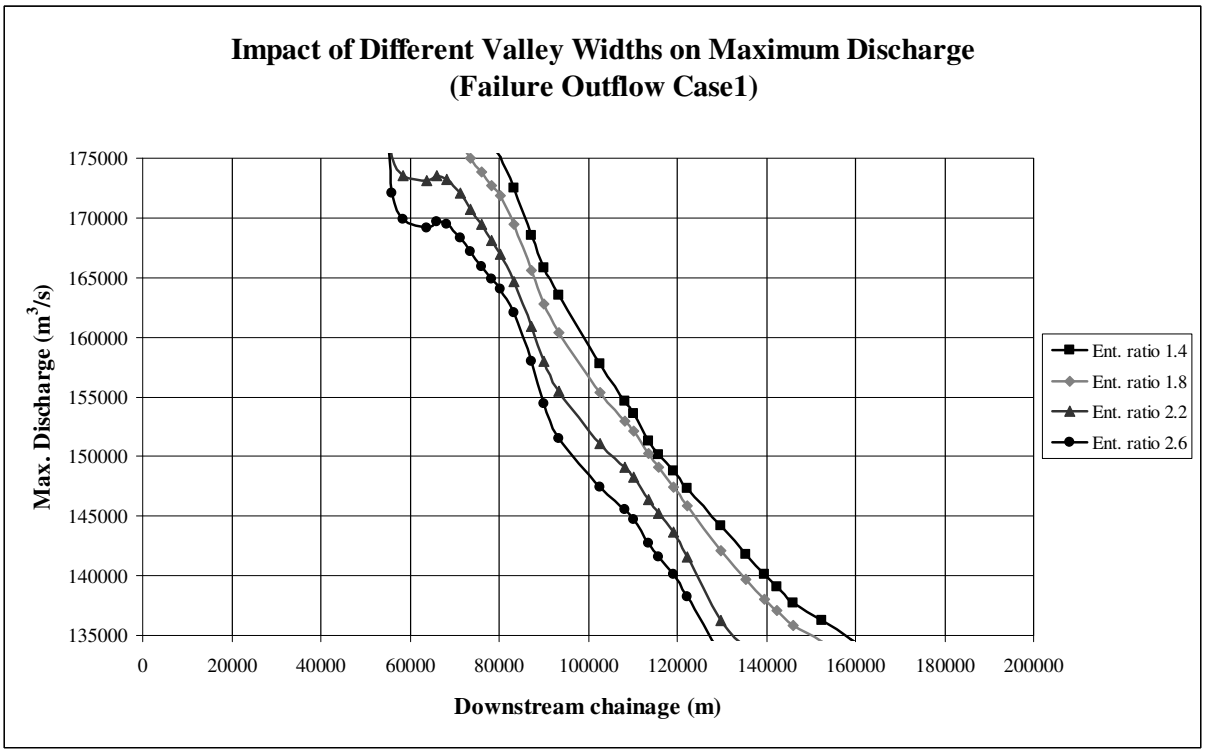

Figure 6.14: Impact of valley widths on discharge (failure outflow case1)

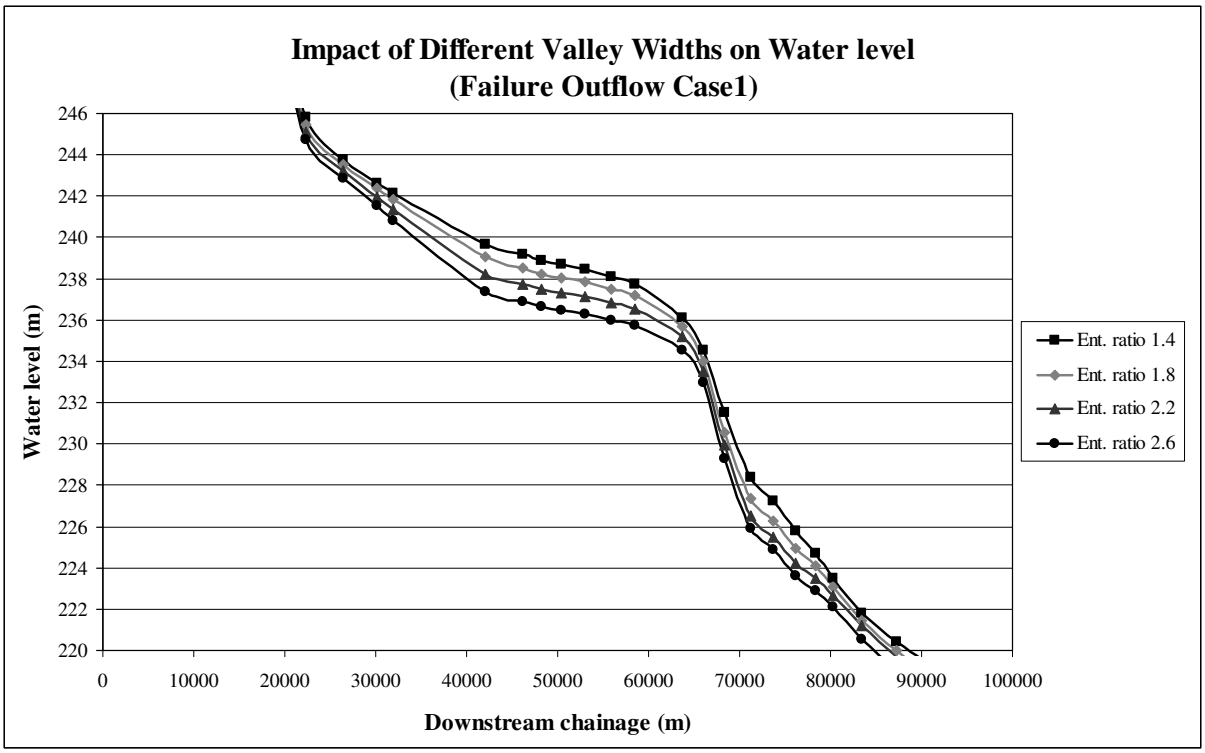

Figure 6.15: Impact of valley widths on water level (failure outflow case1)

6.6 LOSS OF LIFE ESTIMATION

Loss of life has been estimated by using the flood routing results of different flooding scenarios with different changes in the downstream valley shape (section 6.4). All factors for *LOL* estimation have been computed according to the new *LOL* estimation method (section 5.3). In all cases of *LOL* estimation the worst case of warning initiation (30 minutes after failure) has been considered. In the following sections, the results of *LOL* estimation have been discussed for different scenarios of valley shapes.

6.6.1 *LOL* Results for Different Valley Slopes

LOL estimation has been done for suggested valley slopes by using the results of different flooding scenarios. The number of people at risk (*PAR*) has been determined with respect to increase in the flooded areas (section 5.4.1) for different flooding scenarios of valley slopes. Figure 6.16 shows the total *PAR* downstream of Mangla dam for different valley slopes. It is obvious that *PAR* decreases with the increase in slope. This is due to the decrease in the area of influence downstream of the dam (flooded area). The *PAR* is higher for the cases of dam failure as compared to other considered cases without dam failure due to more flooding.

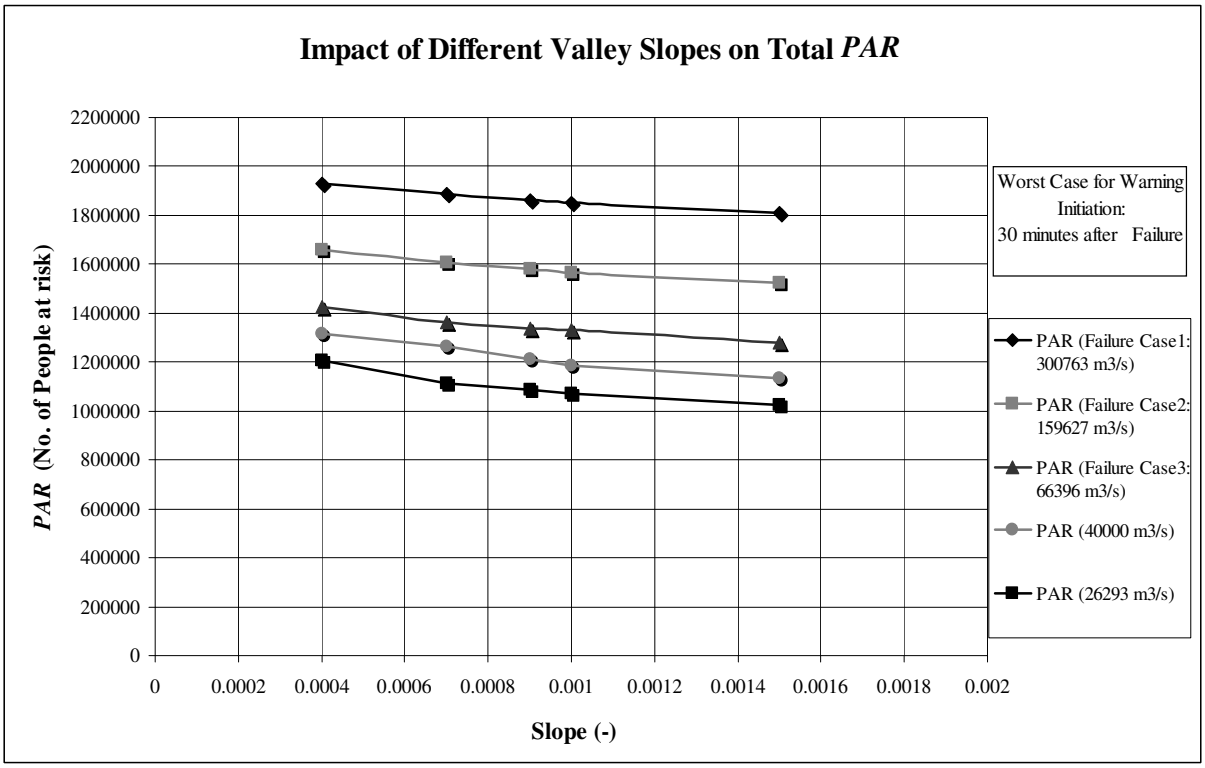

Figure 6.16: Impact of different valley slopes on total *PAR*

The percentage of total loss of life downstream of Mangla dam has been computed with respect to the total *PAR* for different scenarios of valley slopes as shown in figure 6.17. The percentage of total loss of life increases with the increase in valley slope and vice versa. In other words, the steeper the valley the higher the percentage of loss of life. The maximum value is about 4.3% for the failure case1 with the slope of 0.0015. This increase in percentage of total *LOL* is due to the increase in overall flood severity and decrease in warning time (reduction in flood travel time due to fast flooding) with the increase in downstream valley slope.

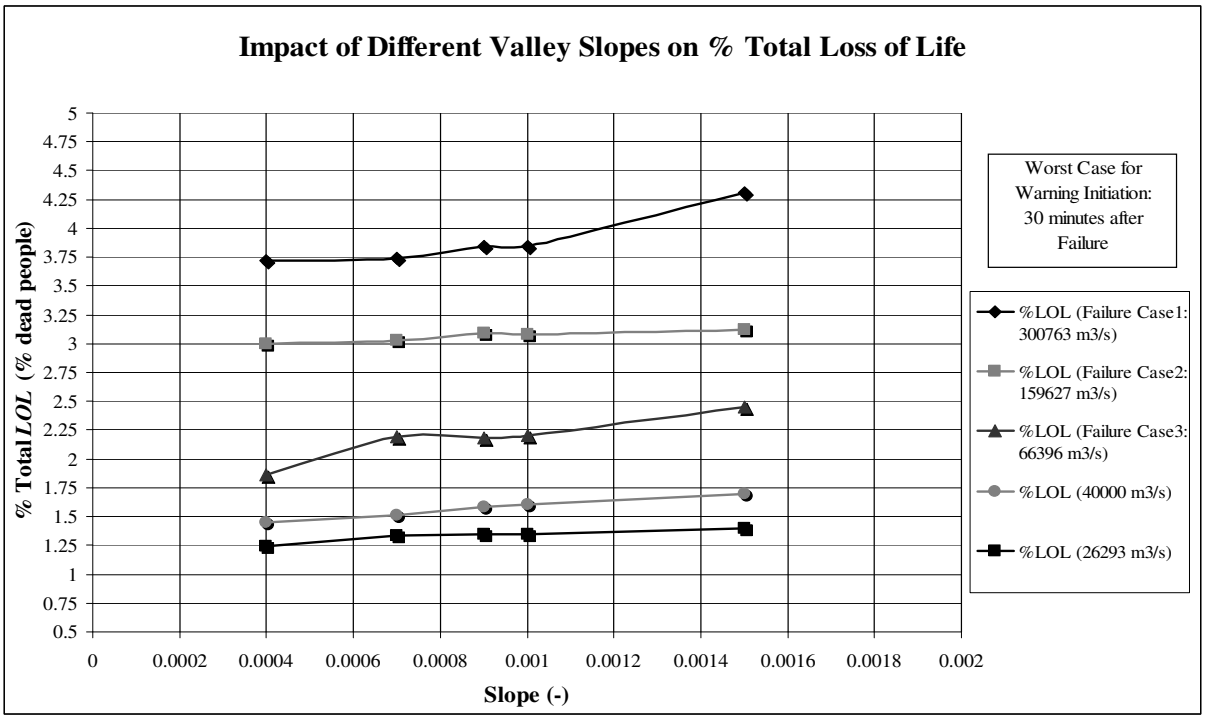

Figure 6.17: Impact of different valley slopes on % total loss of life

In order to compare the loss of life over the distance downstream of the dam for different valley slopes, the computed *LOL* over the reach length for the failure case1 (300,763 m^3/s) has been shown in figure 6.18. The most changes in *LOL* occur up to first 50 km downstream of the dam for different valley slopes.

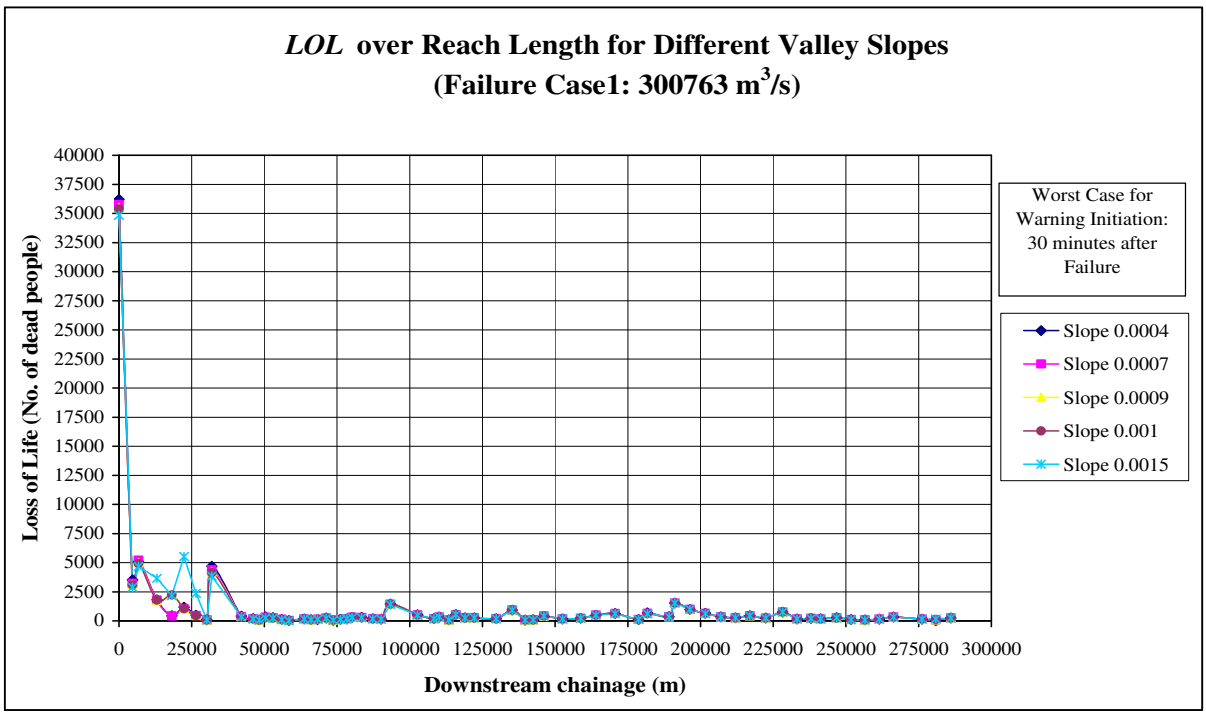

Figure 6.18: *LOL* over reach length for different valley slopes

6.6.2 *LOL* Results for Different Valley Widths

Loss of life estimation has been done for different scenarios of the suggested valley widths (in terms of entrenchment ratio) by using the results of flood routing. Figure 6.19 shows the computed *PAR* for different flooding scenarios with the suggested entrenchment ratios.

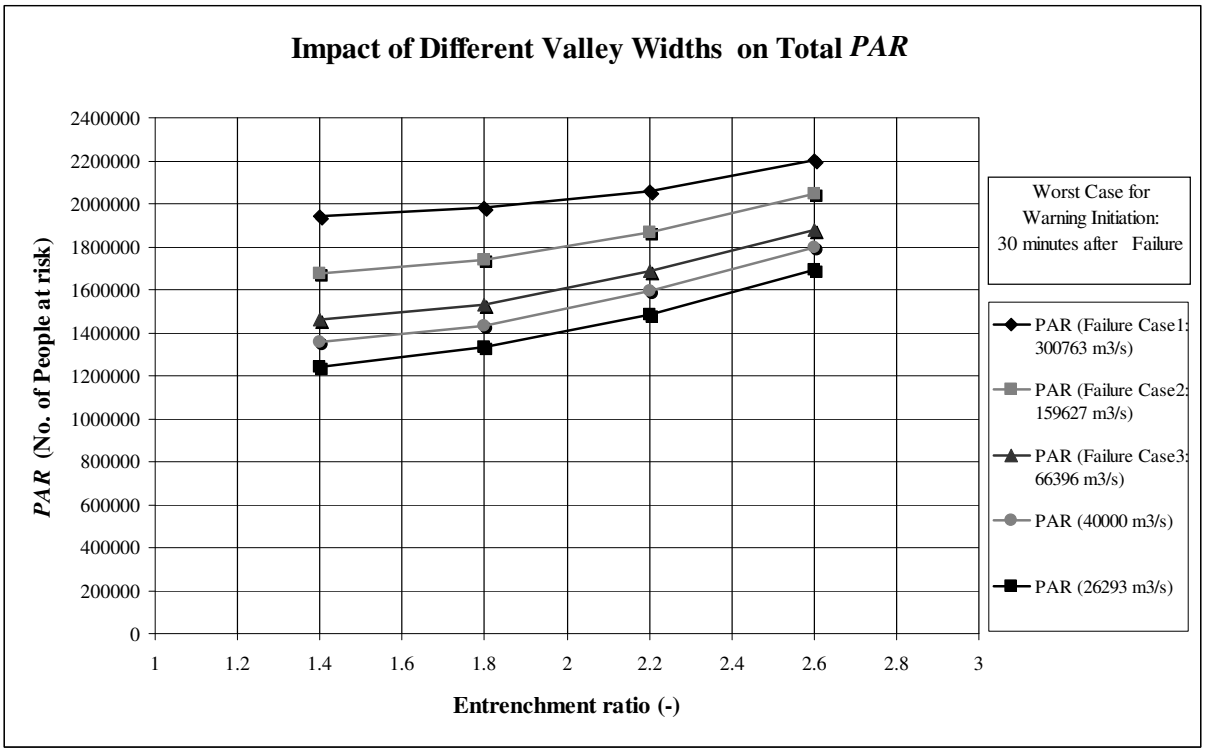

Figure 6.19: Impact of different valley widths (entrenchment ratio) on total *PAR*

The number of people at risk (*PAR*) increases with the increase in the entrenchment ratio. This is due to increase in the area of influence (flooded area) with the increase in valley width (entrenchment ratio). The *PAR* downstream of Mangla dam is higher for the dam failure cases than the other cases. In order to analyze the impact of valley width on loss of life, the percentage of total loss of life for different scenarios has been computed as shown in figure 6.20. The percentage of total loss of life decreases with the increase in the entrenchment ratio of the valley and vice versa. The broader the valley the lower the percentage of loss of life. The maximum percentage of total loss of life is close to 4% for the failure case1 having an entrenchment ratio of 1.4. The decrease in percentage of total *LOL* with the increase in valley width (entrenchment ratio) is because of the decrease in overall flood severity and increase in warning time (increase in flood travel time).

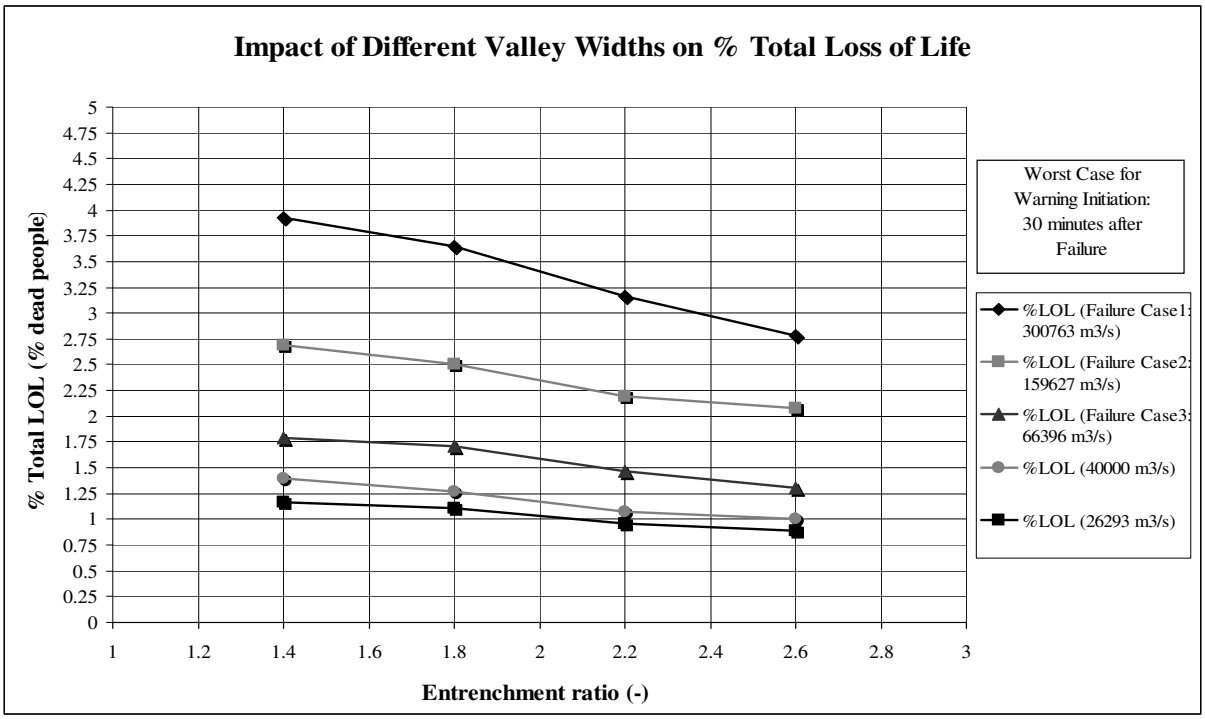

Figure 6.20: Impact of different valley widths (entrenchment ratio) on total *PAR*

The change of computed *LOL* over the reach length downstream of the dam for different valley widths has been shown in figure 6.21 for the failure case1 (300,763 m^3/s). The main variation in *LOL* is up to first 50 km downstream of the dam for different valley widths.

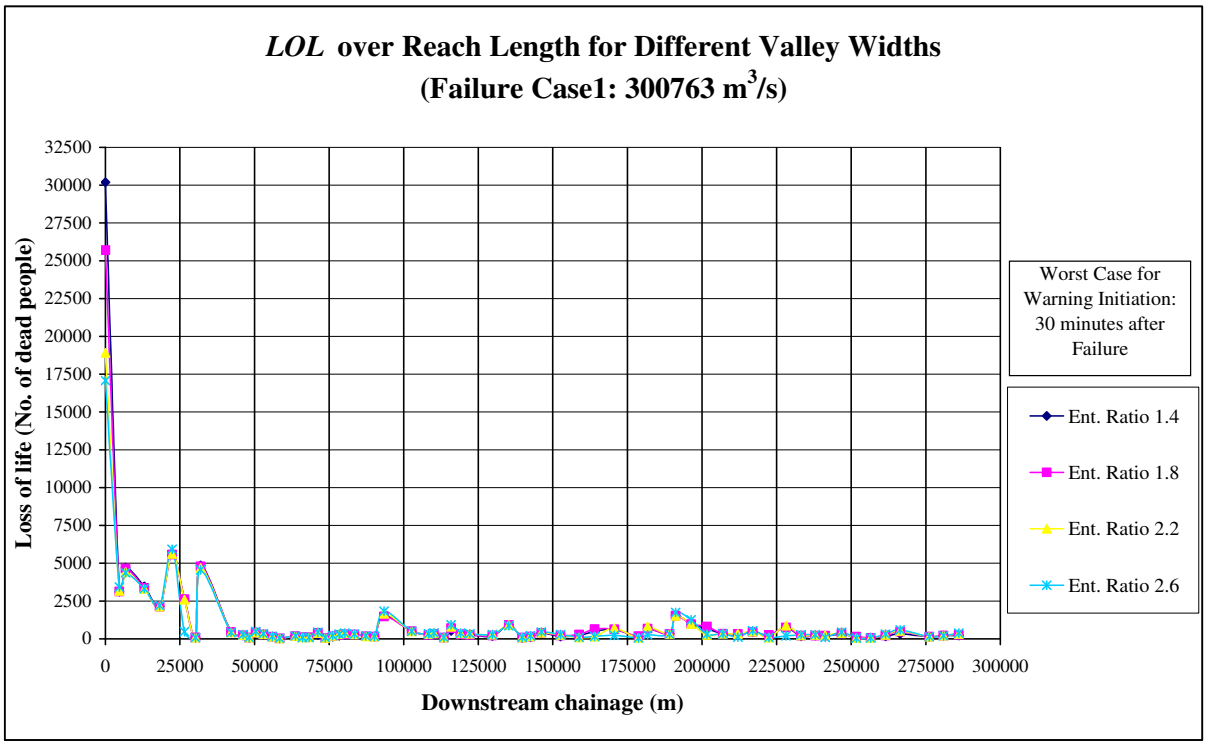

Figure 6.21: *LOL* over reach length for different valley widths

6.7 RISK DETERMINATION

As mentioned in section 5.7, the residual risk can be determined in terms of individual and societal risks. In the following, the impact of different changes in the valley shape on residual risks has been discussed.

6.7.1 Individual Risk for Different Valley Slopes

By using the *LOL* results of different scenarios with and without dam failure (section 6.6), the annual individual risk has been calculated as shown in figure 6.22. For dam failure cases, the overall failure probability (*2.63 E-3*) has been considered for individual risk. But for the cases without dam failure, the corresponding probabilities of occurrence (by the available flood frequency curve: figure 2.1) have been used in the computation of individual risks.

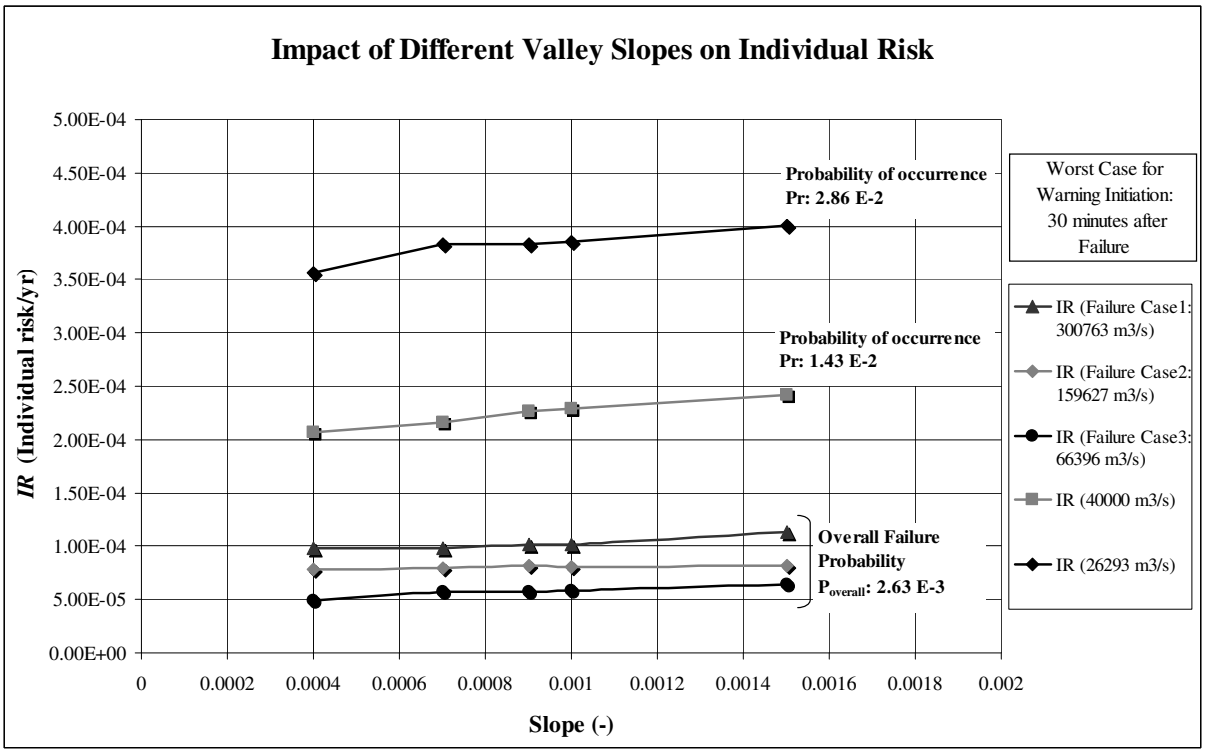

Figure 6.22: Impact of different valley slopes on individual risk

It is quite clear from the results that the individual risk per year increases with the increase in valley slope. For the worst case of dam failure with valley slopes up to 0.001, the individual risk per year is very close to the tolerable limit of 1.0 E-4 by (*ANCOLD (2003)* [3]), (*Bowles (2007)* [10]). Moreover, for the slope of 0.0015 (steepest considered) in the worst case of dam

failure, the individual risk crosses the ANCOLD limit. On the other hand, the individual risk per year is significantly higher than the tolerable limit of (*ANCOLD (2003)* [3]) for all slope categories in the considered cases without dam failure. This is mainly due to higher probability of occurrence for the flooding cases without dam failure. The individual risk is the highest for the flood of 26,293 m^3/s in different slope categories due to the highest probability of occurrence. Collectively, it can be said that the steeper the valley the higher the individual risk and vice versa. This increase in individual risk per year is due to the increase in overall flood severity and decrease in warning time (reduction in flood travel time due to fast flooding) with the increase in downstream valley slope.

6.7.2 Individual Risk for Different Valley Widths

In order to analyze the impact of changes in valley width on individual risk, the individual risk per year has been computed for different scenarios of valley widths (entrenchment ratio). Different flooding scenarios with and without dam failure have been considered. The overall failure probability (*2.63 E-3*) for dam failure cases and corresponding probabilities of occurrence for other cases without failure have been used in the computation of individual risk. Figure 6.23 shows the individual risk per year for different flooding scenarios with different valley widths.

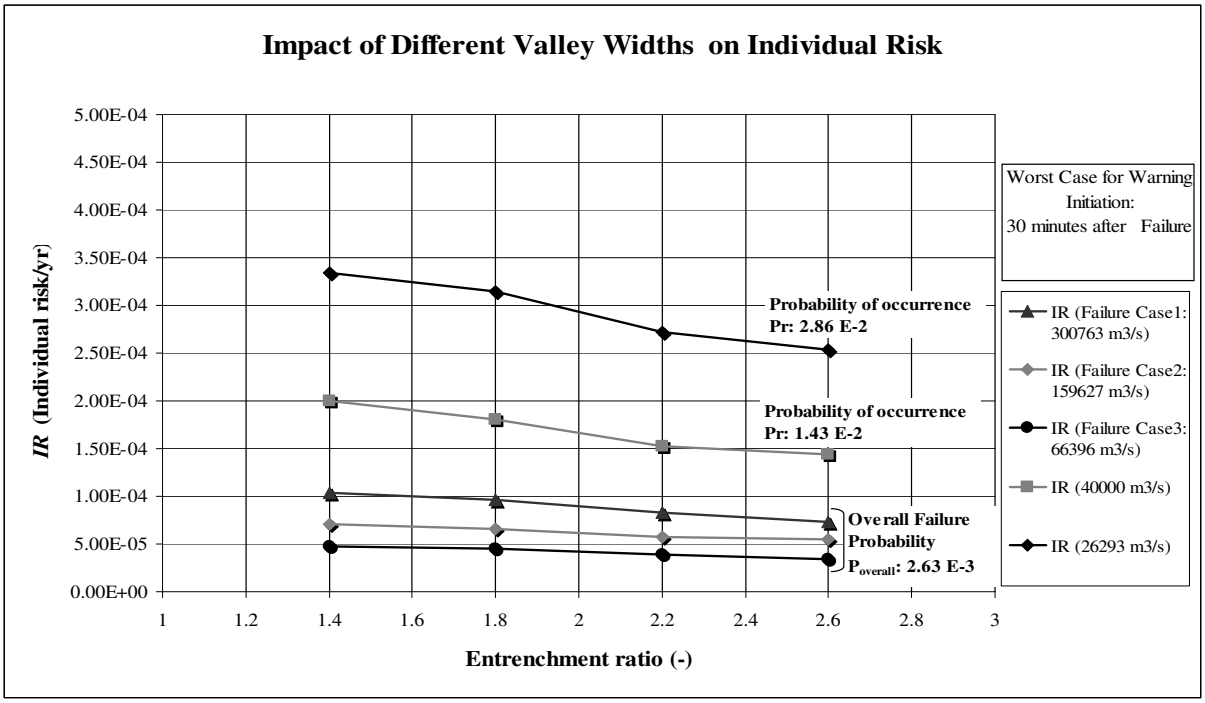

Figure 6.23: Impact of different valley widths on individual risk

The individual risk decreases with the increase in valley width (in terms of entrenchment ratio). In the worst case of dam failure, the individual risk is equal to the tolerable limit of 1.0 E-4 given by (*ANCOLD (2003)* [3]) for the entrenchment ratio of 1.4 (most confined). For other flooding cases without dam failure, the individual risk is quite higher than the tolerable limit of (*ANCOLD (2003)* [3]) for all considered entrenchment ratios due to high probabilities of occurrence. The individual risk is the highest for the flood of 26,293 m^3/s in all entrenchment cases with respect to the corresponding probability of occurrence. The broader the valley the lower the individual risk and vice versa. The decrease in individual risk with the increase in valley width (entrenchment ratio) is because of the decrease in overall flood severity and increase in warning time (increase in flood travel time).

6.7.3 Societal Risk for Different Valley Shapes

As discussed in section 5.7.2, the societal risk depends on failure probability of a dam and expected loss of life. The F-N charts have been developed basically for dam failure events. But in this case, different flooding scenarios (with and without dam failure) have been considered with the suggested changes in valley shape (slope and width). For dam failure cases, the societal risk has been analyzed with respect to the overall failure probability of Mangla dam (*2.63 E-3*) and respective loss of life in different scenarios of changes in valley shape. The estimated loss of life in all flooding scenarios of suggested changes in valley shape is quite higher than 10,000 (figure 5.11) (*ANCOLD (2003)* [3]), (*Bowles (2007)* [10]), (*McDonald (1999)* [44]).

The overall failure probability is also very high and it is out of the range of F-N chart (*ANCOLD (2003)* [3]), (*Bowles (2007)* [10]). So for dam failure cases with different changes in valley shape (slope and width), the societal risk can be considered to be impermissible (as in section 5.7.2). Moreover, for other flooding scenarios without dam failure, the societal risk is also high and unacceptable due to higher probability of occurrence and estimated loss of life (>10,000). The possible reduction in societal risk has been discussed in section 5.7.3. Collectively, it can be said that the societal risk of very big dams like Mangla dam with different valley shapes remains unacceptable for different extreme flooding scenarios with and without dam failure. It strongly justifies the need of improving the existing structural and non-structural risk reduction measures and also planning new useful measures in order to minimize the residual risks of big dams.

6.8 SUMMARY

In order to generalize the *LOL* results of Jhelum river valley for other river valleys in the world, the impact of changes in the downstream valley shape on possible loss of life has been analyzed. For this purpose, different classification systems of rivers have been studied and the Jhelum river valley downstream of Mangla dam has been classified with respect to different important parameters. Different changes in the valley shape downstream of Mangla dam have been suggested with respect to valley slope and width. New valley shapes have been developed for analysis according to these suggested changes. Unsteady flow simulations were run for these valley shapes considering different extreme flooding scenarios with and without dam failure. In order to analyze the impact of different valley shapes on possible loss of life, *LOL* estimation has been done for different scenarios using the flood routing results.

It was found that with the increase in valley slope, discharge increases and the water level decreases. On the other hand, with an increase in valley width (in terms of entrenchment ratio) both discharge and the water level decrease. The percentage of total loss of life increases with the increase in valley slope and it decreases with the increase in valley width. The residual risks (individual and societal) have also been estimated with respect to the probability of occurrence (overall failure probability for dam failure cases) and estimated loss of life for different flooding scenarios with and without dam failure. The individual risk per year increases with the increase in valley slope and it decreases with the increase in valley width.

The individual risk per year is significantly higher than the tolerable risk limit of 1 in 10,000 by (*ANCOLD (2003)* [3]) for different flooding scenarios of all valley shapes (without dam failure) due to higher probability of occurrence. The individual risk is more than the tolerable limit in the worst case of dam failure for the slope of 0.0015 (steepest considered). Moreover, the individual risk is almost equal to the tolerable limit in the worst case of dam failure for the most confined case of valley width with the entrenchment ratio of 1.4. (details in section 6.7.1 and 6.7.2)

The increase in individual risk per year with the increase in valley slope is due to the increase in overall flood severity and decrease in warning time (fast flooding). Moreover, the decrease in individual risk with the increase in valley width (entrenchment ratio) is because of the decrease in overall flood severity and increase in warning time.

The societal risk for all flooding scenarios (with and without dam failure) with different valley shapes remains intolerable according to the F-N chart by ANCOLD (2003) due to very high probability of occurrence (overall failure probability for dam failure cases) and estimated loss of life (details in section 6.7.3). The analysis of the impact of different valley shapes on possible loss of life and residual risks downstream of the dam is deemed to be helpful in improving the risk reduction measures (structural and non-structural) for existing dams and in planning more useful measures for new dams in Pakistan and also in other parts of the world.

7 CONCLUSIONS

7.1 ACHIEVEMENTS OF RESEARCH WORK

In the following, the achievements of this research work are discussed.

- Depending on data availability, the overall failure probability of Mangla dam has been computed by taking into consideration different possible failure scenarios. The computed failure probability is *2.63 E-3* which is comparatively very high. This justifies the importance of risk assessment study on Mangla dam (details in chapter 2).

- Flood routing for Jhelum river valley for a reach of about 329 km downstream of Mangla dam has been done using MIKE 11 with unsteady flow conditions for different flooding scenarios.

- Depending on the available data, an erosion based overtopping failure of Mangla dam has been modeled with MIKE 11 with respect to different dam breach cases which are based on case studies. The peak failure outflow for the worst case is more than 300,000 m^3/s which can be considered to be the highest possible discharge after the failure of Mangla dam.

- Flood severity indication has been done at downstream locations for Jhelum river valley by using different available criteria which are based on specific flood severity definitions. In order to have more realistic and meaningful information about flood severity, an improved criterion for flood severity indication has been developed which includes necessary parameters responsible for flood severity downstream of a dam.

- Different available methods for loss of life (*LOL*) estimation have been studied. For more precise and realistic estimation, a new elaborate method for *LOL* estimation has been developed. Different important factors have been considered according to available data and plausibility analysis. The loss of life has been estimated for different flooding scenarios with and without dam failure for different categories of warning initiation.

- For the actual validation of the *LOL* estimation method, detailed reliable information is required for the estimation of different *LOL* factors. Getting access to reliable data for a specific flood event is very difficult and time consuming. The available data of past floods do not fulfill the requirements of the introduced method. As an attempt, the loss of life due to past floods and computed *LOL* in considered flooding scenarios have been compared with respect to the specific flood severity and warning information (detail in section 5.5).

- The maximum percentage of total *LOL* estimated for the worst case of dam failure is close to 4% which seems to be very high. The extent of loss of life in terms of downstream distance has also been determined. This study verifies and also adjusts other past predictions about the extent of possible *LOL* downstream of the dam due to dam failure (detail in section 5.6).

- The individual and societal risks for Mangla dam due to dam failure have been analyzed by taking into consideration the overall failure probability and estimated loss of life. Individual risk for the worst case of dam failure is higher than the limit of individual tolerable risk (1 in 10,000) for existing dams suggested by ANCOLD (2003).

- According to F-N chart by ANCOLD (2003) (figure 5.11), the societal risk for all failure scenarios is totally unacceptable due to a very high overall probability of failure and estimated loss of life of more than 10,000 (detail in section 5.7.2).

- In order to generalize the *LOL* results of Jhelum river valley for other river valleys in the world, the impact of downstream valley shape on possible loss of life due to extreme flooding has been analyzed.

- Based on the available data, the Jhelum river valley downstream of Mangla dam has been classified as ‘very broad and shallow valley’ with gentle slope (slope category of <0.001) according to different systems of river classification.

- In order to analyze the impact of changes in the valley shape on possible loss of life, different changes in the valley shape downstream of Mangla dam with respect to valley slope and width (in terms of entrenchment ratio) have been suggested. Different valley shapes have been developed according to the suggested changes.

- Different scenarios of extreme flooding with and without dam failure have been modeled for different valley shapes. By the analysis of flood routing results it was found that the steeper the valley the higher the discharge and lower the water level. Moreover, the broader the valley the lower the discharge and water level.

- Loss of life estimation has also been done for different flooding scenarios with different valley shapes. The percentage of total loss of life with respect to the people at risk (*PAR*) increases with the increase in valley slope and it decreases with the increase in valley width.

- The individual risk increases with the increase in valley slope and it decreases with the increase in valley width. The individual risk is quite higher than the tolerable limit of 1.0 E-4 by ANCOLD (2003) for different flooding scenarios of all valley shapes (without dam failure) due to higher probability of occurrence.

- The individual risk exceeds the tolerable limit of 1.0 E-4 by ANCOLD (2003) in the worst case of dam failure for the steepest considered slope of 0.0015 (detail in section 6.7.1).

- The individual risk is almost equal to the tolerable limit of 1.0 E-4 by ANCOLD (2003) in the worst case of dam failure for the most confined case of valley width with the entrenchment ratio of 1.4 (detail in section 6.7.2).

- The increase in individual risk with the increase in valley slope is due to the increase in overall flood severity and decrease in warning time (fast flooding).

- The decrease in individual risk with the increase in valley width (entrenchment ratio) is due to the decrease in overall flood severity and increase in warning time (increase in flood travel time).

- The societal risk for different flooding scenarios (with and without dam failure) with different valley shapes remains unacceptable according to F-N chart by ANCOLD (2003) due to very high probability of occurrence (overall failure probability for dam failure cases) and estimated loss of life of more than 10,000 (detail in section 6.7.3).

7.2 SUGGESTIONS AND RECOMMENDATIONS

Based on the achievements of this research work, following suggestions and recommendations are given:

- The computed overall failure probability of Mangla dam can be considered as guidance to assess the possible overall failure probability of other large dams in the world.

- For new dams, the annual exceedance probability (AEP) of hazards should be considered in acceptable ranges for the computation of overall failure probability in order to achieve safer designs.

- The new criterion for flood severity indication (*GA*) should be used for risk assessment studies on other dams in the world. The accuracy of the results will certainly depend on the available data for flood routing and further analysis.

- The new *LOL* estimation method should be used for other risk assessment studies of dams. As it provides an elaborate understanding of necessary factors responsible for possible loss of life downstream of the dam due to extreme flooding with and without failure. For more realistic and precise estimates, the data availability for downstream valley is very important. The *LOL* factors are based on available guidelines and data but some of them need more improvement.

- The true validation of the *LOL* estimation method with the help of detailed data and information of different flood disasters is recommended for future research.

- More research is needed to estimate precisely the risk posed by different age groups, more storey houses and the very low strength houses (Kucha houses) in the project area. The considered risk for corresponding factors can be taken as a first guideline for further research.

- No proper guidelines are available for estimating the ease of evacuation at the time of emergency. The ease of evacuation would be obviously different for rural and urban areas. It depends on mainly the evacuation facilities and warning efficiency. More research is required to estimate the ease of evacuation for both rural and urban areas in order to have more realistic *LOL* estimation. The considered factor is based on adopted warning efficiency and likelihood of no rescue which certainly needs more improvement.

- For existing dams like the Mangla dam, the residual risks of life loss (individual and societal) can be minimized by improving the existing structural and non-structural risk reduction measures and also introducing new useful measures. Structural measures include repair of existing levees and dykes, construction of new levees and dykes and dam raising or possible reduction in maximum operating level of the reservoir (if required to avoid possible overtopping) etc. The non-structural measures could be e.g. improvement and introduction of new techniques in warning efficiency, emergency evacuation and safe operating procedures. The people living near the flood plains should also be relocated to safe places. Moreover, the awareness in *PAR* about the possible flood severity should also be enhanced.

- For new dams the residual risks can be reduced by making safer design of dams (based on the acceptable AEP of possible hazards) and planning proper structural and non-structural risk reduction measures.

- The impact of the downstream valley shape on possible loss of life has been analyzed in this study. This should be an important consideration at the time of dam planning in order to reduce the residual risks due to extreme flooding downstream of the dam with and without failure. Unfortunately it has been ignored for many aging dams.

- The estimated change in possible residual risks for different valley shapes (with and without dam failure) gives very useful guidelines for dam authorities in advance to plan suitable structural and non-structural risk reduction measures for new dams with respect to particular valley shapes. For existing dams it can also guide in improving the existing risk reduction measures and introducing new measures with respect to the downstream valley shape.

8 REFERENCES

[1] Aboelata, M., Bowles, D.S. and McClelland, D.M. (2003) A model for estimating dam failure life loss, Proceedings of the Australian Committee on Large dams risk Workshop, Australia.

[2] Abbott, M.B. and Ionescu, F. (1967) On the numerical computation of nearly-horizontal flows, *Journal of Hydraulic Research*, Vol. 5, pp. 97-117.

[3] ANCOLD (Australian National Committee on Large Dams) (2003) Guidelines on risk assessment, Australia.

[4] ANCOLD (Australian National Committee on Large Dams) (1994a) Guidelines on dam safety management, Australia.

[5] ANCOLD (Australian National Committee on Large Dams) (1994b) Guidelines on risk assessment, Australia.

[6] Binnie Deacon and Gourley, in association with Harza Engineering Company International andd Preece Cardew & Rider (1959) The Probable maximum flood on the river Jhelum at Mangla, Mangla Dam Project.

[7] Binnie and Partners Consulting Engineers (1971) Mangla Dam Project: Completion Report, Volume III: River Control, Chapter 10: Hydrology.

[8] Bisson, P.A. and Montgomery, D.R. (1996) Valley segments, stream reaches, and channel units, in R. F. Hauer and G. A. Lambert (eds.) Methods in stream ecology, Academic Press, San Diego, California, pp. 23-42.

[9] Bowles, D.S. (1996) Reservoir safety: A risk management approach, *International Conference* on aspects of conflicts in reservoir development and management, London.

[10] Bowles, D.S. (2007) Tolerable Risk for Dams: How safe is safe enough? US Society on Dams *Annual Conference*, Philadelphia, Pennsylvania.

[11] Bowles, D.S. (2004) ALARP evaluation: Using cost effectiveness and disproportionality to justify risk reduction, *ANCOLD Bulletin* 127:89-106.

[12] Bowles, D.S. (2003) ALARP Evaluation: Using cost/benefit disproportionality to justify risk reduction, Proceedings of the Australian Committee on Large Dams Risk Workshop, Launceston, Tasmania, Australia.

[13] Brown, C.A. and Graham, W.J. (1988) Assessing the threat to life from dam failure, *Water Resources Bulletin*, Vol. 24, no. 6, pp. 1303-1309.

[14] Byrne, M.P. and Seid-Karbasi, M. (2003) Seismic stability of impoundments, 17th *Annual Symposium*, Vancouver Geotechnical Society.

[15] Canada-British Columbia Water Supply Expansion Program (CBCWSEP): Technical Standards, Earthfill Dam Technical Requirements. (http://www4.agr.gc.ca/AAFC-AAC/display-afficher.do?id=1184592752232&lang=e&printable=true), last access on 18.07.2008

[16] Canadian Standard Association (1993) Guidelines and requirements for reliability analysis methods, Q636-93.

[17] Cartwright, F., Mussio, J. and Boughton, C. (2006) Developing the composite learning index, A Framework, Canadian Council on learning, Canada.

[18] Clausen, L. and Clark, P.B. (1990) The development of criteria for predicting dam-break flood damages using modeling of historical dam failures, *International Conference* on River Flood Hydraulics, edited by W. R. White. 17. - 20. September, 1990, John Wiley and Sons Ltd. Hydraulics Research Limited, pp. 369-380.

[19] Dahms, S.H. (2004) Damage caused to earth embankment dams by earthquakes in the United States, Global Tectonics, Emporia State University, Emporia, Kansas. (http://www.emporia.edu/earthsci/student/dahms3/web1.htm), last access on 16.07.2008

[20] Dam Safety Inspection Manual (2003) Risk and hazards of dam failure, Part 1: Chapter 5, Indiana department of natural resources.

[21] Debreu, G. (1960) Topological methods in cardinal utility theory, in Arrow K.J., Karlin S. and Suppes P. (eds.) Mathematical methods in social sciences, Stanford University Press, Stanford.

[22] DeKay, M.L. and McClelland, G.H. (1993) Predicting loss of life in cases of dam failure and flash flood, *Risk Analysis*, Vol. 13, no. 2, pp. 193-205.

[23] Dewey, R.L. and Gillette, D.R. (1993) Prediction of embankment dam breaching for hazard assessment, Proceedings, ASCE *Specialty Conference* on Geotechnical Practice in Dam Rehabilitation, Raleigh, North Carolina.

[24] DIN 19700-11 (2004) Stauanlagen, Teil: 11, Talsperren.

[25] DVWK Merkblätter zur Wasserwirtschaft 246/1997: Freibordbemessung an Stauanlagen, Kommissionsvertrieb Wirtschafts- und Verlagsgesellschaft Gas und Wasser mbH., Bonn.

[26] Ehsan, S. (2005) Personal communication with NESPAK Engineers.

[27] Engelund, F. and Hansen, E. (1967) A monograph on sediment transport in alluvial streams, Teknisk Forlag, Copenhagen.

[28] Fell, R., Bowles, D.S., Anderson, L.R. and Bell, G. (2000) The status of methods for estimation of the probability of failure of dams for use in quantitative risk assessment, 20th ICOLD *Congress*, Beijing, Q76-R.

[29] Foster, M.A. and Fell, R. (1999) A framework for estimating the probability of failure of embankment dams by internal erosion and piping using event tree methods, UNICIV Report No. R-377, School of Civil and Environmental Engineering, The University of New South Wales, ISBN: 85841-344-2.

[30] Froehlich, D.C. (1987) Embankment-Dam breach parameters, Hydraulic Engineering, Proceedings of the 1987 ASCE *National Conference* on Hydraulic Engineering, Williamsburg, Virginia, pp. 570-575.

[31] Froehlich, D.C. (1995a) Peak outflow from breached embankment dam, *Water Resources Engineering*, Proceedings of the 1995 ASCE *Conference* on Water Resources Engineering, San Antonio, Texas, pp. 887-891.

[32] Froehlich, D.C. (1995b) Embankment Dam Breach Parameters Revisited, *Journal of Water Resources Planning and Management*, Vol. 121, no.1, pp. 90-97.

[33] Graham, W.J. (1999) A procedure for estimating loss of life caused by dam failure (DSO-99-06), U.S. Department of the Interior, Bureau of Reclamation, Denver, Colorado.

[34] Hartford, D.N.D. and Baecher, G.B. (2004) Risk and uncertainty in dam safety, Chapter 2: 2.1, Chapter 4: 4.2 and Chapter 8.

[35] Hartford, D.N.D. (1998) This dam risk business - the challenge of implementation - managing the risks of risk assessment, ANCOLD/NZCOLD *Conference* on Dams, Sydney.

[36] Harrington, B., Maryland Dam Safety: Dam break analysis & Hazard Classifications. (http://www.mde.state.md.us/assets/document/damsafety/workshop/Dam%20Failure%20Analysis%20by%20Bruce%20Harrington.pdf), last access on 25.07.2008

[37] Idel, K.H. (1986) Sicherheitsuntersuchungen auf probalistischer Grundlage für Staudämme, Abschlußbericht: Anwendungsband, Untersuchungen für einen Referenzstaudamm, ed. by Deutsche Gesellschaft für Erd- und Grundbau im Auftrag des Bundesministers für Forschung und Technologie, Essen.

[38] Johnson, F.A. and Illes, P. (1976) A classification of dam failures, *International Water Power and Dam Construction*, Vol. 28, no. 12, pp. 43-45.

[39] Johansen, P.M., Vick, S.G. and Rikartsen, C. (1997) Risk analyis for three Norwegian dams, Hydropower 97, Broch, Lysne, Flatabø and Helland-Hansen (ed.), Balkema, pp. 431-442.

[40] Kail, J. (2006) Morphological risk assessment, Using river sinuosity to assess the ecological status of streams and rivers, Sofia.

[41] Keeney, R. and Raiffa, H. (1976) Decision with multiple objectives: preferences and value trade-offs, Wiley, New York.

[42] Kelman, I. (2002) Physical flood vulnerability of residential properties in coastal Eastern England, Ph.D. Dissertation, University of Cambridge, U.K., pp. 25-26.

[43] Krantz, D.H., Luce, R.D., Suppes, P. and Tversky, A. (1971) Foundations of measurement, Vol. 1, Additive and polynomial representations, Academic Press, New York.

[44] McDonald, L. (1999) Use of risk assessment for dam safety evaluation in Australia, Proceedings of the International Workshop on Risk Analysis in Dam Safety Assessment, Taiwan.

[45] Montgomery, D.R. and Buffington, J. (1993) Channel classification, Prediction of channel response and Assessment of channel condition, Report FW-SH10-93-002, SHAMW committee of Washington state timber-fish-wildlife Agreement.

[46] Munda G. (1995) Multi-criteria evaluation in a fuzzy environment, Physica-Verlag, Contributions to Economics Series, Heidelberg.

[47] Nardo, M., Saisana, M., Saltelli, A., Tarantola, S., Hoffman, A. and Giovannini, E. (2005) Handbook on constructing composite indicators: Methodology and user guide, OECD Statistics working paper, STD/DOC (2005)3, OECD Statistics Directorate, France.

[48] Nardo, M., Tarantola, S., Saltelli, A., Andropoulos, C., Buescher, R., Karageorgos, G., Latvala, A. and Noel, F. (2004) The e-business readiness composite indicator for 2003: a pilot study, EUR 21294.

[49] NEVADA ADMINISTRATIVE CODE: Dams and other Obstructions, NAC (http://www.leg.state.nv.us/NAC), last access on 18.07.2008

[50] Pakistan Water Gateway- Key Water Information, Mangla Dam. (http://www.waterinfo.net.pk/fsmd.htm), last access on 30.06.2008

[51] Patterson, L. (2003) Examination of stream and habitat classification systems to aid in computer habitat modeling, Master's Thesis, Institut für Wasserbau, Universität Stuttgart, Chapter 3.

[52] Podinovskii, V.V. (1994) Criteria importance theory, Mathematical Social Sciences, Vol. 27, pp. 237-252.

[53] Ramsbottom, D., Floyd, P. and Penning-Rowsell, E. (2003) Flood risks to people Phase 1: R& D Technical Report FD2317, DEFRA/ Environment Agency U.K., pp. 12-18 & 28-35.

[54] Reference Manual MIKE 11 (2004) A modeling system for rivers and channels.

[55] Reiter, P. (2001) Loss of life caused by dam failure, the RESCDAM *LOL* Method and its application to Kyrkösjärvi dam in Seinäjoki, Summary of the final report by PR Vesisuunnittelu Oy PR Water Consulting Ltd.

[56] Reiter, P. (2000) International methods of risk analysis, damage evaluation and social impact studies concerning dam-break accidents, International Seminar on the RESCDAM project, Seinäjoki, PR Vesisuunnittelu Oy PR Water Consulting Ltd.

[57] Rettemeier, K., Falkenhagen, B. and Köngeter, J. (2000) Risk Assessment- New Trends in Germany, ICOLD *Congress*, Beijing, Q76.

[58] RESCDAM (2000) The use of physical models in dam break flood analysis, Final report of Helsinki University of Technology.

[59] Rosgen, D.L. (1994) A Classification of natural rivers, Catena, Volume 22, Elsevier Science B.V., pp. 169-199.

[60] Rosgen, D.L. (1996) Applied River Morphology, ISBN: 0-9653289-0-2.

[61] Roy, B. (1996) Multi-criteria methodology for decision analysis, Kluwer, Dordrecht.

[62] Saisana, M. (2005) Aggregation issues in the development of a composite indicator, Composite indicators Workshop Ottawa.

[63] Schumm, S.A. (1977) The Fluvial system, John Wiley and Sons, New York.

[64] Seid-Karbasi, M. and Byrne, P.M. (2004) Embankment dams and Earthquakes, *Hydropower & Dams* Issue two, p. 96.

[65] Short Introduction Tutorial MIKE 11 (2005) A modeling system for rivers and channels.

[66] Singh, K.P. and Snorrason, A. (1982) Sensitivity of outflow peaks and flood stages to the selection of dam breach parameters and simulation models, SWS Contract Report 288, Illinois Department of Energy and Natural Resources, State Water Survey Division, Surface Water Section at the University of Illinois, p. 179.

[67] Singh, K.P. and Snorrason, A. (1984) Sensitivity of outflow peaks and flood stages to the selection of dam breach parameters and simulation models, *Journal of Hydrology*, Vol. 68, pp. 295-310.

[68] Singh, V.P. and Scarlatos, P.D. (1988) Analysis of gradual earth-dam failure, *Journal of Hydraulic Engineering*, Vol. 114, no. 1, pp. 21-42.

[69] Tingsanchali, T. and Khan, N. (1998) Prediction of flooding due to assumed breaching of Mangla dam, Proceedings of 3rd *International Conference* on Hydroscience & Engineering, Bradenburg University of Technology, Cottbus, Germany.

[70] User Guide MIKE 11 (2004) A modeling system for rivers and channels.

[71] U.S. Bureau of Reclamation (1988) Downstream Hazard Classification Guidelines, ACER Technical Memorandum No. 11, Assistant Commissioner-Engineering and Research, Denver, Colorado, p. 57.

[72] Vick, S.G. (1992) Risk in geotechnical practice, *In Geotechnique and Natural Hazards*, Vancouver Geotechnical Society and the Canadian Geotechnical Society, pp. 41-57.

[73] Vincke, P. (1992) Multi-criteria decision aid, Wiley, New York.

[74] Von Thun, J.L. and Gillette, D.R. (1990) Guidance on breach parameters, internal document, U.S. Bureau of Reclamation, Denver, Colorado, p.17.

[75] Wahl, T.L. (1998) Prediction of embankment dam breach parameters, A Literature review and needs assessment (DSO-98-004), Dam safety report, U.S. Department of the Interior, Bureau of Reclamation, Denver.

[76] Wahl, T.L. (2004) Uncertainty of predictions of embankment dam breach parameters, *Journal of Hydraulic Engineering,* Vol. 130, no.5, pp. 389-397.

[77] WAPDA, Pakistan: Mangla Dam Raising Project, Feasibility Study Report (2001) Volume I: Main Report

[78] WAPDA, Pakistan: Mangla Dam Raising Project, Tender Design Report (2004) Volume II: Section 4: Main Spillway.

[79] WAPDA, Pakistan: Mangla Dam Raising Project, Tender Design Report (2004) Volume II: Section 5: Control weir for Emergency Spillway.

[80] WAPDA, Pakistan: Mangla Dam Raising Project, Feasibility Study Report (2001) Volume III: Appendix H, Spillways and Hydraulic Aspects.

[81] WAPDA, Pakistan: Mangla Dam Raising Project, Feasibility Study Report (2001) Volume II: Appendix C, Flood Studies

[82] WAPDA, Pakistan: Mangla Dam Raising Project, Tender design Report (2004) Volume I: Section 3, Embankment Dams.

[83] WAPDA, Pakistan: Mangla Dam Raising Project, Feasibility Study Report (2001) Volume III: Appendix G, Geotechnical.

[84] WAPDA, Pakistan: Mangla Dam Raising Project, Feasibility Study Report (2001) Volume III: Appendix I, Structural Analysis.

[85] WAPDA, Pakistan: Mangla Dam Raising Project, Project Planning Report (2003) Summary Report.

[86] WAPDA, Pakistan: Mangla Dam Raising Project, Study Report (2003) Probable maximum Flood, Section 8: Flood Routings.

[87] WAPDA, Pakistan: Mangla Dam Raising Project, Study Report (2004) Seismic Hazard Evaluation.

[88] WAPDA, Pakistan: Mangla Dam Raising Project (2007) (http://www.wapda.gov.pk/htmls/ongoing-index.html), last access on 15.07.2008

[89]Whitman, R.V. (1984) Evaluating calculated risk in geotechnical engineering, *Journal of Geotechnical Engineering*, Vol. 110, no. 2, pp. 143-188.

[90] Wurbs, R.A. (1987) Dam-Breach Flood Wave Models, *Journal of Hydraulic Engineering*, Vol. 113, no. 1, pp. 29-46.

[91] Internet link (environment.uwe.ac.uk/geocal/glossary/gloss_p.htm), last access on 26.01.2009

[92] Internet link (http://www.dams.org/images/maps/map_tarbela_big.jpg), last access on 25.01.2009

[93] Internet link (http://outdoors.webshots.com/photo/2816634390088693836wePHnc), last access on 26.01.2009

[94] 1998 Census, Basic population and housing data by union councils, Government of Pakistan, Statistics division, Population census organization, Pakistan. Websites: (www.statpak.gov.pk), (www.census.gov.pk), last access on 26.01.2009

[95] Internet link (http://en.wikipedia.org/wiki/Mangla_Dam), last access on 26.01.2009

9 APPENDICES

APPENDIX A

CHECK OF IMPACT OF WEIGHTS FOR *GA*-CRITERION

Table A1: Impact of weights for 40,000 m^3/s (with bridges)

40,000 m^3/s	**Weights (*DV/vh*)**	**Weights (*DV/vh*)**	**Weights (*DV/vh*)**	**Weights (*DV/vh*)**
with bridges	**0.5/0.5**	**0.4/0.6**	**0.3/0.7**	**0.2/0.8**
Chainage (m)	**FSI (GA1)**	**FSI (GA2)**	**FSI (GA3)**	**FSI (GA4)**
0	High	High	High	High
4681	High	High	High	High
6754	High	High	High	High
13050	High	High	High	High
18189	High	High	High	High
22377	High	High	High	High
26479	High	High	High	High
30203	High	High	High	High
31904	High	High	High	High
42118	High	High	High	High
46130	Medium	Medium	Medium	Medium
48225	High	High	High	High
50382	Medium	Medium	High	High
52949	Medium	Medium	Medium	Medium
55947	Medium	Medium	Medium	Medium
58440	Medium	Medium	Medium	Medium
63654	High	High	High	High
66092	High	High	High	High
68304	High	High	High	High
71260	Medium	Medium	Medium	Medium
73703	Medium	Medium	Medium	Medium
76170	Medium	Medium	Medium	Medium
78375	Medium	Medium	Medium	Medium
80249	Medium	Medium	Medium	Medium
83454	Low	Low	Low	Low
87295	Medium	Medium	Low	Low
90205	Low	Low	Low	Low
93361	Medium	Medium	Medium	Medium
102711	Low	Low	Low	Low
108331	Medium	Medium	Medium	Medium
110138	Low	Low	Low	Low
113462	Low	Low	Low	Low
115856	Low	Low	Low	Low
119058	Low	Low	Low	Low
122184	Low	Low	Low	Low
129735	Low	Low	Low	Low
135257	Low	Low	Low	Low
139718	Low	Low	Low	Low
142442	Low	Low	Low	Low
146139	Low	Low	Low	Low
152575	Medium	Medium	Medium	Medium
158810	Low	Low	Low	Low
164039	Low	Low	Low	Low
170618	Low	Low	Low	Low
178697	Low	Low	Low	Low
181759	Low	Low	Low	Low
189127	High	High	High	High
191125	Medium	Medium	Medium	Medium

196388	Low	Low	Low	Low
201645	Low	Low	Low	Low
206975	Low	Low	Low	Low
212052	Low	Low	Low	Low
216966	Low	Low	Low	Low
222405	Low	Low	Low	Low
228196	Low	Low	Low	Low
233169	Medium	Medium	High	High
237966	Medium	Low	Low	Low
241267	Medium	Medium	Medium	Medium
246780	Medium	Medium	Medium	Low
251707	Medium	Low	Low	Low
256548	Medium	Medium	Medium	Medium
261485	Medium	Medium	Medium	Medium
266370	Medium	Medium	Medium	Medium
276190	Medium	Medium	Medium	High
280916	Low	Low	Low	Low
286091	Medium	Medium	Medium	Medium

Table A2: Impact of weights for 50,000 m^3/s (with bridges)

50,000 m^3/s	**Weights (*DV/vh*)**	**Weights (*DV/vh*)**	**Weights (*DV/vh*)**	**Weights (*DV/vh*)**
with bridges	**0.5/0.5**	**0.4/0.6**	**0.3/0.7**	**0.2/0.8**
Chainage (m)	**FSI (GA1)**	**FSI (GA2)**	**FSI (GA3)**	**FSI (GA4)**
0	High	High	High	High
4681	High	High	High	High
6754	High	High	High	High
13050	High	High	High	High
18189	High	High	High	High
22377	High	High	High	High
26479	Medium	Medium	Medium	High
30203	High	High	High	High
31904	High	High	High	High
42118	High	High	High	High
46130	High	High	High	High
48225	High	High	High	High
50382	High	High	High	High
52949	Medium	Medium	Medium	Medium
55947	Medium	Medium	Medium	Medium
58440	Medium	Medium	Medium	Medium
63654	High	High	High	High
66092	High	High	High	High
68304	High	High	High	High
71260	Medium	Medium	Medium	Medium
73703	Medium	Medium	Medium	Medium
76170	High	High	High	Medium
78375	Medium	Medium	Medium	Medium
80249	Medium	Medium	Medium	Medium
83454	Medium	Medium	Low	Low
87295	Medium	Medium	Medium	Medium

90205	Medium	Medium	Medium	Medium
93361	Medium	Medium	Medium	Medium
102711	Medium	Medium	Medium	Medium
108331	Medium	Medium	Medium	Medium
110138	Low	Low	Low	Low
113462	Low	Low	Low	Low
115856	Low	Low	Low	Low
119058	Low	Low	Low	Low
122184	Low	Low	Low	Low
129735	Low	Low	Low	Low
135257	Low	Low	Low	Low
139718	Medium	Low	Low	Low
142442	Low	Low	Low	Low
146139	Low	Low	Low	Low
152575	Medium	Medium	Medium	Medium
158810	Low	Low	Low	Low
164039	Low	Low	Low	Low
170618	Low	Low	Low	Low
178697	Low	Low	Low	Low
181759	Low	Low	Low	Low
189127	Medium	High	High	High
191125	Medium	Medium	Medium	Medium
196388	Low	Low	Low	Low
201645	Low	Low	Low	Low
206975	Low	Low	Low	Low
212052	Low	Low	Low	Low
216966	Low	Low	Low	Low
222405	Low	Low	Low	Low
228196	Low	Low	Low	Low
233169	Medium	Medium	High	High
237966	Medium	Medium	Low	Low
241267	Medium	Medium	Medium	Medium
246780	Medium	Medium	Medium	Medium
251707	Medium	Medium	Low	Low
256548	Medium	Medium	Medium	Medium
261485	Medium	Medium	Medium	Medium
266370	Medium	Medium	Medium	Medium
276190	Medium	Medium	Medium	High
280916	Low	Low	Low	Low
286091	Medium	Medium	Medium	Medium

Table A3: Impact of weights for MDF (61,977 m^3/s: with bridges)

MDF (61,977 m^3/s)	**Weights (*DV/vh*)**	**Weights (*DV/vh*)**	**Weights (*DV/vh*)**	**Weights (*DV/vh*)**
with bridges	**0.5/0.5**	**0.4/0.6**	**0.3/0.7**	**0.2/0.8**
Chainage (m)	**FSI (GA1)**	**FSI (GA2)**	**FSI (GA3)**	**FSI (GA4)**
0	High	High	High	High
4681	High	High	High	High
6754	High	High	High	High
13050	High	High	High	High
18189	High	High	High	High
22377	High	High	High	High
26479	High	High	High	High
30203	High	High	High	High
31904	High	High	High	High
42118	High	High	High	High
46130	High	High	High	High
48225	High	High	High	High
50382	High	High	High	High
52949	High	High	High	High
55947	High	High	High	High
58440	High	High	High	High
63654	High	High	High	High
66092	High	High	High	High
68304	High	High	High	High
71260	Medium	Medium	Medium	Medium
73703	Medium	Medium	Medium	Medium
76170	High	High	High	High
78375	Medium	Medium	Medium	Medium
80249	Medium	Medium	Medium	Medium
83454	Medium	Medium	Medium	Medium
87295	Medium	Medium	Medium	Medium
90205	Medium	Medium	Medium	Medium
93361	Medium	Medium	Medium	Medium
102711	Medium	Medium	Medium	Medium
108331	Medium	Medium	Medium	Medium
110138	Medium	Medium	Low	Low
113462	Low	Low	Low	Low
115856	Medium	Medium	Medium	Medium
119058	Medium	Medium	Medium	Medium
122184	Medium	Medium	Medium	Medium
129735	Medium	Medium	Medium	Medium
135257	Medium	Medium	Medium	Medium
139718	Medium	Medium	Medium	Medium
142442	Medium	Medium	Medium	Medium
146139	Low	Low	Low	Low
152575	Medium	Medium	Medium	Medium
158810	Low	Low	Low	Low
164039	Medium	Medium	Low	Low
170618	Low	Low	Low	Low
178697	Low	Low	Low	Low
181759	Medium	Medium	Medium	Medium

189127	High	High	High	High
191125	Medium	Medium	Medium	High
196388	Low	Low	Low	Low
201645	Low	Low	Low	Low
206975	Medium	Medium	Medium	Medium
212052	Medium	Medium	Low	Low
216966	Medium	Medium	Medium	Low
222405	Low	Low	Low	Low
228196	Medium	Medium	Medium	Medium
233169	High	High	High	High
237966	Medium	Medium	Medium	Medium
241267	Medium	Medium	Medium	Medium
246780	Medium	Medium	Medium	Medium
251707	Medium	Medium	Medium	Medium
256548	Medium	Medium	Medium	Medium
261485	Medium	Medium	Medium	Medium
266370	High	High	High	High
276190	Medium	High	High	High
280916	Low	Low	Low	Low
286091	Medium	Medium	Medium	Medium

Table A4: Impact of weights for 40,000 m^3/s (without bridges)

40,000 m^3/s	**Weights (*DV/vh*)**	**Weights (*DV/vh*)**	**Weights (*DV/vh*)**	**Weights (*DV/vh*)**
without bridges	**0.5/0.5**	**0.4/0.6**	**0.3/0.7**	**0.2/0.8**
Chainage (m)	**FSI (GA1)**	**FSI (GA2)**	**FSI (GA3)**	**FSI (GA4)**
0	High	High	High	High
4681	High	High	High	High
6754	High	High	High	High
13050	Medium	Medium	Medium	Medium
18189	High	High	High	High
22377	High	High	High	High
26479	Medium	Medium	Medium	Medium
30203	Medium	Medium	Medium	Medium
31904	High	High	High	High
42118	High	High	High	High
46130	Medium	Medium	Medium	Medium
48225	High	High	High	High
50382	Medium	Medium	High	High
52949	Medium	Medium	Medium	Medium
55947	Medium	Medium	Medium	Medium
58440	Medium	Medium	Medium	Medium
63654	High	High	High	High
66092	High	High	High	High
68304	High	High	High	High
71260	Medium	Medium	Medium	Medium
73703	Medium	Medium	Medium	Medium
76170	Medium	Medium	Medium	Medium
78375	Medium	Medium	Medium	Medium
80249	Medium	Medium	Medium	Medium

83454	Low	Low	Low	Low
87295	Medium	Low	Low	Low
90205	Low	Low	Low	Low
93361	Medium	Medium	Low	Low
102711	Low	Low	Low	Low
108331	Medium	Medium	Medium	Medium
110138	Low	Low	Low	Low
113462	Low	Low	Low	Low
115856	Medium	Medium	Medium	Low
119058	Medium	Medium	Medium	Medium
122184	Medium	Medium	Low	Low
129735	Medium	Medium	Medium	Low
135257	Medium	Medium	Medium	Low
139718	Medium	Medium	Medium	Medium
142442	Medium	Medium	Medium	Medium
146139	Low	Low	Low	Low
152575	Medium	Medium	Medium	Medium
158810	Low	Low	Low	Low
164039	Low	Low	Low	Low
170618	Low	Low	Low	Low
178697	Low	Low	Low	Low
181759	Low	Low	Low	Low
189127	High	High	High	High
191125	Medium	Medium	Medium	Medium
196388	Low	Low	Low	Low
201645	Low	Low	Low	Low
206975	Medium	Medium	Medium	Low
212052	Low	Low	Low	Low
216966	Medium	Low	Low	Low
222405	Low	Low	Low	Low
228196	Medium	Medium	Medium	Medium
233169	Medium	High	High	High
237966	Medium	Medium	Medium	Medium
241267	Medium	Medium	Medium	Medium
246780	Medium	Medium	Medium	Medium
251707	Medium	Medium	Medium	Medium
256548	Medium	Medium	Medium	Medium
261485	Medium	Medium	Medium	Medium
266370	High	High	High	High
276190	Medium	Medium	High	High
280916	Low	Low	Low	Low
286091	Medium	Medium	Medium	Medium

Table A5: Impact of weights for 50,000 m^3/s (without bridges)

50,000 m^3/s	**Weights (*DV/vh*)**	**Weights (*DV/vh*)**	**Weights (*DV/vh*)**	**Weights (*DV/vh*)**
without bridges	**0.5/0.5**	**0.4/0.6**	**0.3/0.7**	**0.2/0.8**
Chainage (m)	**FSI (GA1)**	**FSI (GA2)**	**FSI (GA3)**	**FSI (GA4)**
0	High	High	High	High
4681	High	High	High	High
6754	High	High	High	High
13050	High	High	High	High
18189	High	High	High	High
22377	High	High	High	High
26479	Medium	Medium	Medium	Medium
30203	High	High	High	High
31904	High	High	High	High
42118	High	High	High	High
46130	High	High	High	High
48225	High	High	High	High
50382	High	High	High	High
52949	Medium	Medium	Medium	Medium
55947	Medium	Medium	Medium	Medium
58440	Medium	Medium	Medium	Medium
63654	High	High	High	High
66092	High	High	High	High
68304	High	High	High	High
71260	Medium	Medium	Medium	Medium
73703	Medium	Medium	Medium	Medium
76170	High	High	High	High
78375	Medium	Medium	Medium	Medium
80249	Medium	Medium	Medium	Medium
83454	Medium	Medium	Low	Low
87295	Medium	Medium	Medium	Medium
90205	Medium	Medium	Low	Low
93361	Medium	Medium	Medium	Medium
102711	Low	Low	Low	Low
108331	Medium	Medium	Medium	Medium
110138	Medium	Medium	Medium	Medium
113462	Low	Low	Low	Low
115856	Medium	Medium	Medium	Medium
119058	Medium	Medium	Medium	Medium
122184	Medium	Medium	Medium	Medium
129735	Medium	Medium	Medium	Medium
135257	Medium	Medium	Medium	Medium
139718	Medium	Medium	Medium	Medium
142442	Medium	Medium	Medium	Medium
146139	Medium	Low	Low	Low
152575	Medium	Medium	Medium	Medium
158810	Low	Low	Low	Low
164039	Medium	Medium	Medium	Low
170618	Medium	Low	Low	Low
178697	Low	Low	Low	Low
181759	Low	Low	Low	Low
189127	High	High	High	High
191125	Medium	Medium	Medium	Medium

196388	Medium	Medium	Low	Low
201645	Medium	Medium	Medium	Medium
206975	Medium	Medium	Medium	Medium
212052	Medium	Medium	Medium	Medium
216966	Medium	Medium	Medium	Medium
222405	Low	Low	Low	Low
228196	Medium	Medium	Medium	Medium
233169	High	High	High	High
237966	Medium	Medium	Medium	Medium
241267	Medium	Medium	Medium	Medium
246780	Medium	Medium	Medium	Medium
251707	Medium	Medium	Medium	Medium
256548	Medium	Medium	Medium	Medium
261485	Medium	Medium	Medium	Medium
266370	High	High	High	High
276190	Medium	High	High	High
280916	Low	Low	Low	Low
286091	Medium	Medium	Medium	Medium

Table A6: Impact of weights for MDF (61,977 m^3/s: without bridges)

MDF(61,977 m^3/s)	**Weights (*DV/vh*)**	**Weights (*DV/vh*)**	**Weights (*DV/vh*)**	**Weights (*DV/vh*)**
without bridges	**0.5/0.5**	**0.4/0.6**	**0.3/0.7**	**0.2/0.8**
Chainage (m)	**FSI (GA1)**	**FSI (GA2)**	**FSI (GA3)**	**FSI (GA4)**
0	High	High	High	High
4681	High	High	High	High
6754	High	High	High	High
13050	High	High	High	High
18189	High	High	High	High
22377	High	High	High	High
26479	High	High	High	High
30203	High	High	High	High
31904	High	High	High	High
42118	High	High	High	High
46130	High	High	High	High
48225	High	High	High	High
50382	High	High	High	High
52949	High	High	High	High
55947	High	High	High	High
58440	High	High	High	High
63654	High	High	High	High
66092	High	High	High	High
68304	High	High	High	High
71260	Medium	Medium	Medium	Medium
73703	Medium	Medium	Medium	Medium
76170	High	High	High	High
78375	Medium	Medium	Medium	Medium
80249	Medium	Medium	Medium	Medium
83454	Medium	Medium	Medium	Medium
87295	Medium	Medium	Medium	Medium

90205	Medium	Medium	Medium	Medium
93361	Medium	Medium	Medium	Medium
102711	Medium	Medium	Medium	Medium
108331	High	Medium	Medium	Medium
110138	Medium	Medium	Medium	Medium
113462	Medium	Medium	Medium	Medium
115856	Medium	Medium	Medium	Medium
119058	Medium	Medium	Medium	Medium
122184	Medium	Medium	Medium	Medium
129735	Medium	Medium	Medium	Medium
135257	Medium	Medium	Medium	Medium
139718	Medium	Medium	Medium	Medium
142442	Medium	Medium	Medium	Medium
146139	Medium	Medium	Medium	Medium
152575	Medium	Medium	Medium	Medium
158810	Medium	Medium	Medium	Low
164039	Medium	Medium	Medium	Medium
170618	Medium	Medium	Medium	Medium
178697	Medium	Medium	Medium	Medium
181759	Medium	Medium	Medium	Medium
189127	High	High	High	High
191125	Medium	Medium	Medium	Medium
196388	Medium	Medium	Medium	Medium
201645	Medium	Medium	Medium	Medium
206975	Medium	Medium	Medium	Medium
212052	Medium	Medium	Medium	Medium
216966	Medium	Medium	Medium	Medium
222405	Medium	Medium	Medium	Medium
228196	Medium	Medium	Medium	Medium
233169	High	High	High	High
237966	Medium	Medium	Medium	Medium
241267	Medium	Medium	Medium	Medium
246780	Medium	Medium	Medium	Medium
251707	Medium	Medium	Medium	Medium
256548	Medium	Medium	Medium	Medium
261485	High	Medium	Medium	Medium
266370	High	High	High	High
276190	High	High	High	High
280916	Medium	Medium	Medium	Medium
286091	Medium	Medium	Medium	Medium

APPENDIX B

CHECK OF IMPACT OF DAM BREACH PARAMETERS

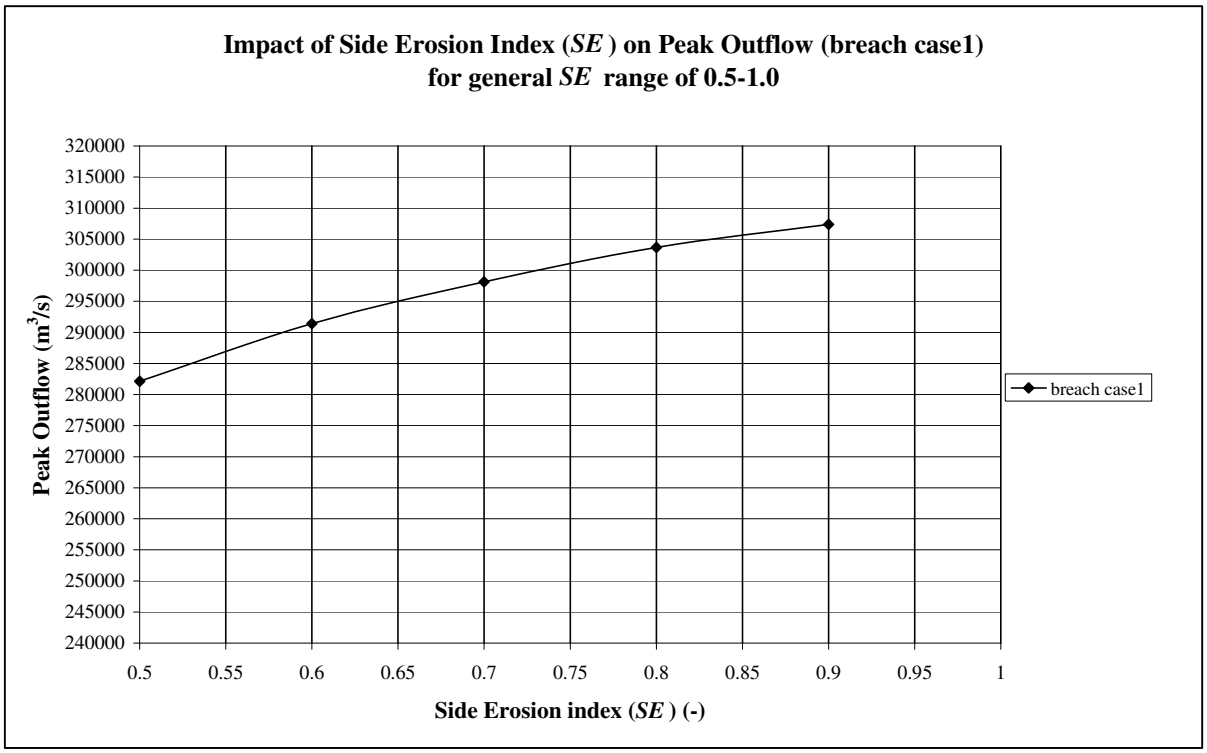

Figure B1: Impact of side erosion index on peak outflow (breach case1)

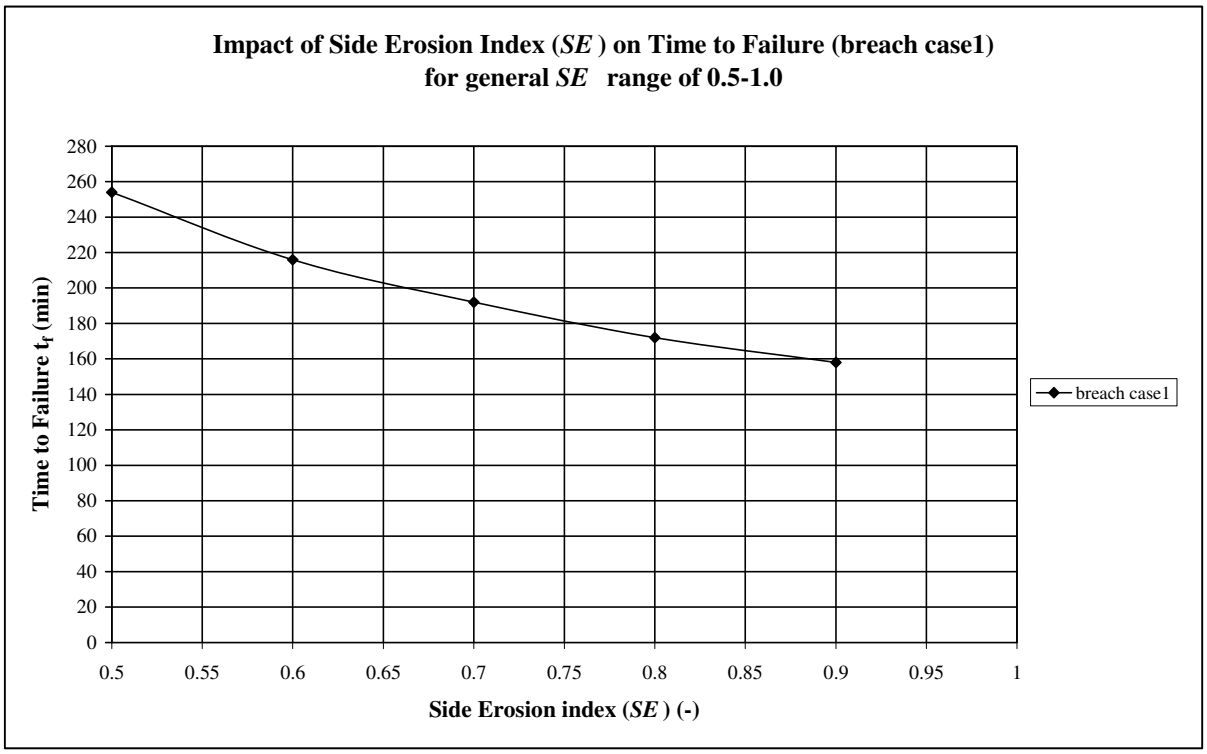

Figure B2: Impact of side erosion index on time to failure (breach case1)

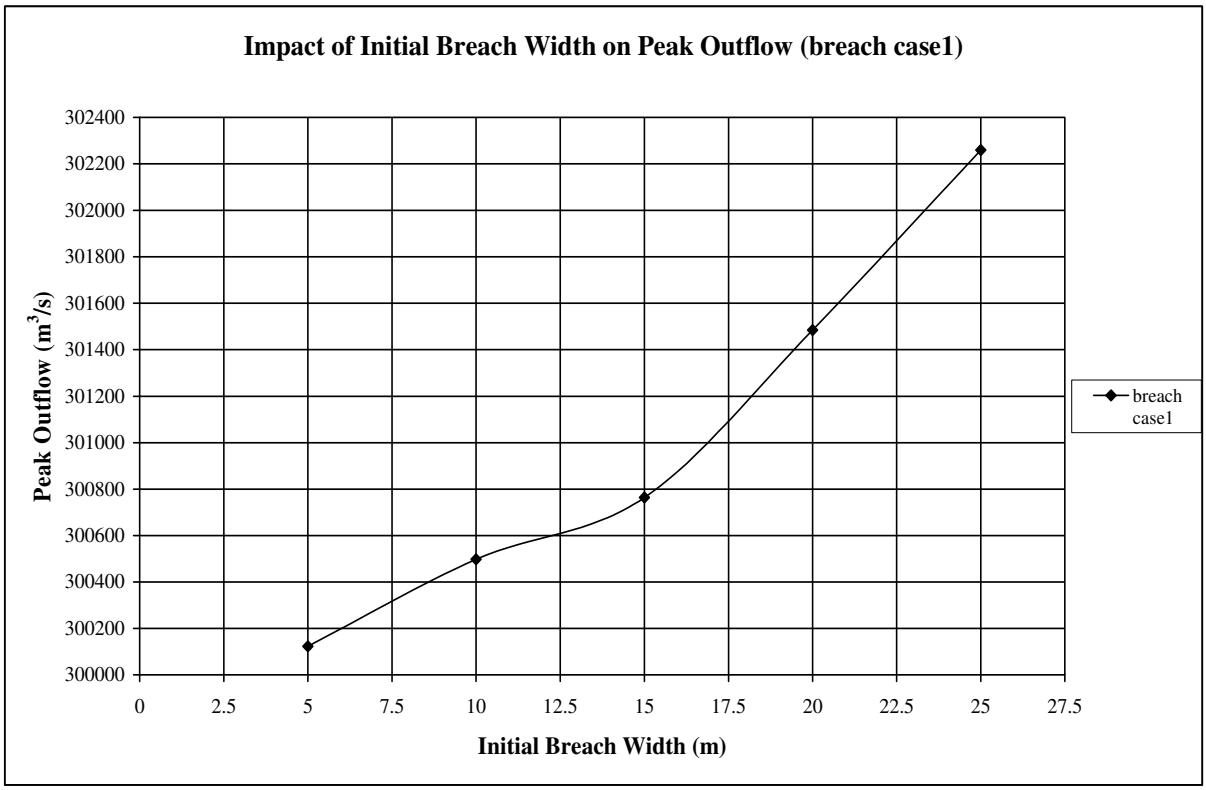

Figure B3: Impact of initial breach width on peak outflow (breach case1)

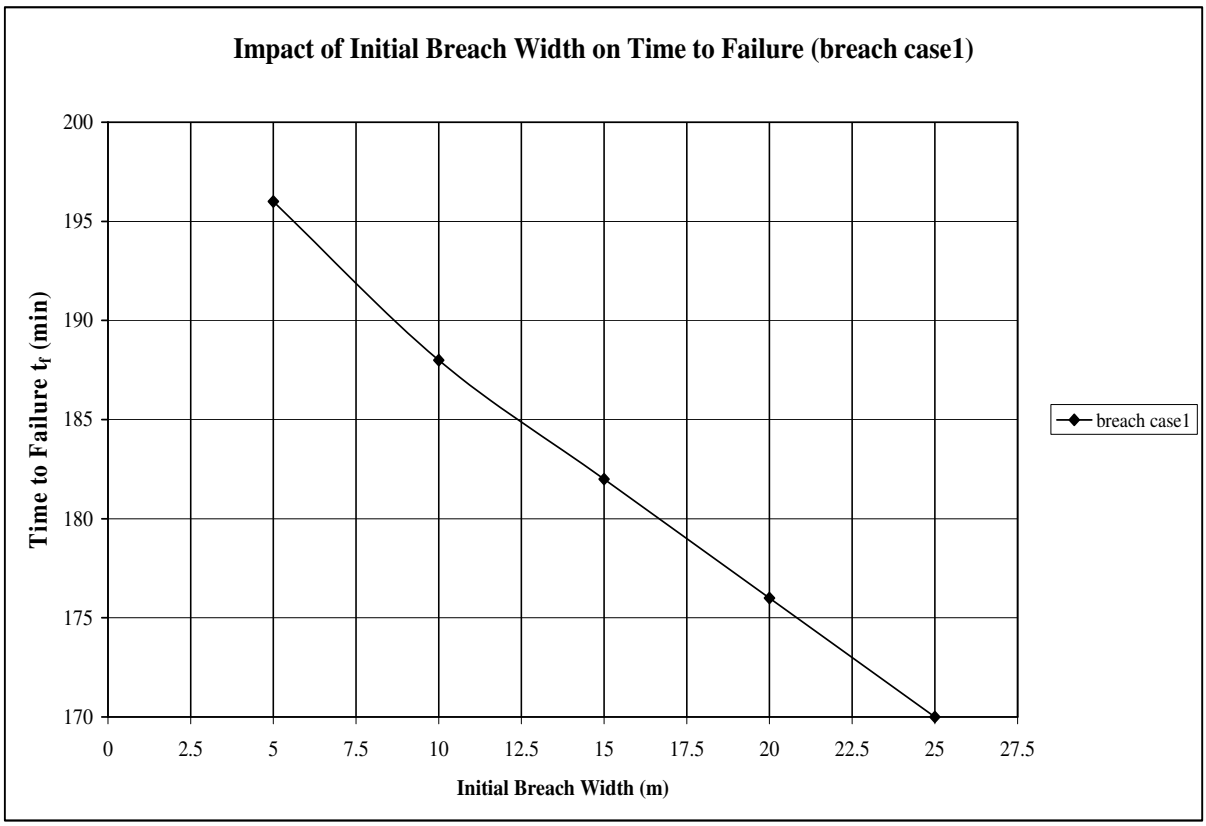

Figure B4: Impact of initial breach width on time to failure (breach case1)

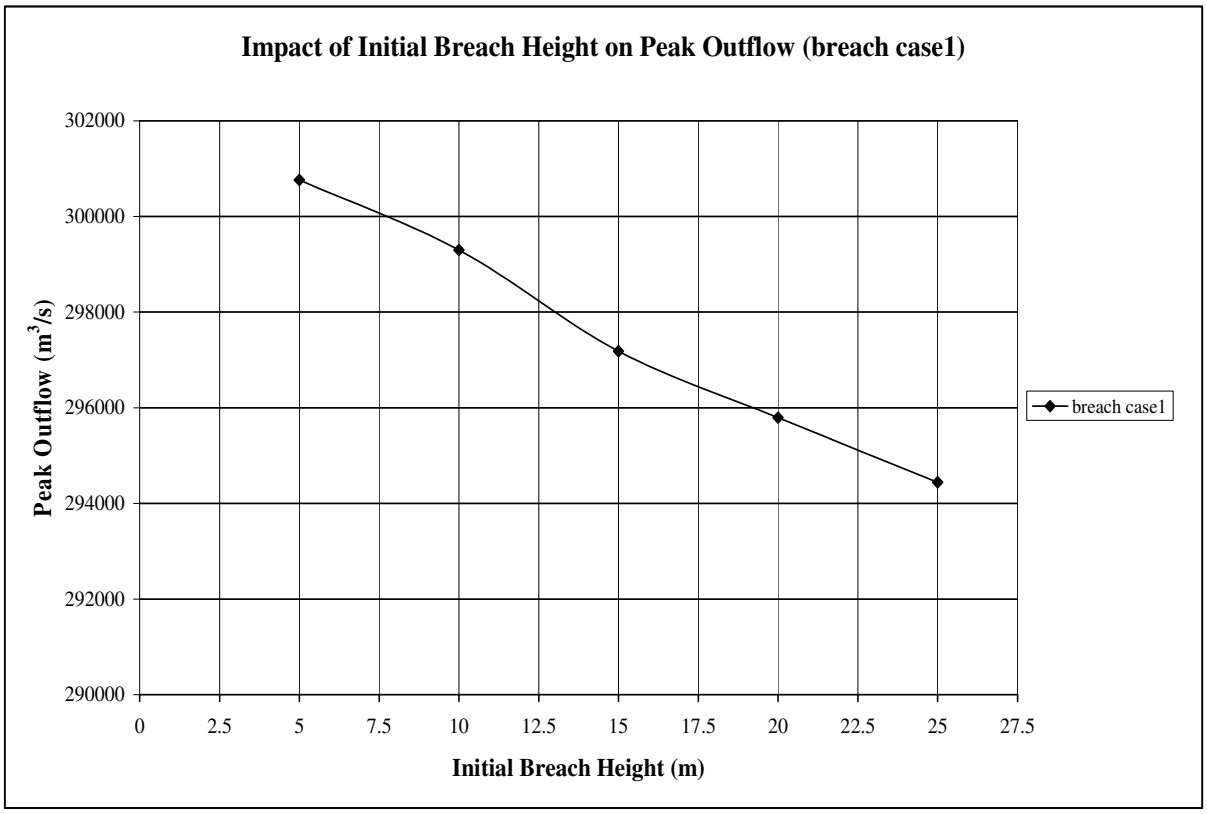

Figure B5: Impact of initial breach height on peak outflow (breach case1)

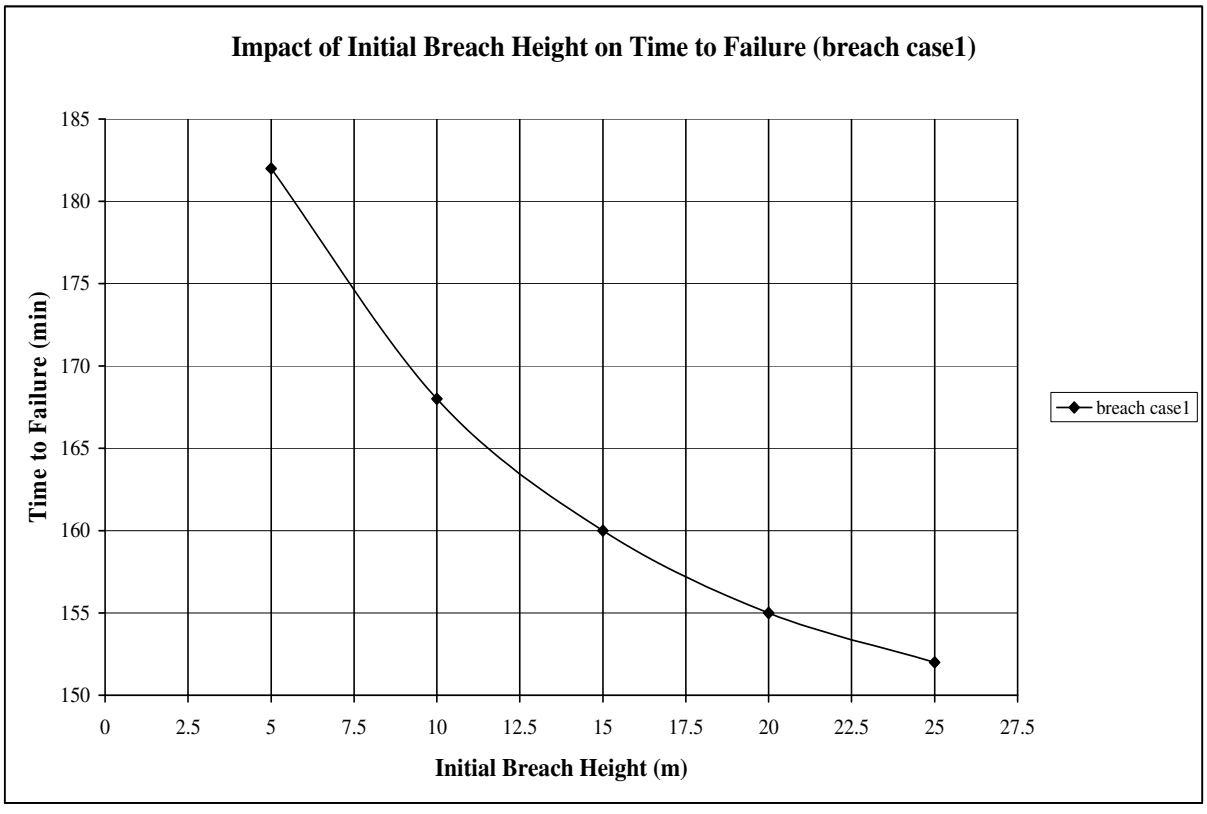

Figure B6: Impact of initial breach height on time to failure (breach case1)

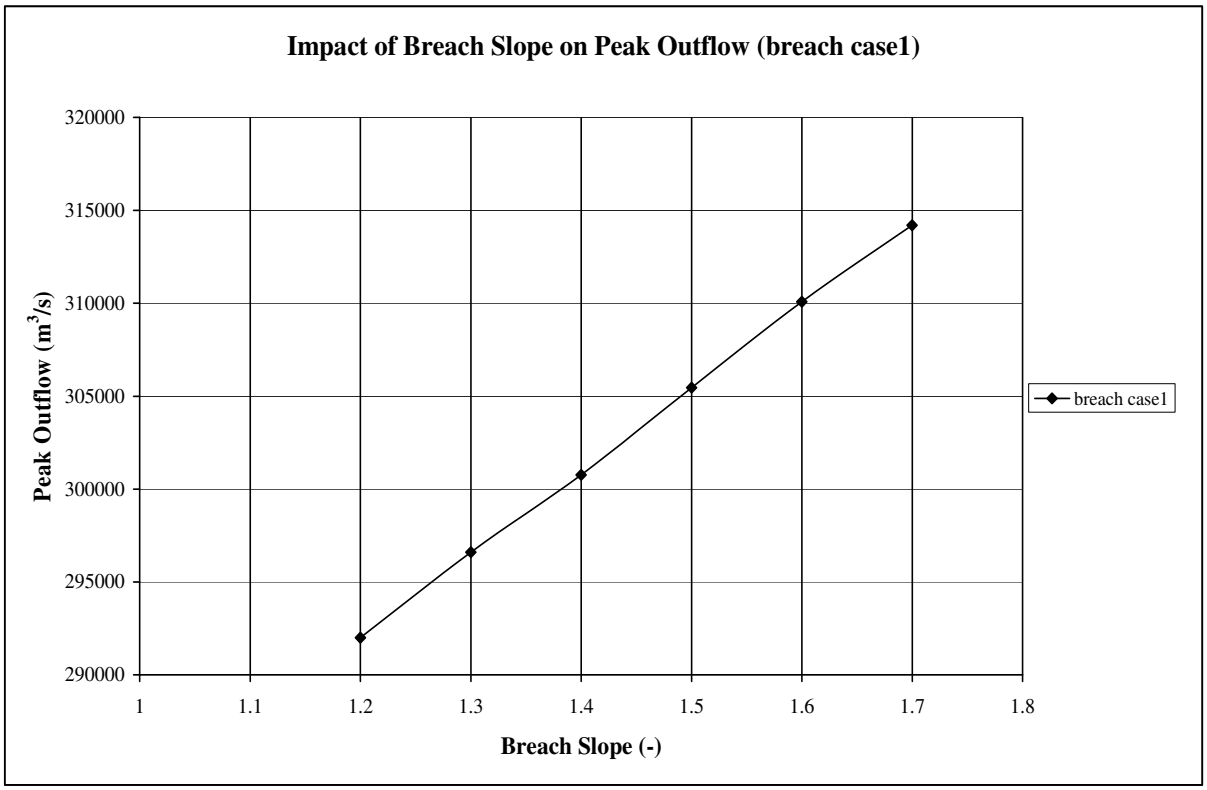

Figure B7: Impact of breach slope on peak outflow (breach case1)

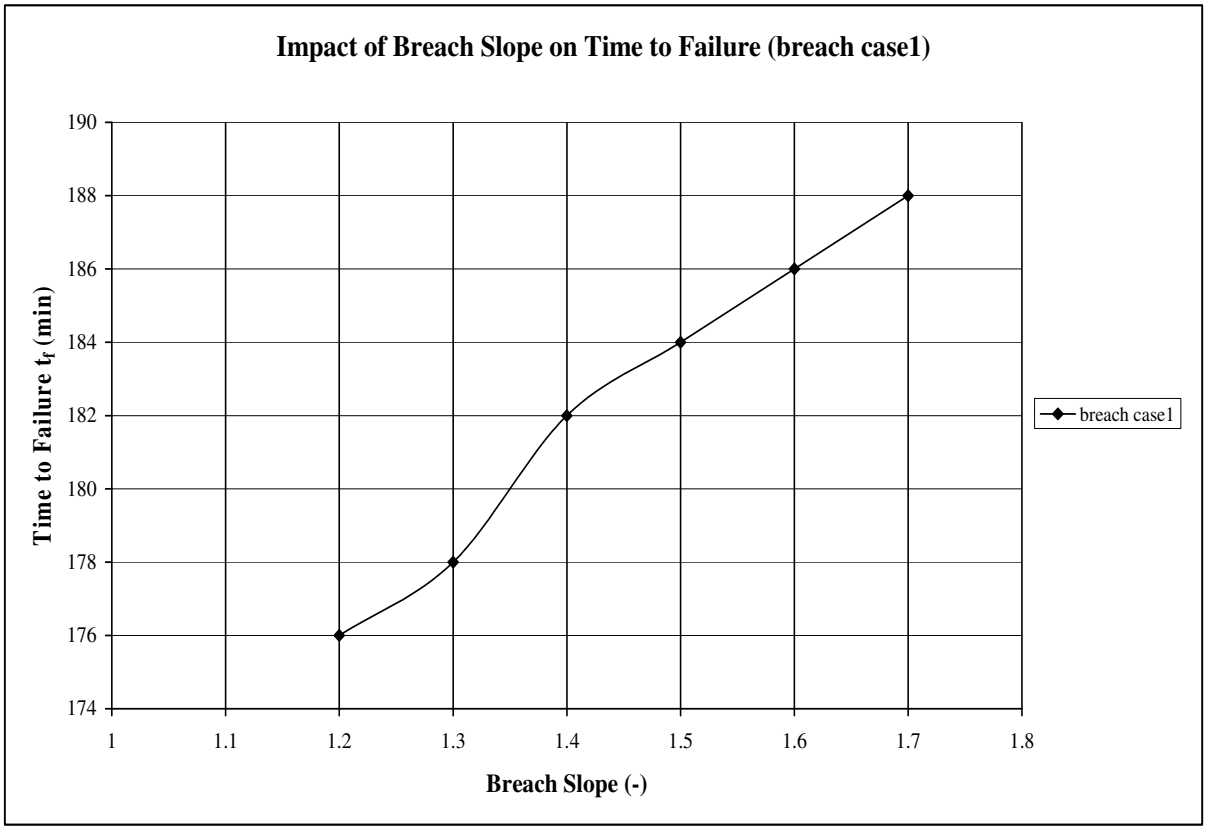

Figure B8: Impact of breach slope on time to failure (breach case1)

Institut für Wasserbau
Universität Stuttgart

Pfaffenwaldring 61
70569 Stuttgart (Vaihingen)
Telefon (0711) 685 - 64717/64749/64752/64679
Telefax (0711) 685 - 67020 o. 64746 o. 64681
E-Mail: iws@iws.uni-stuttgart.de
http://www.iws.uni-stuttgart.de

Verzeichnis der Mitteilungshefte

5 Plate, Erich: *Beitrag zur Bestimmung der Windgeschwindigkeitsverteilung in der durch eine Wand gestörten bodennahen Luftschicht*,
und
Röhnisch, Arthur; Marotz, Günter: *Neue Baustoffe und Bauausführungen für den Schutz der Böschungen und der Sohle von Kanälen, Flüssen und Häfen; Gestehungskosten und jeweilige Vorteile*, sowie Unny, T.E.: *Schwingungsuntersuchungen am Kegelstrahlschieber*, 1967

6 Seiler, Erich: *Die Ermittlung des Anlagenwertes der bundeseigenen Binnenschiffahrtsstraßen und Talsperren und des Anteils der Binnenschiffahrt an diesem Wert*, 1967

7 *Sonderheft anläßlich des 65. Geburtstages von Prof. Arthur Röhnisch mit Beiträgen von* Benk, Dieter; Breitling, J.; Gurr, Siegfried; Haberhauer, Robert; Honekamp, Hermann; Kuz, Klaus Dieter; Marotz, Günter; Mayer-Vorfelder, Hans-Jörg; Miller, Rudolf; Plate, Erich J.; Radomski, Helge; Schwarz, Helmut; Vollmer, Ernst; Wildenhahn, Eberhard; 1967

8 Jumikis, Alfred: *Beitrag zur experimentellen Untersuchung des Wassernachschubs in einem gefrierenden Boden und die Beurteilung der Ergebnisse*, 1968

9 Marotz, Günter: *Technische Grundlagen einer Wasserspeicherung im natürlichen Untergrund*, 1968

10 Radomski, Helge: *Untersuchungen über den Einfluß der Querschnittsform wellenförmiger Spundwände auf die statischen und rammtechnischen Eigenschaften*, 1968

11 Schwarz, Helmut: *Die Grenztragfähigkeit des Baugrundes bei Einwirkung vertikal gezogener Ankerplatten als zweidimensionales Bruchproblem*, 1969

12 Erbel, Klaus: *Ein Beitrag zur Untersuchung der Metamorphose von Mittelgebirgsschneedecken unter besonderer Berücksichtigung eines Verfahrens zur Bestimmung der thermischen Schneequalität*, 1969

13 Westhaus, Karl-Heinz: *Der Strukturwandel in der Binnenschiffahrt und sein Einfluß auf den Ausbau der Binnenschiffskanäle*, 1969

14 Mayer-Vorfelder, Hans-Jörg: *Ein Beitrag zur Berechnung des Erdwiderstandes unter Ansatz der logarithmischen Spirale als Gleitflächenfunktion*, 1970

15 Schulz, Manfred: *Berechnung des räumlichen Erddruckes auf die Wandung kreiszylindrischer Körper*, 1970

16 Mobasseri, Manoutschehr: *Die Rippenstützmauer. Konstruktion und Grenzen ihrer Standsicherheit*, 1970

17 Benk, Dieter: *Ein Beitrag zum Betrieb und zur Bemessung von Hochwasserrückhaltebecken*, 1970

18 Gàl, Attila: *Bestimmung der mitschwingenden Wassermasse bei überströmten Fischbauchklappen mit kreiszylindrischem Staublech*, 1971, vergriffen

19 Kuz, Klaus Dieter: *Ein Beitrag zur Frage des Einsetzens von Kavitationserscheinungen in einer Düsenströmung bei Berücksichtigung der im Wasser gelösten Gase*, 1971, vergriffen

20 Schaak, Hartmut: *Verteilleitungen von Wasserkraftanlagen*, 1971

21 *Sonderheft zur Eröffnung der neuen Versuchsanstalt des Instituts für Wasserbau der Universität Stuttgart mit Beiträgen von* Brombach, Hansjörg; Dirksen, Wolfram; Gàl, Attila; Gerlach, Reinhard; Giesecke, Jürgen; Holthoff, Franz-Josef; Kuz, Klaus Dieter; Marotz, Günter; Minor, Hans-Erwin; Petrikat, Kurt; Röhnisch, Arthur; Rueff, Helge; Schwarz, Helmut; Vollmer, Ernst; Wildenhahn, Eberhard; 1972

22 Wang, Chung-su: *Ein Beitrag zur Berechnung der Schwingungen an Kegelstrahlschiebern*, 1972

23 Mayer-Vorfelder, Hans-Jörg: *Erdwiderstandsbeiwerte nach dem Ohde-Variationsverfahren*, 1972

24 Minor, Hans-Erwin: *Beitrag zur Bestimmung der Schwingungsanfachungsfunktionen überströmter Stauklappen*, 1972, vergriffen

25 Brombach, Hansjörg: *Untersuchung strömungsmechanischer Elemente (Fluidik) und die Möglichkeit der Anwendung von Wirbelkammerelementen im Wasserbau*, 1972, vergriffen

26 Wildenhahn, Eberhard: *Beitrag zur Berechnung von Horizontalfilterbrunnen*, 1972

27 Steinlein, Helmut: *Die Eliminierung der Schwebstoffe aus Flußwasser zum Zweck der unterirdischen Wasserspeicherung, gezeigt am Beispiel der Iller*, 1972

28 Holthoff, Franz Josef: *Die Überwindung großer Hubhöhen in der Binnenschiffahrt durch Schwimmerhebewerke*, 1973

29 Röder, Karl: *Einwirkungen aus Baugrundbewegungen auf trog- und kastenförmige Konstruktionen des Wasser- und Tunnelbaues*, 1973

30 Kretschmer, Heinz: *Die Bemessung von Bogenstaumauern in Abhängigkeit von der Talform*, 1973

31 Honekamp, Hermann: *Beitrag zur Berechnung der Montage von Unterwasserpipelines*, 1973

32 Giesecke, Jürgen: *Die Wirbelkammertriode als neuartiges Steuerorgan im Wasserbau*, und Brombach, Hansjörg: *Entwicklung, Bauformen, Wirkungsweise und Steuereigenschaften von Wirbelkammerverstärkern*, 1974

33 Rueff, Helge: *Untersuchung der schwingungserregenden Kräfte an zwei hintereinander angeordneten Tiefschützen unter besonderer Berücksichtigung von Kavitation*, 1974

34 Röhnisch, Arthur: *Einpreßversuche mit Zementmörtel für Spannbeton - Vergleich der Ergebnisse von Modellversuchen mit Ausführungen in Hüllwellrohren*, 1975

35 *Sonderheft anläßlich des 65. Geburtstages von Prof. Dr.-Ing. Kurt Petrikat mit Beiträgen von*: Brombach, Hansjörg; Erbel, Klaus; Flinspach, Dieter; Fischer jr., Richard; Gàl, Attila; Gerlach, Reinhard; Giesecke, Jürgen; Haberhauer, Robert; Hafner Edzard; Hausenblas, Bernhard; Horlacher, Hans-Burkhard; Hutarew, Andreas; Knoll, Manfred; Krummet, Ralph; Marotz, Günter; Merkle, Theodor; Miller, Christoph; Minor, Hans-Erwin; Neumayer, Hans; Rao, Syamala; Rath, Paul; Rueff, Helge; Ruppert, Jürgen; Schwarz, Wolfgang; Topal-Gökceli, Mehmet; Vollmer, Ernst; Wang, Chung-su; Weber, Hans-Georg; 1975

36 Berger, Jochum: *Beitrag zur Berechnung des Spannungszustandes in rotationssymmetrisch belasteten Kugelschalen veränderlicher Wandstärke unter Gas- und Flüssigkeitsdruck durch Integration schwach singulärer Differentialgleichungen*, 1975

37 Dirksen, Wolfram: *Berechnung instationärer Abflußvorgänge in gestauten Gerinnen mittels Differenzenverfahren und die Anwendung auf Hochwasserrückhaltebecken*, 1976

38 Horlacher, Hans-Burkhard: *Berechnung instationärer Temperatur- und Wärmespannungsfelder in langen mehrschichtigen Hohlzylindern*, 1976

39 Hafner, Edzard: *Untersuchung der hydrodynamischen Kräfte auf Baukörper im Tiefwasserbereich des Meeres*, 1977, ISBN 3-921694-39-6

40 Ruppert, Jürgen: *Über den Axialwirbelkammerverstärker für den Einsatz im Wasserbau*, 1977, ISBN 3-921694-40-X

41 Hutarew, Andreas: *Beitrag zur Beeinflußbarkeit des Sauerstoffgehalts in Fließgewässern an Abstürzen und Wehren*, 1977, ISBN 3-921694-41-8, vergriffen

42 Miller, Christoph: *Ein Beitrag zur Bestimmung der schwingungserregenden Kräfte an unterströmten Wehren*, 1977, ISBN 3-921694-42-6

43 Schwarz, Wolfgang: *Druckstoßberechnung unter Berücksichtigung der Radial- und Längsverschiebungen der Rohrwandung*, 1978, ISBN 3-921694-43-4

44 Kinzelbach, Wolfgang: *Numerische Untersuchungen über den optimalen Einsatz variabler Kühlsysteme einer Kraftwerkskette am Beispiel Oberrhein*, 1978, ISBN 3-921694-44-2

45 Barczewski, Baldur: *Neue Meßmethoden für Wasser-Luftgemische und deren Anwendung auf zweiphasige Auftriebsstrahlen*, 1979, ISBN 3-921694-45-0

46 Neumayer, Hans: *Untersuchung der Strömungsvorgänge in radialen Wirbelkammerverstärkern*, 1979, ISBN 3-921694-46-9

47 Elalfy, Youssef-Elhassan: *Untersuchung der Strömungsvorgänge in Wirbelkammerdioden und -drosseln*, 1979, ISBN 3-921694-47-7

48 Brombach, Hansjörg: *Automatisierung der Bewirtschaftung von Wasserspeichern*, 1981, ISBN 3-921694-48-5

49 Geldner, Peter: *Deterministische und stochastische Methoden zur Bestimmung der Selbstdichtung von Gewässern*, 1981, ISBN 3-921694-49-3, vergriffen

50 Mehlhorn, Hans: *Temperaturveränderungen im Grundwasser durch Brauchwassereinleitungen*, 1982, ISBN 3-921694-50-7, vergriffen

51 Hafner, Edzard: *Rohrleitungen und Behälter im Meer*, 1983, ISBN 3-921694-51-5

52 Rinnert, Bernd: *Hydrodynamische Dispersion in porösen Medien: Einfluß von Dichteunterschieden auf die Vertikalvermischung in horizontaler Strömung*, 1983, ISBN 3-921694-52-3, vergriffen

53 Lindner, Wulf: *Steuerung von Grundwasserentnahmen unter Einhaltung ökologischer Kriterien*, 1983, ISBN 3-921694-53-1, vergriffen

54 Herr, Michael; Herzer, Jörg; Kinzelbach, Wolfgang; Kobus, Helmut; Rinnert, Bernd: *Methoden zur rechnerischen Erfassung und hydraulischen Sanierung von Grundwasserkontaminationen*, 1983, ISBN 3-921694-54-X

55 Schmitt, Paul: *Wege zur Automatisierung der Niederschlagsermittlung*, 1984, ISBN 3-921694-55-8, vergriffen

56 Müller, Peter: *Transport und selektive Sedimentation von Schwebstoffen bei gestautem Abfluß*, 1985, ISBN 3-921694-56-6

57 El-Qawasmeh, Fuad: *Möglichkeiten und Grenzen der Tropfbewässerung unter besonderer Berücksichtigung der Verstopfungsanfälligkeit der Tropfelemente*, 1985, ISBN 3-921694-57-4, vergriffen

58 Kirchenbaur, Klaus: *Mikroprozessorgesteuerte Erfassung instationärer Druckfelder am Beispiel seegangsbelasteter Baukörper*, 1985, ISBN 3-921694-58-2

59 Kobus, Helmut (Hrsg.): *Modellierung des großräumigen Wärme- und Schadstofftransports im Grundwasser*, Tätigkeitsbericht 1984/85 (DFG-Forschergruppe an den Universitäten Hohenheim, Karlsruhe und Stuttgart), 1985, ISBN 3-921694-59-0, vergriffen

60 Spitz, Karlheinz: *Dispersion in porösen Medien: Einfluß von Inhomogenitäten und Dichteunterschieden*, 1985, ISBN 3-921694-60-4, vergriffen

61 Kobus, Helmut: *An Introduction to Air-Water Flows in Hydraulics*, 1985, ISBN 3-921694-61-2

62 Kaleris, Vassilios: *Erfassung des Austausches von Oberflächen- und Grundwasser in horizontalebenen Grundwassermodellen*, 1986, ISBN 3-921694-62-0

63 Herr, Michael: *Grundlagen der hydraulischen Sanierung verunreinigter Porengrundwasserleiter*, 1987, ISBN 3-921694-63-9

64 Marx, Walter: *Berechnung von Temperatur und Spannung in Massenbeton infolge Hydratation*, 1987, ISBN 3-921694-64-7

65 Koschitzky, Hans-Peter: *Dimensionierungskonzept für Sohlbelüfter in Schußrinnen zur Vermeidung von Kavitationsschäden*, 1987, ISBN 3-921694-65-5

66 Kobus, Helmut (Hrsg.): *Modellierung des großräumigen Wärme- und Schadstofftransports im Grundwasser*, Tätigkeitsbericht 1986/87 (DFG-Forschergruppe an den Universitäten Hohenheim, Karlsruhe und Stuttgart) 1987, ISBN 3-921694-66-3

67 Söll, Thomas: *Berechnungsverfahren zur Abschätzung anthropogener Temperaturanomalien im Grundwasser*, 1988, ISBN 3-921694-67-1

68 Dittrich, Andreas; Westrich, Bernd: *Bodenseeufererosion, Bestandsaufnahme und Bewertung*, 1988, ISBN 3-921694-68-X, vergriffen

69 Huwe, Bernd; van der Ploeg, Rienk R.: *Modelle zur Simulation des Stickstoffhaushaltes von Standorten mit unterschiedlicher landwirtschaftlicher Nutzung*, 1988, ISBN 3-921694-69-8, vergriffen

70 Stephan, Karl: *Integration elliptischer Funktionen*, 1988, ISBN 3-921694-70-1

71 Kobus, Helmut; Zilliox, Lothaire (Hrsg.): *Nitratbelastung des Grundwassers, Auswirkungen der Landwirtschaft auf die Grundwasser- und Rohwasserbeschaffenheit und Maßnahmen zum Schutz des Grundwassers*. Vorträge des deutsch-französischen Kolloquiums am 6. Oktober 1988, Universitäten Stuttgart und Louis Pasteur Strasbourg (Vorträge in deutsch oder französisch, Kurzfassungen zweisprachig), 1988, ISBN 3-921694-71-X

72 Soyeaux, Renald: *Unterströmung von Stauanlagen auf klüftigem Untergrund unter Berücksichtigung laminarer und turbulenter Fließzustände*,1991, ISBN 3-921694-72-8

73 Kohane, Roberto: *Berechnungsmethoden für Hochwasserabfluß in Fließgewässern mit überströmten Vorländern*, 1991, ISBN 3-921694-73-6

74 Hassinger, Reinhard: *Beitrag zur Hydraulik und Bemessung von Blocksteinrampen in flexibler Bauweise*, 1991, ISBN 3-921694-74-4, vergriffen

75 Schäfer, Gerhard: *Einfluß von Schichtenstrukturen und lokalen Einlagerungen auf die Längsdispersion in Porengrundwasserleitern*, 1991, ISBN 3-921694-75-2

76 Giesecke, Jürgen: *Vorträge, Wasserwirtschaft in stark besiedelten Regionen; Umweltforschung mit Schwerpunkt Wasserwirtschaft*, 1991, ISBN 3-921694-76-0

77 Huwe, Bernd: *Deterministische und stochastische Ansätze zur Modellierung des Stickstoffhaushalts landwirtschaftlich genutzter Flächen auf unterschiedlichem Skalenniveau*, 1992, ISBN 3-921694-77-9, vergriffen

78 Rommel, Michael: *Verwendung von Kluftdaten zur realitätsnahen Generierung von Kluftnetzen mit anschließender laminar-turbulenter Strömungsberechnung*, 1993, ISBN 3-92 1694-78-7

79 Marschall, Paul: *Die Ermittlung lokaler Stofffrachten im Grundwasser mit Hilfe von Einbohrloch-Meßverfahren*, 1993, ISBN 3-921694-79-5, vergriffen

80 Ptak, Thomas: *Stofftransport in heterogenen Porenaquiferen: Felduntersuchungen und stochastische Modellierung*, 1993, ISBN 3-921694-80-9, vergriffen

81 Haakh, Frieder: *Transientes Strömungsverhalten in Wirbelkammern,* 1993, ISBN 3-921694-81-7

82 Kobus, Helmut; Cirpka, Olaf; Barczewski, Baldur; Koschitzky, Hans-Peter: *Versucheinrichtung zur Grundwasser und Altlastensanierung VEGAS, Konzeption und Programmrahmen*, 1993, ISBN 3-921694-82-5

83 Zang, Weidong: *Optimaler Echtzeit-Betrieb eines Speichers mit aktueller Abflußregenerierung*, 1994, ISBN 3-921694-83-3, vergriffen

84 Franke, Hans-Jörg: *Stochastische Modellierung eines flächenhaften Stoffeintrages und Transports in Grundwasser am Beispiel der Pflanzenschutzmittelproblematik*, 1995, ISBN 3-921694-84-1

85 Lang, Ulrich: *Simulation regionaler Strömungs- und Transportvorgänge in Karstaquiferen mit Hilfe des Doppelkontinuum-Ansatzes: Methodenentwicklung und Parameteridentifikation*, 1995, ISBN 3-921694-85-X, vergriffen

86 Helmig, Rainer: *Einführung in die Numerischen Methoden der Hydromechanik*, 1996, ISBN 3-921694-86-8, vergriffen

87 Cirpka, Olaf: *CONTRACT: A Numerical Tool for Contaminant Transport and Chemical Transformations - Theory and Program Documentation -*, 1996, ISBN 3-921694-87-6

88 Haberlandt, Uwe: *Stochastische Synthese und Regionalisierung des Niederschlages für Schmutzfrachtberechnungen*, 1996, ISBN 3-921694-88-4

89 Croisé, Jean: *Extraktion von flüchtigen Chemikalien aus natürlichen Lockergesteinen mittels erzwungener Luftströmung*, 1996, ISBN 3-921694-89-2, vergriffen

90 Jorde, Klaus: *Ökologisch begründete, dynamische Mindestwasserregelungen bei Ausleitungskraftwerken*, 1997, ISBN 3-921694-90-6, vergriffen

91 Helmig, Rainer: *Gekoppelte Strömungs- und Transportprozesse im Untergrund - Ein Beitrag zur Hydrosystemmodellierung-*, 1998, ISBN 3-921694-91-4, vergriffen

92 Emmert, Martin: *Numerische Modellierung nichtisothermer Gas-Wasser Systeme in porösen Medien,* 1997, ISBN 3-921694-92-2

93 Kern, Ulrich: *Transport von Schweb- und Schadstoffen in staugeregelten Fließgewässern am Beispiel des Neckars*, 1997, ISBN 3-921694-93-0, vergriffen

94 Förster, Georg: *Druckstoßdämpfung durch große Luftblasen in Hochpunkten von Rohrleitungen 1997*, ISBN 3-921694-94-9

95 Cirpka, Olaf: *Numerische Methoden zur Simulation des reaktiven Mehrkomponententransports im Grundwasser*, 1997, ISBN 3-921694-95-7, vergriffen

96 Färber, Arne: *Wärmetransport in der ungesättigten Bodenzone: Entwicklung einer thermischen In-situ-Sanierungstechnologie*, 1997, ISBN 3-921694-96-5

97 Betz, Christoph: *Wasserdampfdestillation von Schadstoffen im porösen Medium: Entwicklung einer thermischen In-situ-Sanierungstechnologie*, 1998, ISBN 3-921694-97-3

98 Xu, Yichun: *Numerical Modeling of Suspended Sediment Transport in Rivers*, 1998, ISBN 3-921694-98-1, vergriffen

99 Wüst, Wolfgang: *Geochemische Untersuchungen zur Sanierung CKW-kontaminierter Aquifere mit Fe(0)-Reaktionswänden,* 2000, ISBN 3-933761-02-2

100 Sheta, Hussam: *Simulation von Mehrphasenvorgängen in porösen Medien unter Einbeziehung von Hysterese-Effekten*, 2000, ISBN 3-933761-03-4

101 Ayros, Edwin: *Regionalisierung extremer Abflüsse auf der Grundlage statistischer Verfahren*, 2000, ISBN 3-933761-04-2, vergriffen

102 Huber, Ralf: *Compositional Multiphase Flow and Transport in Heterogeneous Porous Media*, 2000, ISBN 3-933761-05-0

103 Braun, Christopherus: *Ein Upscaling-Verfahren für Mehrphasenströmungen in porösen Medien*, 2000, ISBN 3-933761-06-9

104 Hofmann, Bernd: *Entwicklung eines rechnergestützten Managementsystems zur Beurteilung von Grundwasserschadensfällen*, 2000, ISBN 3-933761-07-7

105 Class, Holger: *Theorie und numerische Modellierung nichtisothermer Mehrphasenprozesse in NAPL-kontaminierten porösen Medien,* 2001, ISBN 3-933761-08-5

106 Schmidt, Reinhard: *Wasserdampf- und Heißluftinjektion zur thermischen Sanierung kontaminierter Standorte*, 2001, ISBN 3-933761-09-3

107 Josef, Reinhold:, *Schadstoffextraktion mit hydraulischen Sanierungsverfahren unter Anwendung von grenzflächenaktiven Stoffen*, 2001, ISBN 3-933761-10-7

108 Schneider, Matthias: *Habitat- und Abflussmodellierung für Fließgewässer mit unscharfen Berechnungsansätzen*, 2001, ISBN 3-933761-11-5

109 Rathgeb, Andreas: *Hydrodynamische Bemessungsgrundlagen für Lockerdeckwerke an überströmbaren Erddämmen*, 2001, ISBN 3-933761-12-3

110 Lang, Stefan: *Parallele numerische Simulation instätionärer Probleme mit adaptiven Methoden auf unstrukturierten Gittern*, 2001, ISBN 3-933761-13-1

111 Appt, Jochen; Stumpp Simone: *Die Bodensee-Messkampagne 2001, IWS/CWR Lake Constance Measurement Program 2001*, 2002, ISBN 3-933761-14-X

112 Heimerl, Stephan: *Systematische Beurteilung von Wasserkraftprojekten,* 2002, ISBN 3-933761-15-8

113 Iqbal, Amin: *On the Management and Salinity Control of Drip Irrigation,* 2002, ISBN 3-933761-16-6

114 Silberhorn-Hemminger, Annette: *Modellierung von Kluftaquifersystemen: Geostatistische Analyse und deterministisch-stochastische Kluftgenerierung,* 2002, ISBN 3-933761-17-4

115 Winkler, Angela: *Prozesse des Wärme- und Stofftransports bei der In-situ-Sanierung mit festen Wärmequellen,* 2003, ISBN 3-933761-18-2

116 Marx, Walter: *Wasserkraft, Bewässerung, Umwelt - Planungs- und Bewertungsschwerpunkte der Wasserbewirtschaftung,* 2003, ISBN 3-933761-19-0

117 Hinkelmann, Reinhard: *Efficient Numerical Methods and Information-Processing Techniques in Environment Water,* 2003, ISBN 3-933761-20-4

118 Samaniego-Eguiguren, Luis Eduardo: *Hydrological Consequences of Land Use / Land Cover and Climatic Changes in Mesoscale Catchments*, 2003, ISBN 3-933761-21-2

119 Neunhäuserer, Lina: *Diskretisierungsansätze zur Modellierung von Strömungs- und Transportprozessen in geklüftet-porösen Medien*, 2003, ISBN 3-933761-22-0

120 Paul, Maren: *Simulation of Two-Phase Flow in Heterogeneous Poros Media with Adaptive Methods*, 2003, ISBN 3-933761-23-9

121 Ehret, Uwe: *Rainfall and Flood Nowcasting in Small Catchments using Weather Radar*, 2003, ISBN 3-933761-24-7

122 Haag, Ingo: *Der Sauerstoffhaushalt staugeregelter Flüsse am Beispiel des Neckars - Analysen, Experimente, Simulationen -,* 2003, ISBN 3-933761-25-5

123 Appt, Jochen: *Analysis of Basin-Scale Internal Waves in Upper Lake Constance,* 2003, ISBN 3-933761-26-3

124 Hrsg.: Schrenk, Volker; Batereau, Katrin; Barczewski, Baldur; Weber, Karolin und Koschitzky, Hans-Peter: *Symposium Ressource Fläche und VEGAS - Statuskolloquium 2003, 30. September und 1. Oktober 2003,* 2003, ISBN 3-933761-27-1

125 Omar Khalil Ouda: *Optimisation of Agricultural Water Use: A Decision Support System for the Gaza Strip,* 2003, ISBN 3-933761-28-0

126 Batereau, Katrin: *Sensorbasierte Bodenluftmessung zur Vor-Ort-Erkundung von Schadensherden im Untergrund*, 2004, ISBN 3-933761-29-8

127 Witt, Oliver: *Erosionsstabilität von Gewässersedimenten mit Auswirkung auf den Stofftransport bei Hochwasser am Beispiel ausgewählter Stauhaltungen des Oberrheins*, 2004, ISBN 3-933761-30-1

128 Jakobs, Hartmut: *Simulation nicht-isothermer Gas-Wasser-Prozesse in komplexen Kluft-Matrix-Systemen*, 2004, ISBN 3-933761-31-X

129 Li, Chen-Chien: *Deterministisch-stochastisches Berechnungskonzept zur Beurteilung der Auswirkungen erosiver Hochwasserereignisse in Flussstauhaltungen,* 2004, ISBN 3-933761-32-8

130 Reichenberger, Volker; Helmig, Rainer; Jakobs, Hartmut; Bastian, Peter; Niessner, Jennifer: *Complex Gas-Water Processes in Discrete Fracture-Matrix Systems: Upscaling, Mass-Conservative Discretization and Efficient Multilevel Solution,* 2004, ISBN 3-933761-33-6

131 Hrsg.: Barczewski, Baldur; Koschitzky, Hans-Peter; Weber, Karolin; Wege, Ralf: *VEGAS - Statuskolloquium 2004,* Tagungsband zur Veranstaltung am 05. Oktober 2004 an der Universität Stuttgart, Campus Stuttgart-Vaihingen, 2004, ISBN 3-933761-34-4

132 Asie, Kemal Jabir: *Finite Volume Models for Multiphase Multicomponent Flow through Porous Media*. 2005, ISBN 3-933761-35-2

133 Jacoub, George: *Development of a 2-D Numerical Module for Particulate Contaminant Transport in Flood Retention Reservoirs and Impounded Rivers,* 2004, ISBN 3-933761-36-0

134 Nowak, Wolfgang: *Geostatistical Methods for the Identification of Flow and Transport Parameters in the Subsurface,* 2005, ISBN 3-933761-37-9

135 Süß, Mia: *Analysis of the influence of structures and boundaries on flow and transport processes in fractured porous media*, 2005, ISBN 3-933761-38-7

136 Jose, Surabhin Chackiath: *Experimental Investigations on Longitudinal Dispersive Mixing in Heterogeneous Aquifers,* 2005, ISBN: 3-933761-39-5

137 Filiz, Fulya: *Linking Large-Scale Meteorological Conditions to Floods in Mesoscale Catchments,* 2005, ISBN 3-933761-40-9

138 Qin, Minghao: *Wirklichkeitsnahe und recheneffiziente Ermittlung von Temperatur und Spannungen bei großen RCC-Staumauern*, 2005, ISBN 3-933761-41-7

139 Kobayashi, Kenichiro: *Optimization Methods for Multiphase Systems in the Subsurface - Application to Methane Migration in Coal Mining Areas*, 2005, ISBN 3-933761-42-5

140 Rahman, Md. Arifur: *Experimental Investigations on Transverse Dispersive Mixing in Heterogeneous Porous Media,* 2005, ISBN 3-933761-43-3

141 Schrenk, Volker: *Ökobilanzen zur Bewertung von Altlastensanierungsmaßnahmen,* 2005, ISBN 3-933761-44-1

142 Hundecha, Hirpa Yeshewatesfa: *Regionalization of Parameters of a Conceptual Rainfall-Runoff Model*, 2005, ISBN: 3-933761-45-X

143 Wege, Ralf: *Untersuchungs- und Überwachungsmethoden für die Beurteilung natürlicher Selbstreinigungsprozesse im Grundwasser,* 2005, ISBN 3-933761-46-8

144 Breiting, Thomas: *Techniken und Methoden der Hydroinformatik - Modellierung von komplexen Hydrosystemen im Untergrund*, 2006, 3-933761-47-6

145 Hrsg.: Braun, Jürgen; Koschitzky, Hans-Peter; Müller, Martin: *Ressource Untergrund: 10 Jahre VEGAS: Forschung und Technologieentwicklung zum Schutz von Grundwasser und Boden,* Tagungsband zur Veranstaltung am 28. und 29. September 2005 an der Universität Stuttgart, Campus Stuttgart-Vaihingen, 2005, ISBN 3-933761-48-4

146 Rojanschi, Vlad: *Abflusskonzentration in mesoskaligen Einzugsgebieten unter Berücksichtigung des Sickerraumes,* 2006, ISBN 3-933761-49-2

147 Winkler, Nina Simone: *Optimierung der Steuerung von Hochwasserrückhaltebecken-systemen,* 2006, ISBN 3-933761-50-6

148 Wolf, Jens: *Räumlich differenzierte Modellierung der Grundwasserströmung alluvialer Aquifere für mesoskalige Einzugsgebiete*, 2006, ISBN: 3-933761-51-4

149 Kohler, Beate: *Externe Effekte der Laufwasserkraftnutzung*, 2006, ISBN 3-933761-52-2

150 Hrsg.: Braun, Jürgen; Koschitzky, Hans-Peter; Stuhrmann, Matthias: *VEGAS-Statuskolloquium 2006,* Tagungsband zur Veranstaltung am 28. September 2006 an der Universität Stuttgart, Campus Stuttgart-Vaihingen, 2006, ISBN 3-933761-53-0

151 Niessner, Jennifer: *Multi-Scale Modeling of Multi-Phase - Multi-Component Processes in Heterogeneous Porous Media*, 2006, ISBN 3-933761-54-9

152 Fischer, Markus: *Beanspruchung eingeerdeter Rohrleitungen infolge Austrocknung bindiger Böden,* 2006, ISBN 3-933761-55-7

153 Schneck, Alexander: *Optimierung der Grundwasserbewirtschaftung unter Berücksichtigung der Belange der Wasserversorgung, der Landwirtschaft und des Naturschutzes*, 2006, ISBN 3-933761-56-5

154 Das, Tapash: *The Impact of Spatial Variability of Precipitation on the Predictive Uncertainty of Hydrological Models,* 2006, ISBN 3-933761-57-3

155 Bielinski, Andreas: *Numerical Simulation of CO_2 sequestration in geological formations*, 2007, ISBN 3-933761-58-1

156 Mödinger, Jens: *Entwicklung eines Bewertungs- und Entscheidungsunterstützungssystems für eine nachhaltige regionale Grundwasserbewirtschaftung*, 2006, ISBN 3-933761-60-3

157 Manthey, Sabine: *Two-phase flow processes with dynamic effects in porous media - parameter estimation and simulation,* 2007, ISBN 3-933761-61-1

158 Pozos Estrada, Oscar: *Investigation on the Effects of Entrained Air in Pipelines,* 2007, ISBN 3-933761-62-X

159 Ochs, Steffen Oliver: *Steam injection into saturated porous media – process analysis including experimental and numerical investigations*, 2007, ISBN 3-933761-63-8

160 Marx, Andreas: *Einsatz gekoppelter Modelle und Wetterradar zur Abschätzung von Niederschlagsintensitäten und zur Abflussvorhersage, 2007,* ISBN 3-933761-64-6

161 Hartmann, Gabriele Maria: *Investigation of Evapotranspiration Concepts in Hydrological Modelling for Climate Change Impact Assessment*, 2007, ISBN 3-933761-65-4

162 Kebede Gurmessa, Tesfaye: *Numerical Investigation on Flow and Transport Characteristics to Improve Long-Term Simulation of Reservoir Sedimentation*, 2007, ISBN 3-933761-66-2

163 Trifković, Aleksandar: *Multi-objective and Risk-based Modelling Methodology for Planning, Design and Operation of Water Supply Systems*, 2007, ISBN 3-933761-67-0

164 Götzinger, Jens: *Distributed Conceptual Hydrological Modelling - Simulation of Climate, Land Use Change Impact and Uncertainty Analysis*, 2007, ISBN 3-933761-68-9

165 Hrsg.: Braun, Jürgen; Koschitzky, Hans-Peter; Stuhrmann, Matthias: *VEGAS – Kolloquium 2007,* Tagungsband zur Veranstaltung am 26. September 2007 an der Universität Stuttgart, Campus Stuttgart-Vaihingen, 2007, ISBN 3-933761-69-7

166 Freeman, Beau: *Modernization Criteria Assessment for Water Resources Planning; Klamath Irrigation Project, U.S.*, 2008, ISBN 3-933761-70-0

167 Dreher, Thomas: *Selektive Sedimentation von Feinstschwebstoffen in Wechselwirkung mit wandnahen turbulenten Strömungsbedingungen*, 2008, ISBN 3-933761-71-9

168 Yang, Wei: *Discrete-Continuous Downscaling Model for Generating Daily Precipitation Time Series*, 2008, ISBN 3-933761-72-7

169 Kopecki, Ianina: *Calculational Approach to FST-Hemispheres for Multiparametrical Benthos Habitat Modelling,* 2008*,* ISBN 3-933761-73-5

170 Brommundt, Jürgen: *Stochastische Generierung räumlich zusammenhängender Niederschlagszeitreihen*, 2008, ISBN 3-933761-74-3

171 Papafotiou, *Alexandros: Numerical Investigations of the Role of Hysteresis in Heterogeneous Two-Phase Flow Systems*, 2008, ISBN 3-933761-75-1

172 He, Yi: *Application of a Non-Parametric Classification Scheme to Catchment Hydrology*, 2008, ISBN 978-3-933761-76-7

173 Wagner, Sven: *Water Balance in a Poorly Gauged Basin in West Africa Using Atmospheric Modelling and Remote Sensing Information*, 2008, ISBN 978-3-933761-77-4

174 Hrsg.: Braun, Jürgen; Koschitzky, Hans-Peter; Stuhrmann, Matthias; Schrenk, Volker: *VEGAS-Kolloquium 2008 Ressource Fläche III*, Tagungsband zur Veranstaltung am 01. Oktober 2008 an der Universität Stuttgart, Campus Stuttgart-Vaihingen, 2008, ISBN 978-3-933761-78-1

175 Patil, Sachin: *Regionalization of an Event Based Nash Cascade Model for Flood Predictions in Ungauged Basins*, 2008, ISBN 978-3-933761-79-8

176 Assteerawatt, Anongnart: *Flow and Transport Modelling of Fractured Aquifers based on a Geostatistical Approach,* 2008, ISBN 978-3-933761-80-4

177 Karnahl, Joachim Alexander: *2D numerische Modellierung von multifraktionalem Schwebstoff- und Schadstofftransport in Flüssen*, 2008, ISBN 978-3-933761-81-1

178 Hiester, Uwe: *Technologieentwicklung zur In-situ-Sanierung der ungesättigten Bodenzone mit festen Wärmequellen,* 2009, ISBN 978-3-933761-82-8

179 Laux, Patrick: *Statistical Modeling of Precipitation for Agricultural Planning in the Volta Basin of West Africa,* 2009, ISBN 978-3-933761-83-5

180 Ehsan, Saqib: *Evaluation of Life Safety Risks Related to Severe Flooding,* 2009, ISBN 978-3-933761-84-2

Die Mitteilungshefte ab der Nr. 134 (Jg. 2005) stehen als pdf-Datei über die Homepage des Instituts: www.iws.uni-stuttgart.de zur Verfügung.